THE UNIVERSITY OF ALABAMA

COLLEGE OF ENGINEERING
BUREAU OF ENGINEERING RESEARCH

Contract Number MASG-R/ER-3
Grant Number NA81AA-D-00050

HYDRODYNAMICS OF MOBILE BAY AND MISSISSIPPI SOUND - NET CROSS CHANNEL FLOWS IN MOBILE BAY

by

Donald C. Raney
Professor of Engineering Mechanics

and

John N. Youngblood
Professor of Mechanical Engineering

Prepared for

Mississippi-Alabama Sea Grant Consortium

October 1982

BER Report No. 285-112

MASGP-82-011

UNIVERSITY, ALABAMA 35486

BUREAU OF ENGINEERING RESEARCH

Members of the faculty who teach at the undergraduate and graduate levels, along with their graduate students, generate and conduct the investigations that make up the College's research program. The College of Engineering of The University of Alabama believes that research goes hand in hand with teaching. Early in the development of its graduate program, the College recognized that men and women engaged in research should be as free as possible of the administrative duties involved in sponsored research. Therefore, the Bureau of Engineering Research (BER) was established and assigned the administrative responsibility for such research within the College.

The director of BER—himself a faculty member and researcher—maintains familiarity with the support requirements of both proposals and research in progress. He is aided by the College of Engineering Research Committee which is made up of faculty representatives from the academic departments of the College. This committee serves to inform BER of the needs and perspectives of the research program.

In addition to administrative support, BER is charged with providing certain technical assistance. Because it is not practical for each department to become self-sufficient in all phases of the supporting technology essential to present-day research, BER makes services available through support groups such as the machine shop, the electronics shop, and publication services.

ACKNOWLEDGEMENT

This work is a result of research sponsored in part by NOAA Office of Sea Grant, Department of Commerce under Grant Number NA81AA-D-00050, the Mississippi - Alabama Sea Grant Consortium and The University of Alabama. The U.S. Government is authorized to reproduce and distribute reprints for governmental purposes notwithstanding any copyright notation which may appear.

HYDRODYNAMICS OF MOBILE BAY AND MISSISSIPPI SOUND - NET CROSS CHANNEL FLOWS IN MOBILE BAY

by

Donald C. Raney
Professor of Engineering Mechanics
The University of Alabama

and

John N. Youngblood
Professor of Mechanical Engineering
The University of Alabama

Prepared for

Mississippi-Alabama Sea Grant Consortium

Grant Number NA81AA-D-00050

October 1982

TABLE OF CONTENTS

I. SUMMARY

Mobile Bay is located on the northeastern shoreline of the Gulf of Mexico east of the Mississippi River delta. The estuary is about 31 miles long and varies in width from 8 to 10 miles in the northern half to about 24 miles wide in the southern portion. The bay is connected by passes to the Gulf of Mexico and also to Eastern Mississippi Sound.

The bay is the terminus of the Mobile River system which consists of more than 43,000 square miles of drainage basin. As a result of the large region drained and the relatively high river flows during the rainy season, suspended sediment loads equivalent to about 5.5×10^6 tons/year are carried into the bay. To maintain navigation channels in the bay, it is necessary for the Corps of Engineers to engage in yearly maintenance dredging activities. During the time period 1970-1977 an average of 6.4 million ft^3/year of sediment was dredged from navigation channels, most of which came from the main channel which runs from Main Pass to the Port of Mobile. The sediment dredged from the main channel is placed in disposal areas adjacent to and on both sides of the channel. Current open water disposal of dredge spoil from the main ship channel is by contract limited to about a 2000 ft. wide strip adjacent to the channel center.

Some seismic surveys have indicated a possible redistribution of spoil material far outside the contract disposal areas. This apparent redistribution of spoil material is asymmetric, a considerable eastward

spreading is indicated with only a slight westward spreading of the material. If this preliminary sesimic information is valid, serious consideration must be given to future dredge spoil disposal practices and locations within Mobile Bay.

The study was initiated to determine whether a numerical hydrodynamic model would indicate any tendency to produce circulation patterns consistent with an asymmetric spreading of the dredged material. The sediment transport problem is extremely complex to model properly. The deposition and resuspension process combined with the generally long time frame associated with sediment movement are difficult to represent in a numerical model. As a first approximation to the problem, sediment transport is considered as being related to net fluid transport. A partially calibrated and verified numerical model of Mobile Bay and East Mississippi Sound is applied and net flow rates across the main channel are evaluated. Net flow rates across the channel are considered for various tide, river and wind conditions.

In order for sediment from the channel aprons to actually be deposited in an area it is not necessary or sufficient that there be net cross-channel flows in the direction of the area under consideration. A more complex flow pattern can exist which results in sediment following a more indirect path before deposition. In addition, if fluid velocities are strong in an area the sediment will move through the area without being deposited. To investigate this aspect of the sediment transport problem, overall circulation patterns at hourly intervals were considered. In addition, a normalized average hydrodynamic energy level over a tidal cycle was calculated for each finite difference cell. The average hydrodynamic energy level is

based upon a mean square of the velocity over the tidal cycle. Regions of low average hydrodynamic energy levels are much more susceptible to sediment deposition than are regions of higher average energy levels. Erosion rather than deposition should occur in regions of very high hydrodynamic energy levels.

The numerical hydrodynamic model results do not indicate a tendency for net west to east flows across the main channel which might be directly consistent with the preliminary seismic survey results. Net flows, depending primarily on the wind condition can be either west to east or east to west. Actually, a slight general tendency appears to exist for net east to west flows across the main channel. There does appear to be some correlation between hydrodynamic energy levels predicted by the model and possible deposition patterns identified by the preliminary seismic surveys. Thus, the numerical model results appear to indicate a possible asymmetric deposition pattern rather than net cross-channel flows as the mechanism for any asymmetric spreading of the dredge spoil which may exist. A strong asymmetric spreading of the dredge spoil cannot be established based upon hydrodynamic model results.

II. OBJECTIVE OF STUDY

Some preliminary seismic surveys suggest redistribution of spoil material from dredge disposal areas adjacent to the main ship channel in Mobile Bay. The spreading of the spoil material appears to be asymmetric with a larger eastward than westward movement. A numerical hydrodynamic model is used to determine if circulation patterns in Mobile Bay are consistent with a net west to east transport relative to the main ship channel.

III. APPROACH TO PROBLEM

Sediment transport is an extremely complex process involving erosion, entrainment, suspension, transportation and deposition. Most measurable sediment movements also occur over rather large time frames (months or years as opposed to hours or days). Sediment movement is therefore difficult to simulate with a numerical model. As a first approximation to the problem the complex details of the processes are neglected and it is assumed that sediment transport is related, in some manner, to net water movement. A partially calibrated and verified numerical hydrodynamic model of Mobile Bay is used to investigate circulation patterns in the bay. New volumetric flows across the main channel are investigated for various tide, river and wind forcing functions. An attempt is made to determine if net flows across the main channel and hydrodynamic energy levels are consistent with an asymmetric spreading of material from the spoil disposal areas. Possible deposition patterns, based upon an average hydrodynamic energy level, are also considered as a possible source of any asymmetric spreading of the dredge spoil from the channel aprons.

IV. THE NUMERICAL MODEL

Formulation of the Model

A complete mathematical description of the hydrodynamic flow in a harbor, bay or estuary would require that the velocity and density be completely specified for every point in the system at all times:

$$u = u(x,y,z,t)$$

$$\rho = \rho(x,y,z,t)$$

where

x = longitudinal coordinate measured along the estuary axis

y = transverse coordinate

z = vertical coordinate

t = time

Because of the difficulties in formulating, executing and verifying a three-dimensional model, researchers have devised a variety of numerical models of various degrees of simplification.

A two-dimensional depth averaged model (BAY) is used in this investigation. The vertical components of velocity and acceleration are neglected and the general three-dimensional governing hydrodynamic equations are integrated over the water depth. A pseudo-three-dimensional effect is present since the equations are forced to satisfy the boundary conditions at the bottom and surface of the water column. A depth-averaged two-dimensional flow field is obtained but three-dimensional geometry can be considered. The most important approximations used in the model are those of constant density and relatively small variations of velocity over the depth, conditions which are reasonably valid much of the time in Mobile Bay. Where these conditions are approximately valid, this type of numerical

model can provide accurate representations of tidal elevations and velocities.

The rectangular coordinate system is located in the plane of the undisturbed water surface as shown in Figure 1. The equations

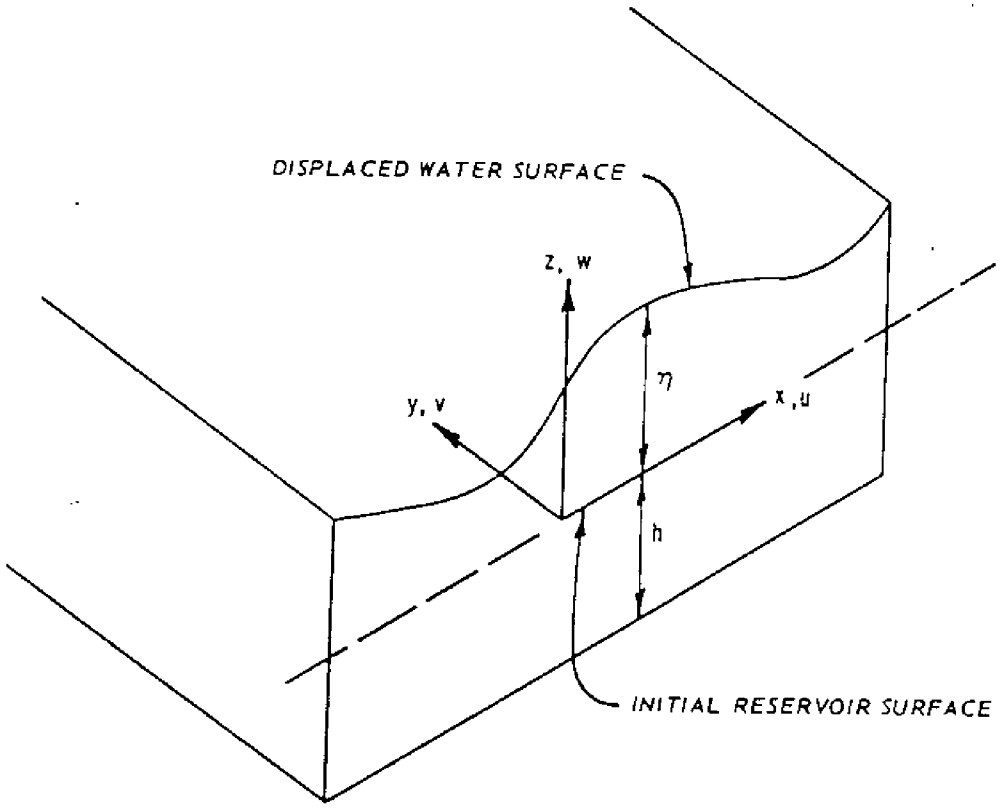

Figure 1. Coordinate system for problem formulation

of motion and the equation of continuity are written as follows:

$$\frac{\partial u}{\partial t} + u\frac{\partial u}{\partial x} + v\frac{\partial u}{\partial y} + g\frac{\partial \eta}{\partial x} - fv = R_x + L_x \tag{1}$$

$$\frac{\partial v}{\partial t} + u\frac{\partial v}{\partial x} + v\frac{\partial v}{\partial y} + g\frac{\partial \eta}{\partial y} + fu = R_y + L_y \tag{2}$$

and

$$\frac{\partial \eta}{\partial t} + \frac{\partial}{\partial x}[(h + \eta)u] + \frac{\partial}{\partial y}[(h + \eta)v] = 0 \tag{3}$$

where

u = depth-averaged velocity component in the x direction

t = time

x,y = rectangular coordinate variables

v = depth-averaged velocity component in the y direction

g = acceleration due to gravity

η = water level displacement with respect to datum elevation

f = Coriolis parameter

R_x, R_y = the effect of bottom roughness in x and y directions

L_x, L_y = the acceleration effect of the wind stress acting on the water surface in the x and y directions

h = water depth

The continuity equation has been obtained by integrating across the water depth and applying kinematic and dynamic boundary conditions at the surface and bottom of the reservoir. The bottom friction terms are represented using a Chezy coefficient in the following form:

$$R_x = \frac{-gu(u^2 + v^2)^{1/2}}{C^2(h + \eta)} \tag{4}$$

$$R_y = \frac{-gv(u^2 + v^2)^{1/2}}{C^2(h + \eta)} \tag{5}$$

where C is the Chezy coefficient. The terms L_x and L_y represent the wind shear stress effect on the water surface. These terms are of the form:

$$L_x = \frac{T_x}{(h + \eta)} \tag{6}$$

$$L_y = \frac{T_y}{(h + n)} \tag{7}$$

where T_x and T_y are the wind stress components acting on the water surface.

A major advantage of BAY is the capability of applying a smoothly varying grid to the given study region. This allows efficient simulation of complex geometries by locally increasing grid resolution in critical areas. For each coordinate direction, a piecewise reversible transformation is independently used to map prototype or real space (x,y space) into a computational space (α_1,α_2 space). The transformation takes the form

$$x = a + b\alpha^c$$

where a, b and c are arbitrary constants. By applying a smoothly varying grid transformation which is continuous and which has continuous first derivatives, many stability problems commonly associated with variable grid schemes are eliminated provided that all derivatives are centered in α space[2]. The transformed equations in α space can be written as

$$\frac{\partial u}{\partial t} + \frac{1}{\mu_1} u \frac{\partial u}{\partial \alpha_1} + \frac{1}{\mu_2} v \frac{\partial u}{\partial \alpha_2} + \frac{g}{\mu_1} \frac{\partial n}{\partial \alpha_1} - fv = R_x + L_x \tag{8}$$

$$\frac{\partial v}{\partial t} + \frac{1}{\mu_1} u \frac{\partial v}{\partial \alpha_1} + \frac{1}{\mu_2} v \frac{\partial v}{\partial \alpha_2} + \frac{g}{\mu_2} \frac{\partial n}{\partial \alpha_2} + fu = R_y + L_y \tag{9}$$

$$\frac{\partial n}{\partial t} + \frac{1}{\mu_1} \frac{\partial}{\partial \alpha_1} [(h+n)u] + \frac{1}{\mu_2} \frac{\partial}{\partial \alpha_2} [(h+n)v] = 0 \tag{10}$$

To solve the governing equations, a finite difference approximation of the equations and an alternating direction technique are employed. A space-staggered scheme is used in which velocities, water-level displacement, bottom displacement, and water depth are described at different locations within a grid cell as shown in Figure 2. This solution scheme is similar to that originally proposed by Leendertse[3].

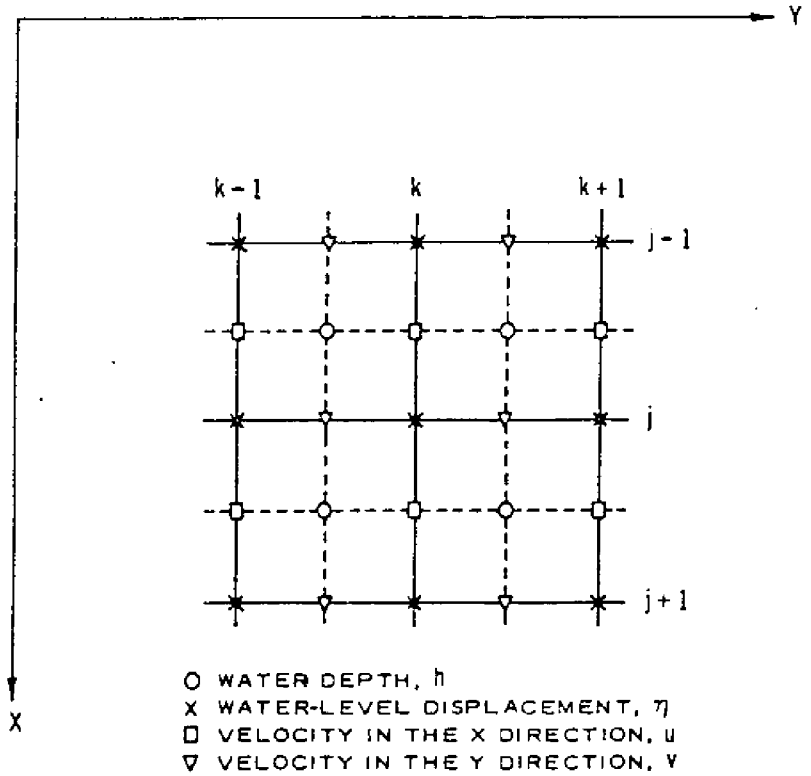

Figure 2. Grid system and variable definition locations

The first step in the calculation consists of computing u and η implicitly and v explicitly, advancing from time $n\Delta t$ to $(n + 1/2)\Delta t$. The parameter n is an integer representing the time step at which the calculations are being conducted. The second step computes η and v implicitly and u explicitly, advancing from time $(n + 1/2)\Delta t$

to $(n + 1)\Delta t$. Central differences are used for evaluating all derivatives in the governing equations. The application of these difference approximations gives rise to corresponding difference equations centered about different points within a grid cell. These expressions require the evaluation of certain quantities at locations different from those defined in the grid system. Such quantities are replaced by values computed from a one- and two-dimensional averaging of neighboring values. The time interval Δt is taken as the time required to complete the full cycle in the computational procedure; however, each half cycle is treated by a different set of equations so a system of six operational equations is used.

Three types of boundaries are involved in the calculations: solid boundaries at fixed coastlines, artificial tidal input boundaries arising from the need to truncate the region of computation and river inflows into the bay.

A condition of complete reflection is adopted at solid boundaries. While some dissipation does occur at the shoreline, this should not be significant in this application. The actual boundary condition for the solid boundary can be written as

$$\vec{V}_n = 0 \tag{11}$$

where $\vec{V}_n$ denotes the normal component of velocity.

Artificial tidal boundaries were used in the model to describe the tidal action that occurs at the ocean computational boundaries. These boundaries must be accurately defined since the tides applied at these boundaries represent the major forcing function driving the hydrodynamic system. The water-surface elevation time history for

the desired tidal cycle is specified at each such boundary and applied during the operation of the model. River inflow boundaries are required to simulate the river hydrograph for those significant streams discharging into the bay.

V. Mobile Bay Estuary System

The Mobile Bay Estuary System is illustrated in Figure 3. Mobile Bay is a moderate-sized,shallow, semi-enclosed coastal embayment with a simple pear shape and a small tidal amplitude. The bay width varies from about 8 miles at the northern end to 23 miles between Pass aux Herons and the eastern shore of Bon Secour Bay. The length of the bay is approximately 31 miles. The bay is also the terminus of the fourth largest river system in the United States in terms of discharge. The average depth of the bay is 9 feet except for the Mobile Ship Channel. The channel is 29 miles long by 400 feet wide with a controlled depth of 40 feet. The Bay is separated from the Gulf of Mexico by Fort Morgan Peninsula to the southeast and Dauphin Island to the southwest. The 4.1 mile wide Main Pass connects Mobile Bay to the Gulf of Mexico between these barriers. Most of the salt water entering the Bay enters from the Gulf through the Main Pass.

Mobile is connected to East Mississippi Sound by Pass aux Herons. Pass aux Herons is about 1.9 miles wide along a line between Cedar Point and North Point of Little Dauphin Island. The majority of the pass is shallow, depths being generally less than 4 feet. The Gulf Intracoastal Channel, dredged through Pass aux Herons, has a controlled depth of 12 feet.

Most investigations have indicated that Main Pass is responsible for approximately 85% and Pass aux Herons for approximately 15% of the exchange of waters in and out of Mobile Bay. Schroeder[4] indicates that river waters favor the western shore as they move to the south while the Gulf of Mexico waters favor the eastern shore as they move north, although it is not uncommon for movement of river water down the eastern shore.

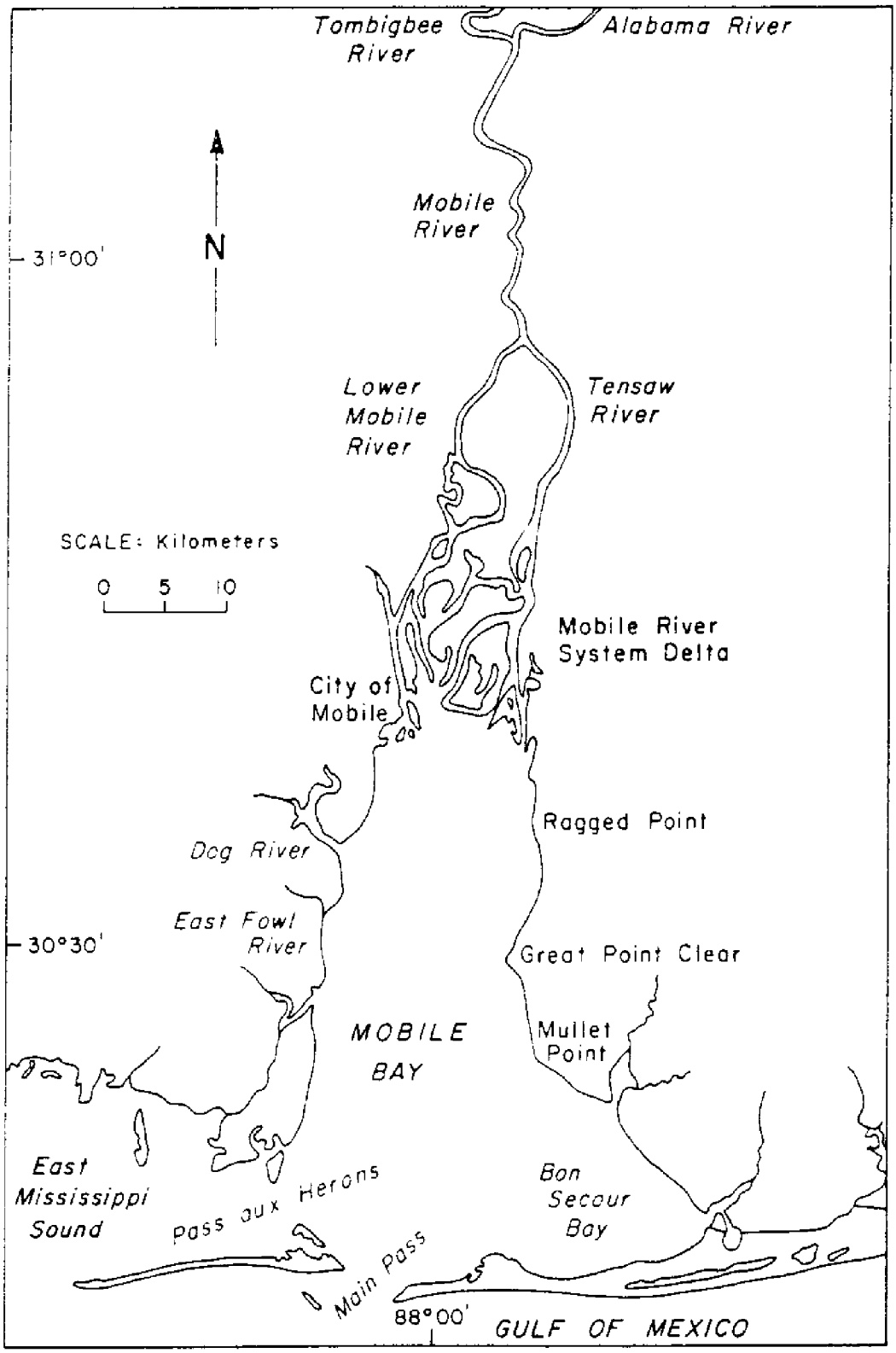

Figure 3. Mobile Bay Estuary System

Dauphin Island Wind Roses, Schroeder[5], for 1974-1977 indicate a predominate northwest to northeast system during the late fall and winter and a southeast to southwest system in the spring and summer. The Annual Wind Roses presented by Schroeder[4] indicate that most of the larger winds (over 15 knots) are from northeast to northwest in direction although as observed in Figure 4, the percent occurrence is just about equal between the northeast to northwest system and the southeast to southwest system.

The interaction between Mobile Bay, East Mississippi Sound and the Gulf of Mexico is complex. Natural changes from storms and long term sediment transport combine with man made changes such as dredging and spoil deposition to produce a dynamically changing system. Small changes in current patterns and salinity levels often have significant effects on the acquatic environment of the area. Observed shifting patterns of productive oyster reefs and fluctuations in other seafood species are evidence of past changes which have occurred in the bay.

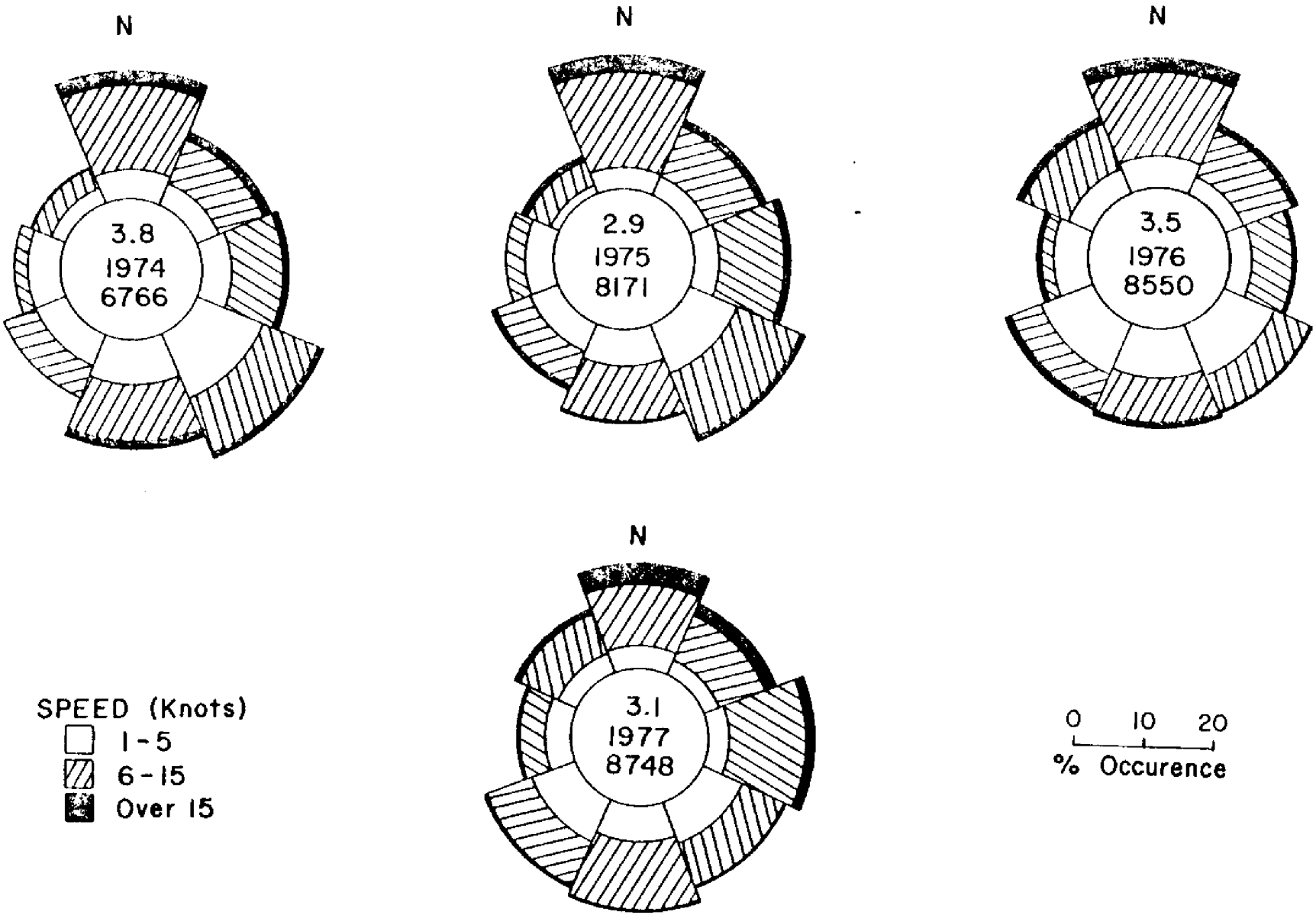

Figure 4. Dauphin Island Annual Wind Roses

VI. PROTOTYPE DATA FOR MODEL CALIBRATION AND VERIFICATION

Very rarely are there sufficient prototype data available to completely calibrate and verify a numerical model to the extent that the modeler would desire. As is often the case, some prototype data are available allowing the numerical model to be partially calibrated and verified. Such a model can generally be used to predict basic trends in the system being modeled, but detailed flow patterns from such a model should be viewed with caution.

Two sets of tidal elevation and current velocity data were available for calibrating and verifying the Mobile Bay model. These data were obtained from the U.S. Army Corps of Engineers, Mobile, Alabama.[6] The data were originally used for the calibration and verification of a physical model of Mobile Bay located at the Waterways Experiment Station, U.S. Army Corps of Engineers, Vicksburg, Mississippi. An additional tide elevation record from Hill[7] that was not included with the Corps of Engineers data was also used.

The data were collected over two 25 hr time periods. The first period was from 1200 CST May 15, 1972 to 1300 CST May 16, 1972. The second data set was collected from 0900 CST June 13, 1973 to 1000 CST June 14, 1973. The locations of some of the tide-elevation and current-velocity stations vary between the two data sets. The average flow rates (cfs) during these two time periods for the Mobile and Tensaw Rivers were included in the data. The 1972 data also included flow-rate calculations for Main Pass and Pass aux Herons over the data collection period.

The tide-elevation data consisted of a continuous paper-tape record of elevation (ft) over time (hrs). The current-velocity data

consisted of readings of the current-velocity magnitude and compass direction at hourly intervals over the 25 hr collection periods.

For calibration and verification of the model, tide elevations at each gage were obtained from the tide record at hourly intervals corresponding to the times of the velocity data. In most cases the elevation could be read to ±0.20 ft at any given hour. At stations where the current velocity and direction were measured at depth intervals, the velocity magnitude and direction were taken as the average of these measurements since they were to be compared with a depth averaged velocity from the numerical model.

1972 Data

Tide elevation, current velocity and pass flow-rate data were available for the 25 hour period starting 1200 CST May 15, 1972. Notes on the raw velocity data indicated the presence of a variable wind of 5-20 k. The wind data were not in sufficient detail to allow inclusion of its effect in the numerical model. The actual locations of each gage station are shown in Figure 5.

A constant, total river flow of 63,500 cfs was used. Of this amount, 33,270 cfs was introduced into the Mobile River and 30,230 cfs into the Tensaw River.

The tidal boundary condition at the Gulf of Mexico was obtained using the tide record at the Dauphin Island Gulf station obtained from Hill.[7] The tidal record at Cedar Point was used to obtain the tidal boundary condition for East Mississippi Sound. In both cases the tidal records of the indicated gages were backed off to the computational boundary based on the free-gravity wave speed.

B-12 = Buoy 12
Dauphin Island = Dauphin Island Gulf
E-1 = West Main Pass
E-3 = East Main Pass

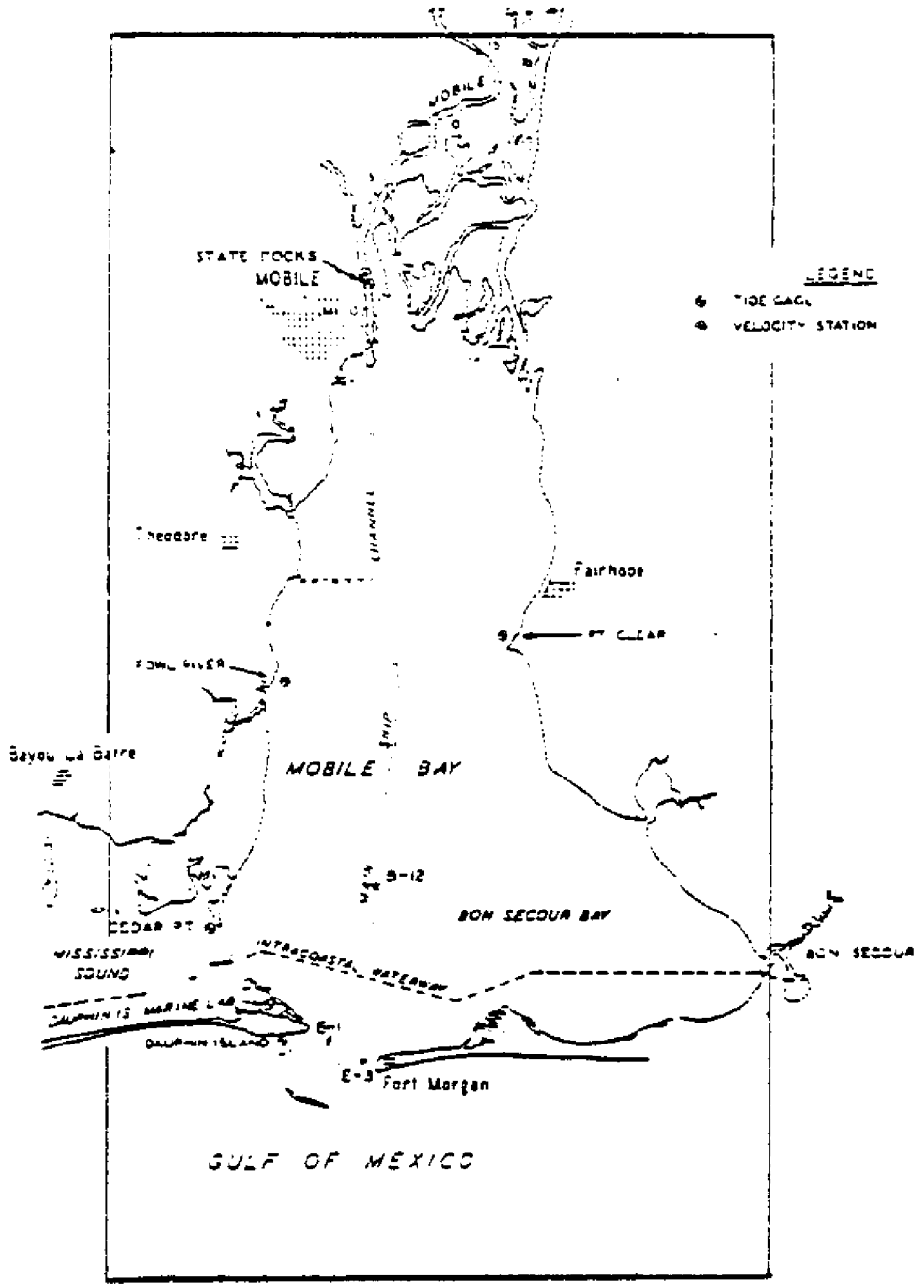

Figure 5. Location of Field Data Stations for May 15-16, 1972.

1973 Data

The field data were collected over the 25 hr period from 0900 CST June 13 through 1000 CST June 14, 1973. Notes on the raw velocity-data sheets indicated low wind conditions. The data consisted of tide-elevation and velocity stations only. No pass flow-rate calculations were available. The locations of the gages are shown in Figure 6.

A constant total river flow of 116,000 cfs was used. The flow was divided equally between the Mobile and Tensaw Rivers.

A tide-elevation record for Dauphin Island Gulf was not available in the 1973 field data for the specification of the Gulf of Mexico boundary condition. The only alternative for setting any reasonable boundary condition at the Gulf was the use of the predicted or astronomical tide for this time period. The Tide Tables[8] provided the predictions of the elevations and times of the high and low tides at the MLW datum. By interpolation of the tide elevations between these times, an approximation of the predicted tide elevation as a function time was obtained. The data were obtained for June 13 and 14, 1973 at Bayou La Batre, Alabama and Dauphin Island (Fort Gaines). These tide-elevation curves were corrected to MSL and used as the initial boundary conditions for East Mississippi Sound and the Gulf of Mexico, respectively. This constructed tidal boundary condition was then adjusted slightly to produce results more consistent with the prototype data.

B-12 = Buoy 12
B-32 = Buoy 32
E-3 = East Main Pass
2-12 = Dauphin Island Bridge

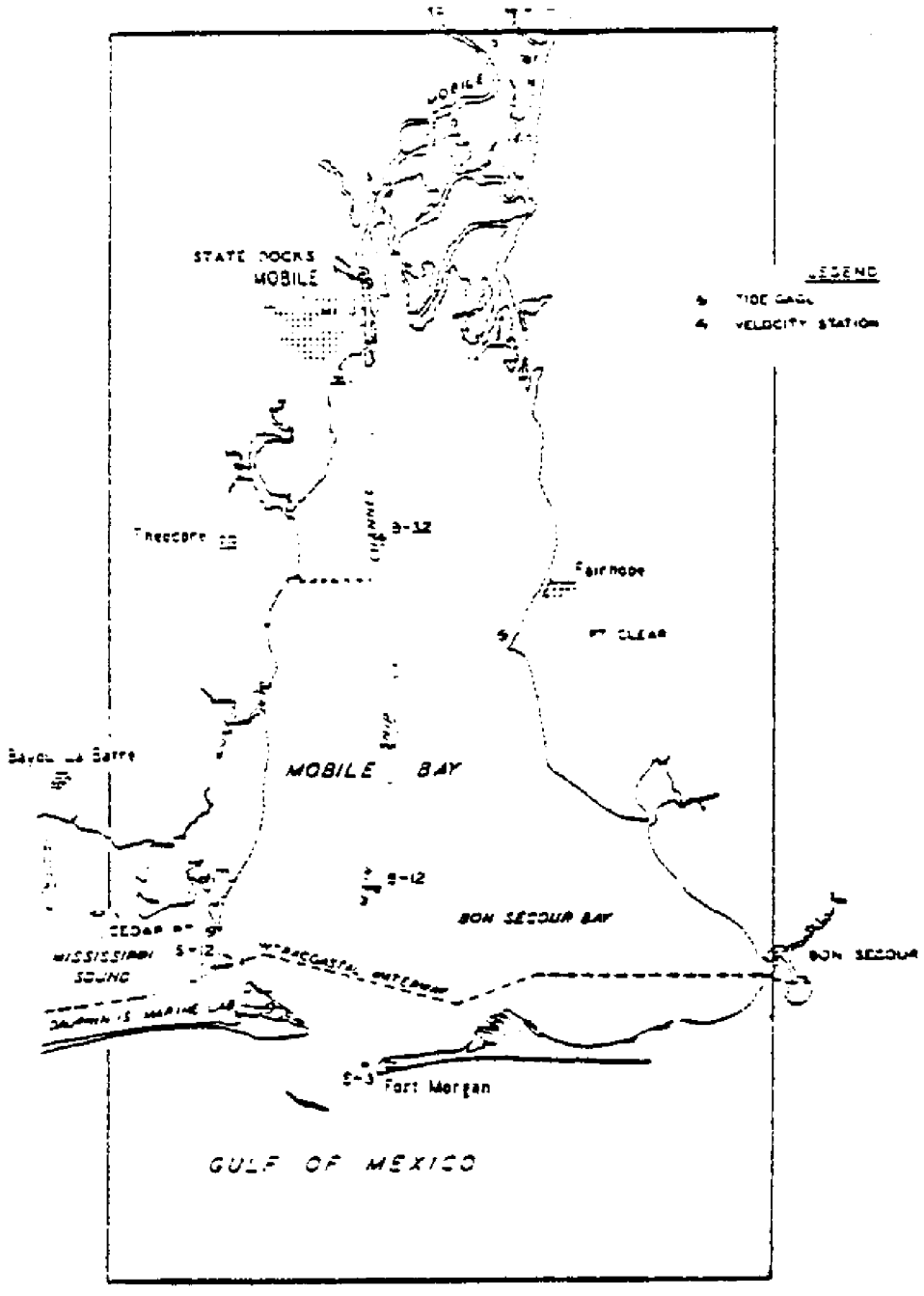

Figure 6. Location of Field Data Stations for June 13-14, 1973.

VII. THE FINITE DIFFERENCE GRID

The area of Mobile Bay and East Mississippi Sound chosen for representation by a variable-size finite difference grid is shown in Figure 7. This area includes Mobile Bay, the Mobile River delta up to about 5 miles north of the I-20 Causeway, East Mississippi Sound to 6.9 miles west of Dauphin Island Bridge and the Gulf of Mexico southward to 8.5 miles south of Fort Morgan.

The finite difference grid, Figure 8, used for the model of Mobile Bay-East Mississippi Sound was developed using a 1:80000 scale nautical chart[9]. A variable grid was developed with the primary objective of good resolution of the main ship channel as well as reasonable representation of other geometric and bathymetric features. The dimension of the resulting grid was 55 by 56 cells or 3080 cells. After mapping the grid, it was used as an overlay on the nautical chart to assign boundaries, depths and Manning friction coefficients for each finite difference cell. The manner in which the grid fits the land boundaries, channels and other features of the bay is illustrated in Figure 9.

The smallest cells were used in representing the main ship channel since this was the region of primary interest. Small cells were also used in the inlets since these are critical areas for the tidal hydraulics. Larger cells were used in Bon Secour Bay, the Gulf of Mexico and in upper Mobile Bay where the bathymetry was reasonably constant and/or boundary geometry was relatively simple. No attempt was made to accurately represent the Mobile River delta except for providing a constant river flow at appropriate points on the system boundary.

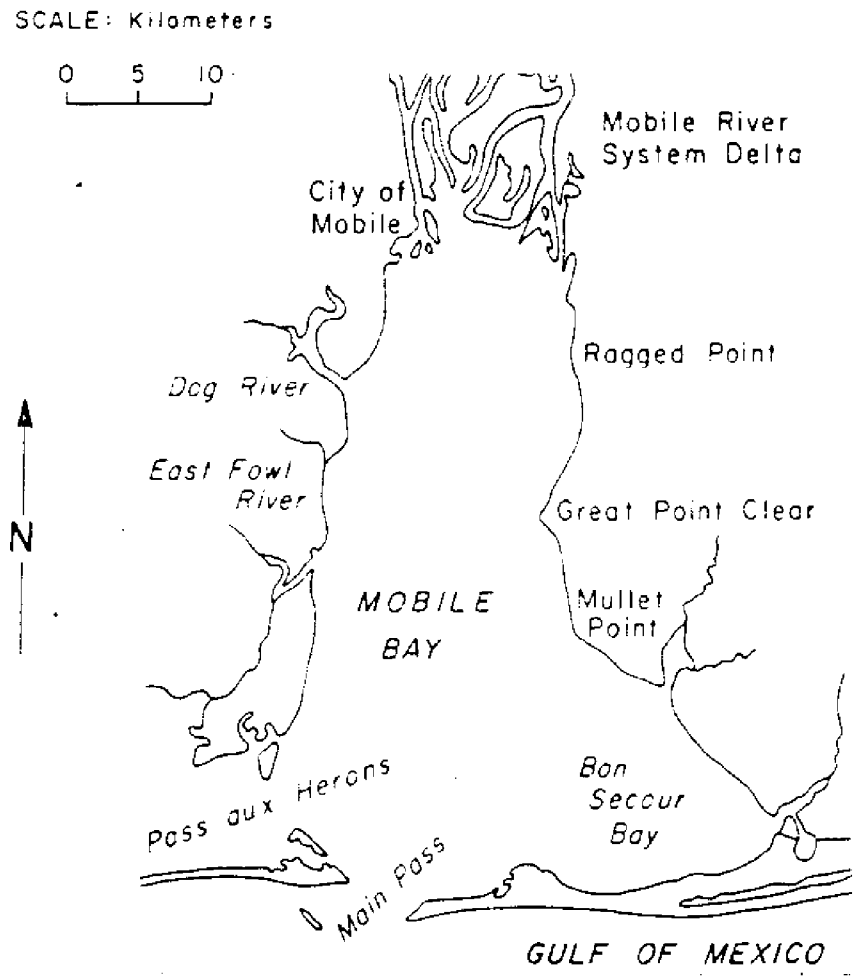

Figure 7. The Study Area.

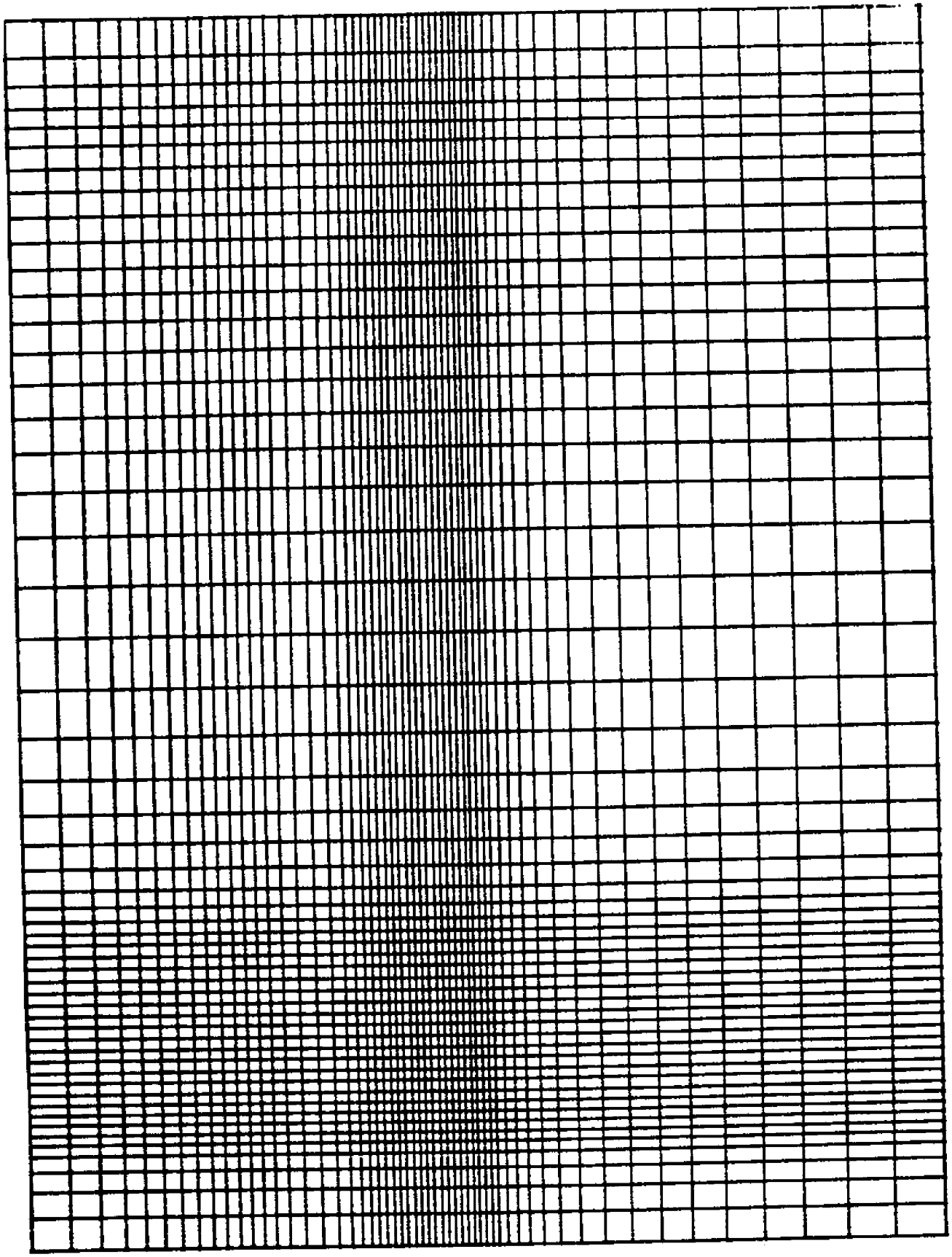

Figure 8. Variable Size Finite Difference Grid.

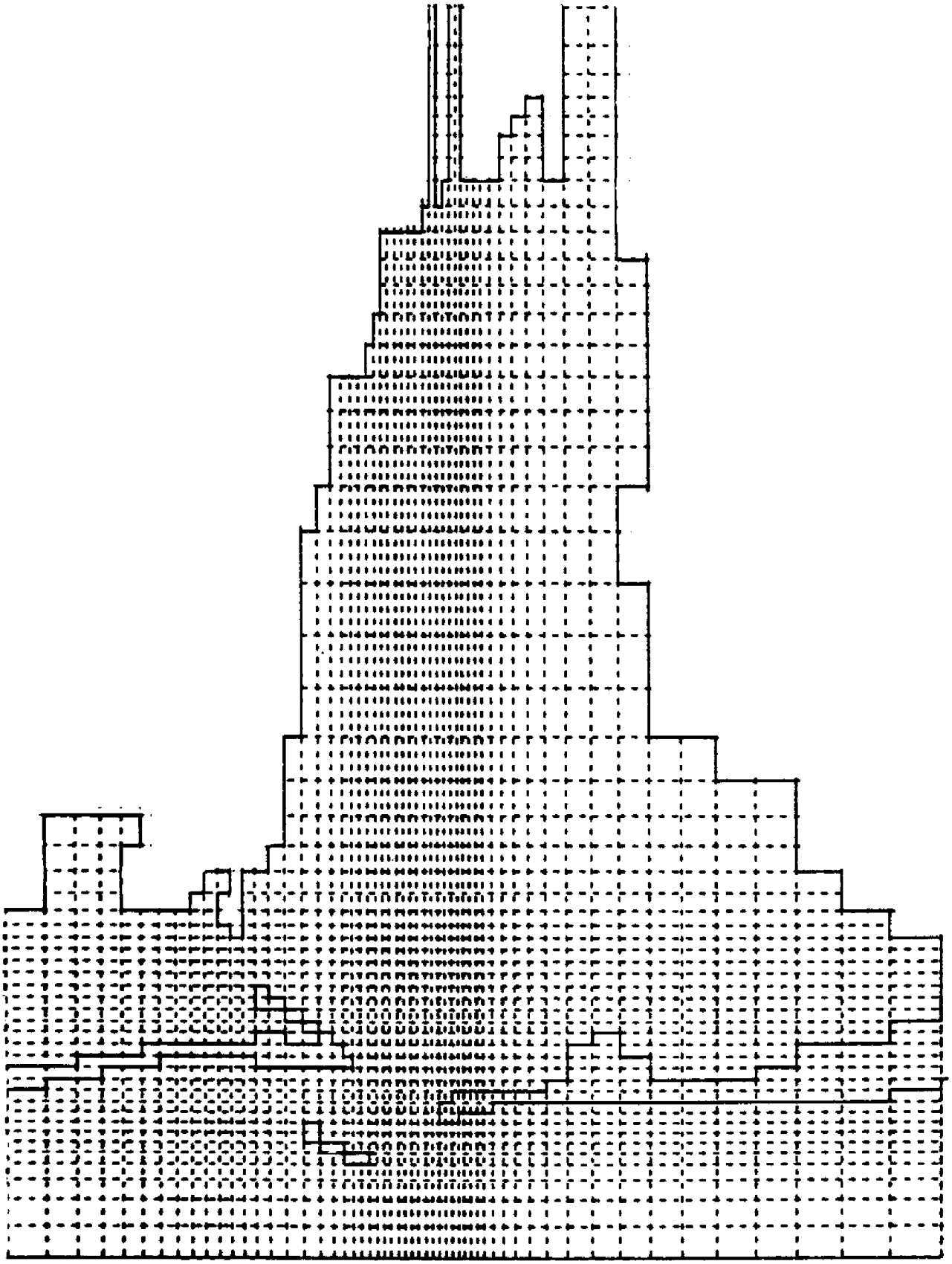

Figure 9. Finite Difference Grid Representation of Mobile Bay.

The smallest cell size was 1000 ft and the maximum depth was 60 feet. Thus the maximum propogation speed of an infinitesimal disturbance is approximately 44 ft/sec. A half time step of 90 sec will yield a reasonable Courant number for the calculations.

Tide-elevation boundary conditions were specified at the Gulf of Mexico boundary and the East Mississippi Sound boundary. River-flow boundary conditions were specified for the Mobile and Tensaw Rivers. River flows were not included for Dog River, Fowl River, or any of the other small rivers emptying into the model region. The flows from these rivers are insignificant with respect to the overall hydrodynamics of the Mobile Bay-East Mississippi Sound region as stated above.

The datum of the nautical chart was the Gulf Coast Low Water Datum (LWD) which was established in 1880 as an average of 60 consecutive low-water readings according to MacPhearson,[10] Figure 10. The datum of the Tide Tables was Mean Low Water (MLW). The datum of the field data used in this study was Mean Sea Level (MSL). In applying the model, the depth of each cell was corrected to MSL to correspond to the field data.

Depths were assigned to each water cell as delineated by the land boundary. The depth of each cell was determined as a weighted average of the charted depths within that cell. Due to the slowly varying bottom depth over large portions of the Bay, most of the depths assigned to the grid cells reflected the actual bathymetry of the Bay. This did not hold for the grid cells in which the ship channel was located. The ship channel is 400 ft. wide, and therefore

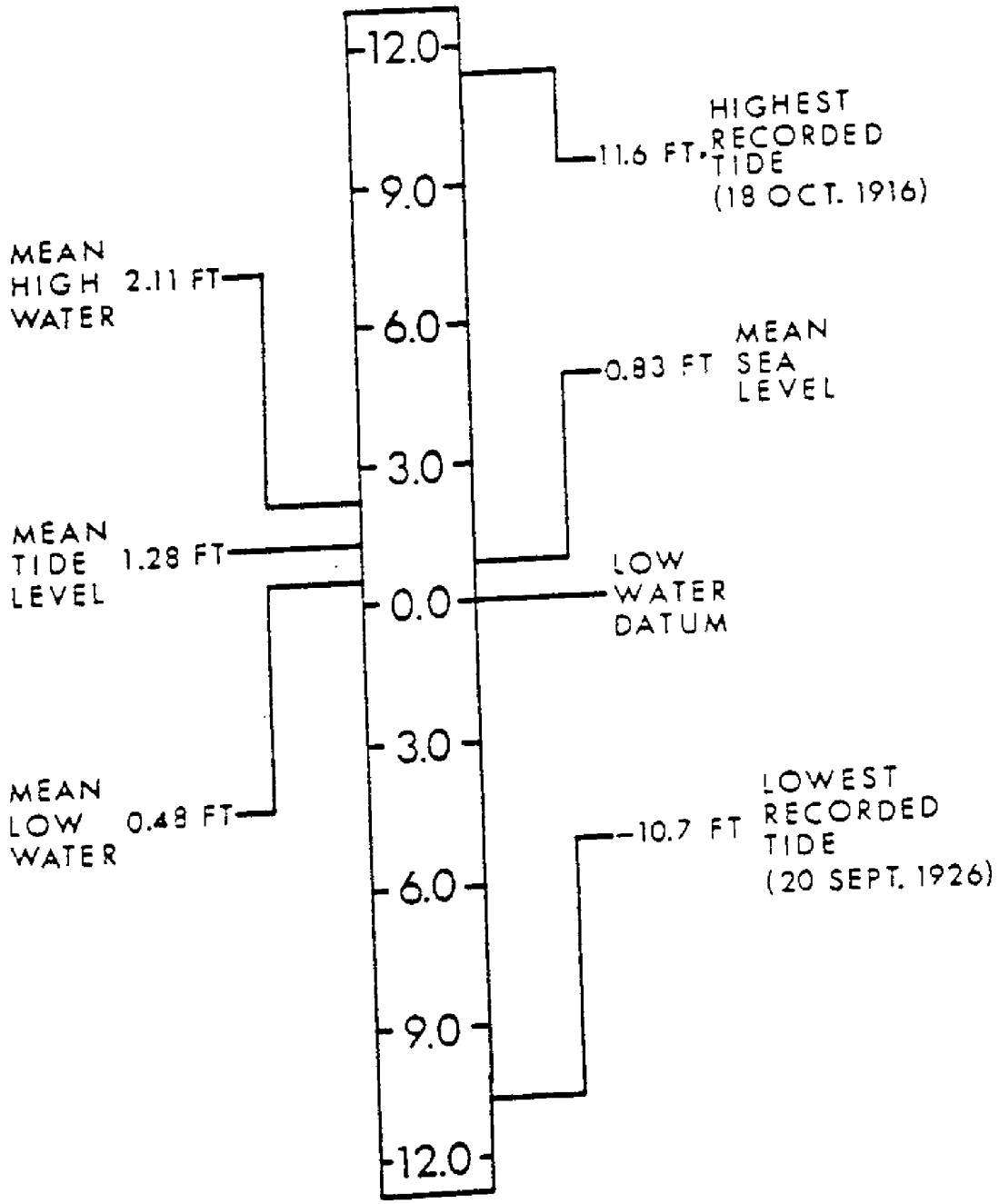

Figure 10. Significant Water Levels Relative to Low Water Datum.

smaller than the minimum grid dimension of 1000 ft. Its 40 ft. depth is deeper than the average 10 ft. depth of the Bay. Depths for these cells were assigned by a carefully weighted average.

Manning's n friction values for bottom roughness were assigned on a relative basis according to the bottom type specified by the nautical chart. The Manning coefficients ranged from .021 clean sandy areas to .050 in the river-marsh area of the Mobile River delta.

VIII. MODEL CALIBRATION AND VERIFICATION

The 1972 prototype data were selected for model calibration with the 1973 prototype data used for model verification. The tide gage and velocity station locations on the model grid were designated as the grid cells closest to the physical location in the bay. The tide elevation and velocity used for comparison purposes with each protoype gage was the calculated elevation and velocity of the designated grid cell.

Calibration

As indicated previously, elevation and velocity data were available at selected locations for the 25 hour period starting 1200 CST May 15, 1972. A variable 5-20 knot wind was present but detailed time variation of the wind was not available for inclusion as a model boundary condition. A constant total river flow of 63,500 cfs was used. The flow was split with 33,270 cfs introduced into the Mobile River and 30,230 cfs into the Tensaw River.

The tidal boundary conditions at the Gulf of Mexico and in East Mississippi Sound were established from the tidal gage records nearest to these two boundaries. Thus, the Dauphin Island Gulf and Cedar Point gages were "backed off" to the tidal boundary using the free gravity wave speed. The tidal boundary condition was then adjusted slightly until the model essentially reproduced the prototype tidal elevations at these two gages.

The model was run with a half time step of 90 seconds over a period of 27 hours. Previous model applications had established that only about 3 or 4 hours of model warm-up time are required if the model is started at high tide where velocities are small.

The comparison of model results with prototype data is presented in Figures 11 thru 20. In general, the hydrodynamic model produced results that were in very good areement with prototype data.

Dauphin Island Gulf, Cedar Point, Bon Secour and Point Clear tidal elevations predicted by the model are essentially identical with the prototype data. These results are shown in Figures 11, 12, 13, and 14. In Figure 15, the Dauphin Island Marine Lab tidal elevation predicted by the model is observed to agree in magnitude with prototype data, but there is a slight phase error. This difference is attributed to the numerical model grid resolution being insufficient to allow representation of Pass Drury between Dauphin Island and Little Dauphin Island. As a result, the Dauphin Island Marine Lab location in the numerical model is more heavily dependent upon the East Mississippi Sound tide than is the actual case. In the actual case this gage will feel some direct influence from the Gulf of Mexico tide through Pass Drury.

The model and prototype tidal elevations at Fowl River are shown in Figure 16. These results agree in magnitude but there is a phrase difference. Other investigators[11] have had difficulty with the prototype data from this gage and a timing problem with the gage is suspected. The model and prototype elevations at the State Docks agree well in magnitude but there is a slight phrase difference. This is shown in Figure 17.

The model and prototype velocities at East Main Pass, Figure 18, are in extremely good agreement. The velocity agreement for West Main Pass, Figure 19, is satisfactory. Buoy 12 velocities agree well for about 14 hours then disagree during the latter part of the test period. As observed in Figure 20, the prototype data has a discontinuity in the record suggesting some possible problems with these data.

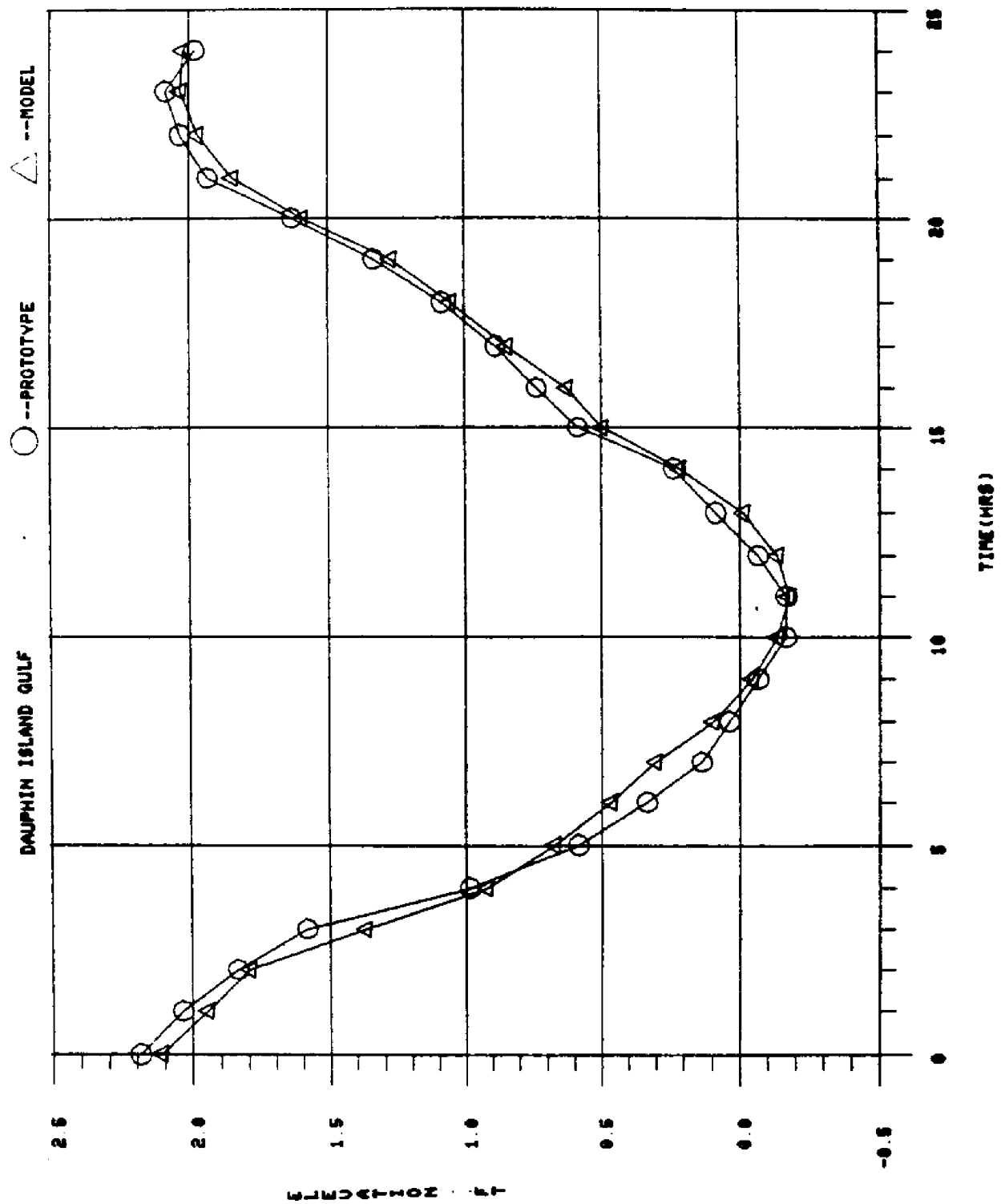

Figure 11. Comparison of Model Tidal Elevation Results at Dauphin Island Gulf with 1972 Prototype Data

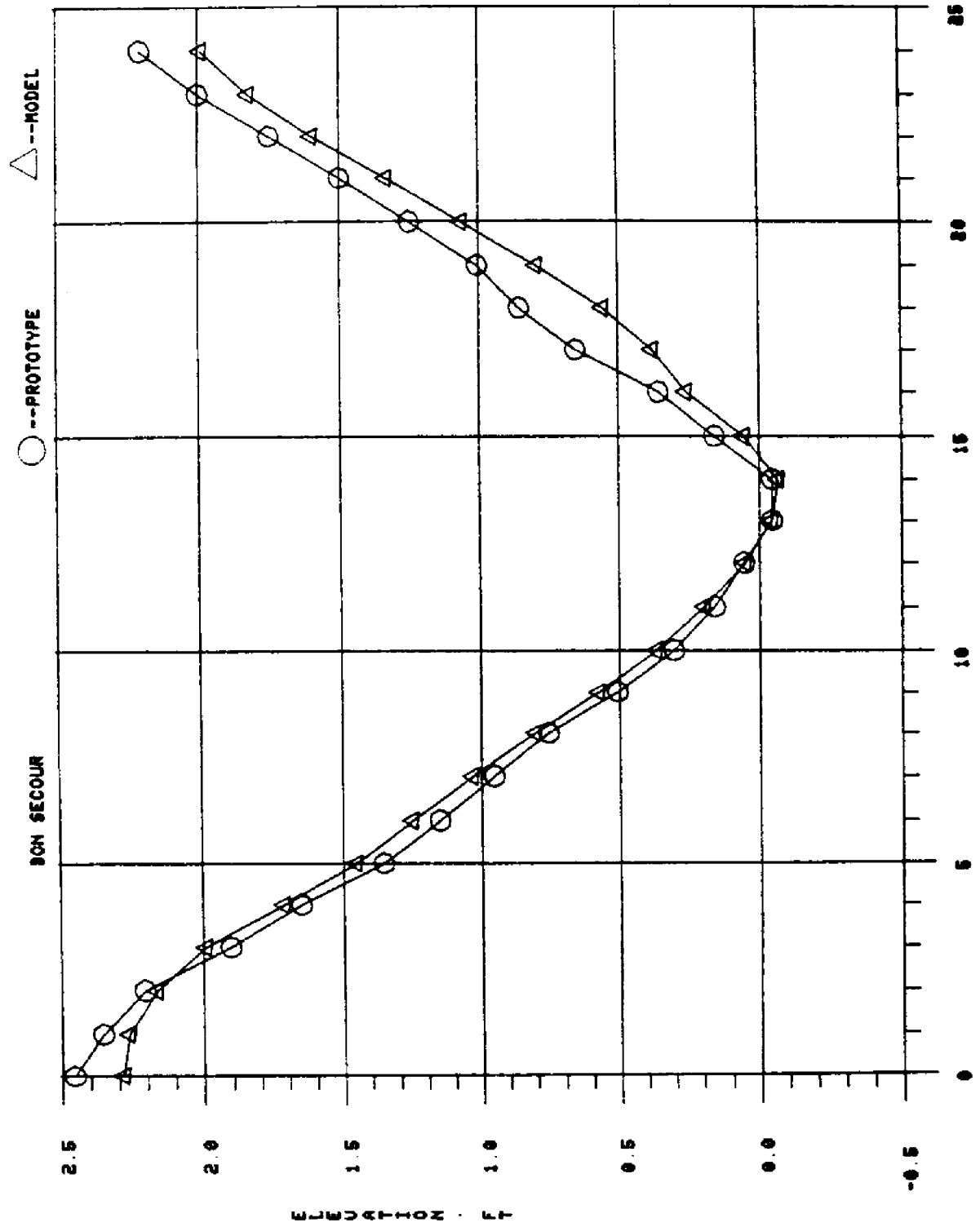

Figure 12. Comparison of Model Tidal Elevation Results at Bon Secour with 1972 Prototype Data

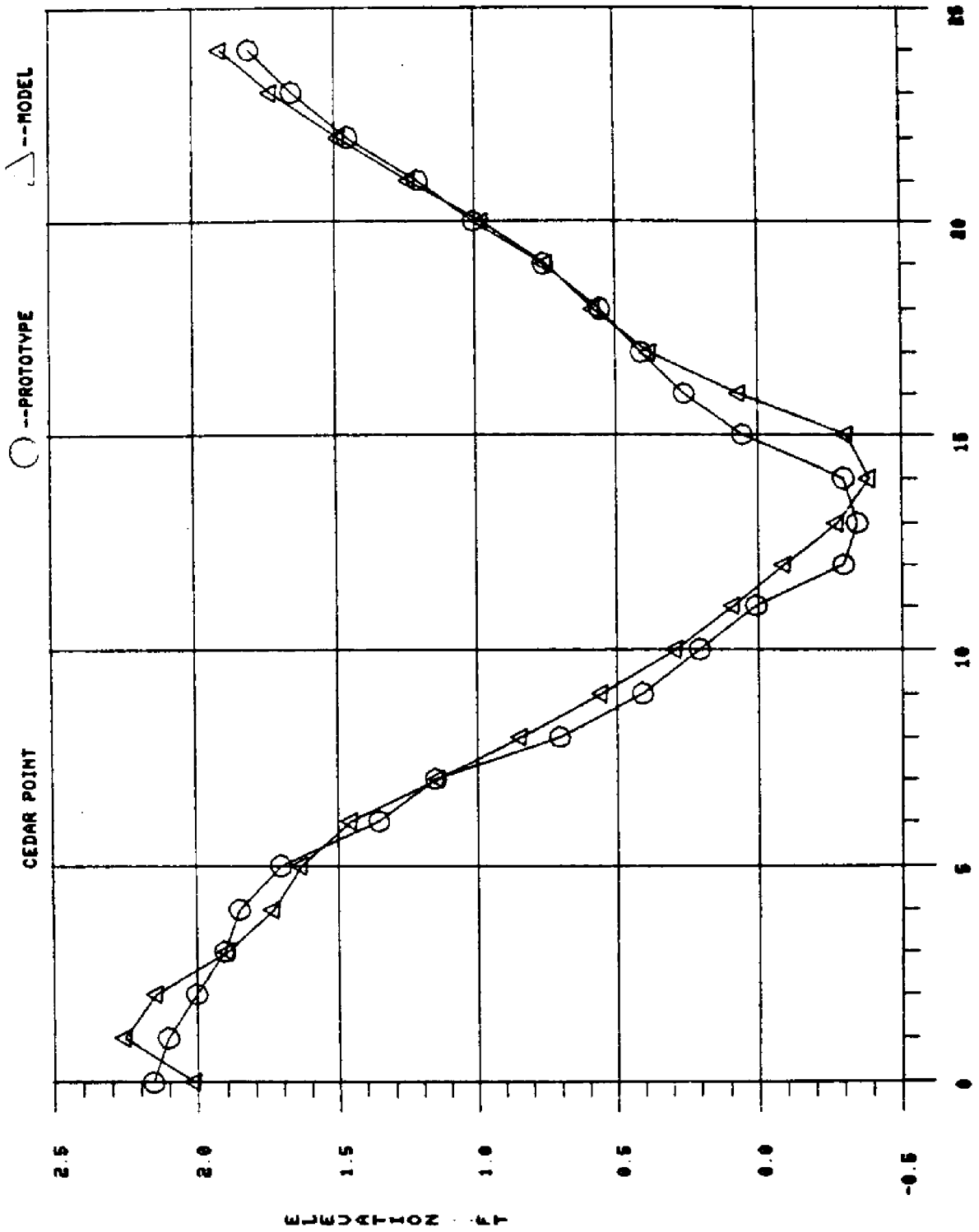

Figure 13. Comparison of Model Tidal Elevation Results at Cedar Point with 1972 Prototype Data.

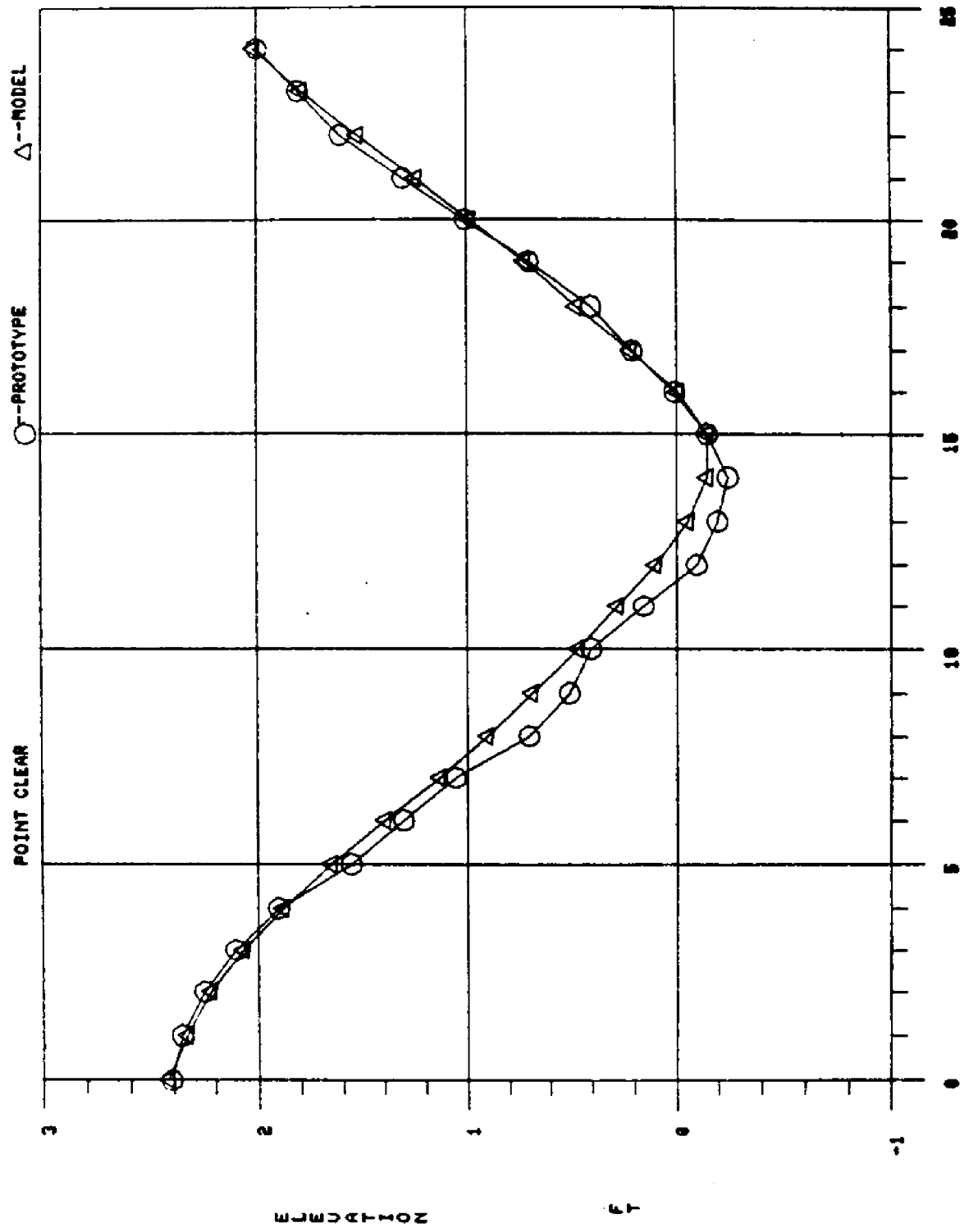

Figure 14. Comparison of Model Tidal Elevation Results at Point Clear with 1972 Prototype Data.

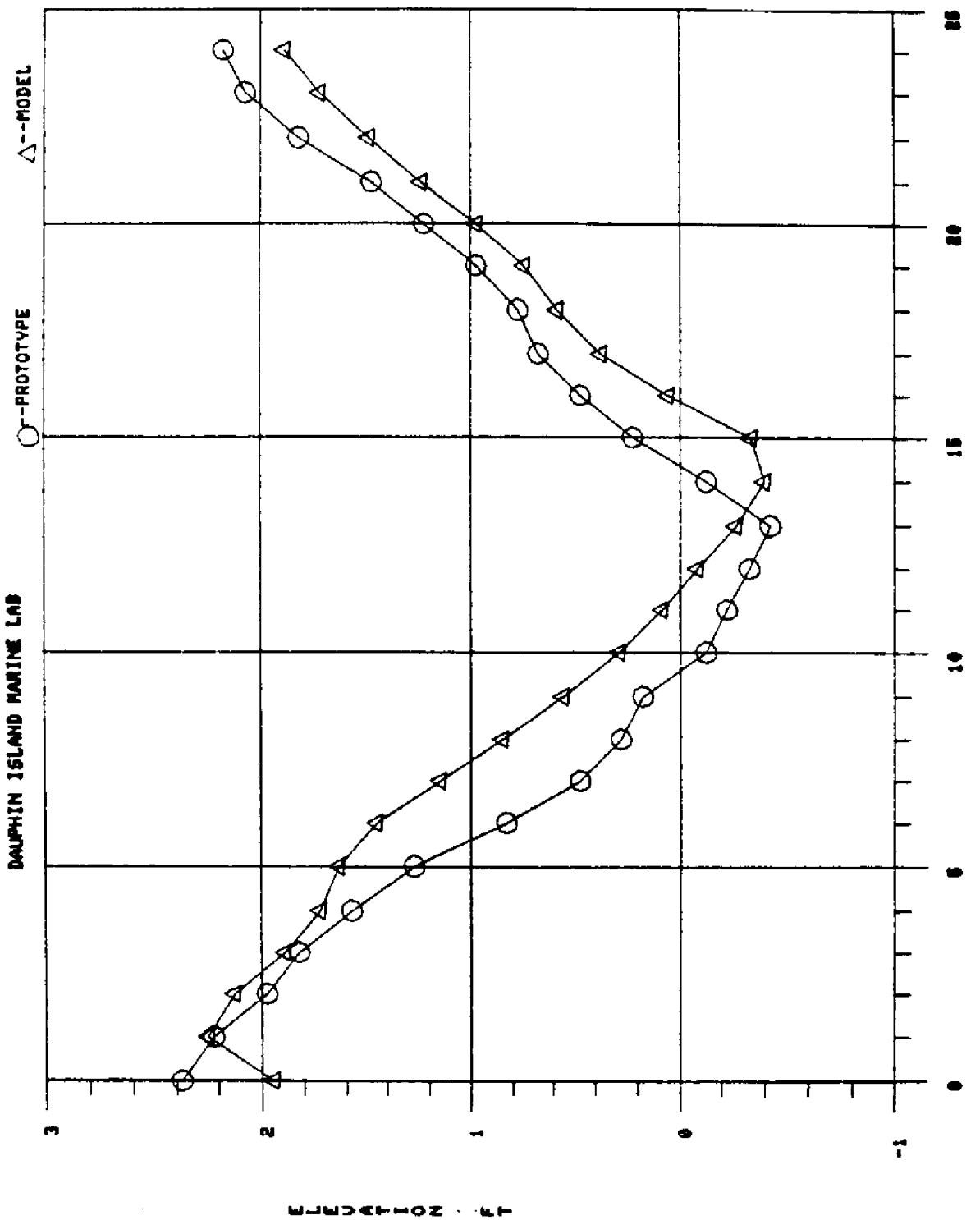

Figure 15. Comparison of Model Tidal Elevations Results at Dauphin Island Marine Lab with 1972 Prototype Data.

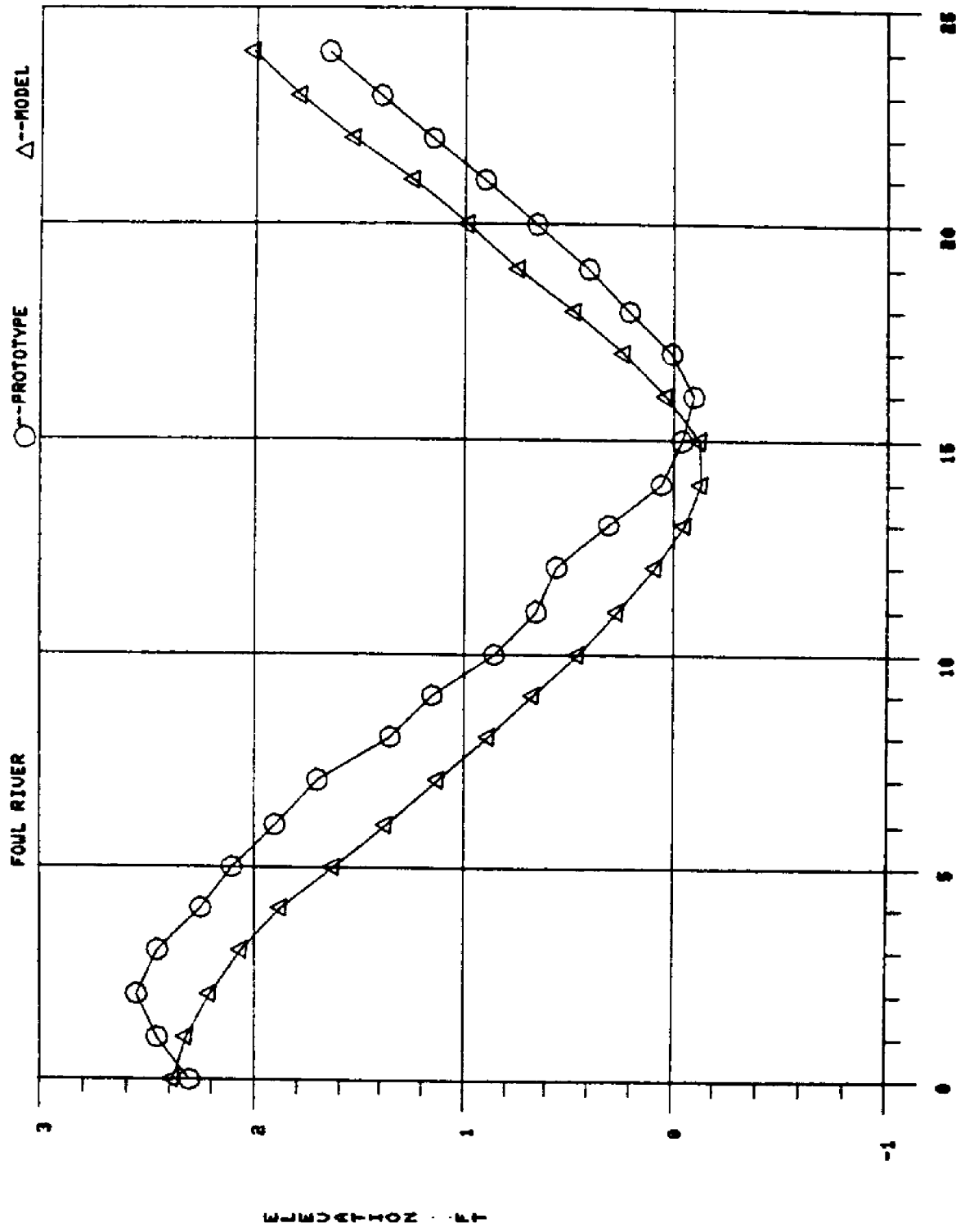

Figure 16. Comparison of Model Tidal Elevation Results at Fowl River with 1972 Prototype Data.

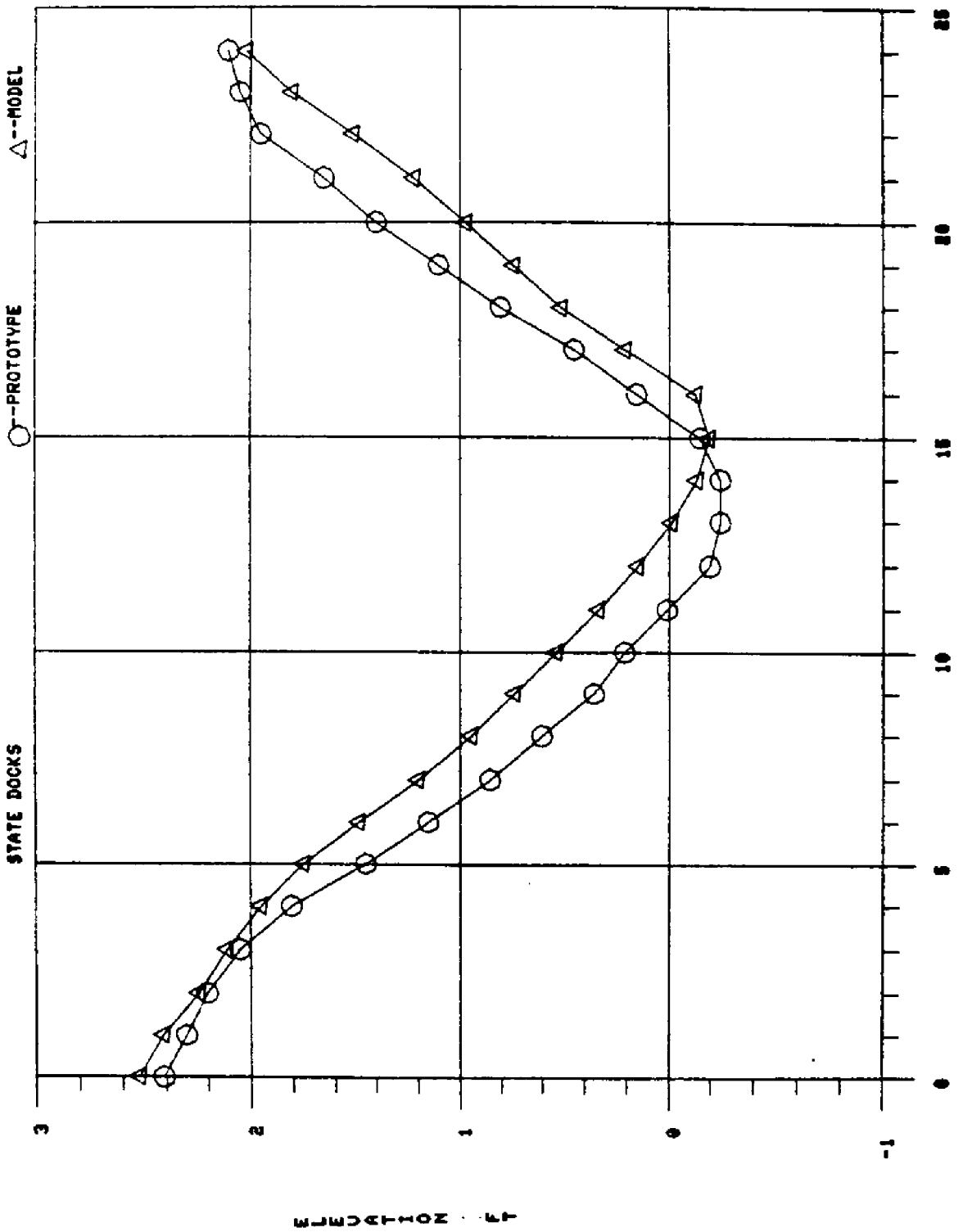

Figure 17. Comparison of Model Tidal Elevation Results at the State Docks with 1972 Prototype Data.

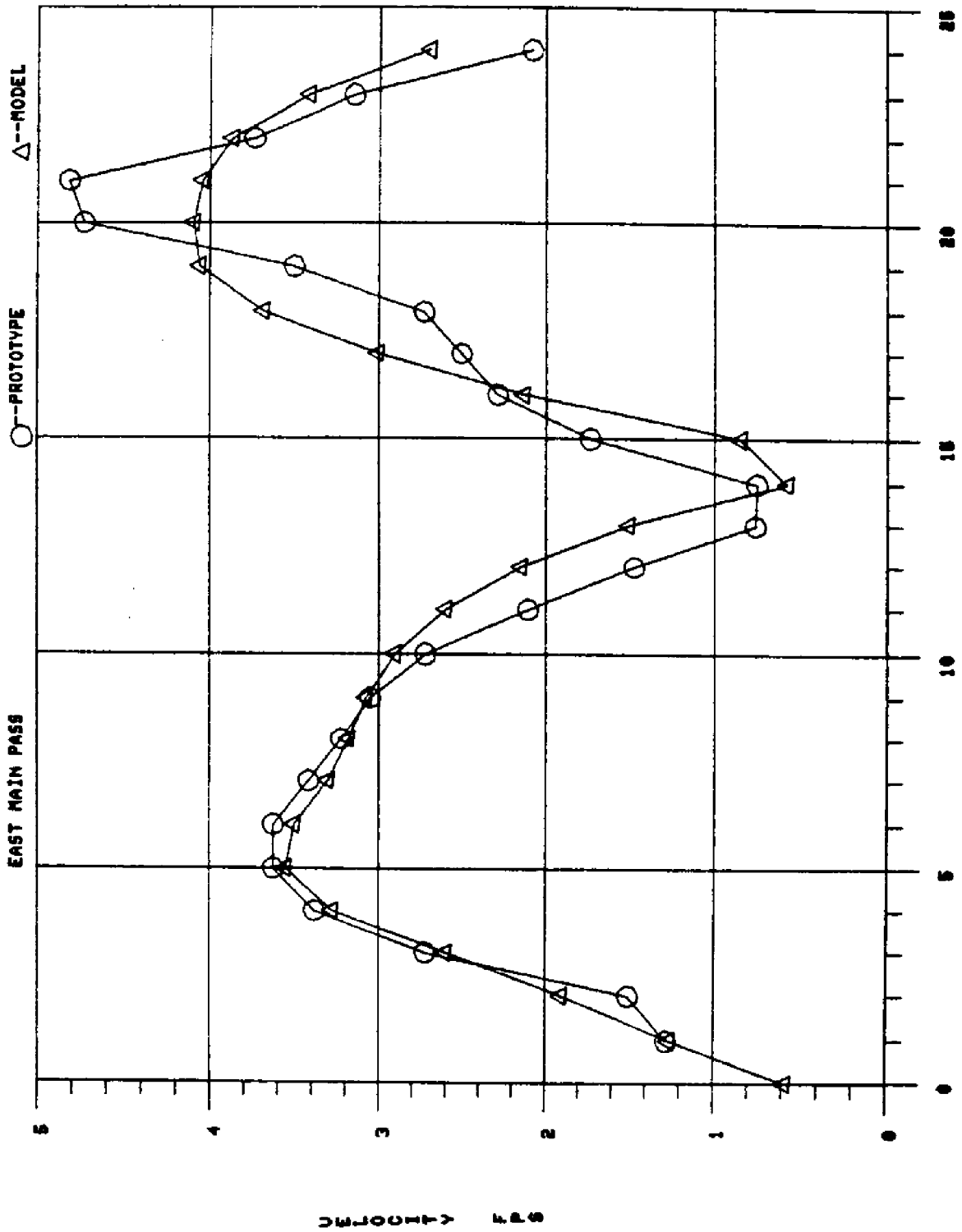

Figure 18. Comparison of Model Velocity Results at East Main Pass with 1972 Prototype Data.

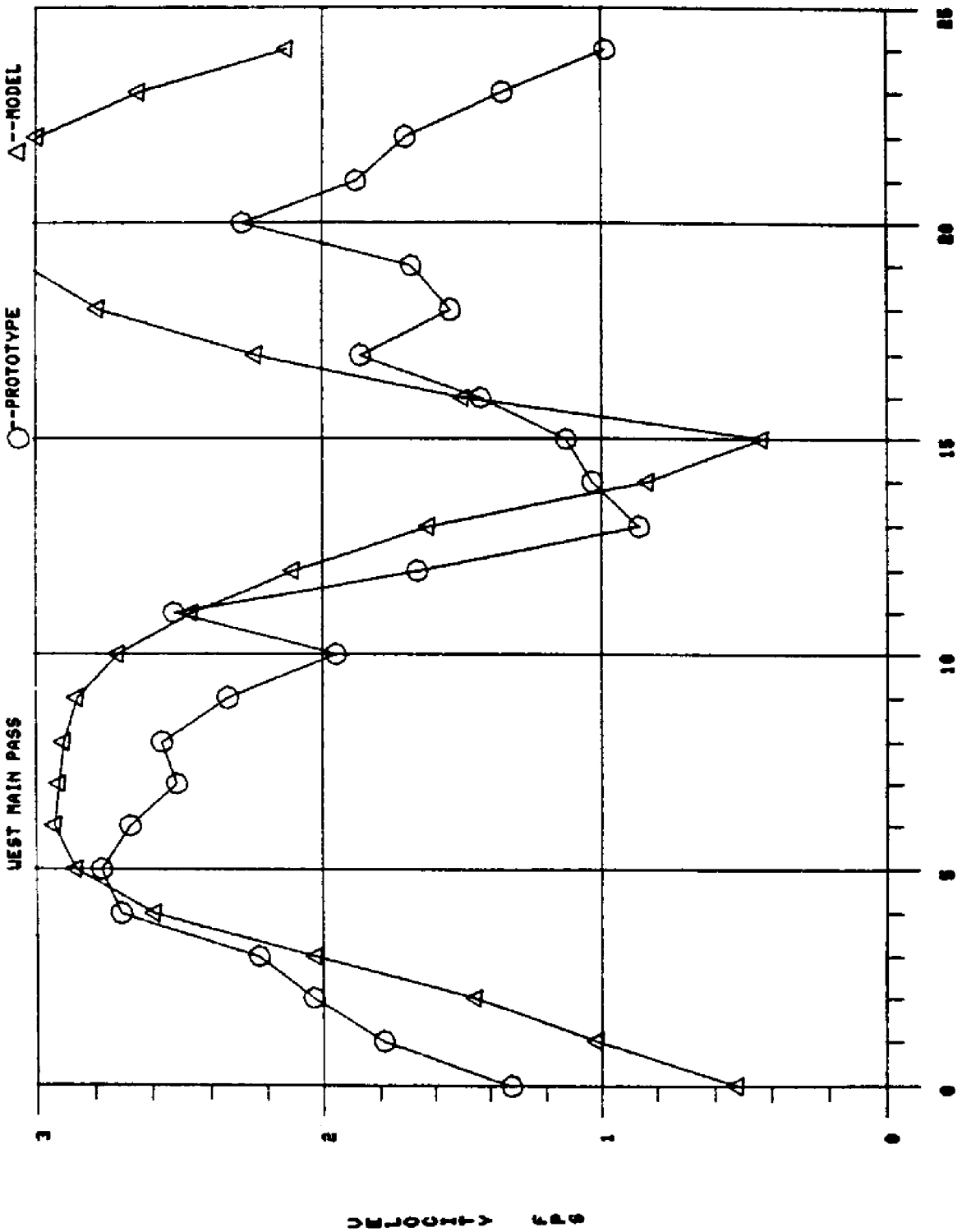

Figure 19. Comparison of Model Velocity Results at West Main Pass with 1972 Prototype Data.

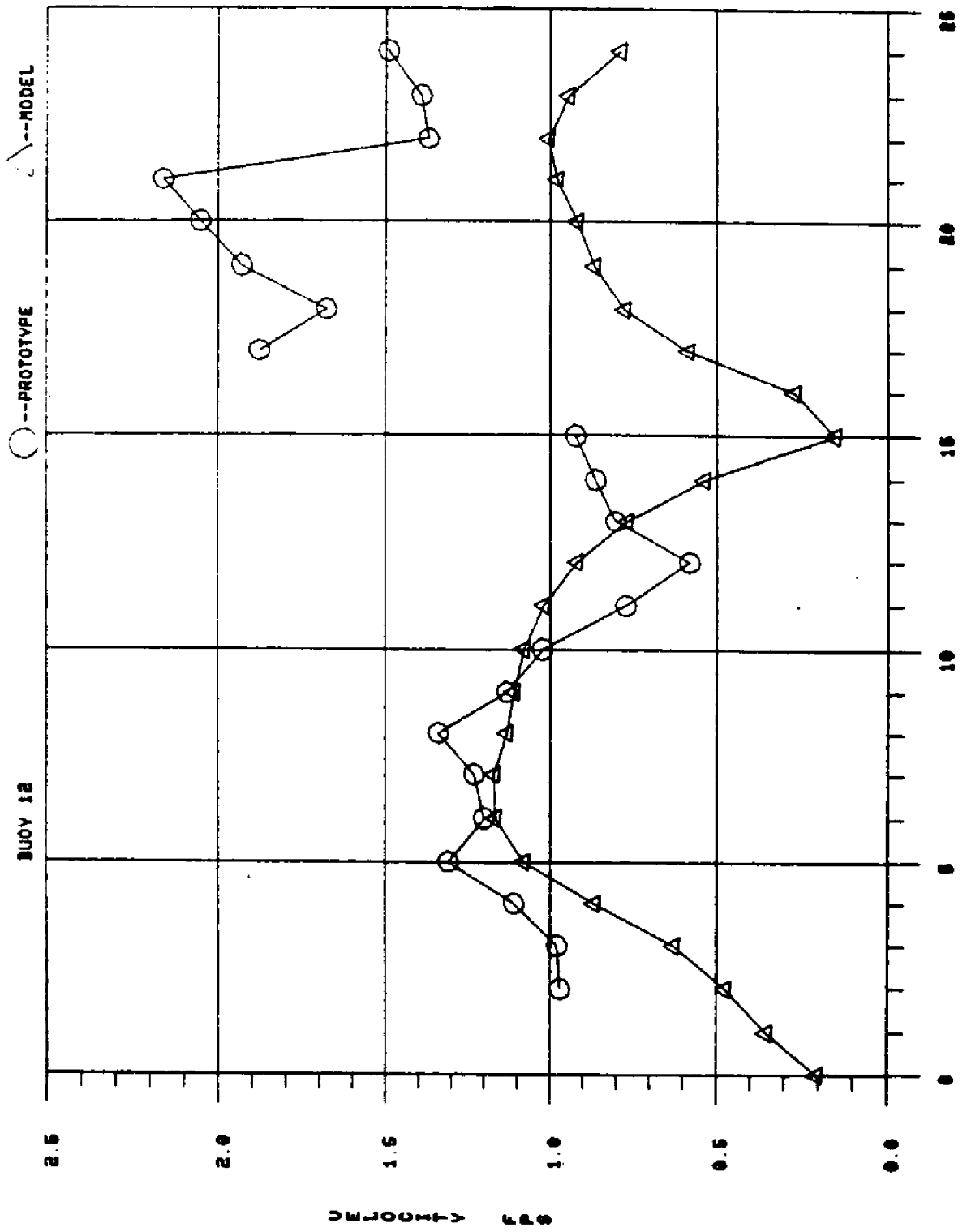

Figure 20. Comparison of Model Velocity Results at Buoy 12 with 1972 Prototype Data.

In general, considering the unknown wind situation during the prototype data collection period, the numerical model calibrates very well to the prototype data.

VERIFICATION

To verify the model it was run with all model parameters (i.e. depths, friction coefficients, etc.) the same as for the 1972 calibration run; only the model boundary conditions were changed to reflect the 1973 prototype conditions.

The 1973 field data were collected over a 25 hour period between 0900 CST June 13 and 1000 CST June 14, 1973. The wind was indicated as being small, however no detailed wind data were available. A constant total river flow of 116,000 cfs was used, split equally between the Mobile and Tensaw Rivers.

There was no Dauphin Island Gulf tide gage data available for the 1973 prototype data set. This complicated the establishment of a gulf tide boundary condition. A modified astronomical tide was used. The Tide Tables[6] provided the prediction of elevations and times of high and low tides. This predicted tide was backed off to the gulf tidal boundary using the free gravity wave speed. This predicted tide was then adjusted slightly to better fit the available prototype data. The results for the verification run are shown in Figures 21 thru 27.

Considering the approximate nature of the gulf tide boundary condition and the unknown wind condition, the model is considered to adequately reproduce the 1973 prototype data. Tidal elevations and velocities indicate that the model is representing the fundamental behavior of the physcial system.

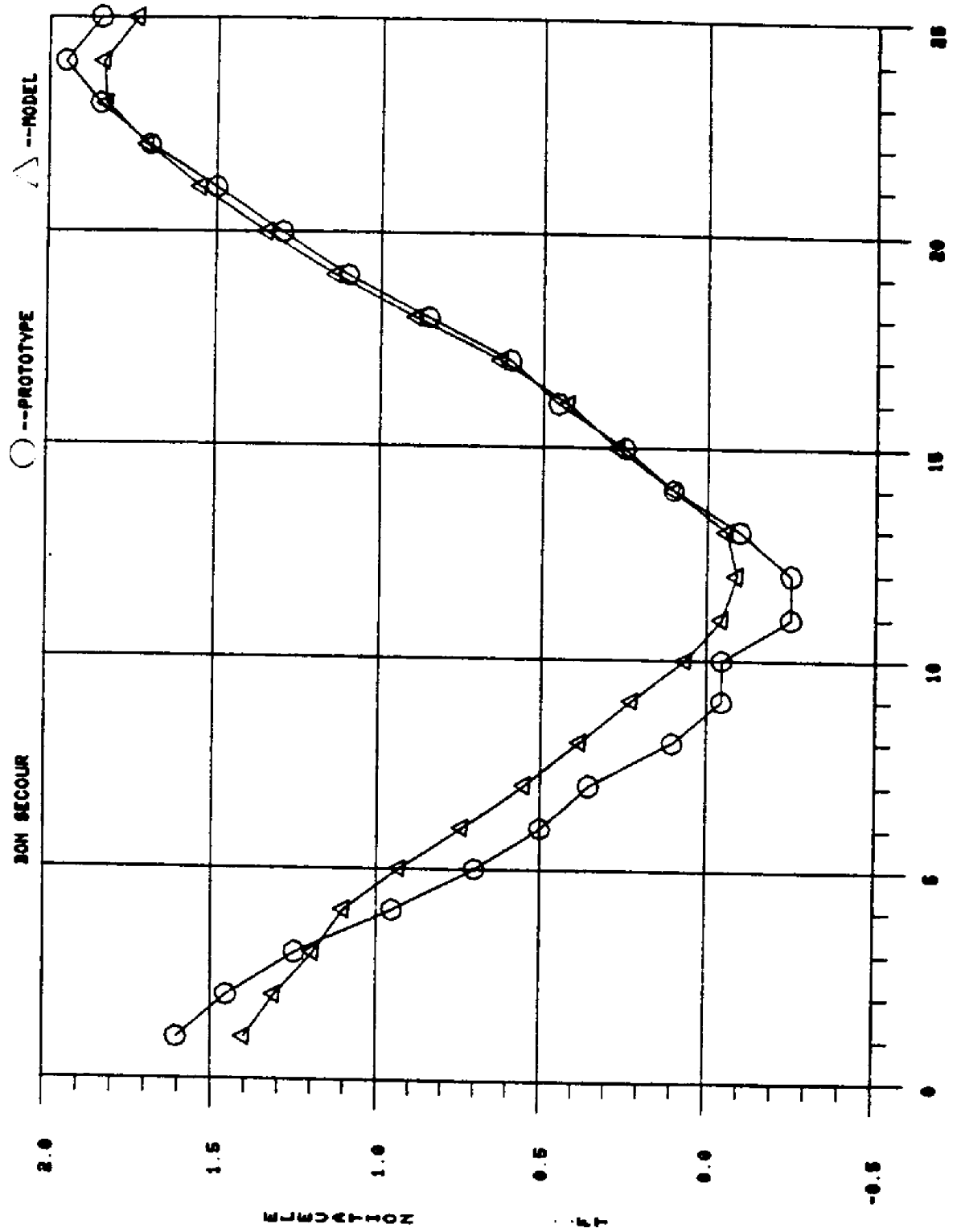

Figure 21. Comparison of Model Tidal Elevation Results at Bon Secour with 1973 Prototype Data.

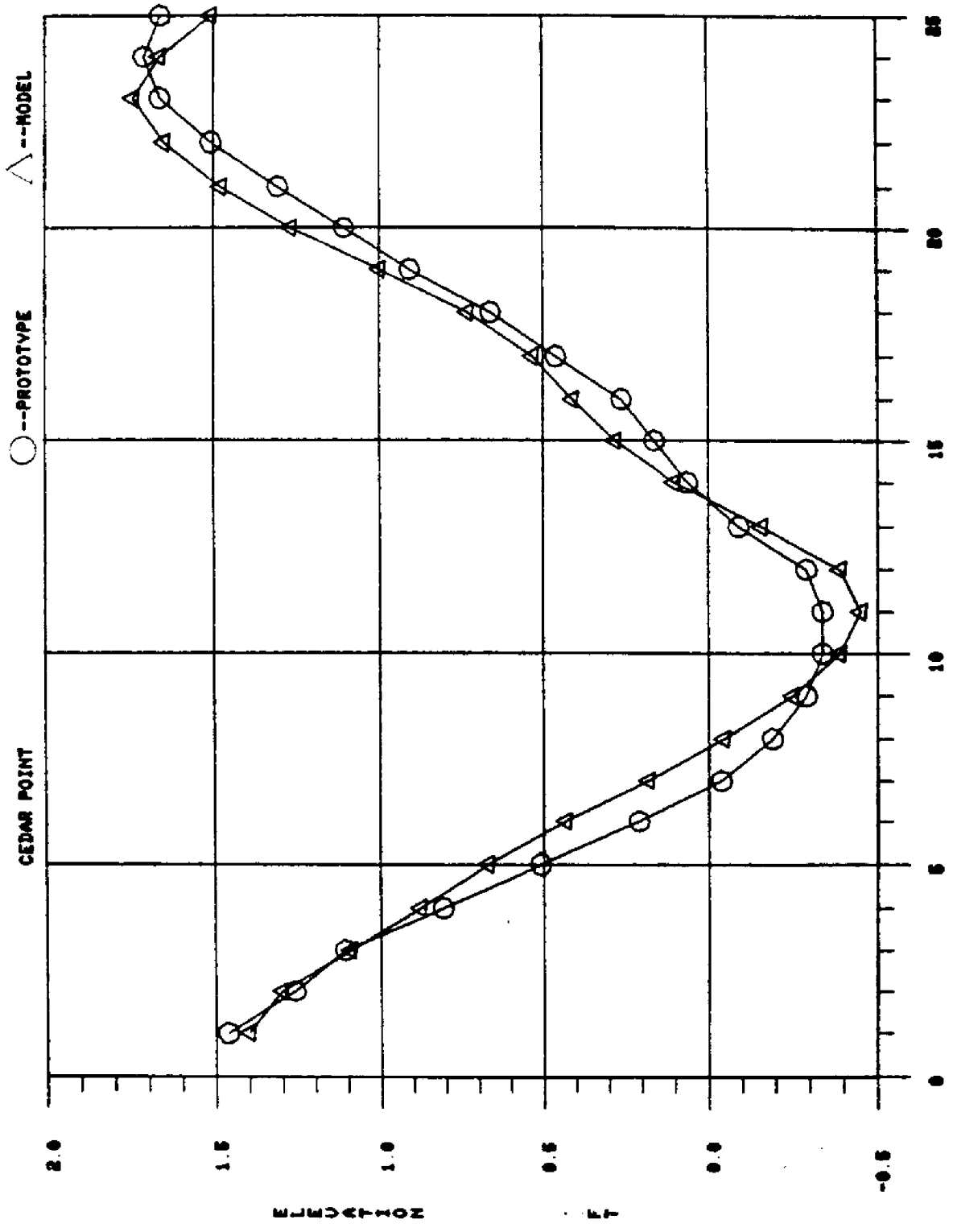

Figure 22. Comparison of Model Tidal Elevation Results at Cedar Point with 1973 Prototype Data.

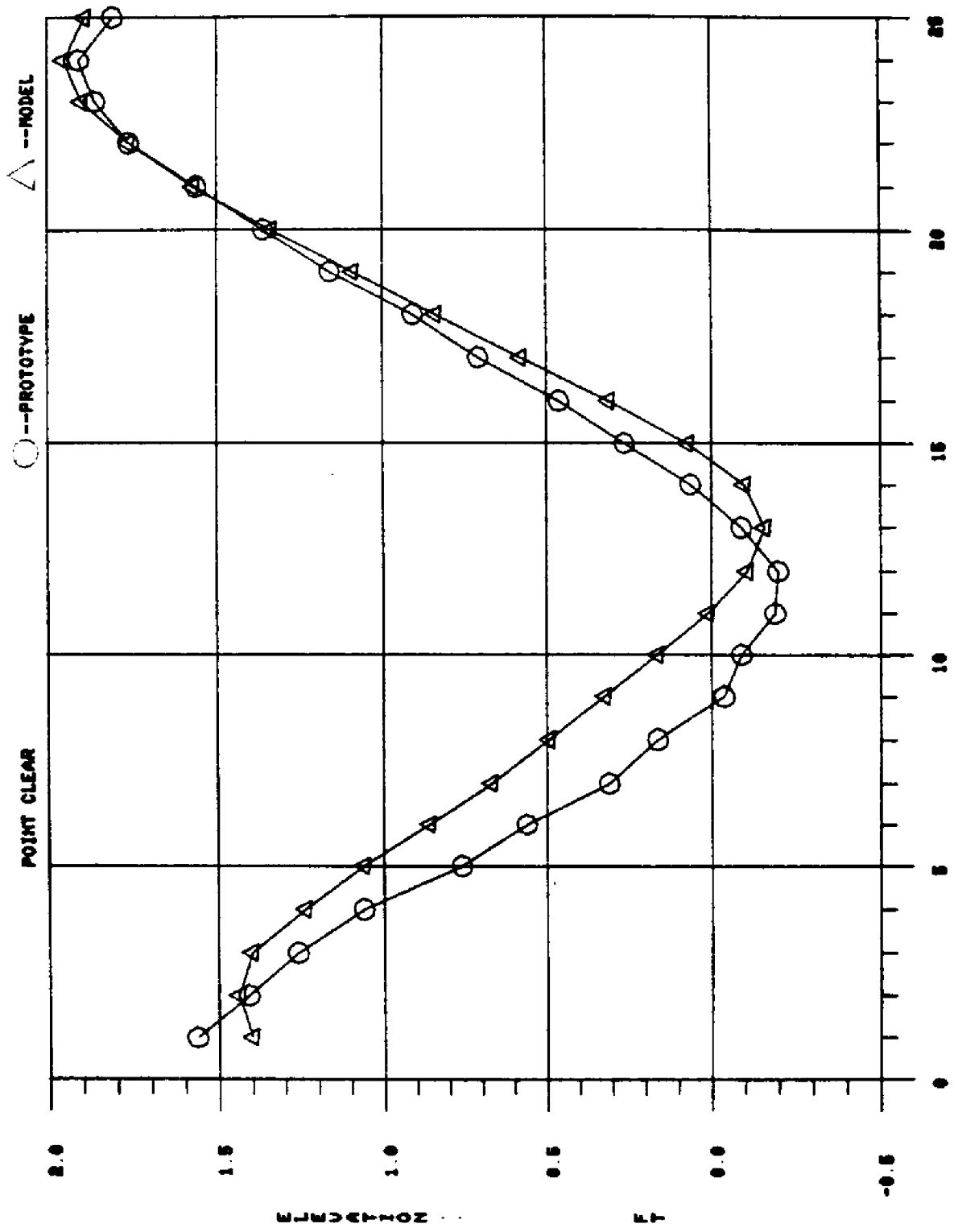

Figure 23. Comparison of Model Tidal Elevation Results at Point Clear with 1973 Prototype Data.

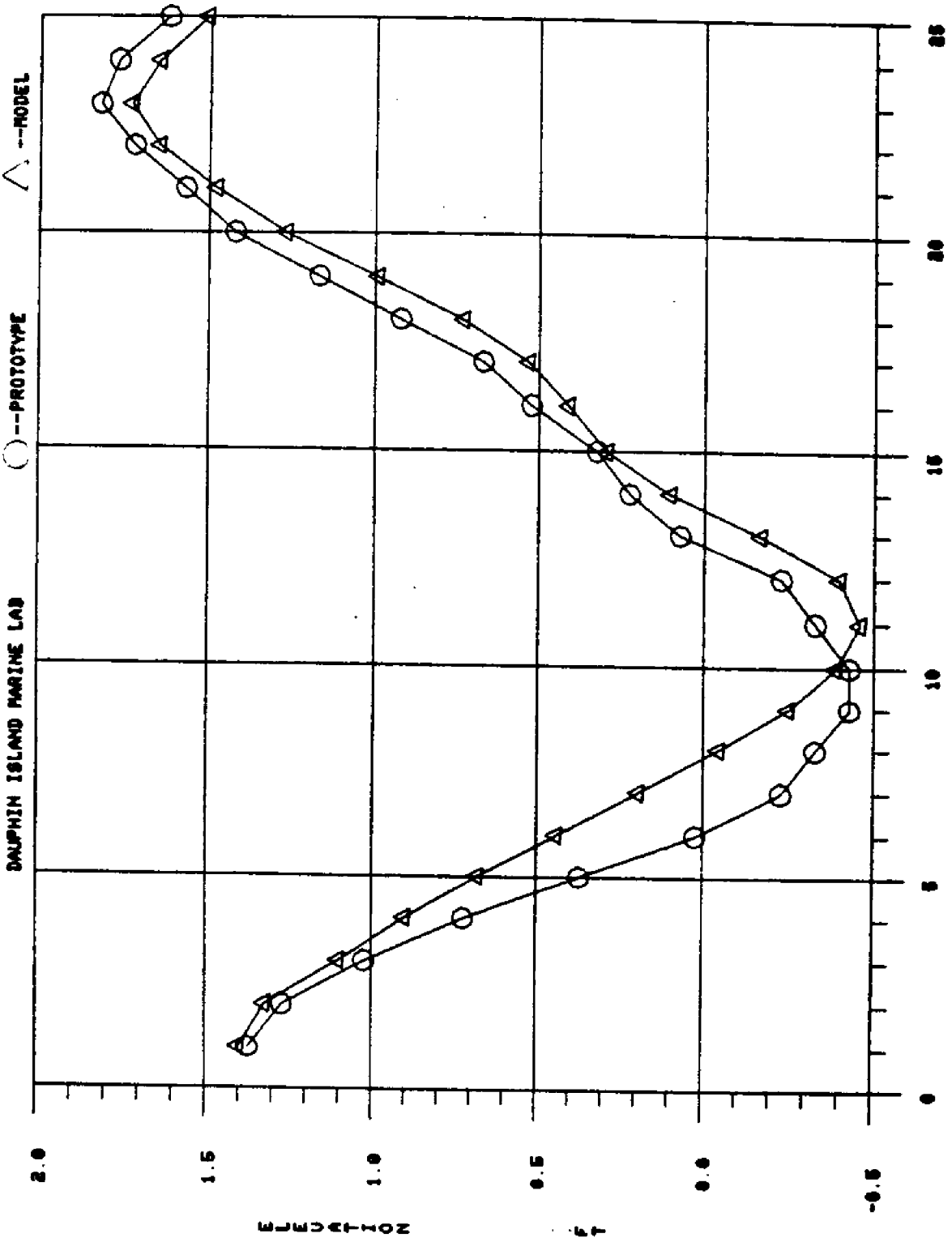

Figure 24. Comparison of Model Tidal Elevation Results at Point Clear with 1973 Prototype Data.

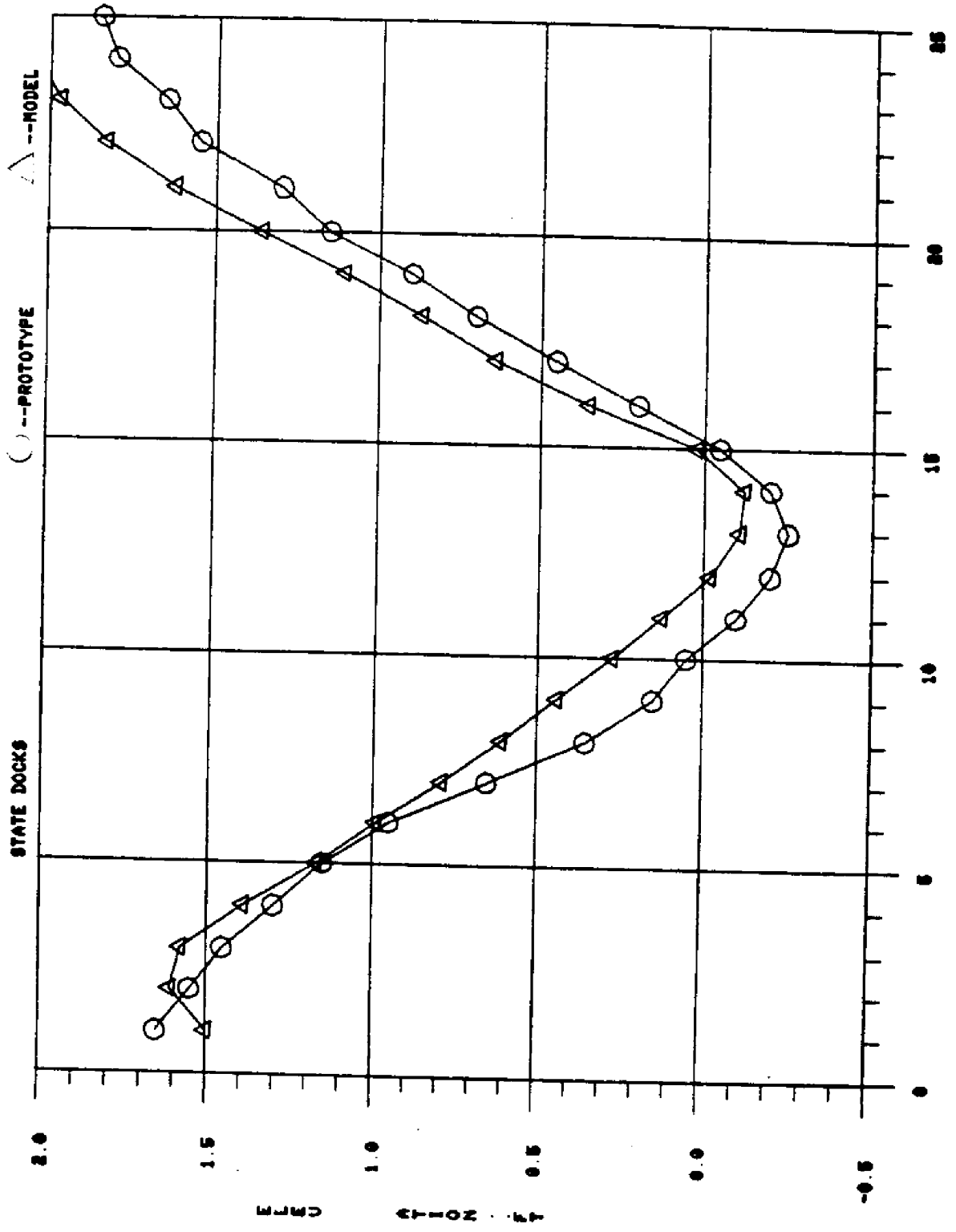

Figure 25. Comparison of Model Tidal Elevation Results at the State Docks with 1973 Prototype Data.

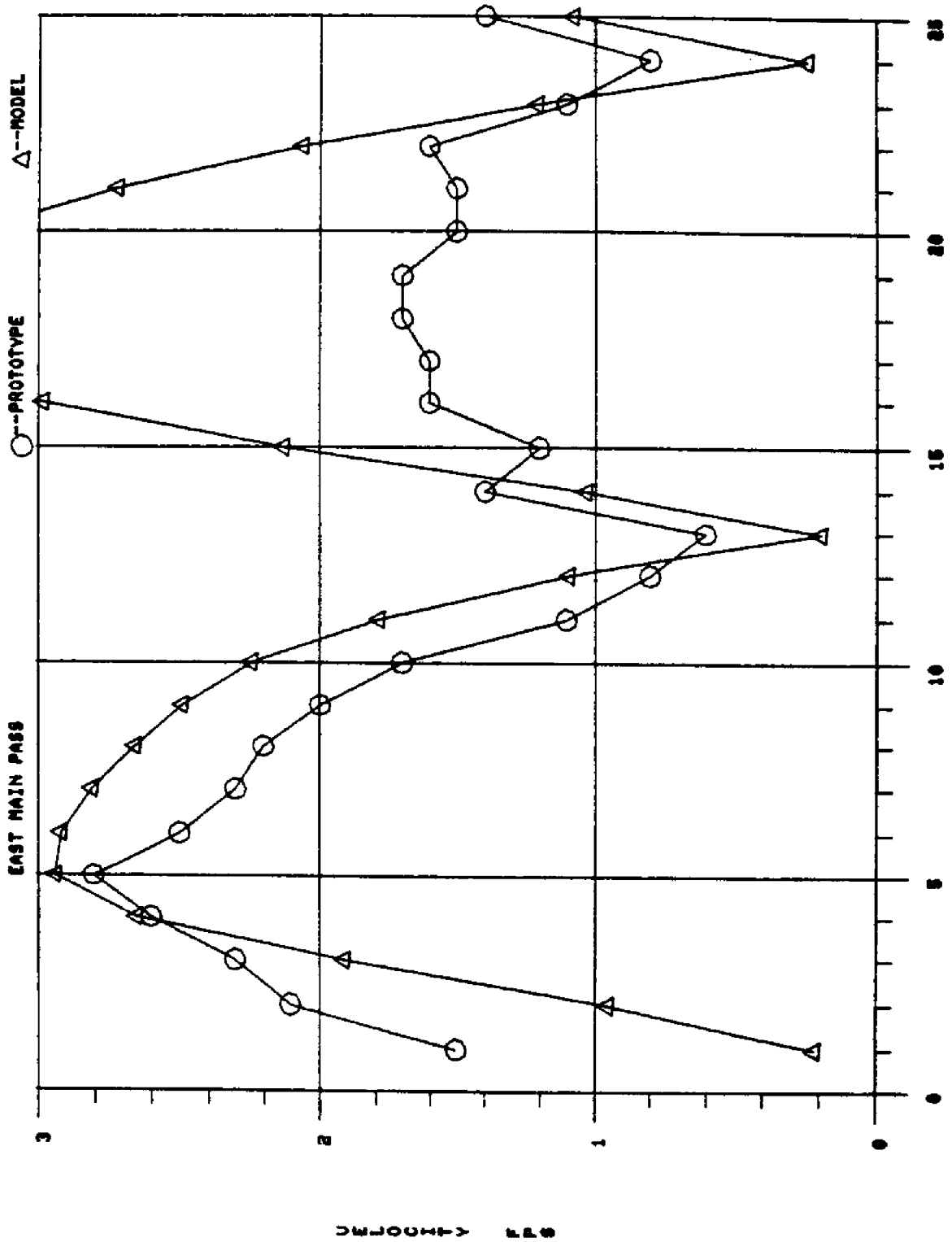

Figure 26. Comparison of Model Velocity Results at East Main Pass with 1973 Prototype Data.

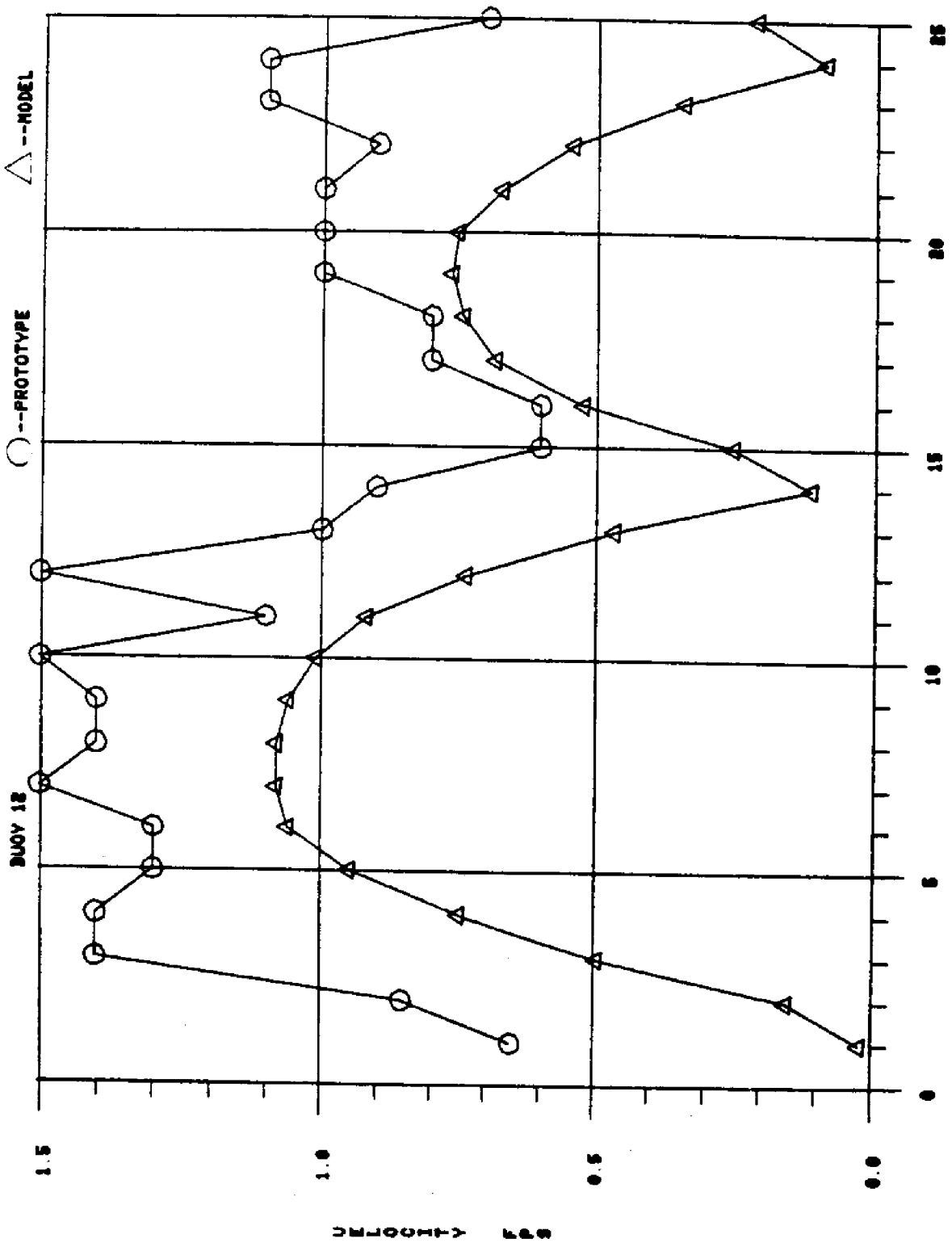

Figure 27. Comparison of Model Velocity Results at Buoy 12 with 1973 Prototype Data.

Overall Calibration/Verification Results

The hydrodynamic model is now considered to be calibrated and verified based upon the available prototype data. As such, the model can be used in a predictive mode to investigate the behavior of the system under different boundary conditions of river inflow, tide, and wind. As long as extreme boundary conditions are avoided the model should approximate the behavior of the system. The model should be more completely calibrated and verified for extremely detailed hydrodynamic investigations; however, it should be capable in its current form to predict overall trends in the system under different boundary conditions.

Some typical circulation patterns for Mobile Bay are shown in Figures 28, 29 and 30 for flood, ebb and slack water tide conditions. In Figure 28 it can be observed that during flood tide conditions some flow comes into Mobile Bay through the main pass and almost immediately passes into East Mississippi Sound through Pass Aux Herons. In Figure 29, during ebb conditions, the flow in the entire main channel is very apparent. Most flow activity near slack water is associated with the river inflow into the upper end of the bay and some activity in the main pass.

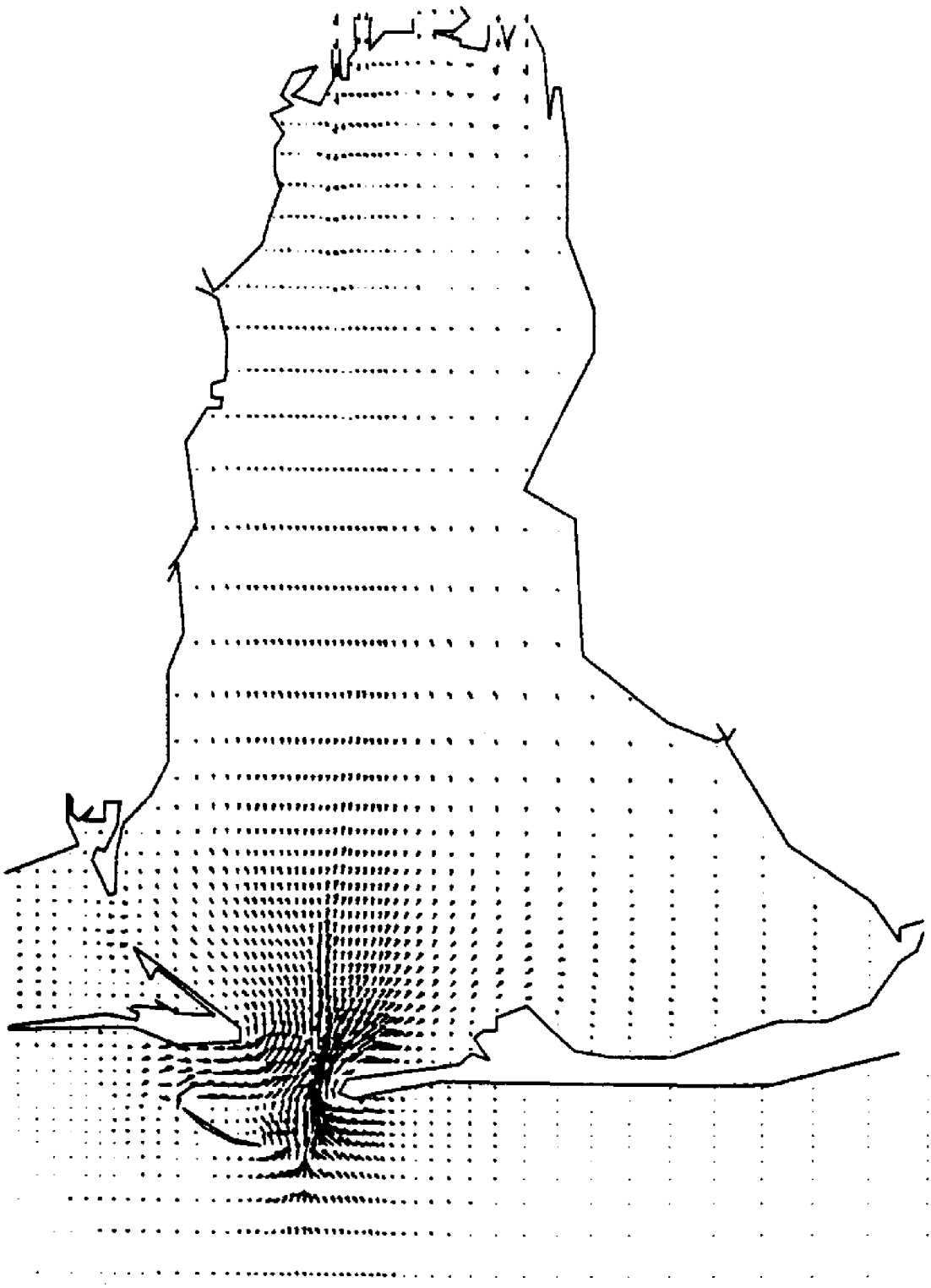

Figure 28. Typical Circulation Pattern in Mobile Bay Near Maximum Flood Condition.

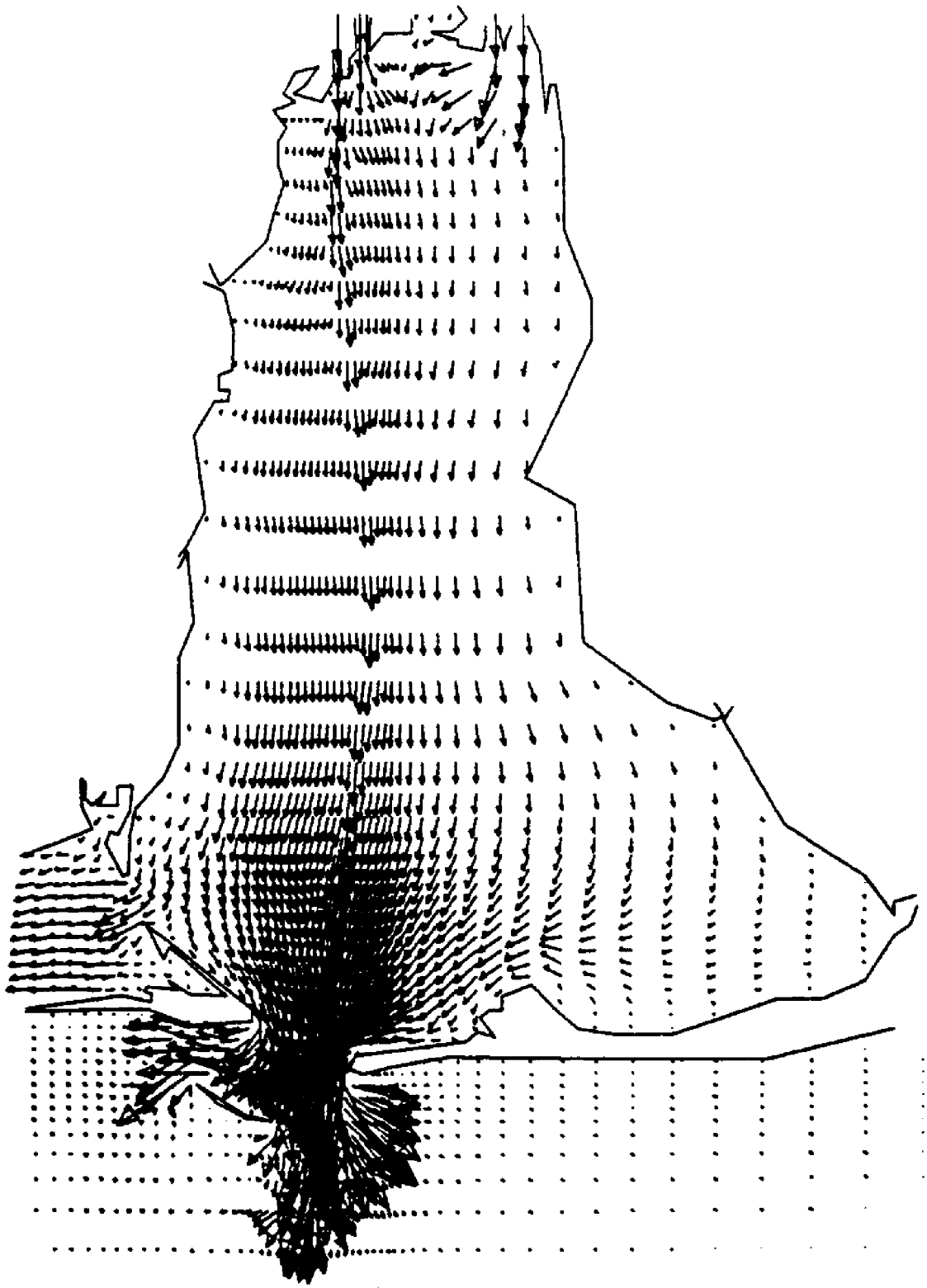

Figure 29. Typical Circulation Pattern in Mobile Bay Near Maximum Ebb Condition.

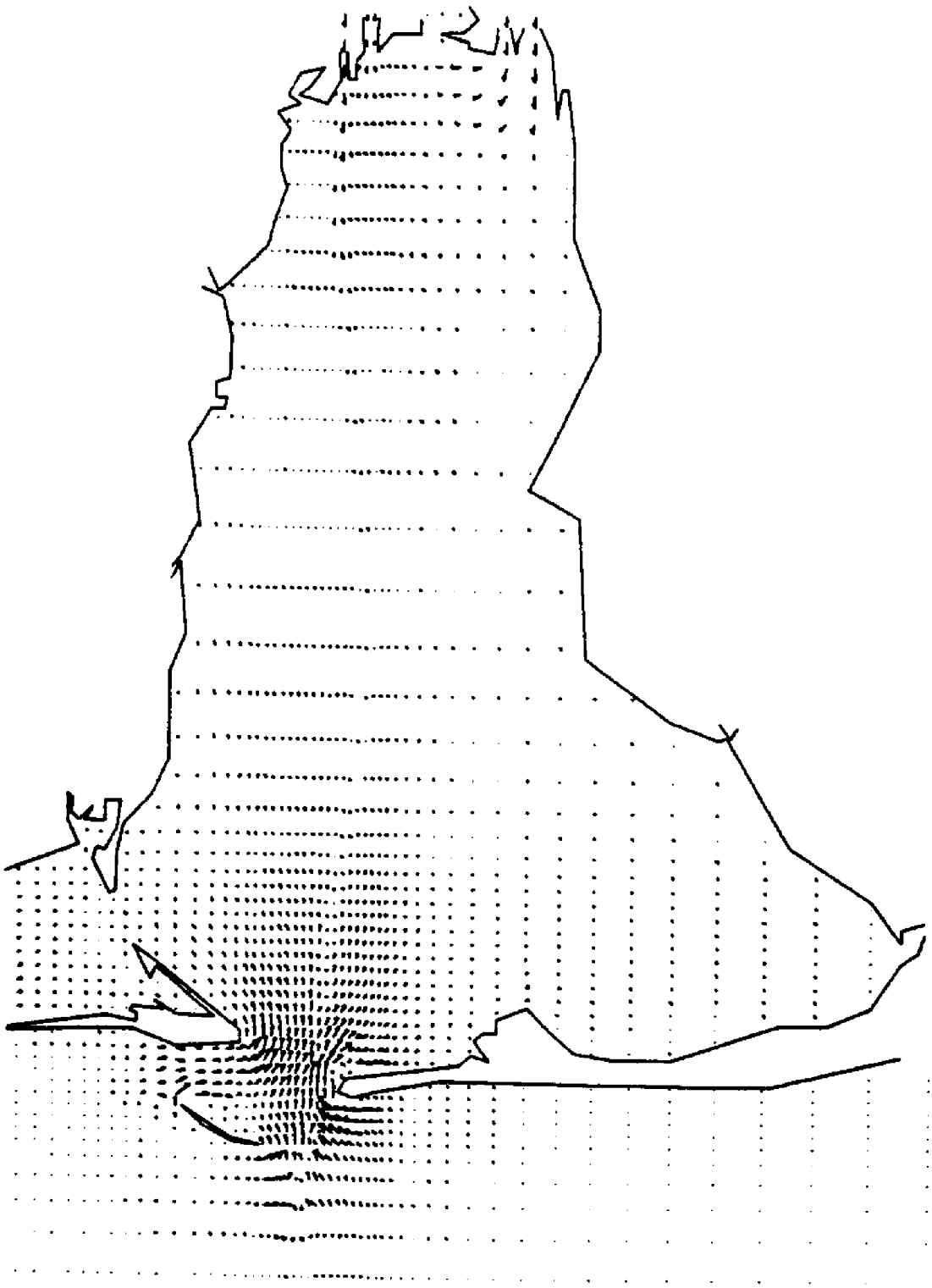

Figure 30. Typical Circulation Pattern in Mobile Bay Near Slack Water Tide Condition.

IX. BASIC CONCEPTS OF SEDIMENT TRANSPORT

Sediment transport in an estuary is a problem which has interested scientists and engineers for a long time. An estuary is subjected to tidal, wind and freshwater flow boundary conditions which result in hydrodynamics and sedimentary patterns which are not completely understood because of their complex nature. Basically the transport processes are composed of several components; erosion, entrainment, suspension, transportation, and deposition. Each of these components involve variable parameters which may be difficult to establish.

Relations between erosion, transportation and deposition velocities and the grain size of sediments have been the subject of many investigations.[12,13] The "critical erosion velocity" is the minimum current velocity at which sediment of a particular size begins to move. The movement stops at a flow velocity called the "deposition velocity." The deposition velocity is generally about two-thirds of the erosion velocity magnitude. The difference in the velocity between erosion and deposition is of great importance for the behavior of suspended matter. For smaller diameter particles, cohesiveness and duration of consolidation become extremely important in establishing the critical erosion velocity. Recently deposited, very loose and unconsolidated fine-grained matter may easily be carried away by a small current velocity. When the material has been deposited for a longer time, it gradually loses water, hardens and becomes increasingly difficult to erode.

In tidal inlets and larger channels the tidal currents may become very large. The strength of the currents decreases rapidly toward the tidal flats bordering these channels. Near the coast the currents can be small or there may be significant current parallel to the shoreline.

The decrease is less rapid along the axis of a channel. Generally high current velocities are accompanied by strong turbulence and vertical density differences are obliterated.

Tidal currents are generally sufficiently strong and turbulent to set in motion considerable amounts of suspended matter. The quantities and grain sizes of the material at a fixed point fluctuate with current velocity. In any detailed study of the variations of suspended matter over a tidal cycle, the behavior of "sand" and fine grained suspended matter or "silt" must be considered separately due to their different reactions to tidal currents.

Fine grained suspended matter reacts with a certain inertia or lag time to changes of current velocity. This is explained by the low setting velocities of the small particles. This lag effect has been used to explain why, proceeding landward in a tidal flat area, the grains in the bottom sediment gradually become smaller. The decrease of grain size on the bottom is primarily, a result of the reduced average and maximum velocities from the open sea toward the coast. It is evident that in and near the inlets, the bottom will consist of coarse sand because fine sand and silt are transported out by the strong currents. Near the coast and on tidal flats where currents are weaker, fine grained matter prevails; the coarse sand cannot reach these places and the fine material can.

The strong currents prevailing during spring tides will generally bring more material into suspension than the neap tide currents. During the neap tide period; material may remain on the bottom for longer periods and more consolidation will occur. In an estuary where strong freshwater inflows exist the sediment transport is strongly dependent

on the freshwater flow rate. Not only is the inflow bringing sediment into the estuary but the high currents and turbulence levels entrain bottom sediment into the flow.

Coarse grained material (sand) is transported with greater difficulty than unconsolidated fine-grained matter, and is at the same time transported closer to the bottom, partially as bed load. Besides strong currents, wave action may also be required to set sand into motion. As a result important sand transport may occur primarily in periods of strong winds. The settling velocity for the larger particles is too fast for a significant lag time effect to be present.

Sediments in Mobile Bay include all sizes of material from relatively clean sand to relatively pure clay with various admixtures of sand, silt and clay. A distribution presented by Ryan[14] is shown in Figure 31. The sand in the upper reaches of the bay and around the perimeter is indicative of relatively strong currents and shallow waters in these areas. The large areas of clay depositions indicates areas of relatively low energy levels characteristic of eddy currents which do not feel the general tidal current variations. The areas of mixed sediment size are taken to be areas of variable (but not extremely large) currents. The coarser sediment mixtures indicate stronger currents in that portion of the Bay. Sediment transport in Mobile Bay therefore involves materials with a wide range of sizes. The varying tidal, river and wind condition combine with the range of sediment sizes available to produce a complex sediment transport problem not readily amenable to analysis.

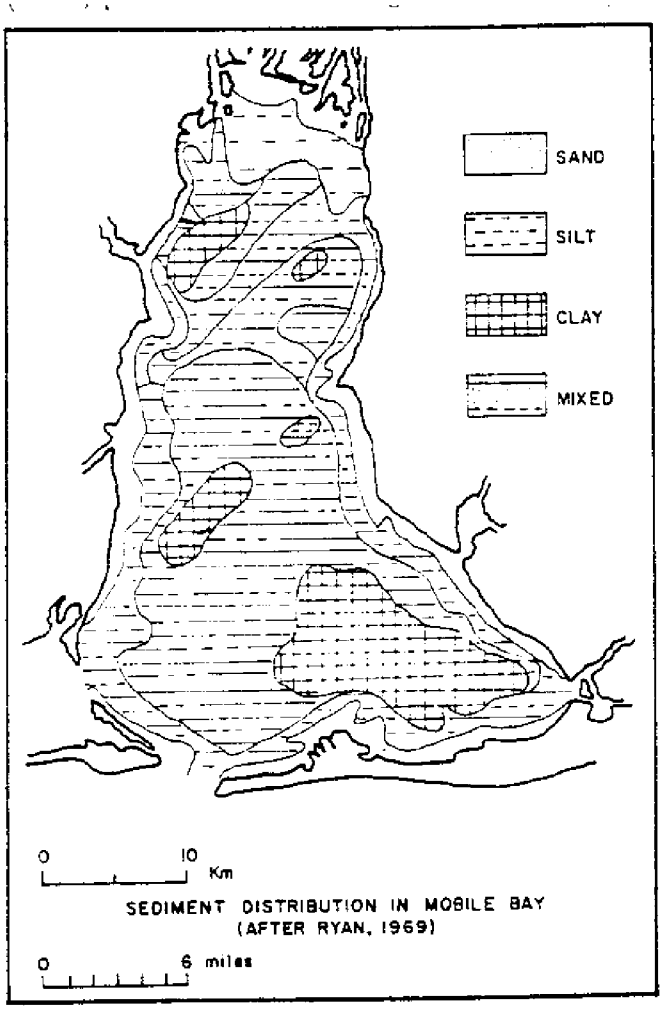

Figure 31. Sediment Distribution on Mobile Bay

X. MODEL APPLICATIONS AND RESULTS

As indicated previously, the sediment transport process is complex and not readily amenable to direct quantitative analysis. As a first approximation, an indirect, qualitative approach is taken to the problem. Sediment transport in the Bay certainly depends on the bay hydrodynamics. It can further be reasoned that since a wide spectrum of particle sizes are available in the sediment, sediment movement should be related in some manner with net volumetric flows over some significant time interval. In this analysis sediment transport from short period wave action is not considered since the hydrodynamic models are not capable of simulating this type event. The model can simulate tidal action, river inflows and relatively steady state wind conditions and predict their effects upon bay hydrodynamics and thus indirectly indicate qualitative information about sediment transport.

In particular possible asymmetric spreading of sediment from the channel aprons will be investigated by considering net cross-channel flows over a representative tidal cycle. The sediment transport will then be assumed to be related in some manner to the net flows. Hydrodynamic energy levels will also be investigated to determine the tendency for sediment to be deposited in a given area of the bay.

A representative 24 hour tide for Mobile Bay is shown in Figure 32. This tide is considered to repeat itself in the model applications. This tide was applied to the partially calibrated and verified hydrodynamic model of Mobile Bay. The main channel representation in the model for the central portion of the bay is shown in Figure 33.

The hydrodynamic model was initially run with a small river inflow (63,5000 cfs) and no wind. The model was run for 1½ complete

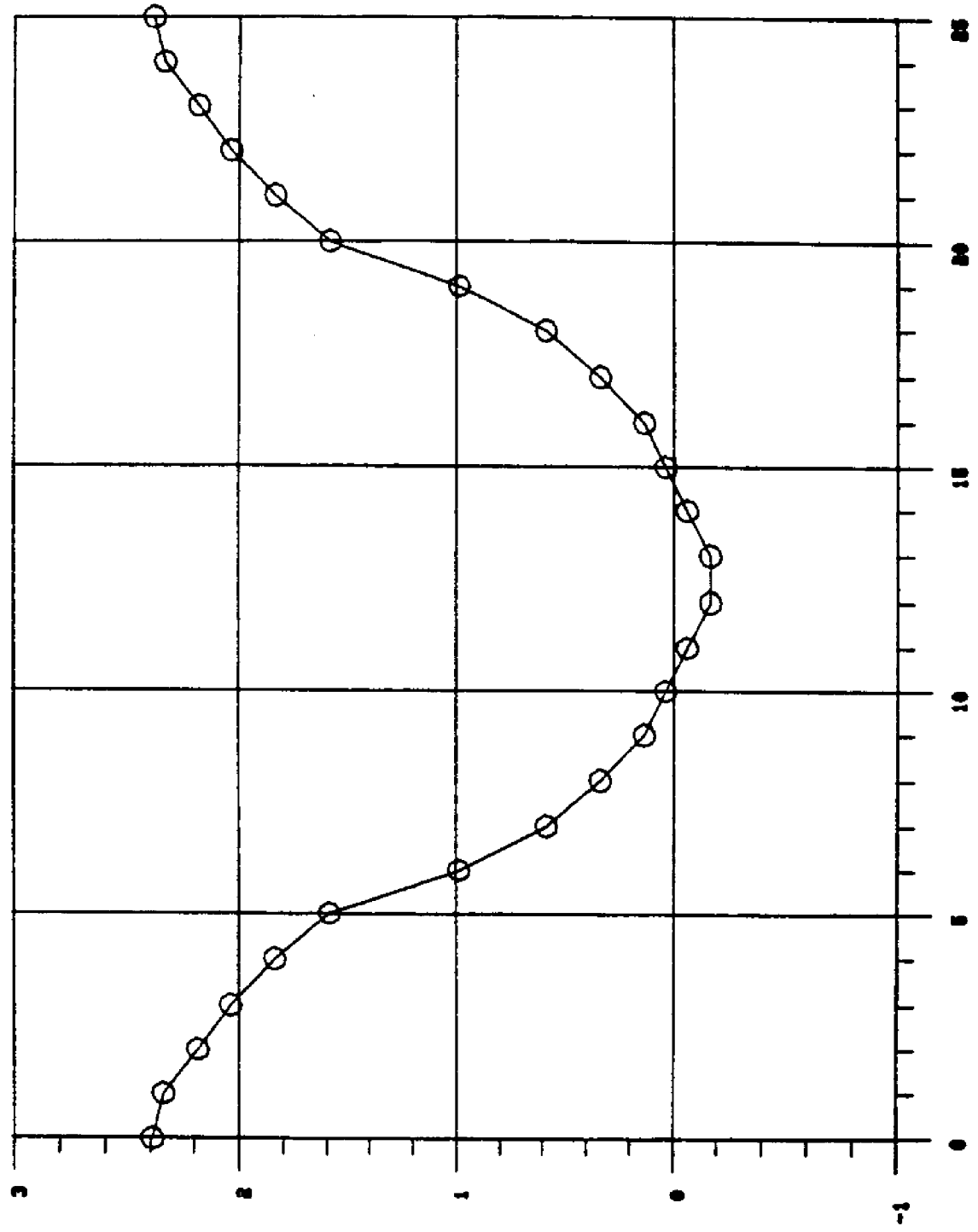

Figure 32. Representative Tide Used in Net Cross-Channel Flow Applications of Hydrodynamic Model.

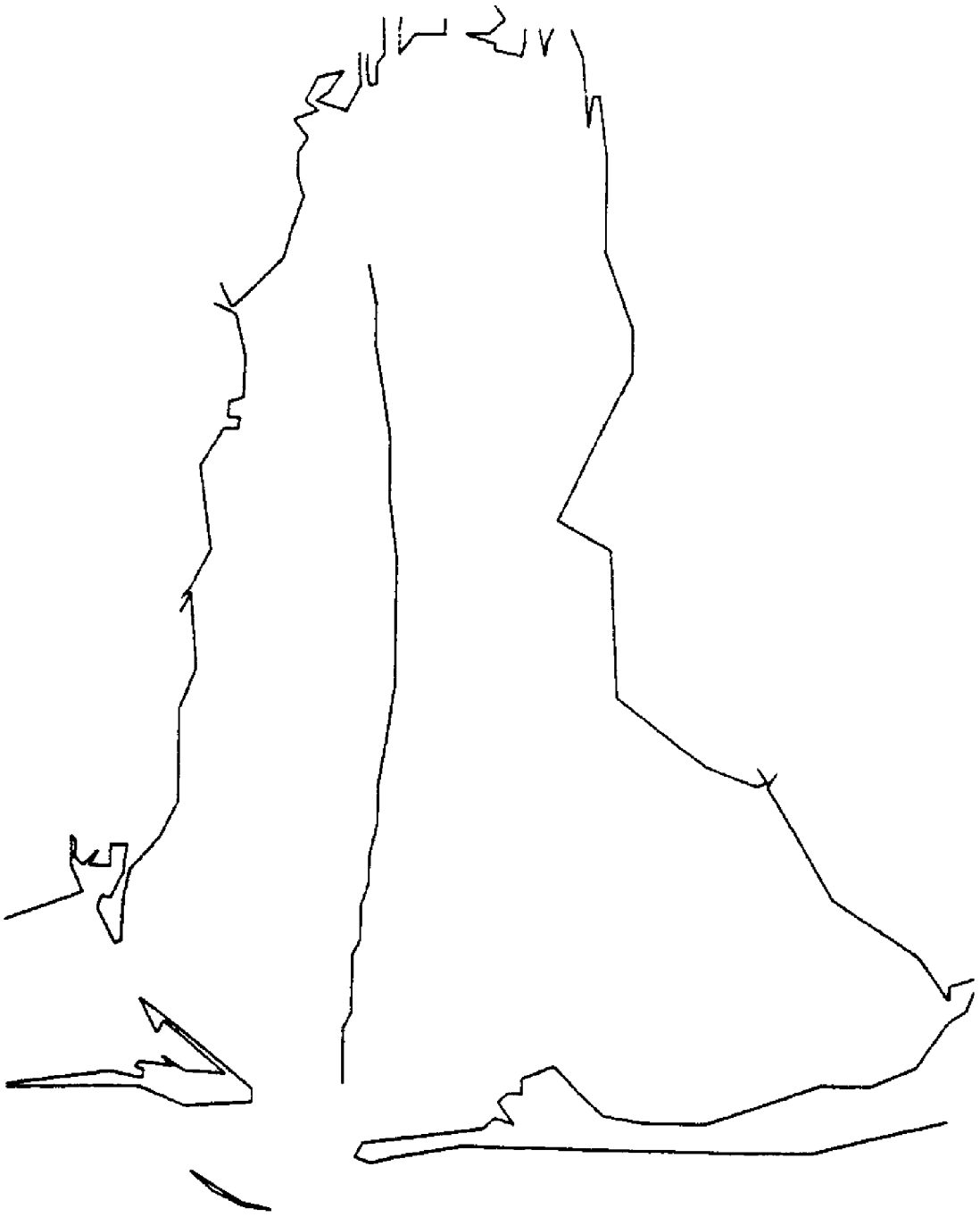

Figure 33. Representation of the Main Channel in Mobile Bay.

tidal cycles with the net flows across each cell of the channel calculated after the last complete tidal cycle. The actual magnitudes of the net flows are not directly related to sediment movement so the values were normalized by dividing by the largest net flow for any channel cell. The resulting normalized values were plotted in Figure 34, on a representation of Mobile Bay and the ship channel. The arrows indicate the direction and relative magnitude of net cross-channel flows for each finite difference cell making up the central section of the ship channel. These results are interpreted as a tendency for sediment transport in the direction indicated by the arrows.

The no wind application of the model indicates relatively small net flows across the channel over most of its length. The basic flow in the Bay is north-south along the bay's length rather than east-west across the bay's width. In the lower bay some larger east to west net flows are observed.

To examine the effect of wind magnitude upon net cross-channel flows, various wind magnitudes were used as boundary conditions in the model. Figure 35 indicates results from a model application with a 20 mph wind from the south-west. The net cross-channel flow pattern is observed to have changed. Generally there is an east to west net flow in the upper bay and an west to east movement in the lower bay. Figures 36 and 37 indicate similar results for winds from southwest winds of 40 mph and 60 mph magnitude. The normalized net cross-channel flow patterns are observed to be almost identical for 20 mph, 40 mph, and 60 mph.

To examine the effect of wind direction on net cross-channel flows, a 20 mph wind from the southeast, northeast and northwest was applied to the model. These applications together with the prior 20 mph south-

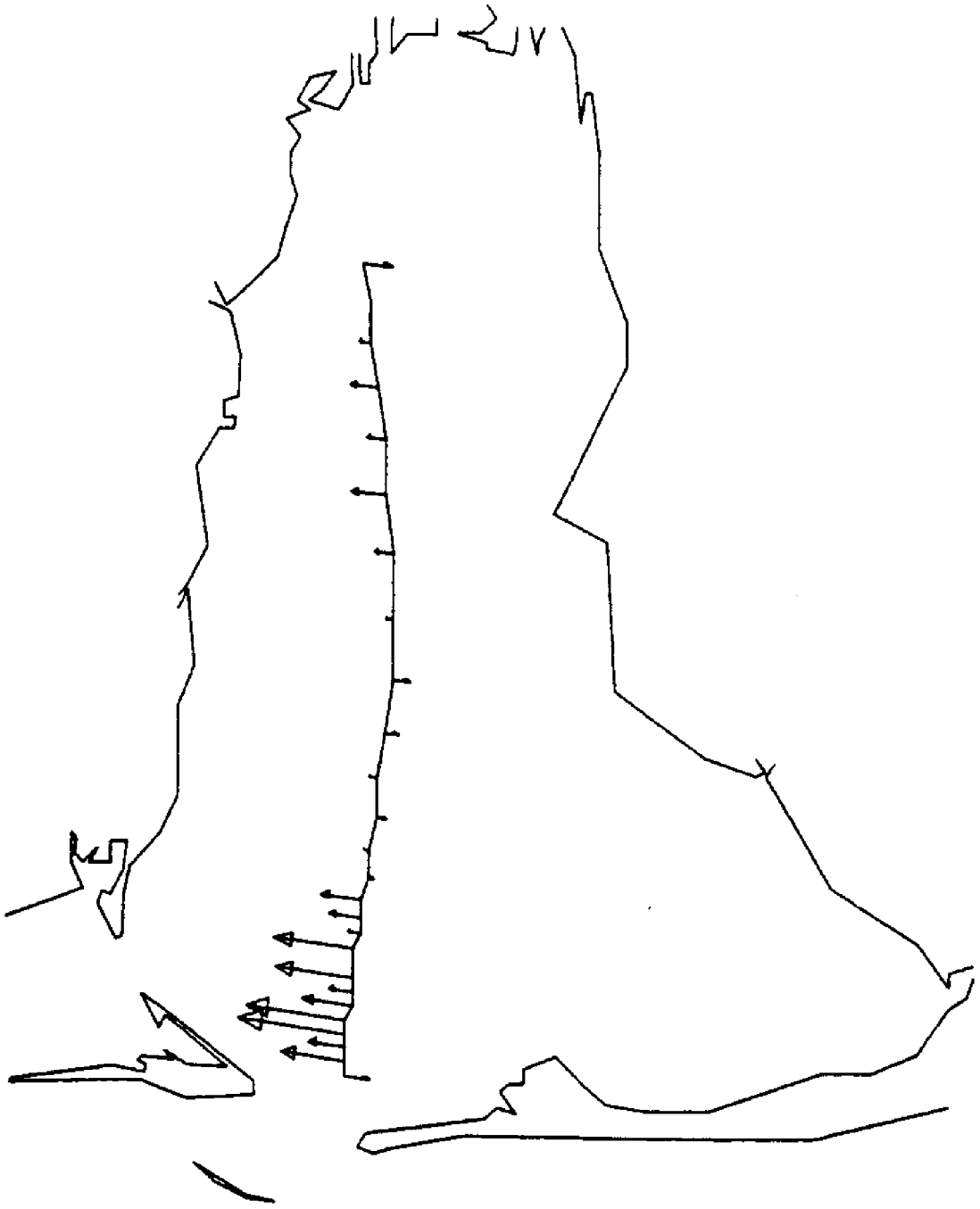

Figure 34. Normalized Net Cross-Channel Flows Over a Tidal Cycle With No Wind and a Relatively Small River Flow Rate.

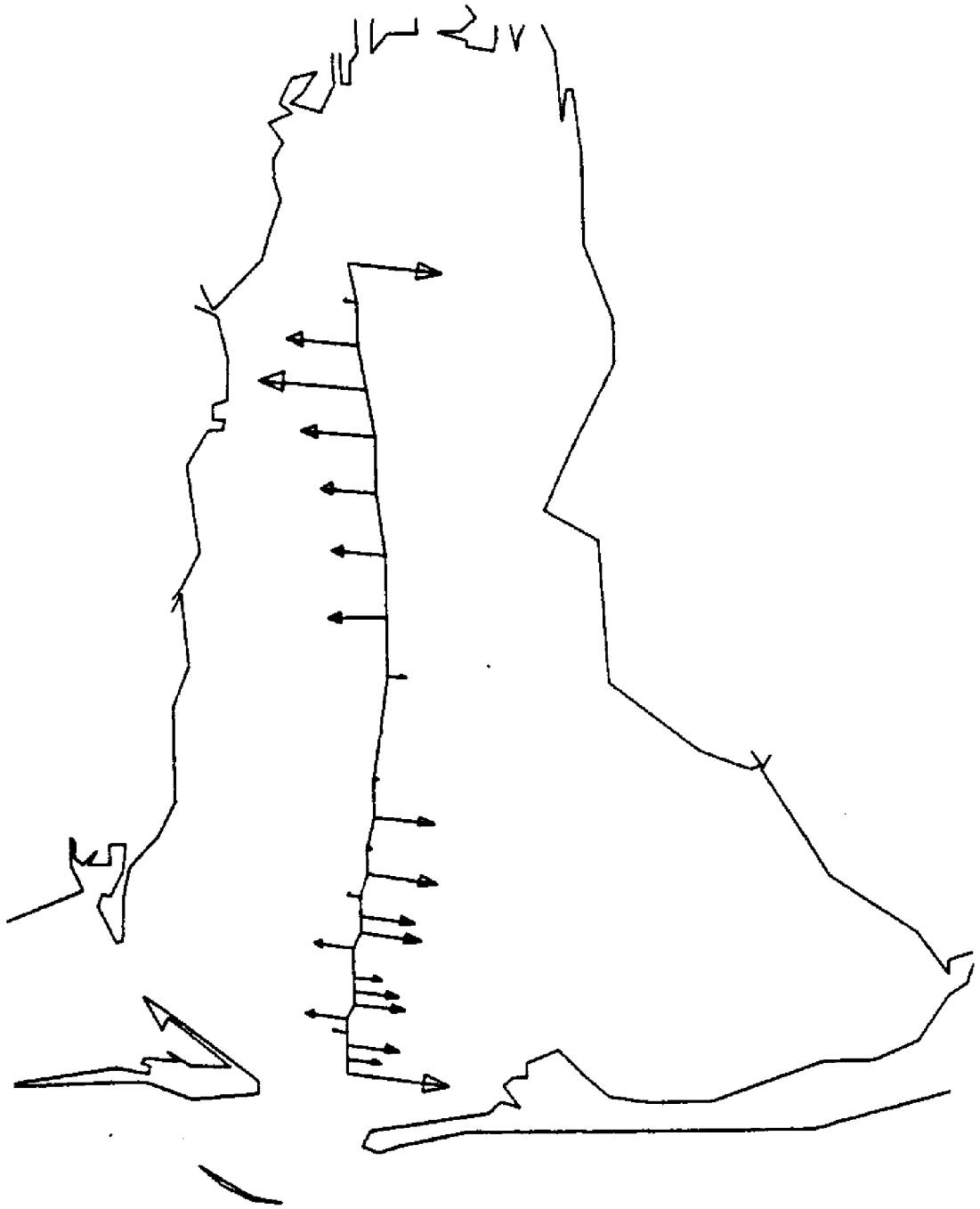

Figure 35. Normalized Net Cross-Channel Flows Over a Tidal Cycle with a 20 MPH Wind From the SW and a Relatively Small River Flow Rate.

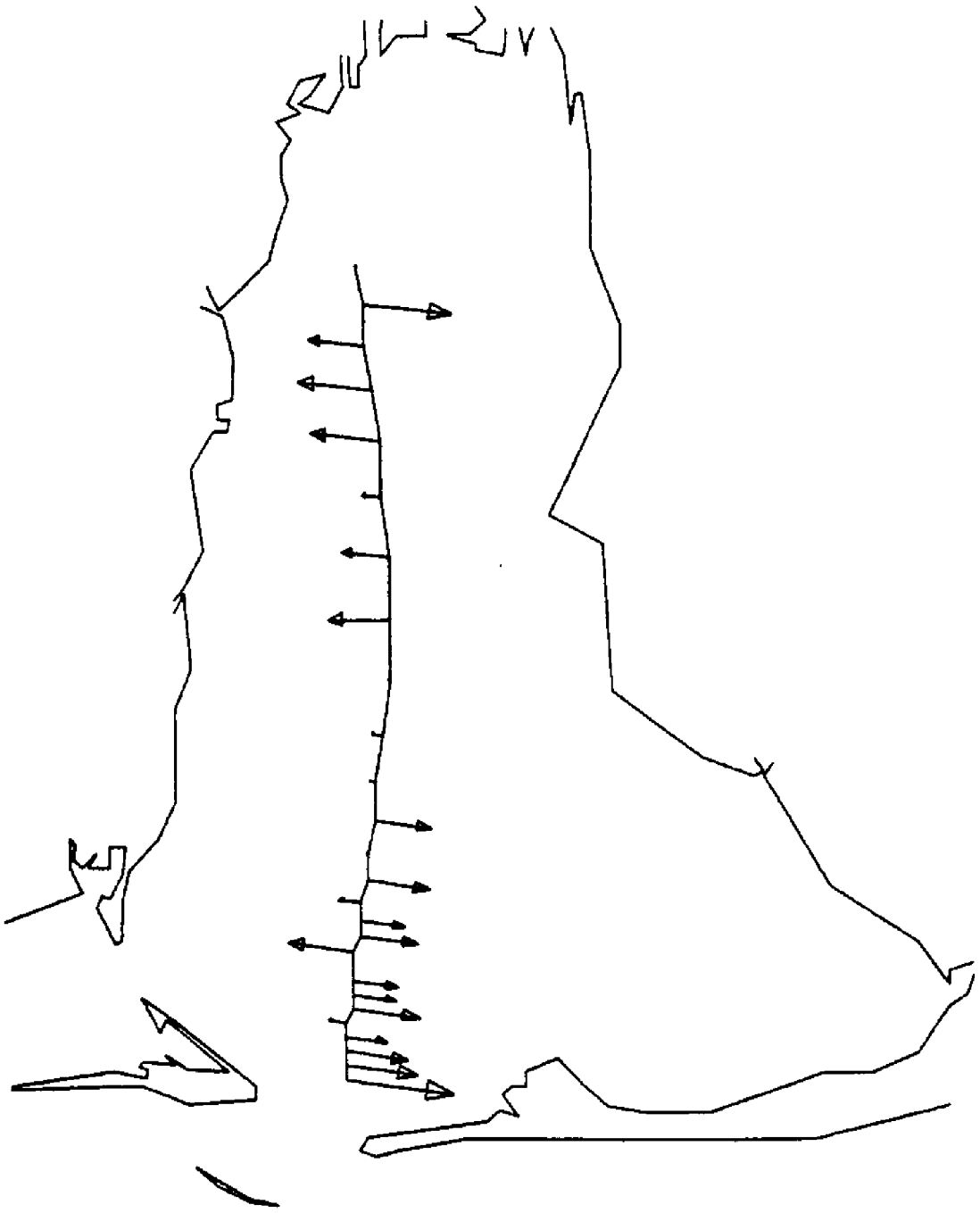

Figure 36. Normalized Net Cross-Channel Flows Over a Tidal Cycle With a 40 MPH Wind From the SW and a Relatively Small River Flow Rate.

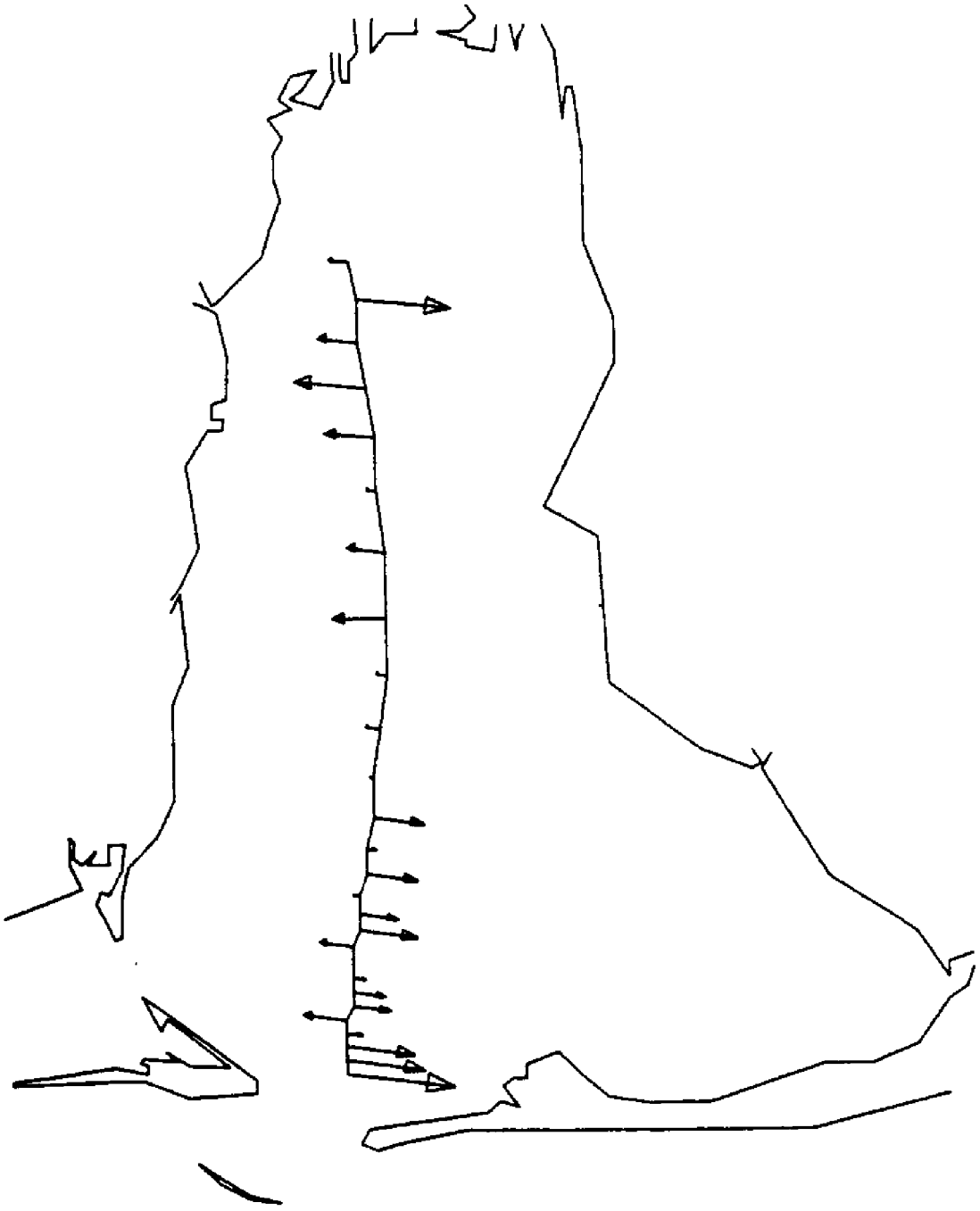

Figure 37. Normalized Net Cross-Channel Flows Over a Tidal Cycle With a 60 MPH Wind From the SW and a Relatively Small River Flow Rate.

west application provided a general coverage of wind directions. The net cross-channel flow patterns for the southwest, northeast and northwest winds are shown in Figures 38, 39, and 40. Generally, depending upon the wind condition, net cross-channel flows in both the upper and lower bay can be either to the east or west. There is however a general tendency for the flows in both the upper and lower bay to be from east to west. In the center of the bay there appears to be only very small net cross-channel flows regardless of the wind condition.

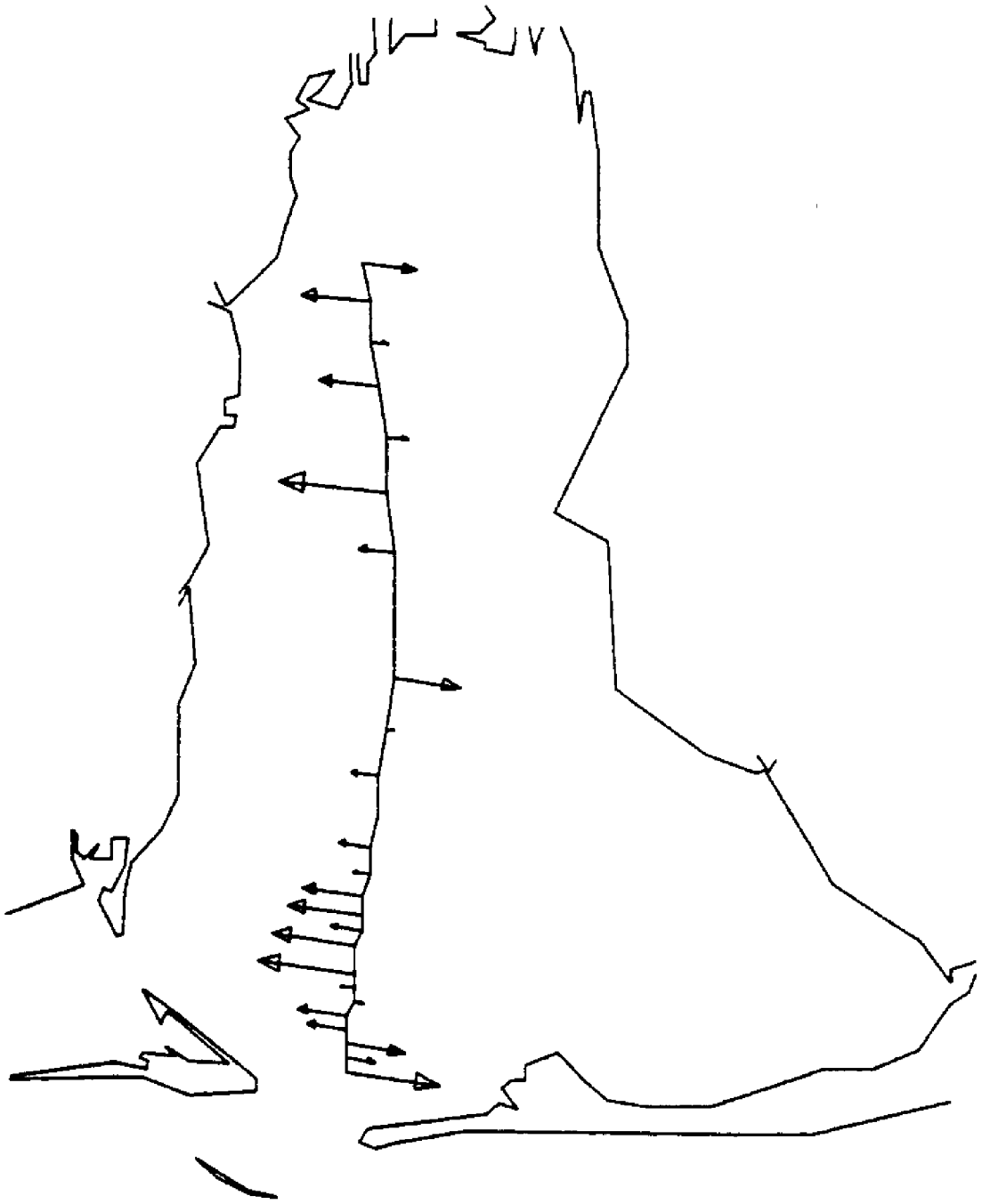

Figure 38. Normalized Net Cross-Channel Flows Over a Tidal Cycle With a 20 MPH Wind From the SE and a Relatively Small River Flow Rate.

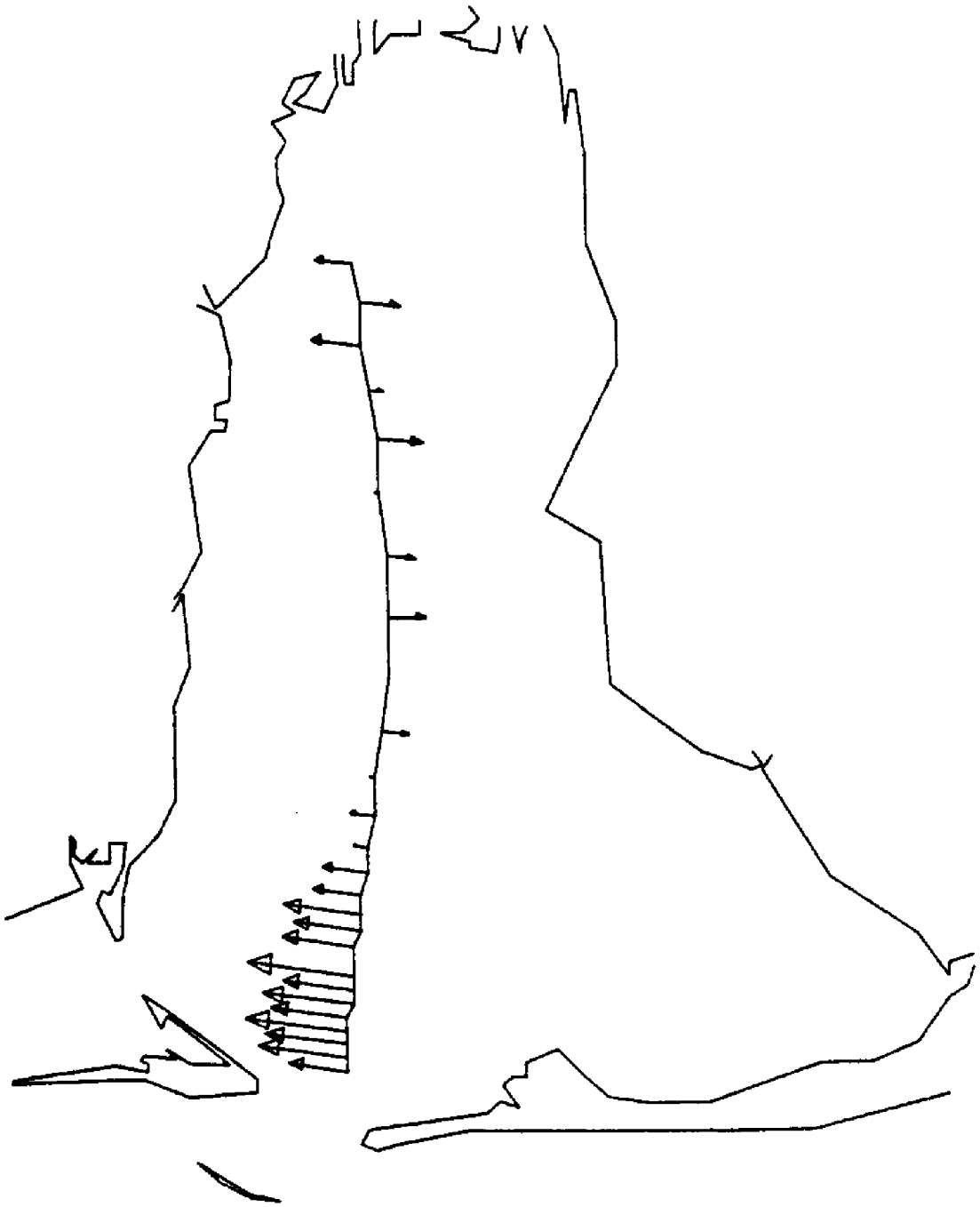

Figure 39. Normalized Net Cross-Channel Flows Over a Tidal Cycle With a 20 MPH Wind From the NE and a Relatively Small River Flow Rate.

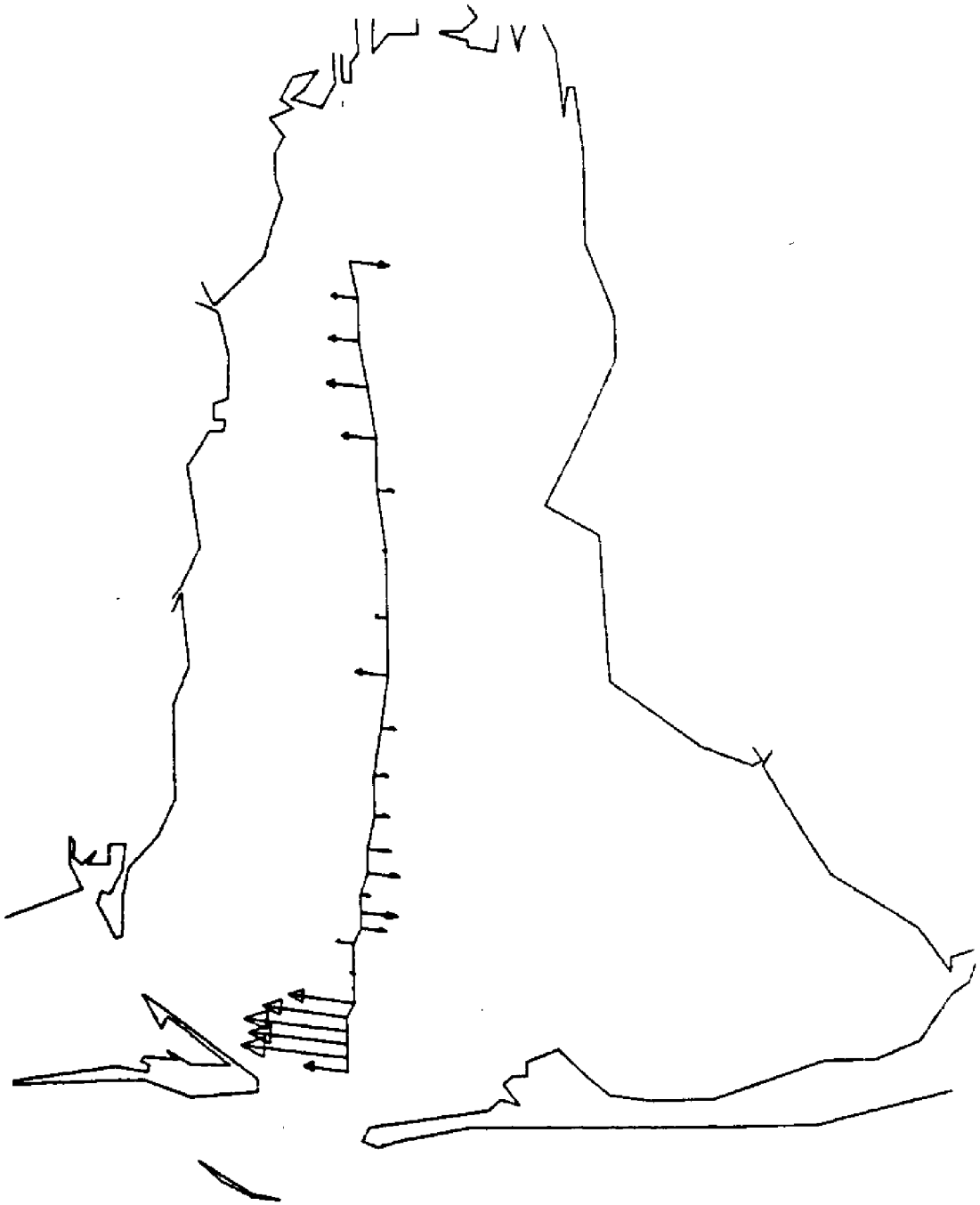

Figure 40. Normalized Net Cross-Channel Flows Over a Tidal Cycle With a 20 MPH Wind From the NW and a Relatively Small River Flow Rate.

To examine the effect of river inflow on net cross-channel flows, different river conditions were considered. Figure 41 indicates the net cross-channel flow rate results for a 20 mph wind from the southwest and a river inflow of 200,000 cfs. When compared with Figure 35 (similar conditions except for river flow), only small differences are observed in the basic net cross-channel flow patterns.

After a wide range of model applications, it appears that river inflow and wind magnitude have a smaller effect than wind direction on the general net cross-channel flow patterns. Considering the spectrum of wind magnitudes, wind directions and river inflow conditions it appears that sediment from the channel aprons can move either east or west from the channel. In general, however, it would appear that sediment movement from east to west is more probable based upon the net cross-channel flows predicted by the hydrodynamic model.

In order for sediment from the channel aprons to actually spread into an area it is not necessary or sufficient that there be net cross-channel flows in the direction of the area under consideration. A more complex flow pattern can exist which results in sediment following a more indirect path before deposition. In addition, if fluid velocities are strong in an area the sediment will move on through the area without being deposited. To investigate this aspect of the sediment transport problem, overall circulation patterns were plotted at hourly intervals. Circulation patterns are presented in Appendix A for the no wind condition and for a 20 mph wind from the SW, SE, NE and NW. The wind is observed to have a much larger effect for the shallower regions of the bay. The main channel flow is not greatly affected in a direct manner by the wind. The tide and inner forces

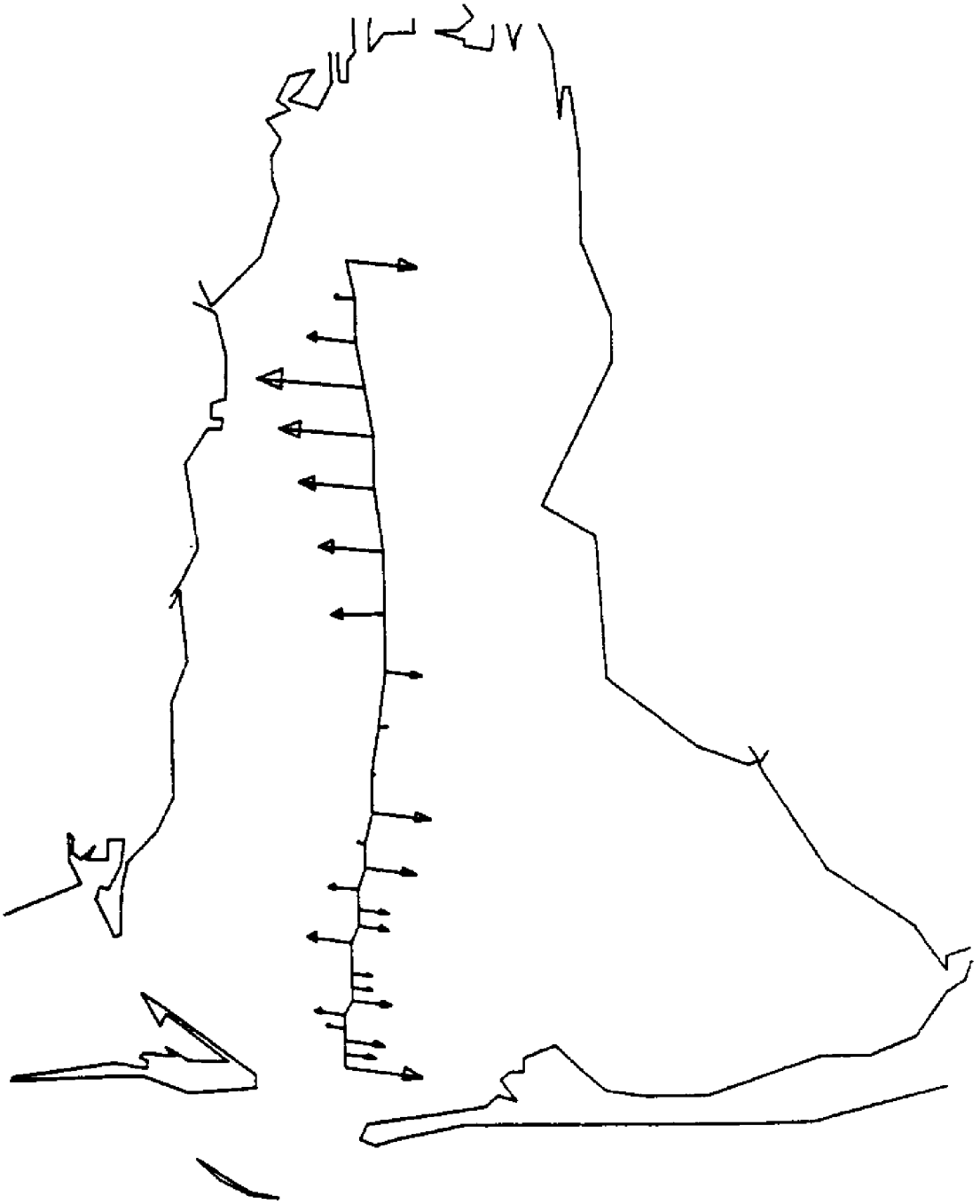

Figure 41. Normalized Net Cross-Channel Flows Over a Tidal Cycle With a 20 MPH Wind From the SW and a Large River Flow Rate.

still have a predominant effect in the main channel. Indeed, the flow in the main channel is often altered in a direction opposite to the wind effect. This can be attributed to the hydraulic gradient established by the water movement in the shallow regions as a result of wind effects.

To more readily observe the effect of wind on circulation patterns, difference vector plots are presented in Appendix B. These plots represent the difference between the velocity at a point for a given wind condition and the velocity at the point for a "no wind" condition. These difference plots are observed to vary greatly with the wind direction. Generally a wind from the north blows water out of the bay, a wind from the east blows water into Mississippi Sound, a wind from the south blows additional water into the bay, and a wind from the west blows water from Mississippi Sound into the bay. Some complex flow patterns are established in the bay when winds with various components from the north, east, south, or west are applied to the bay.

In addition to investigating the circulation patterns, a normalized average hydrodynamic energy level was calculated for each finite difference cell. The average hydrodynamic energy level is based upon the mean square of the velocity over the tidal cycle for each finite difference cell. The average hydrodynamic energy level results are presented in Figure 42. Regions of low average hydrodynamic energy levels are much more susceptible to sediment deposition than are regions of higher average energy levels. Erosion rather than deposition should occur in regions of very high average hydrodynamic energy levels. The model results indicate Bon Secour and the region above Point Clear as possible regions where deposition might be likely. Of course this

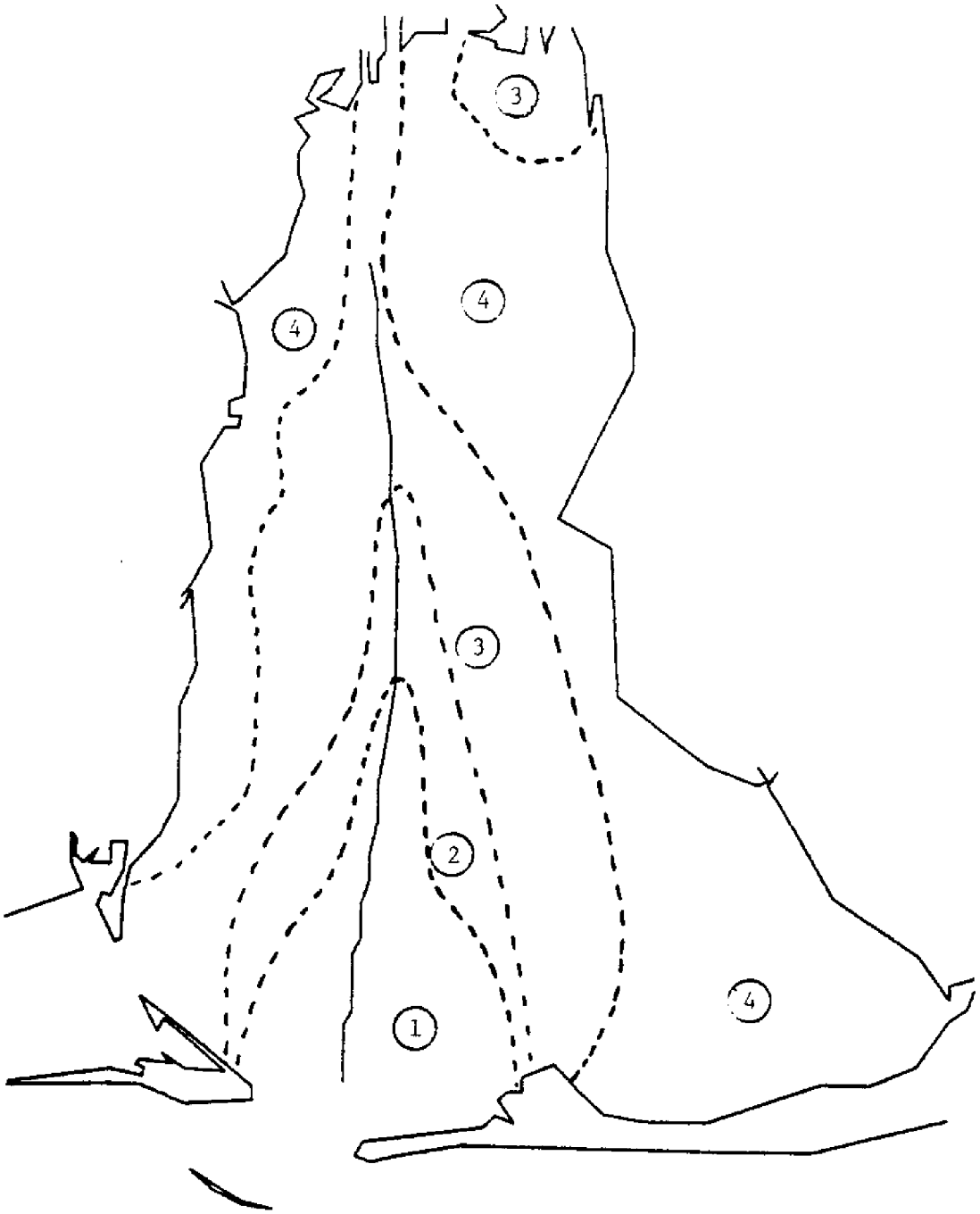

Region 1 - High Hydrodynamic Energy Level
Region 2 - Moderately High Hydrodynamic Energy Level
Region 3 - Medium Hydrodynamic Energy Level
Region 4 - Low Hydrodynamic Energy Level

Figure 42. Average Hydrodynamic Energy Levels in Mobile Bay Over a Typical Tidal Cycle.

does not mean that the actual deposition in these areas will be greater than in other parts of the bay since sediment must be available in the water column before it can be deposited in these regions. However, if the sediment load was the same over the bay then deposition should be largest in these regions.

From the average hydrodynamic energy profile in the bay and based upon the overall circulation patterns presented in Appendix A, an asymmetric deposition pattern appears possible. Sediment disturbed from the channel apron on the west side of the channel appears to have a much greater chance of being flushed from the bay through Main pass or Pass aux Herons than does sediment from the channel apron on the east side of the channel. Sediment disturbed from the east side of the channel appears to have an excellent chance of being deposited in Bon Secour or in the uppear eastern part of the bay because of low average hydrodynamic energy levels in these regions.

XI. CONCLUSIONS

The numerical model results do not indicate a tendency for net west to east flows across the main channel which might be directly consistent with the preliminary seismic survey results. Net flows, depending on the wind condition, can be either west to east or east to west. A slight general tendency appears to exist for net east to west flows across the main channel. There does appear to be some correlation between hydrodynamic energy levels predicted by the model and possible deposition patterns identified by the preliminary seismic surveys. Thus, the numerical model results appear to indicate a possible asymmetric deposition pattern rather than net cross-channel flows as the mechanism for any asymmetric spreading of the dredge spoil from the channel aprons.

XII. REFERENCES

1. Brande, Scott, "Dredge Spoil Mapping by Seismic Survey and Sedi-Analysis in Mobile Bay, Alabama," 1982 Sea Grant College Program Proposal by Mississippi-Alabama Sea Grant Consortium, Volume II, August 1981.

2. Wanstrath, J. J., Whitaker, R. E., Reid, R. O., and Vastano, A. C., "Storm Surge Simulation in Transformed Coordinates, Vol. I - Theory and Applications," Technical Report 76-3, U.S. Army Coastal Engineering Research Center, CE, Fort Belvoir, VA, November 1976.

3. Leendertse, J. J., "Aspects of Computational Model for Long-Period Water-Wave Propagation," RM-5294-PR, Rand Corporation, Santa Monica, California, 1967.

4. Schroeder, W. W., "Riverine Influence on Estuaries: A Case Study," In M. S. Wiley [ed.], Estuarine Interactions, Academic Press, Inc., New York, 1978, pp 347-364.

5. Schoreder, W. W., "Physical Environment Atlas of Coastal Alabama," Mississippi-Alabama Sea Grant Program, 76-034, 1976.

6. U.S. Department of Commerce, National Ocean Survey, "Tide Tables: East Coast of North and South America including Greenland, 1972-73.

7. Hill, Donald O., "A Hydrodynamic And Salinity Model For Mobile Bay," Ph.D. Dissertation, The University of Alabama, 1975.

8. Personal communication from Lawrence R. Green, chief of the Planning Division, U.S. Army Corps of Engineers, Mobile, Alabama to Dr. Gary C. April, Professor, The University of Alabama.

9. U.S. Department of Commerce, The National Ocean Survey, "U.S. Gulf Coast: Alabama: Mobile Bay, 1:80000 Mercator Projection at Lat 30 25' ", September 23, 1978.

10. MacPhearson, Jr., Roland M. "The Hydrography of Mobile Bay and Mississippi Sound, Alabama," Journal of Marine Science 1, August 1970, pp 1-83.

11. Jarrell, John P., "Hydrodynamics of Mobile Bay and Mississippi Sound - Pass Exchange Studies," Bureau of Engineering Research Report 271-112, The University of Alabama, July 1981.

12. Sundborg, F. A., "The River Klaralveu, A Study of Fluvial Processes, Geogr. Ann. Arg; 37:125-316, 1956.

13. Postma, H., "Sediment Transport and Sedimentation in the Estuarine Environment," Estuaries (George Lauff, editor), American Association for the Advancement of Science, Publication No. 83, 1967, pp 158-179.

14. Ryan, J. J., "A Sedimentalogic Study of Mobile Bay, Alabama," Florida State University Department of Geology, Contract No. 30, 1969.

APPENDIX A

CIRCULATION PATTERNS IN MOBILE BAY FOR VARIOUS WIND CONDITIONS

1. No wind.
2. 20 mph wind from SW.
3. 20 mph wind from NE.
4. 20 mph wind from NW.
5. 20 mph wind from SE.

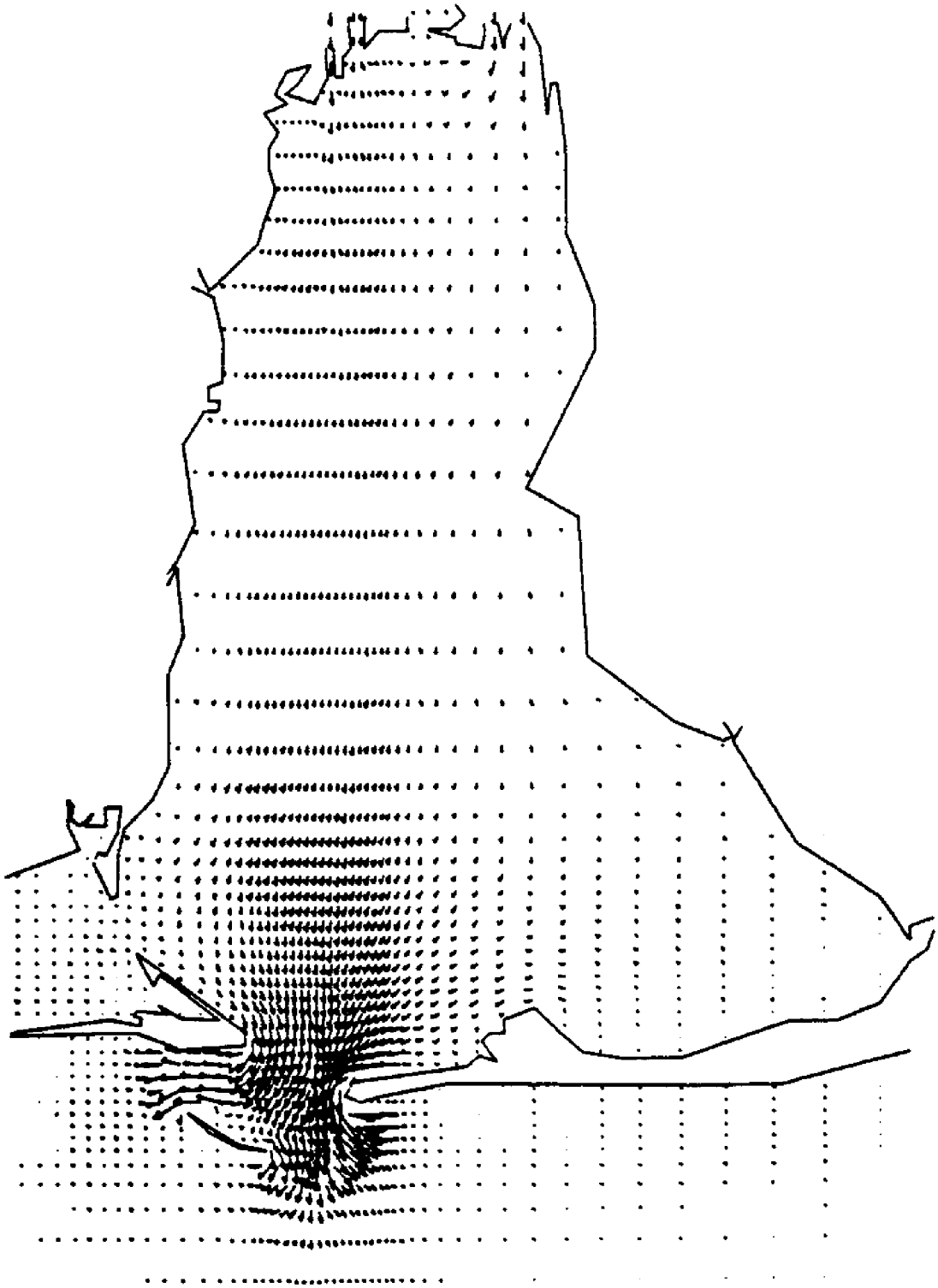

FLOW RATE FIELD AT T(HR) = 4.00
MAXIMUM VELOCITY (FT/SEC) = 1.81

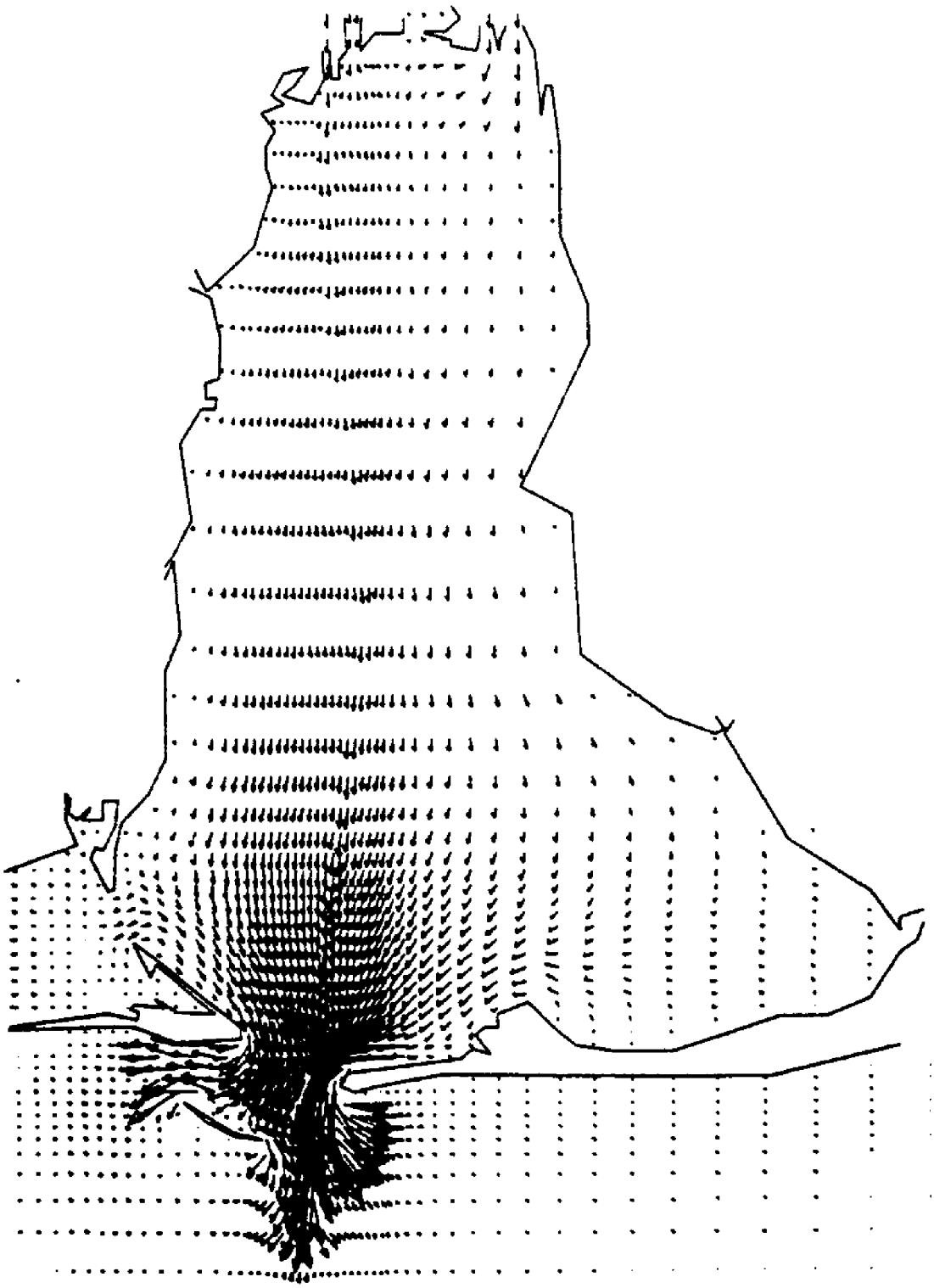

FLOW RATE FILED AT T(HR) = 8.00
MAXIMUM VELOCITY (FT/SEC) = 4.25

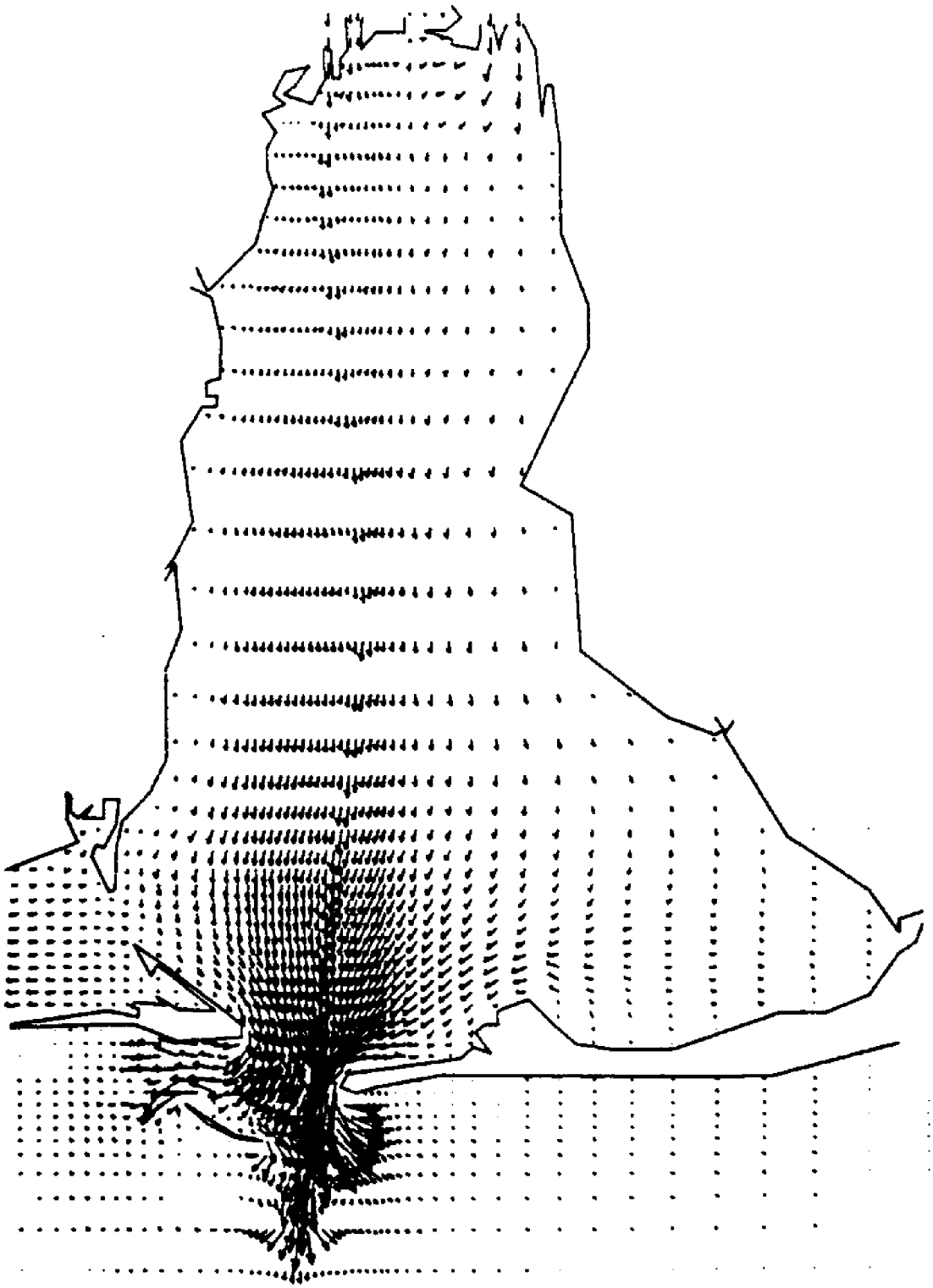

FLOW RATE FIELD AT T(HR) = 12.00
MAXIMUM VELOCITY (FT/SEC) = 3.74

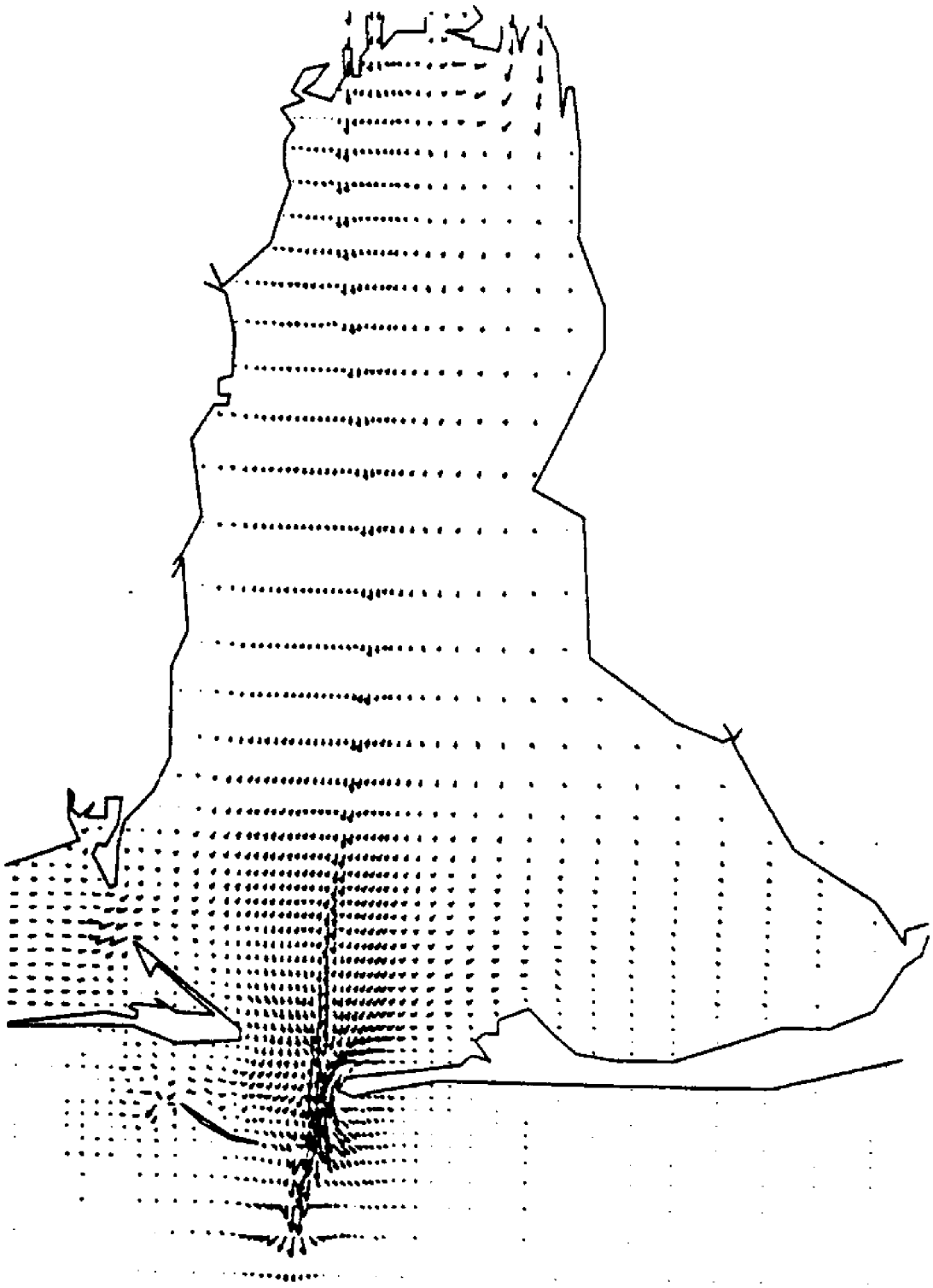

FLOW RATE FIELD AT T(HR) = 16.00
MAXIMUM VELOCITY (FT/SEC) = 1.73

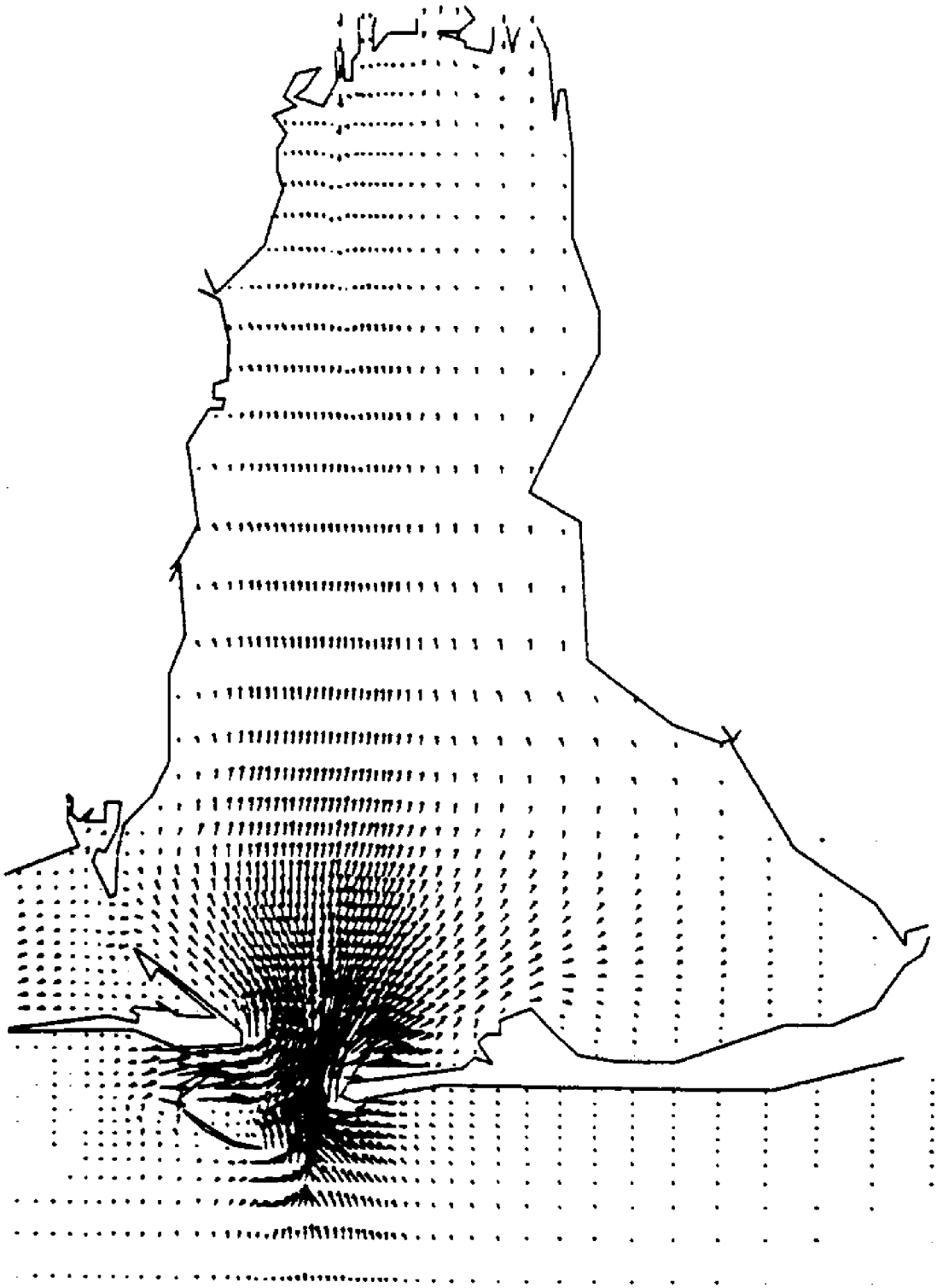

FLOW RATE FIELD AT T(HR) = 20.00
MAXIMUM VELOCITY (FT/SEC) = 3.56

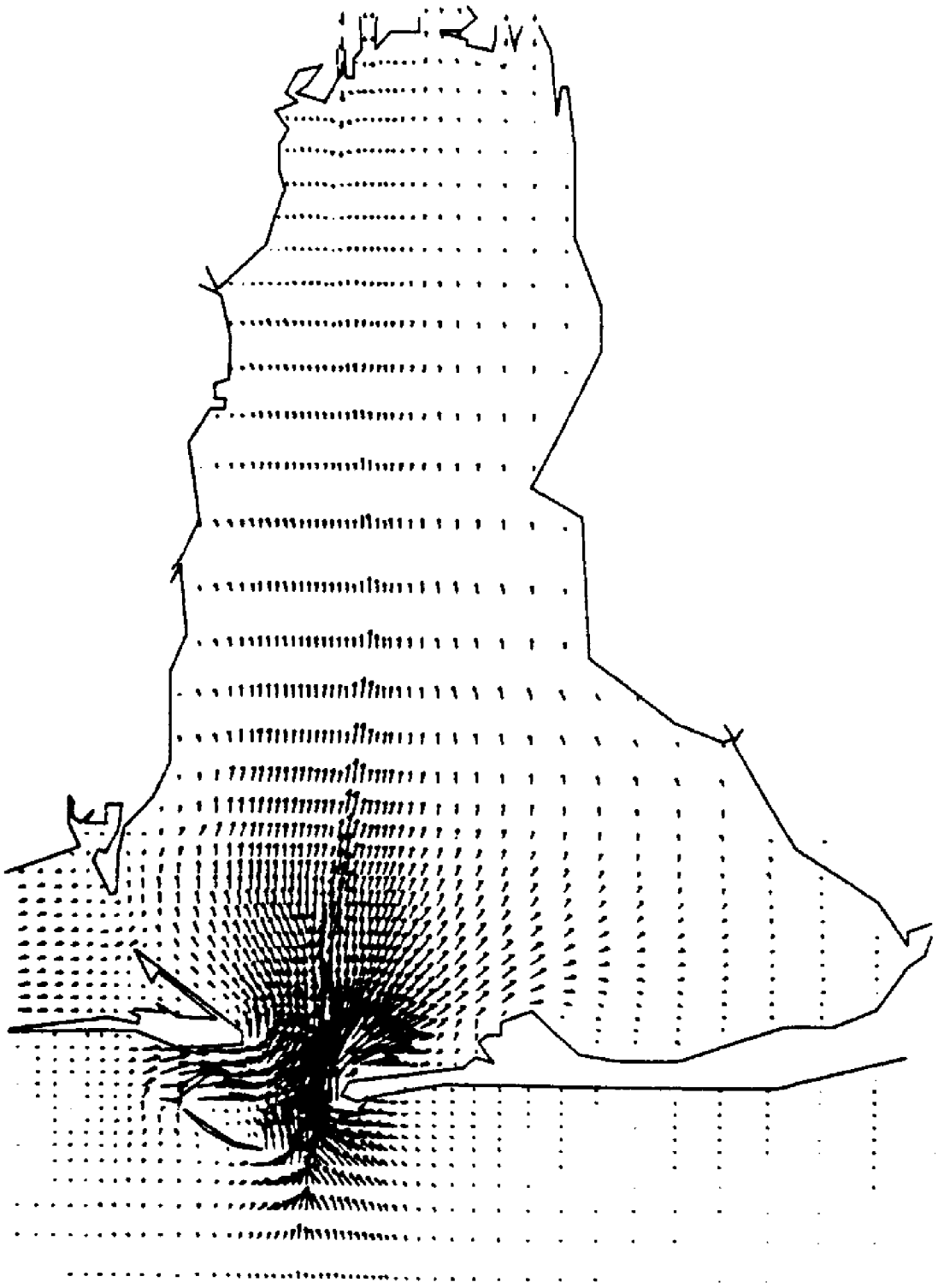

FLOW RATE FIELD AT T(HR) = 24.00
MAXIMUM VELOCITY (FT/SEC) = 3.94

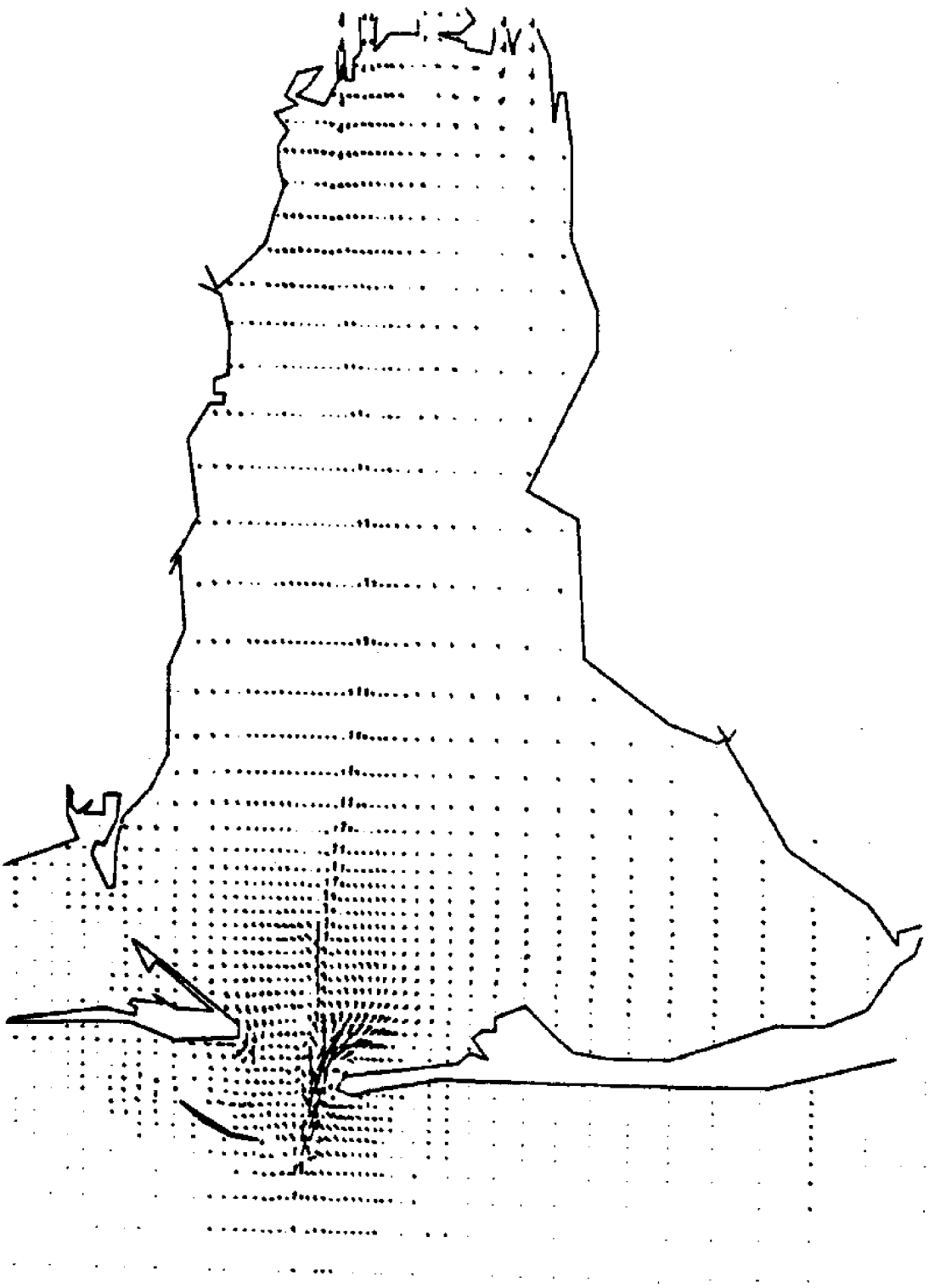

FLOW RATE FIELD AT T(HR) = 28.00
MAXIMUM VELOCITY (FT/SEC) = 1.30

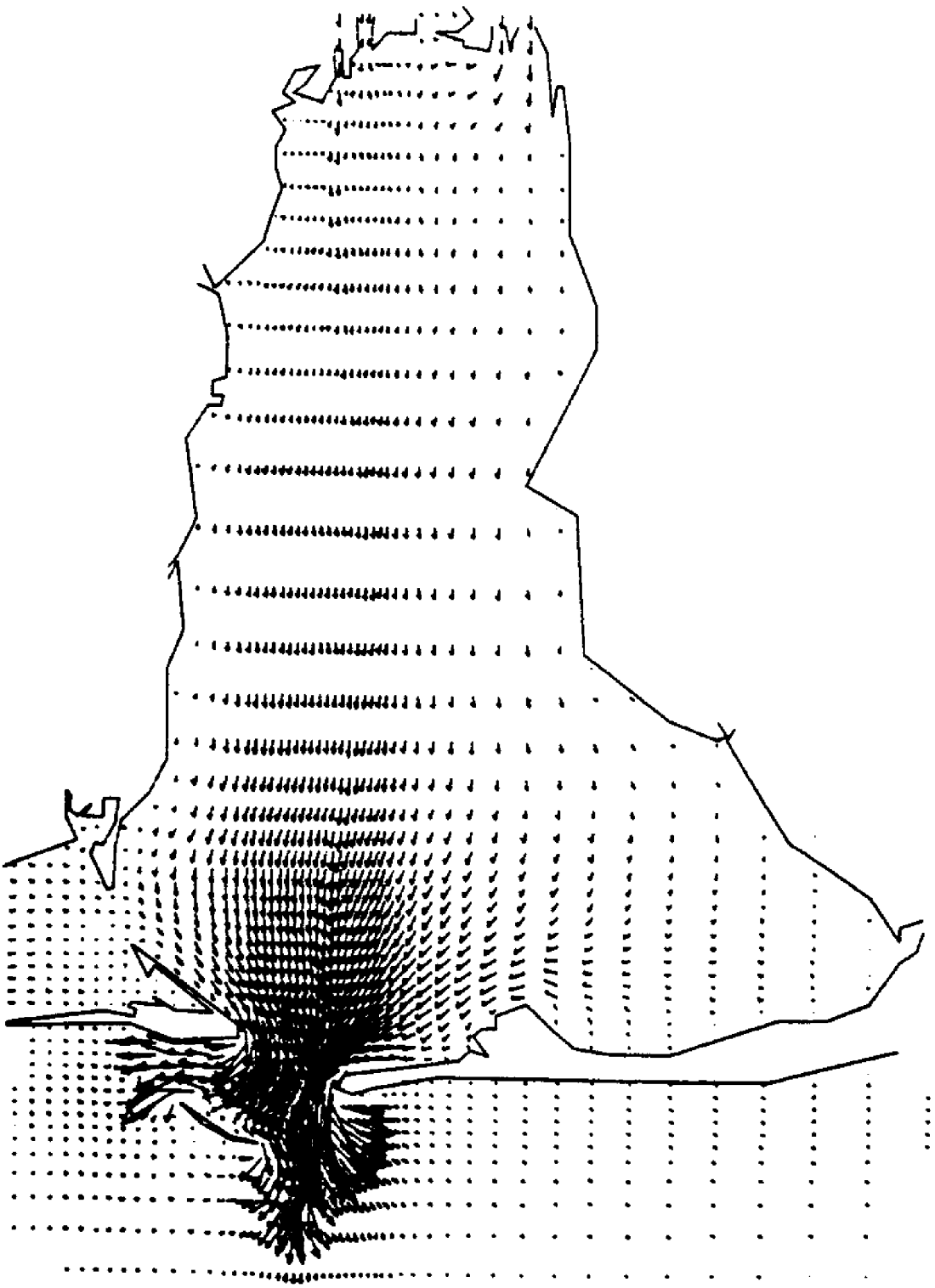

FLOW RATE FIELD AT T(HR) = 32.00
MAXIMUM VELOCITY (FT/SEC) = 4.19

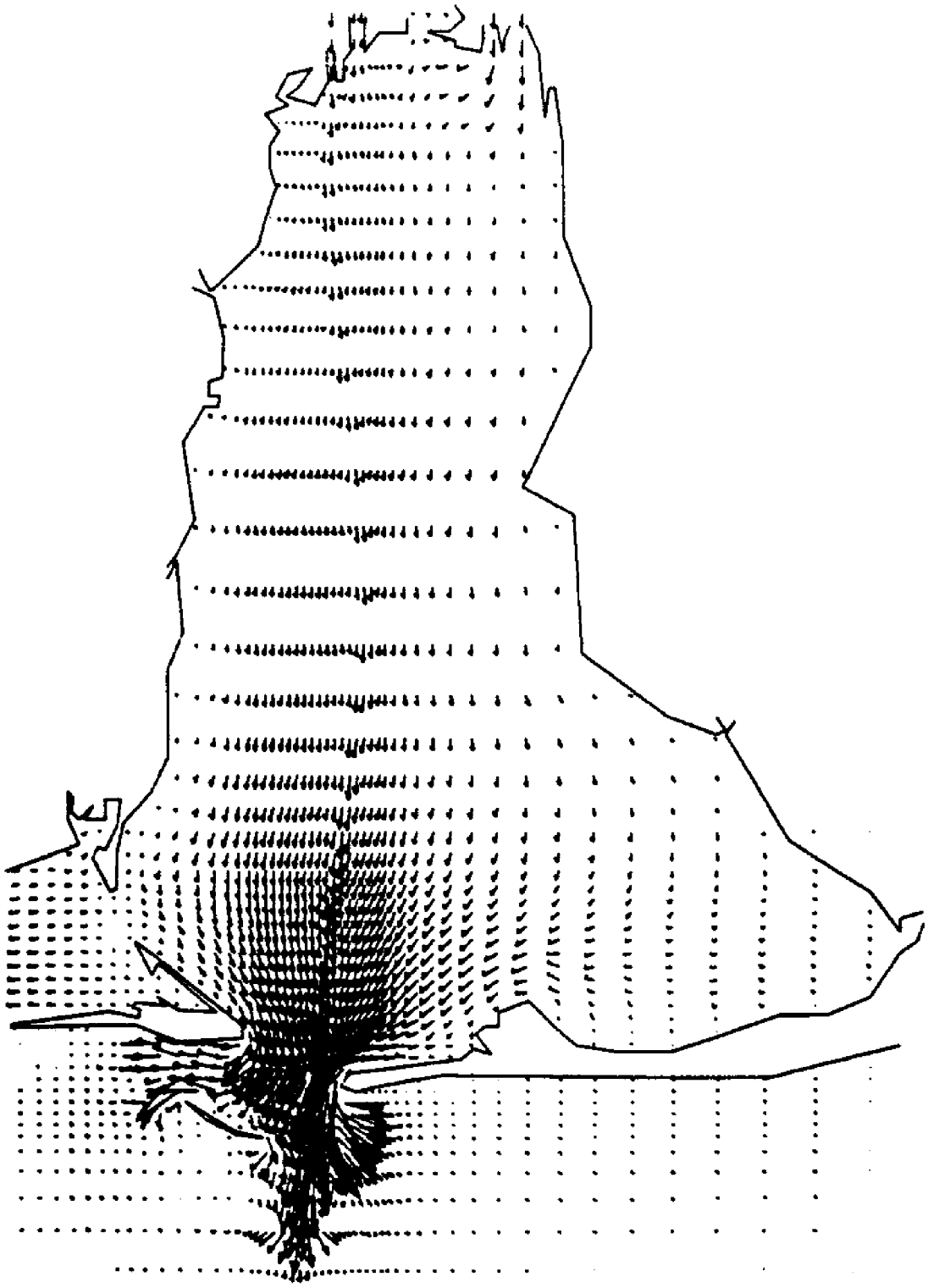

FLOW RATE FIELD AT T(HR) = 36.00
MAXIMUM VELOCITY (FT/SEC) = 4.16

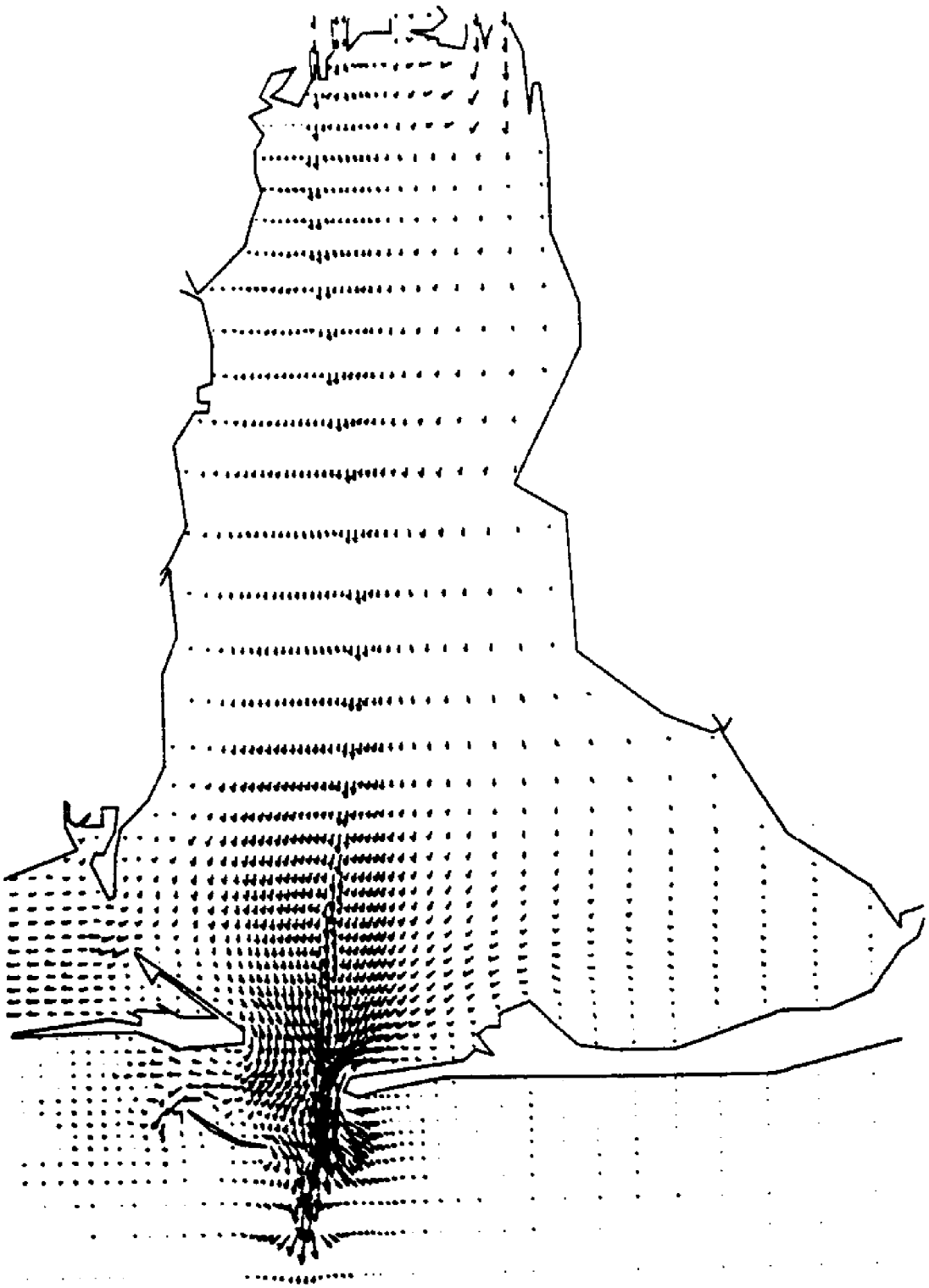

FLOW RATE FIELD AT T(HR) = 40.00
MAXIMUM VELOCITY (FT/SEC) 8.42

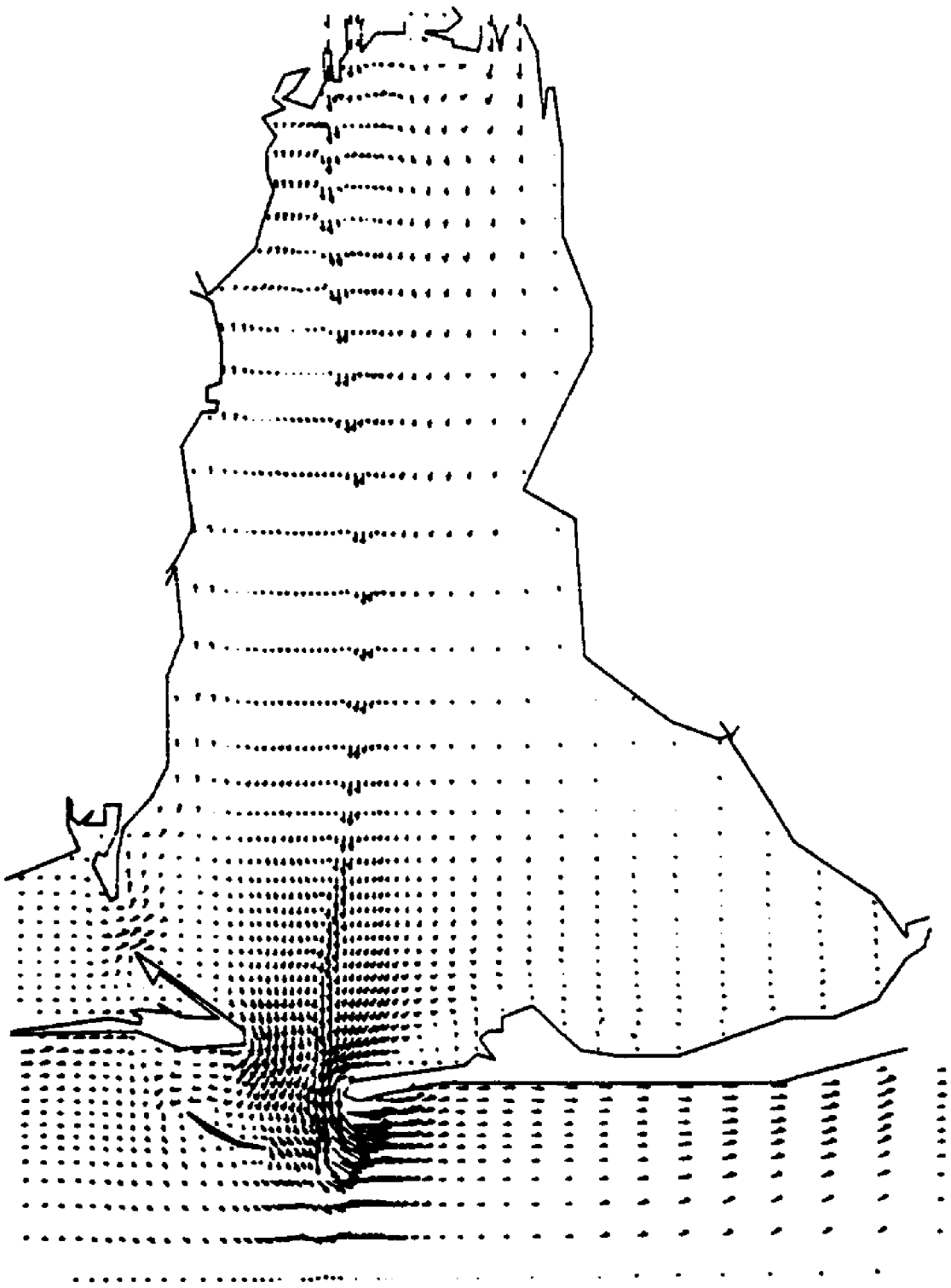

FLOW RATE FIELD AT T(HR) = 4.00
MAXIMUM VELOCITY (FT/SEC) = 1.87

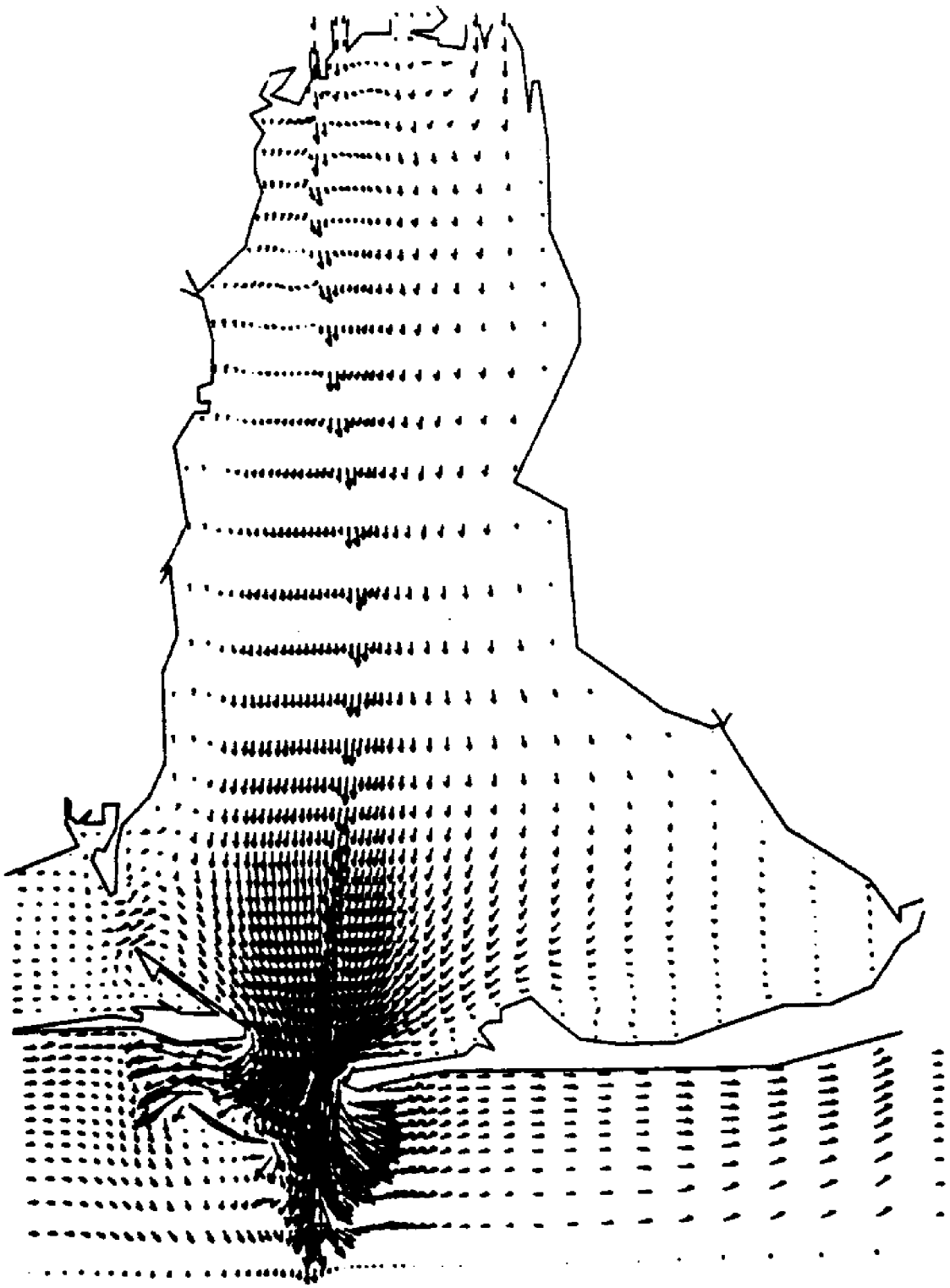

FLOW RATE FIELD AT T(HR) = 8.00
MAXIMUM VELOCITY (FT/SEC) = 4.46

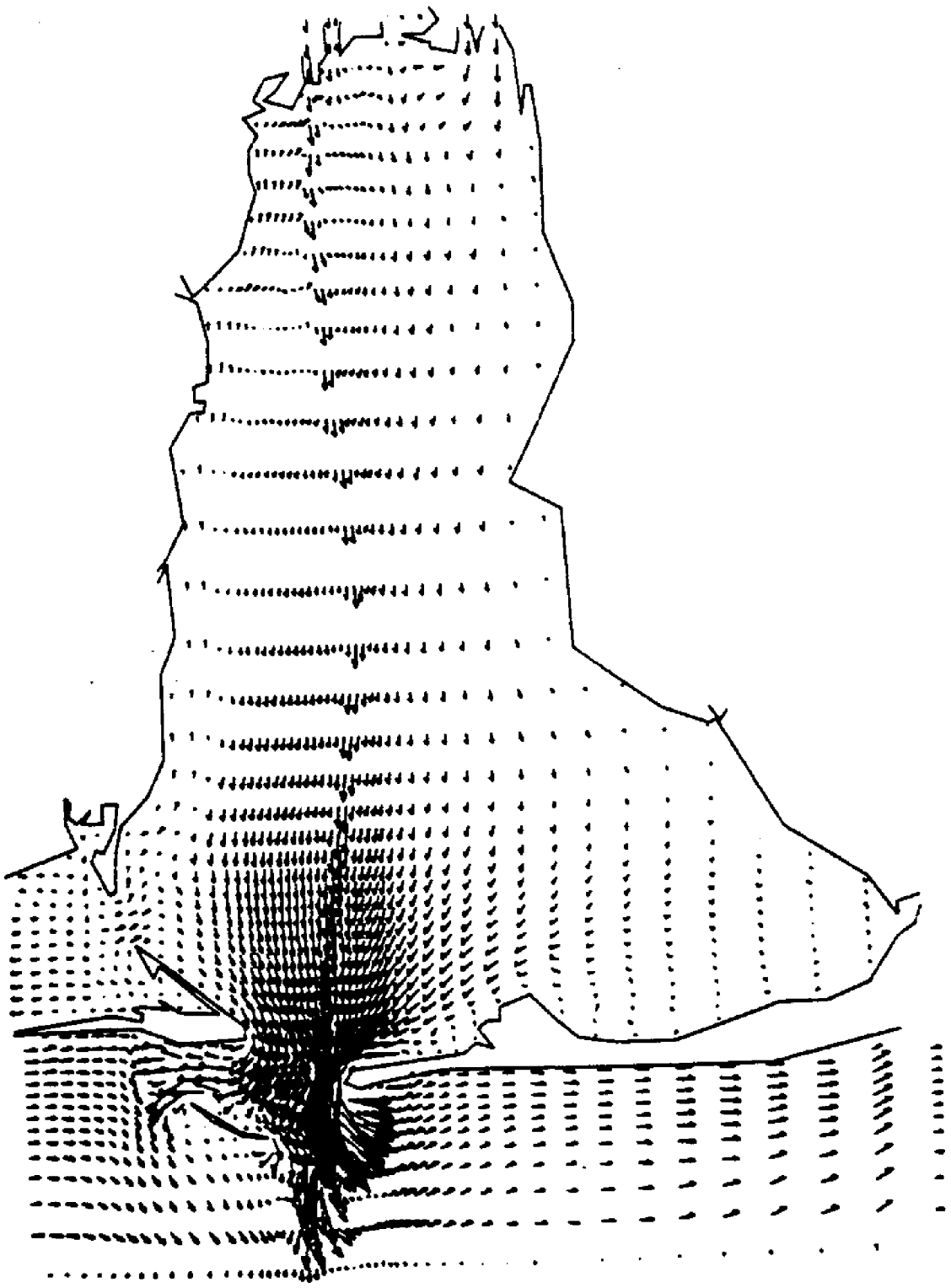

FLOW RATE FIELD AT T(HR) = 12.00
MAXIMUM VELOCITY (FT/SEC) = 3.85

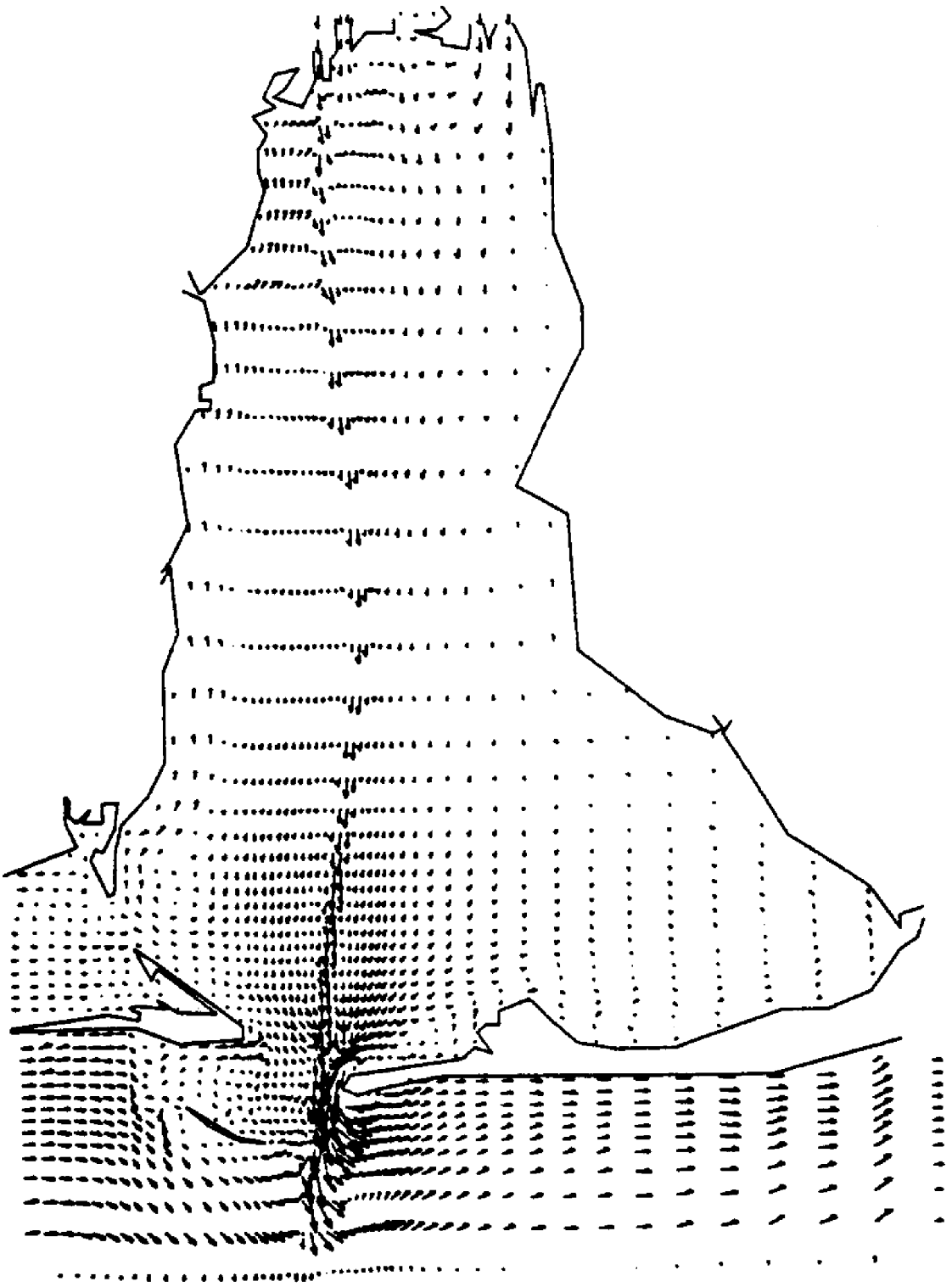

FLOW RATE FIELD AT T(HR) = 16.00
MAXIMUM VELOCITY (FT/SEC) = 1.88

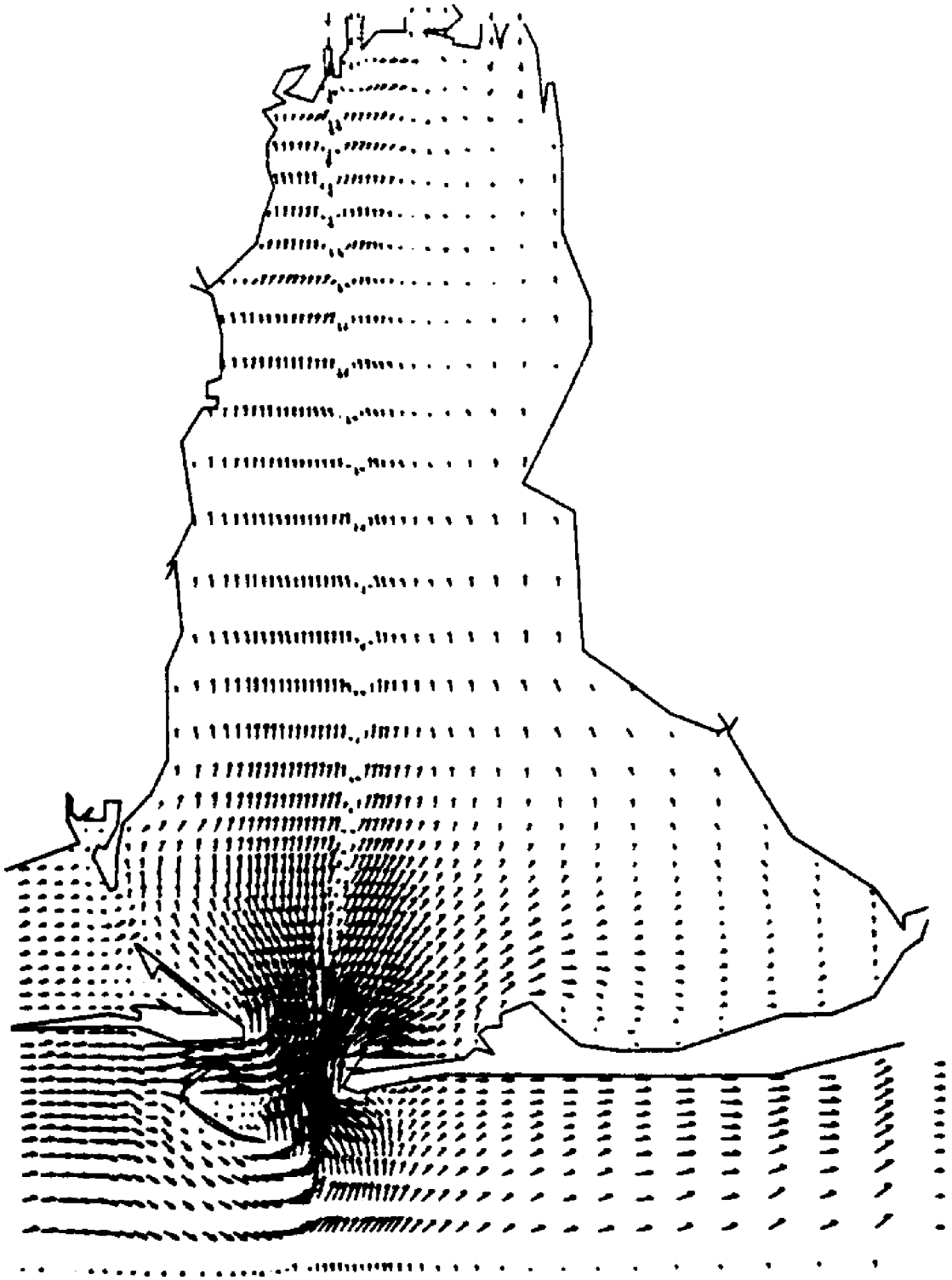

FLOW RATE FIELD AT T(HR) = 20.00
MAXIMUM VELOCITY (FT/SEC) = 3.18

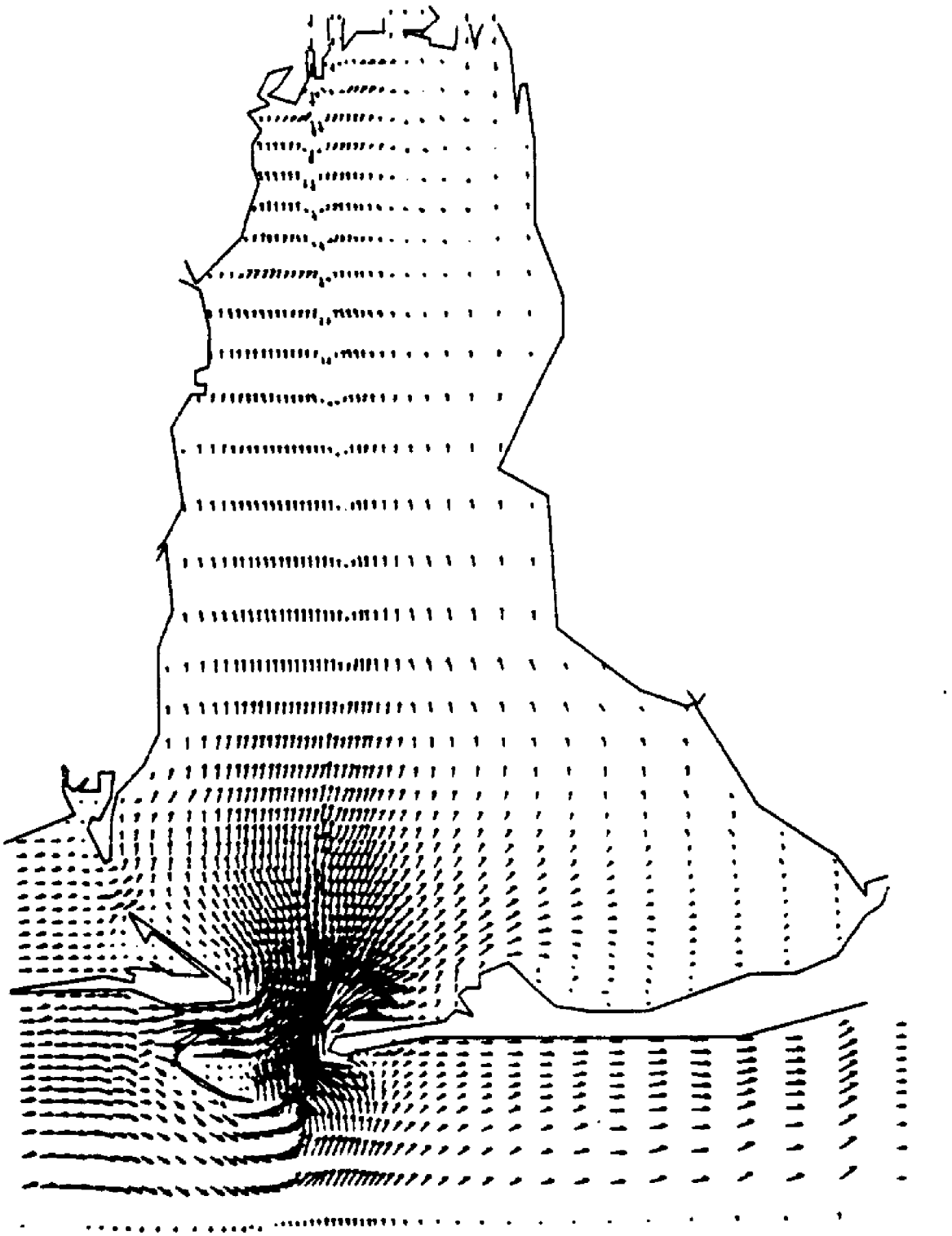

FLOW RATE FIELD AT T(HR) = 24.00
MAXIMUM VELOCITY (FT/SEC) = 3.70

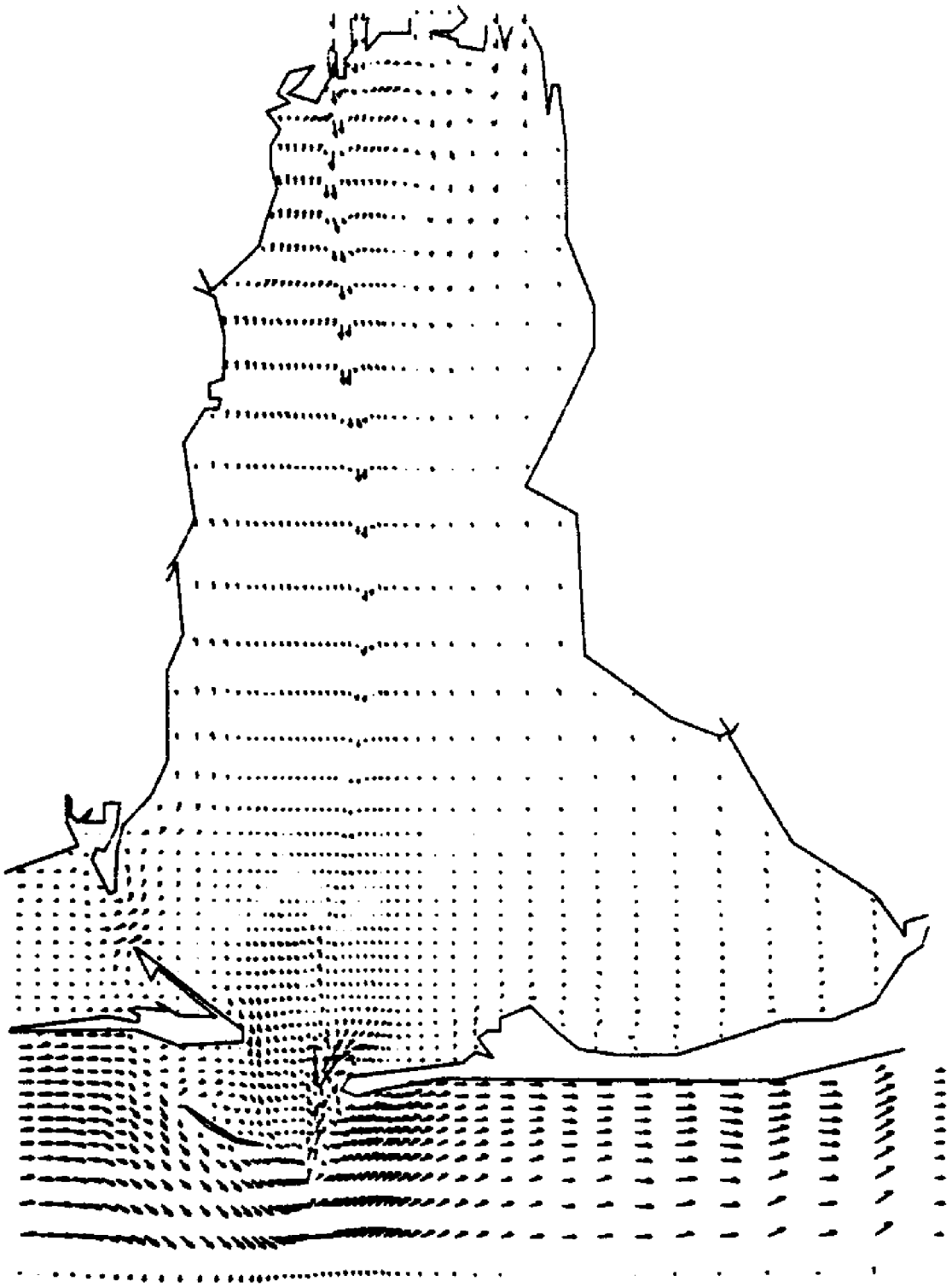

FLOW RATE FIELD AT T(HR) = 28.00
MAXIMUM VELOCITY (FT/SEC) = 1.05

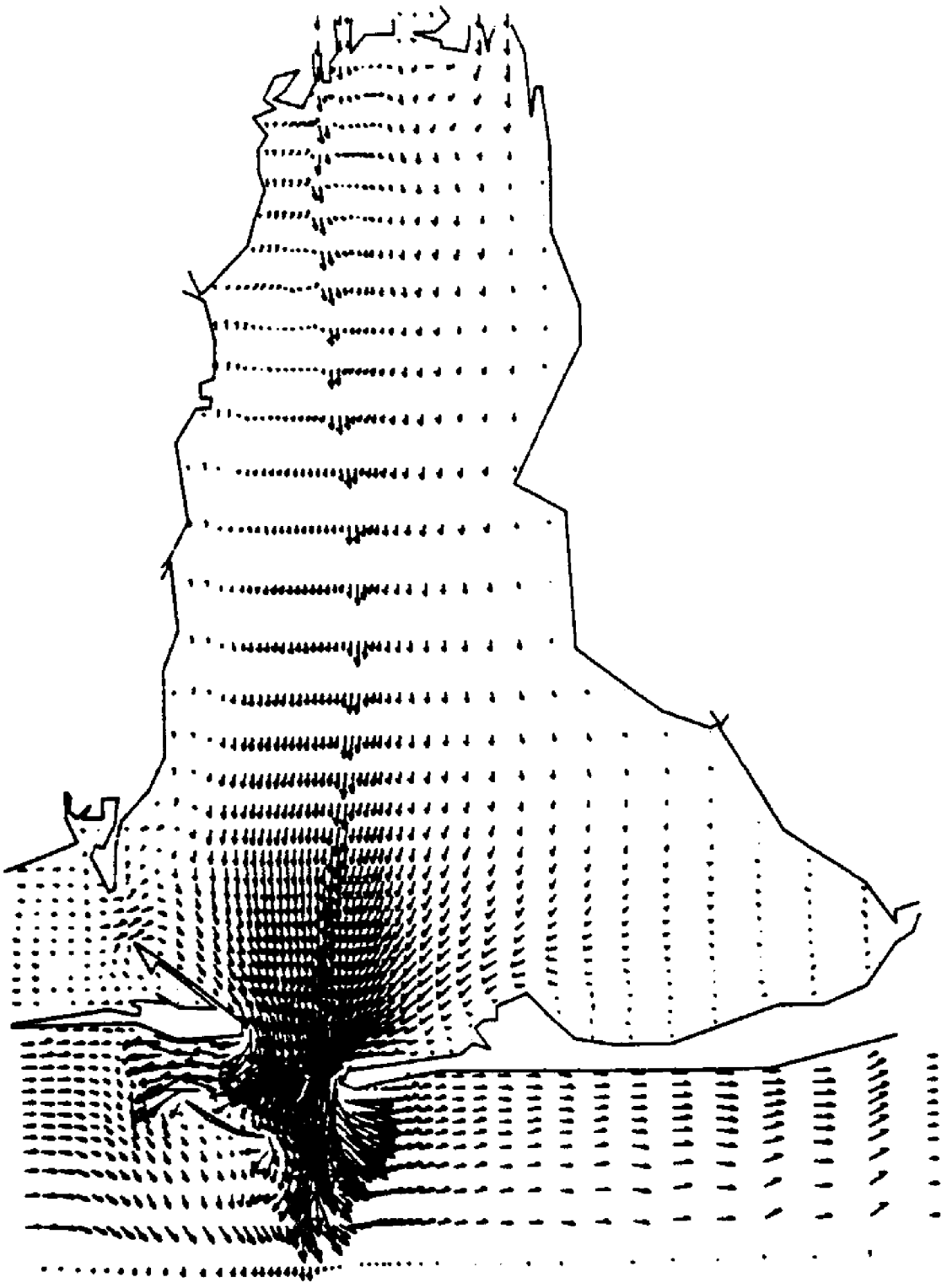

FLOW RATE FIELD AT T(HR) = 32.00
MAXIMUM VELOCITY (FT/SEC) = 4.32

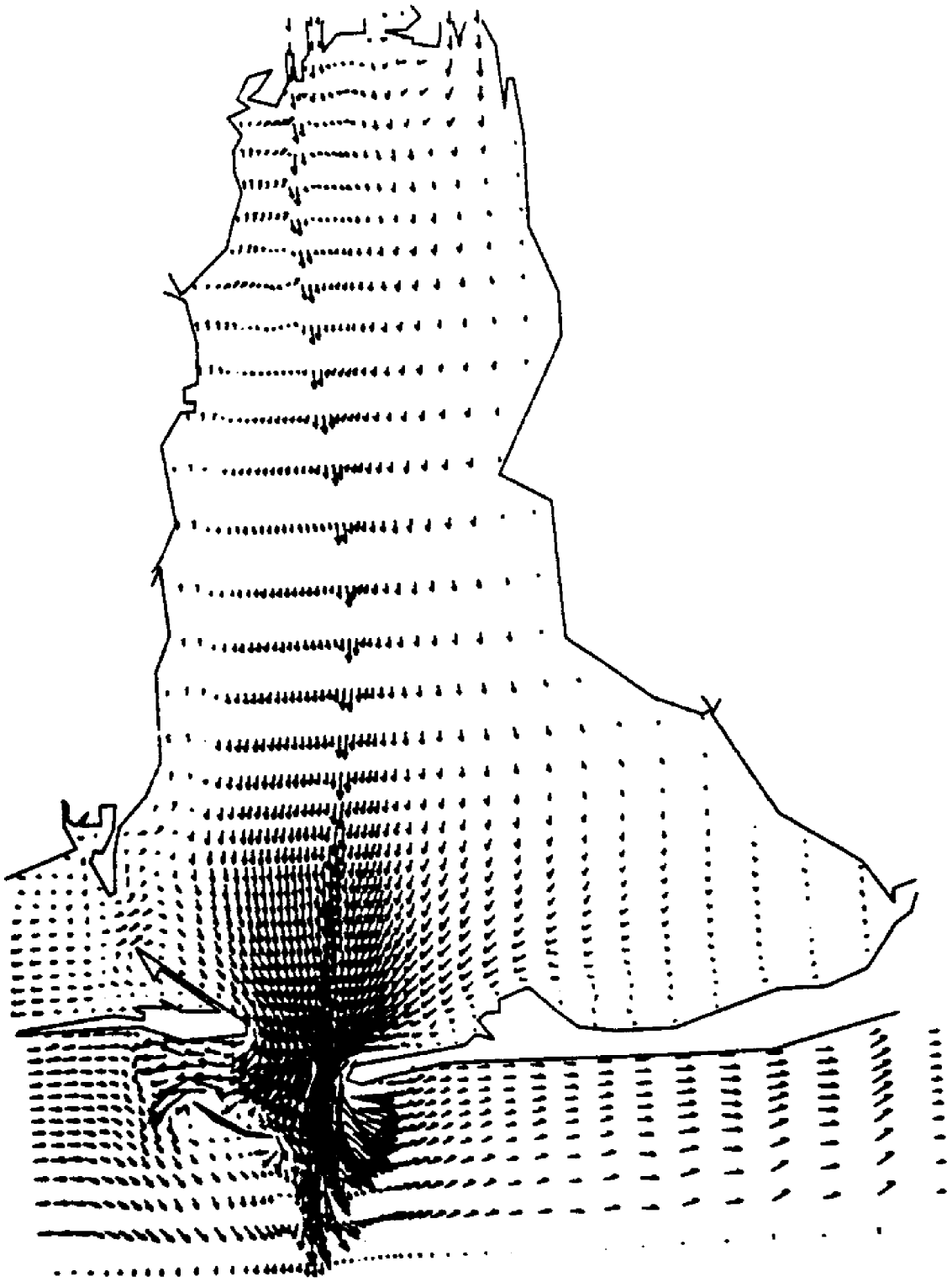

FLOW RATE FIELD AT T(HR) = 36.00
MAXIMUM VELOCITY (FT/SEC) = 4.18

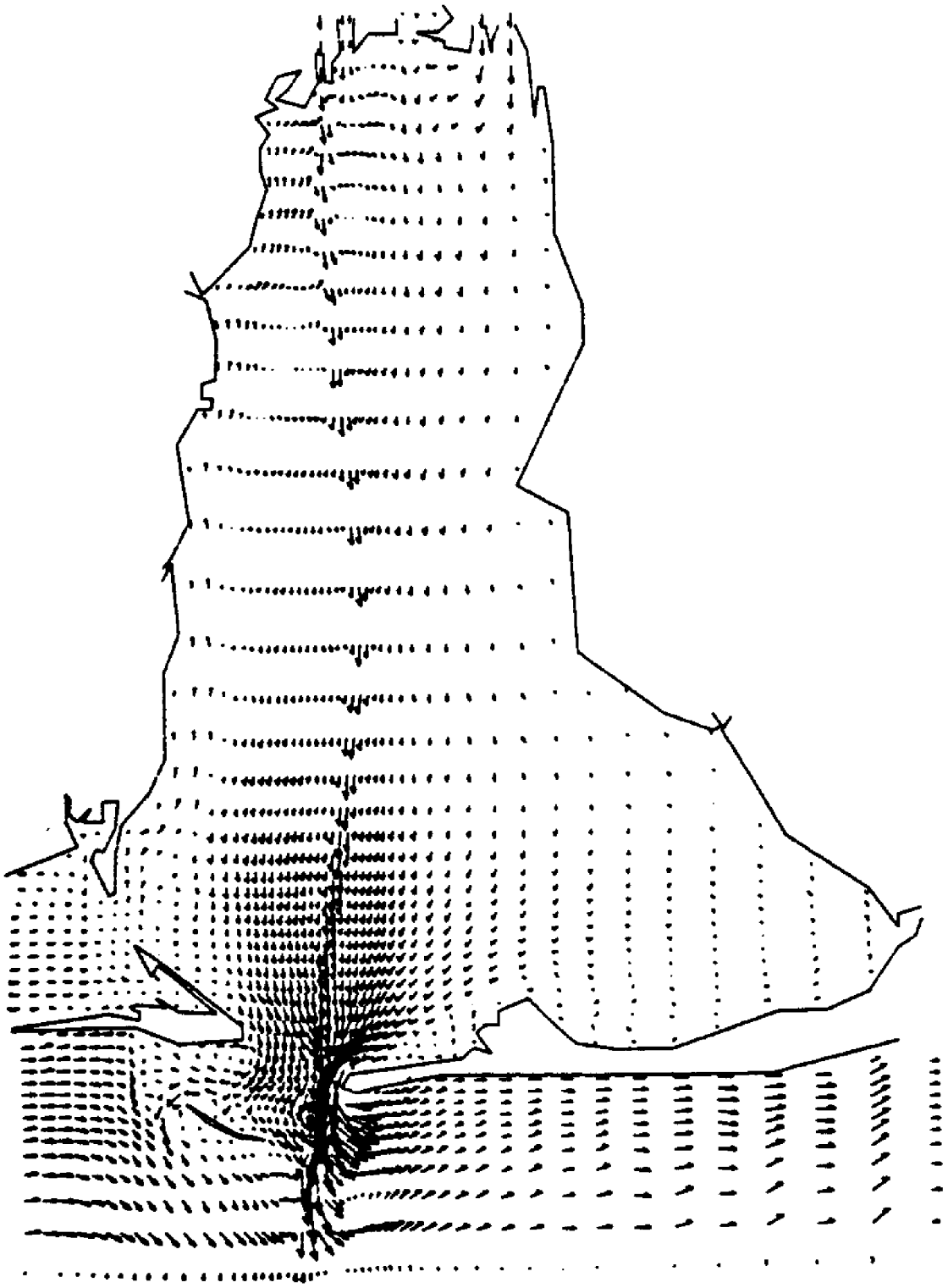

FLOW RATE FIELD AT T(HR) = 40.00
MAXIMUM VELOCITY (FT/SEC) = 2.49

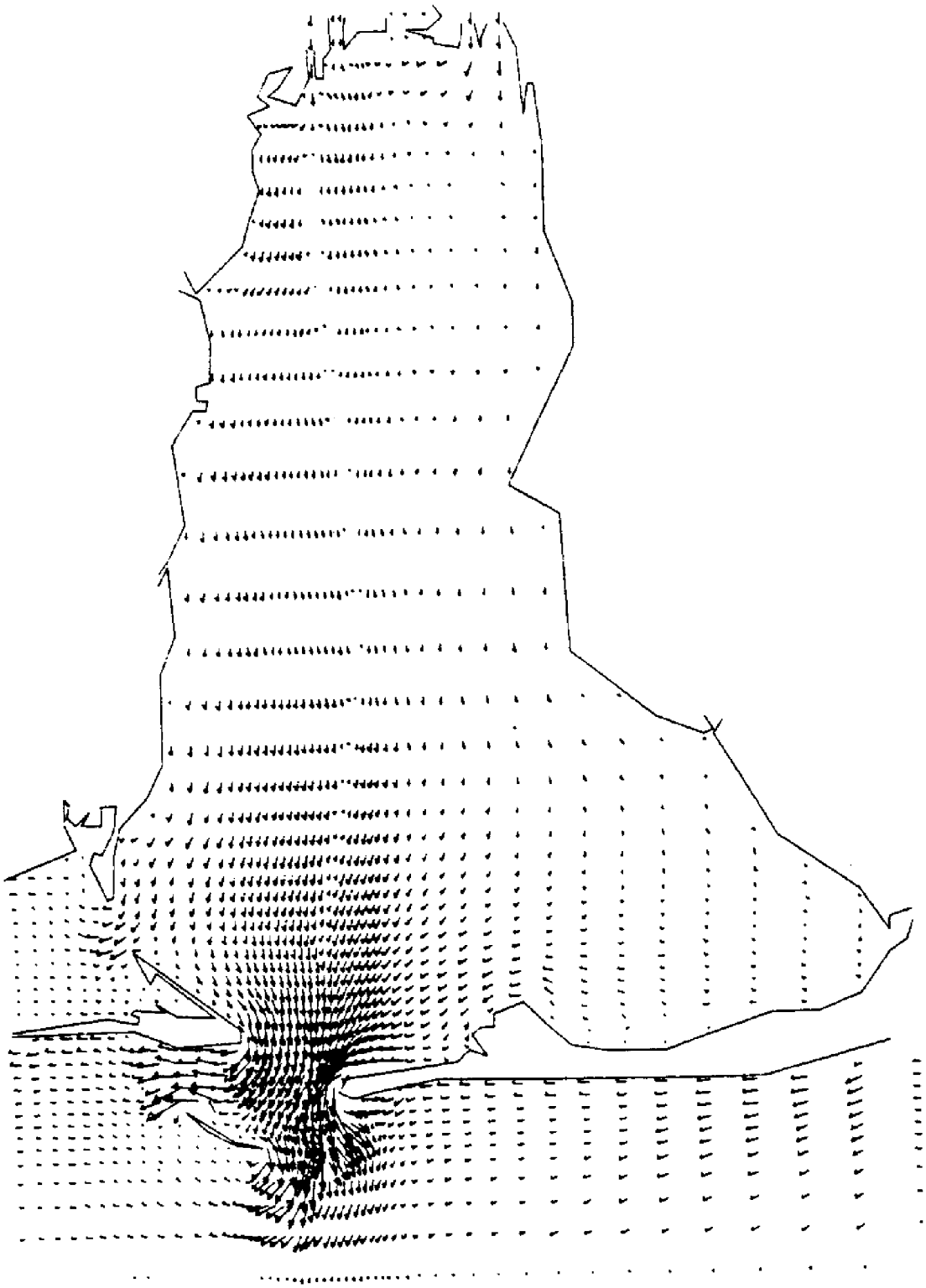

FLOW RATE FIELD AT T(HR) = 4.00
MAXIMUM VELOCITY (FT/SEC) = 2.13

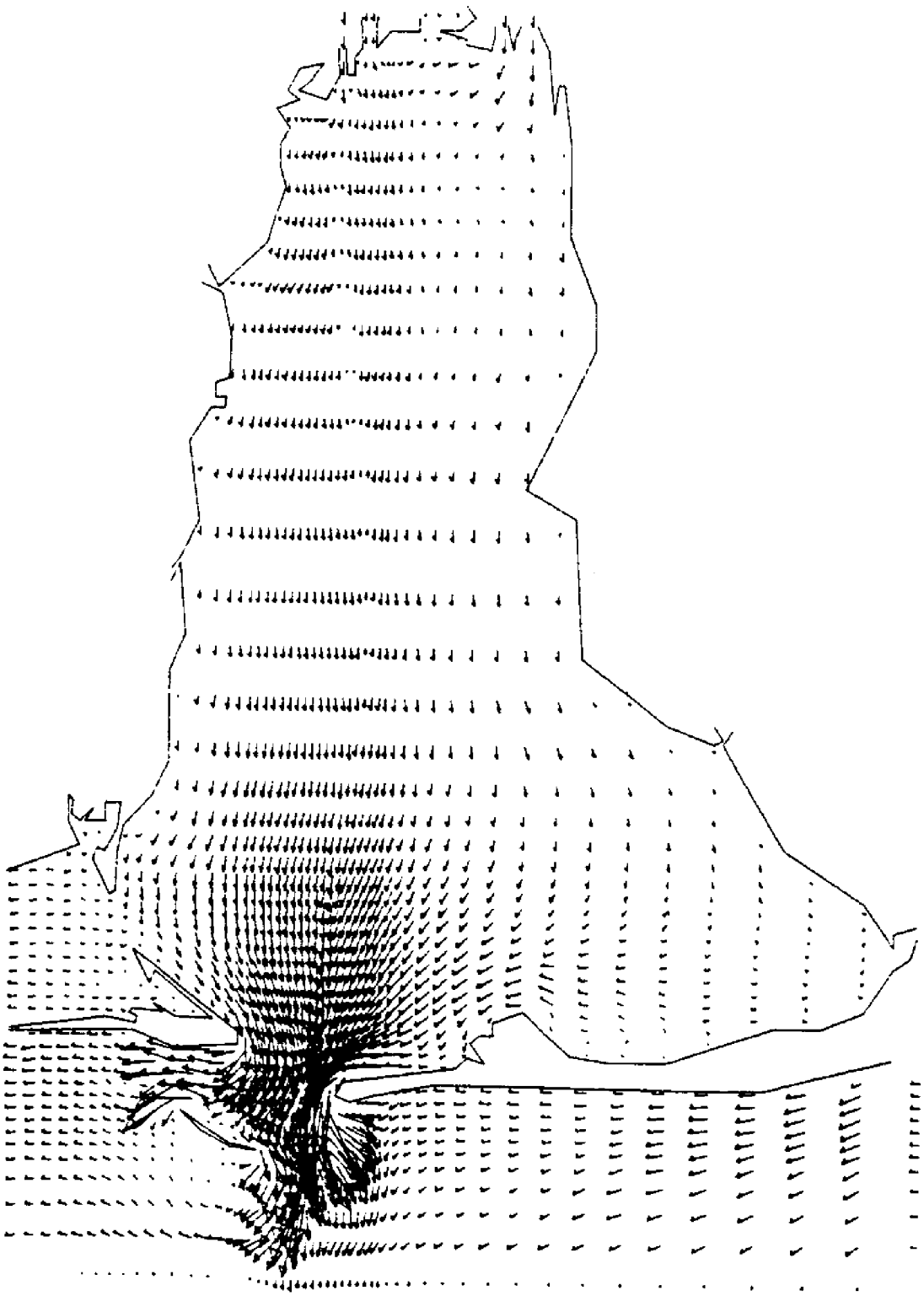

FLOW RATE FIELD AT T(HR) = 8.00
MAXIMUM VELOCITY (FT/SEC) = 4.14

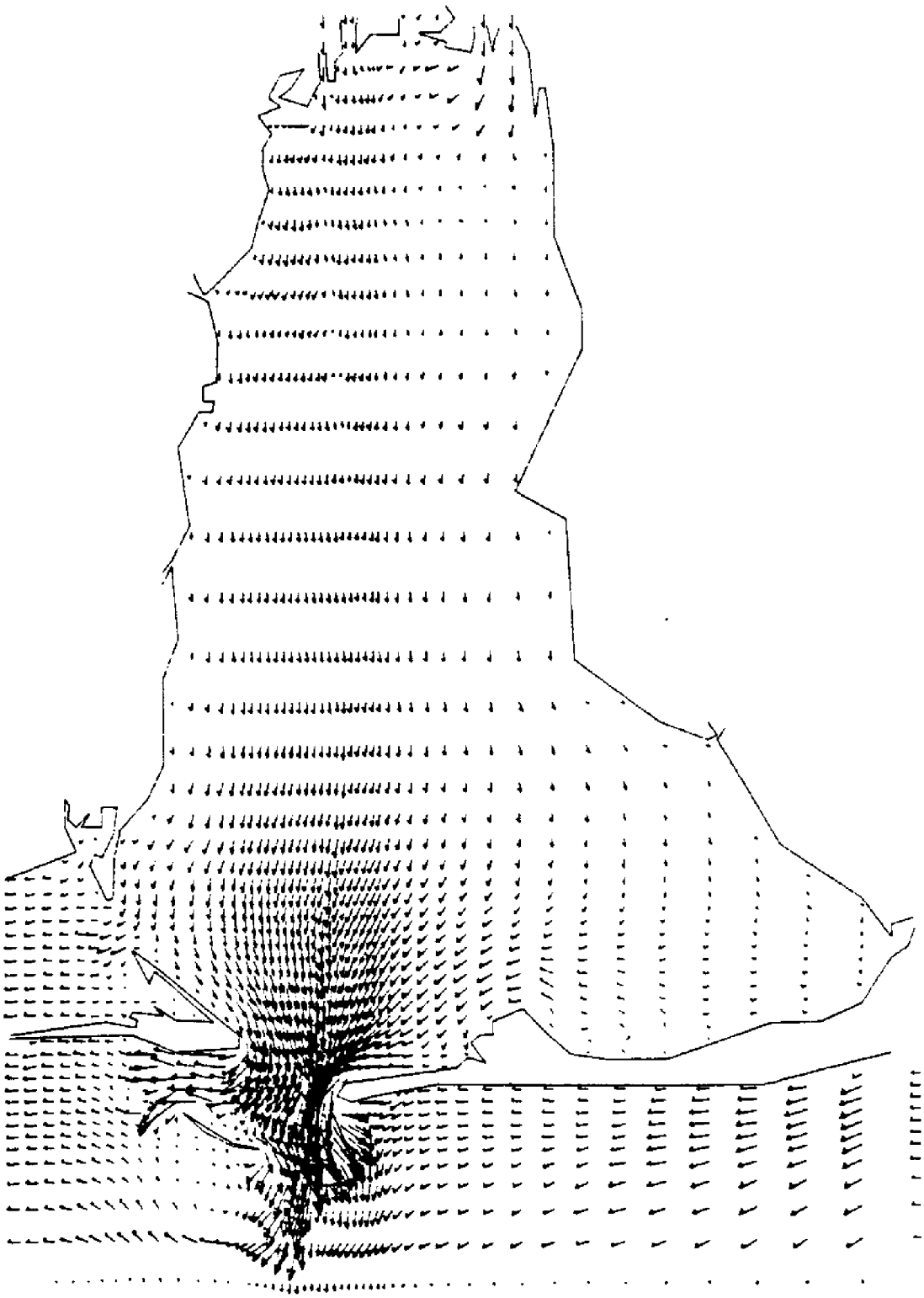

FLOW RATE FIELD AT T(HR) = 12.00
MAXIMUM VELOCITY (FT/SEC) = 3.64

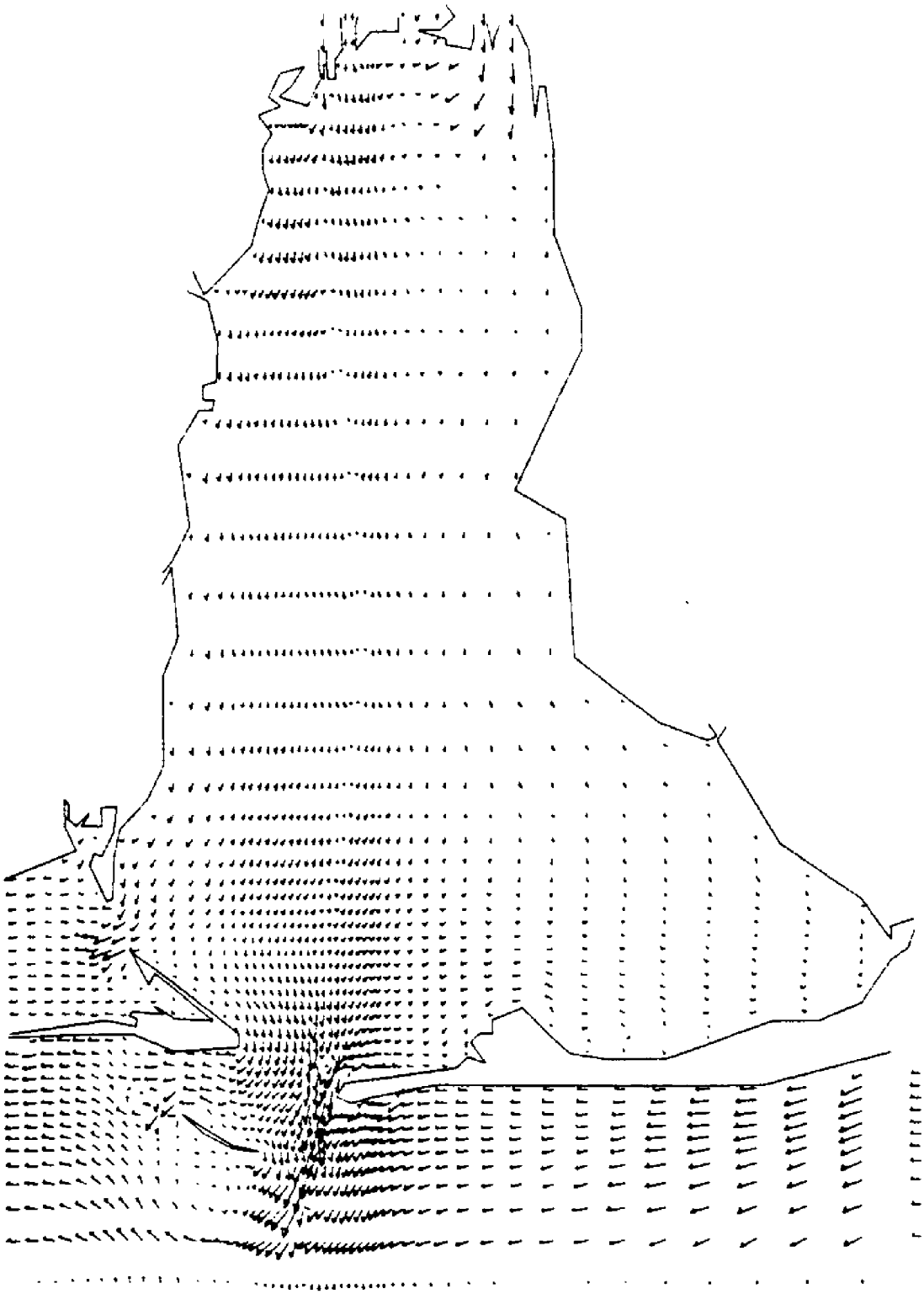

FLOW RATE FIELD AT T(HR) = 16.00
MAXIMUM VELOCITY (FT/SEC) = 1.67

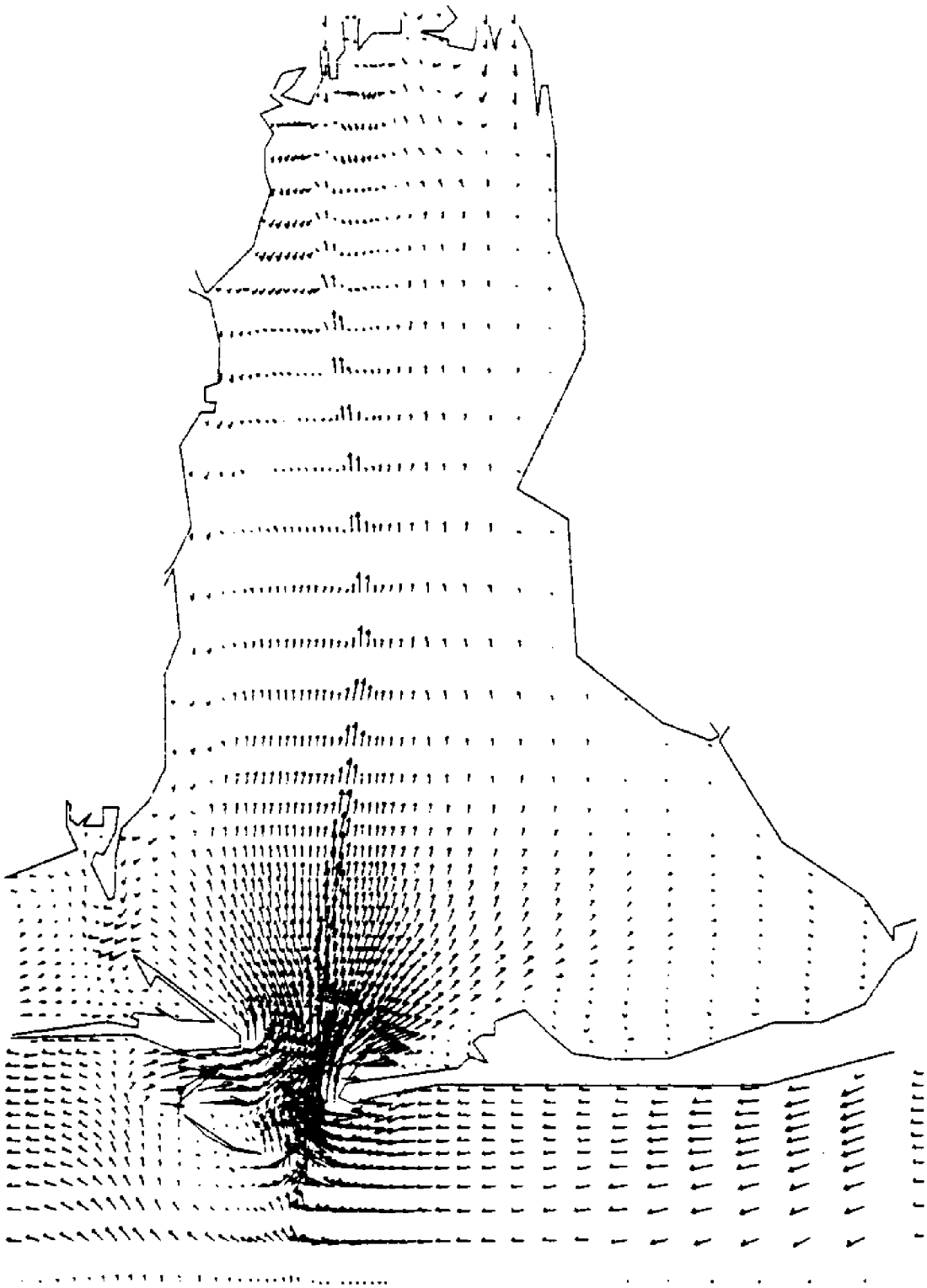

FLOW RATE FIELD AT T(HR) = 20.00
MAXIMUM VELOCITY (FT/SEC) = 3.75

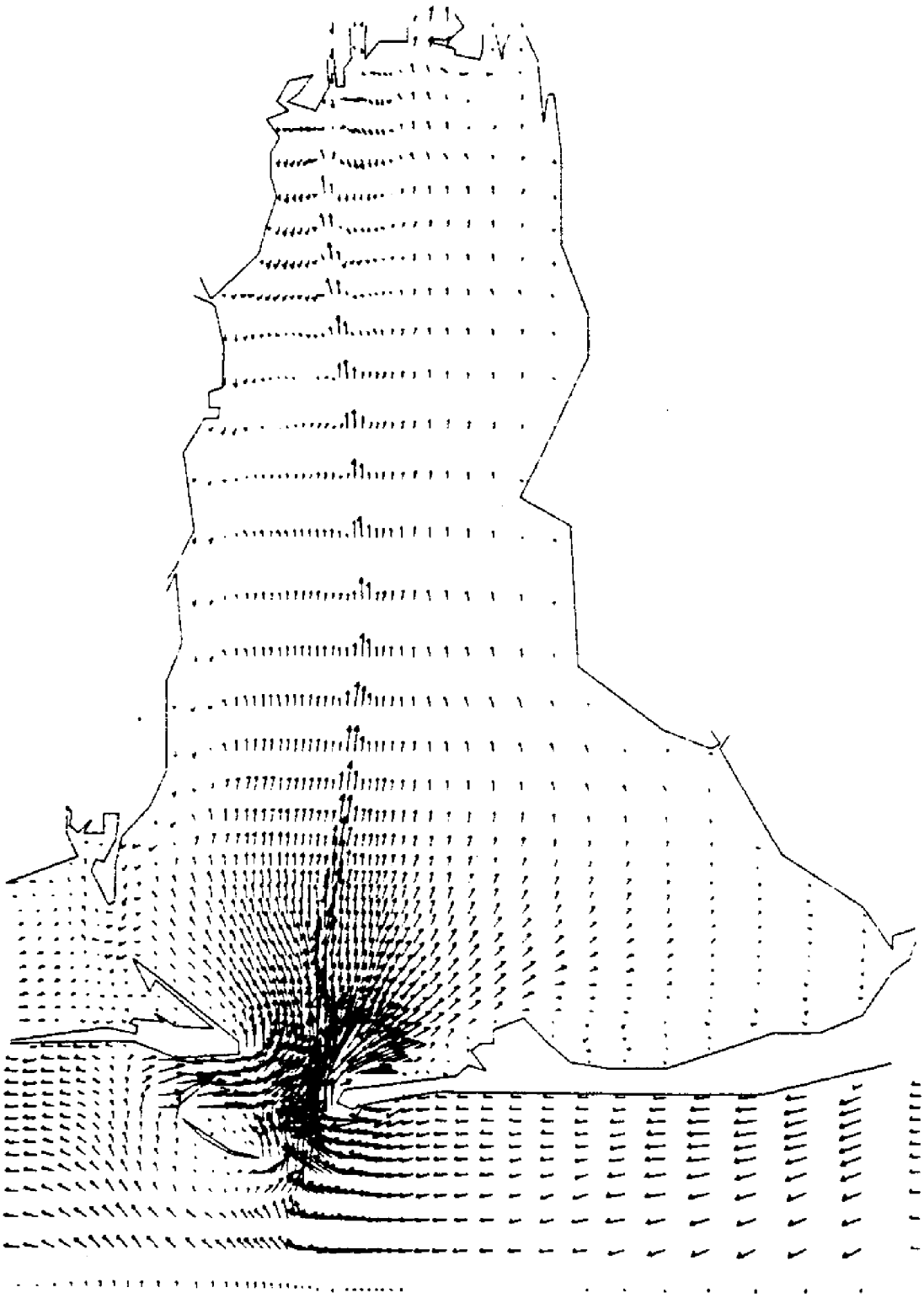

FLOW RATE FIELD AT T(HR) = 24.00
MAXIMUM VELOCITY (FT/SEC) = 4.06

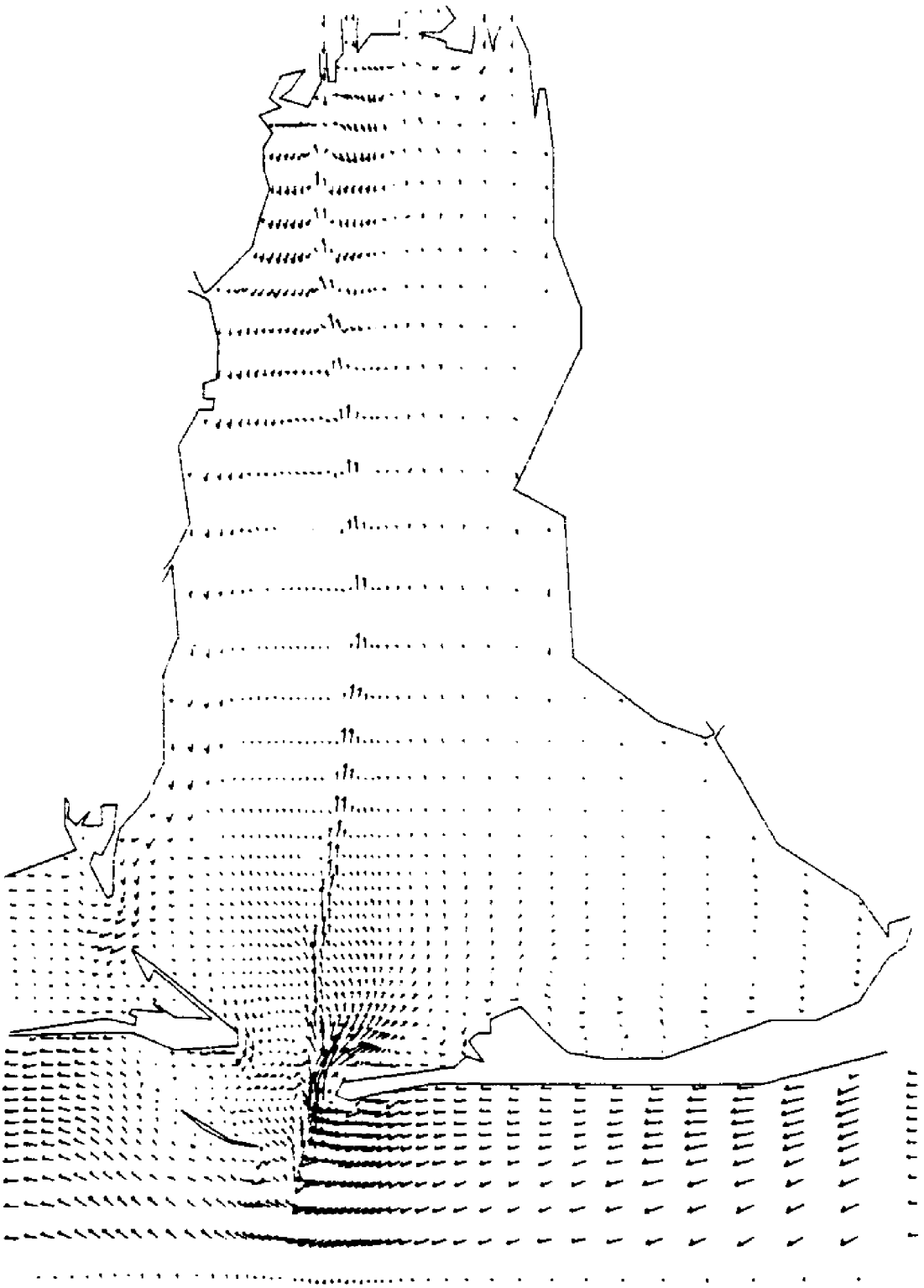

FLOW RATE FIELD AT T(HR) = 28.00
MAXIMUM VELOCITY (FT/SEC) = 1.67

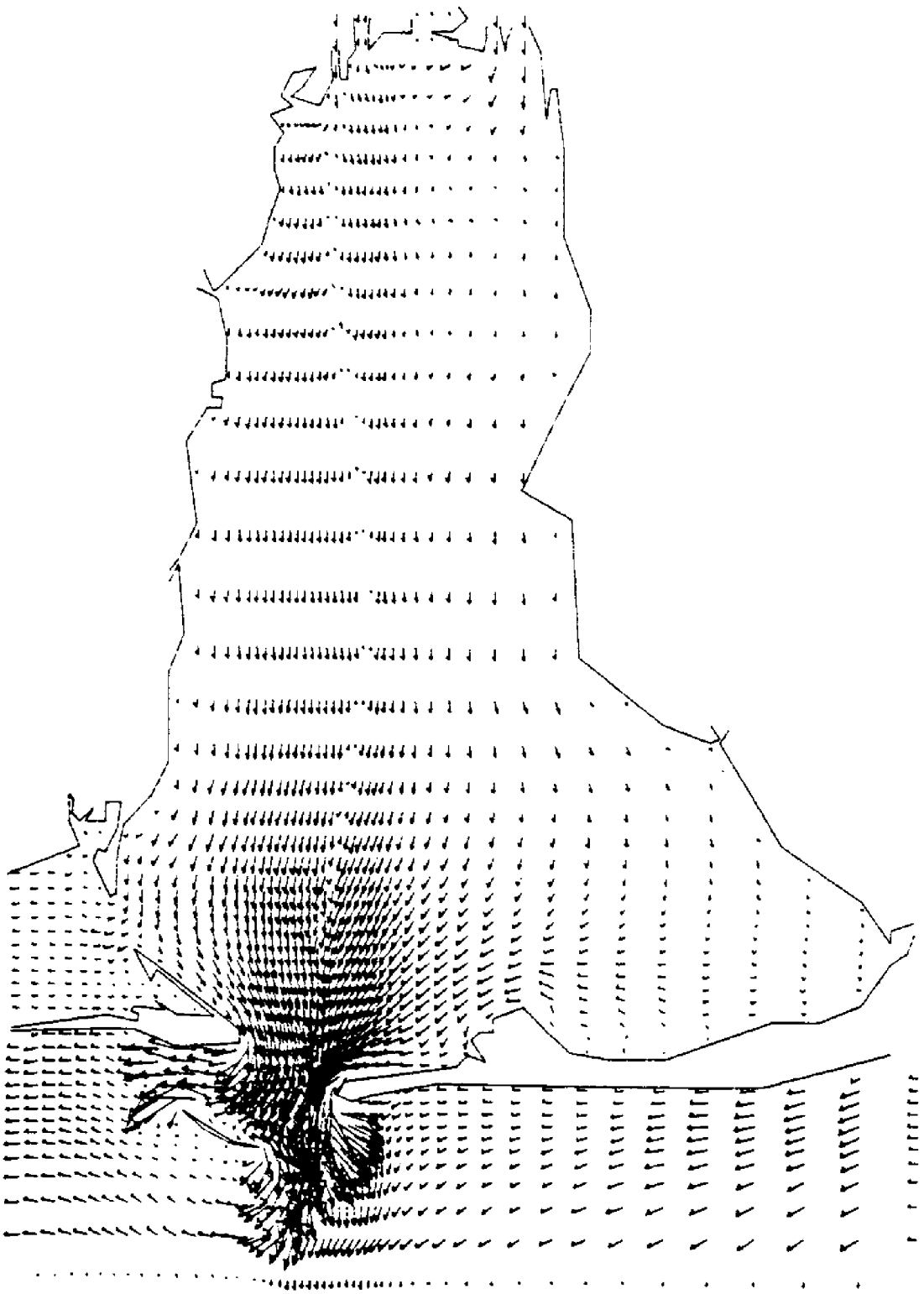

FLOW RATE FIELD AT T(HR) = 32.00
MAXIMUM VELOCITY (FT/SEC) = 3.96

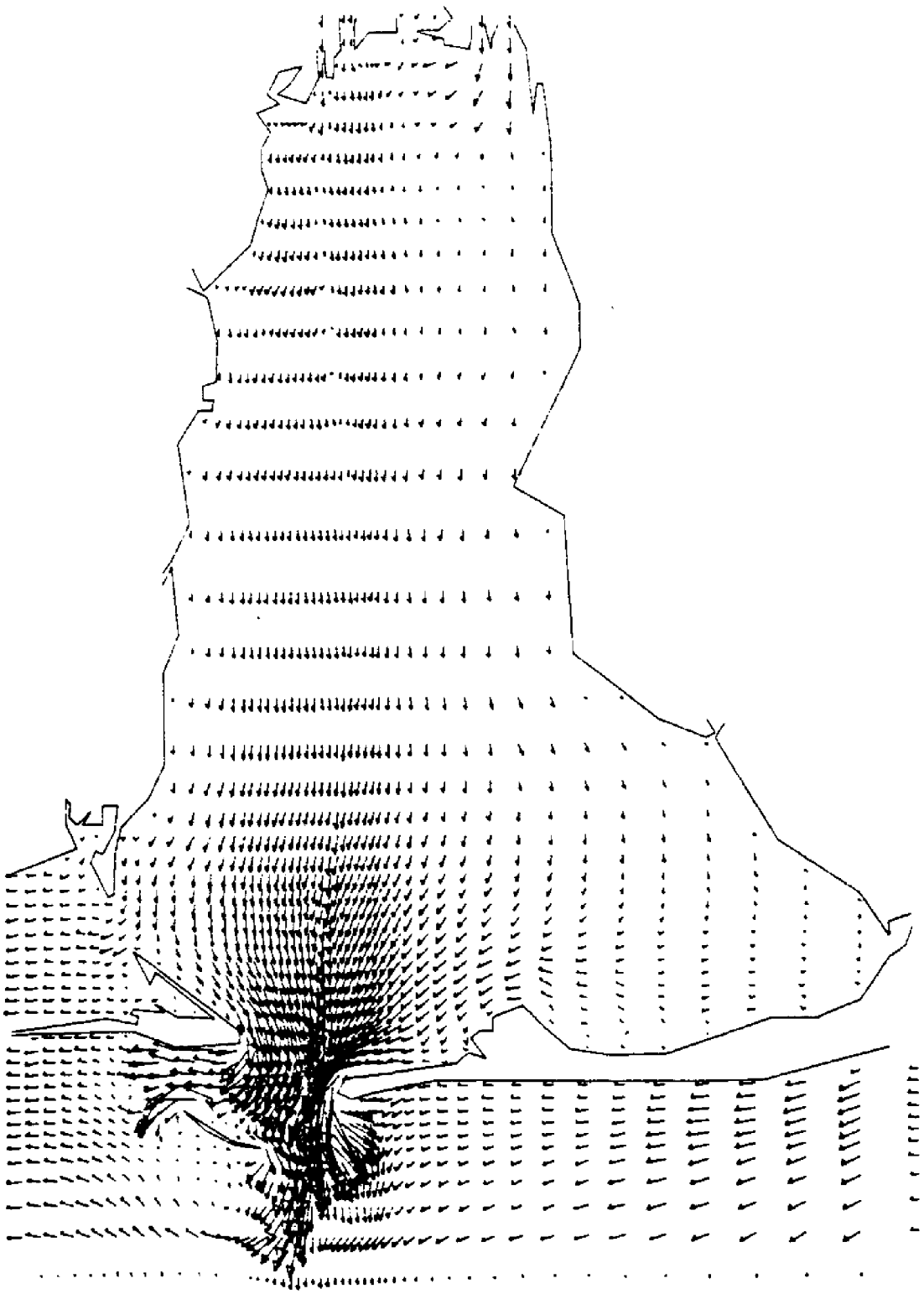

FLOW RATE FIELD AT T(HR) = 36.00
MAXIMUM VELOCITY (FT/SEC) = 4.06

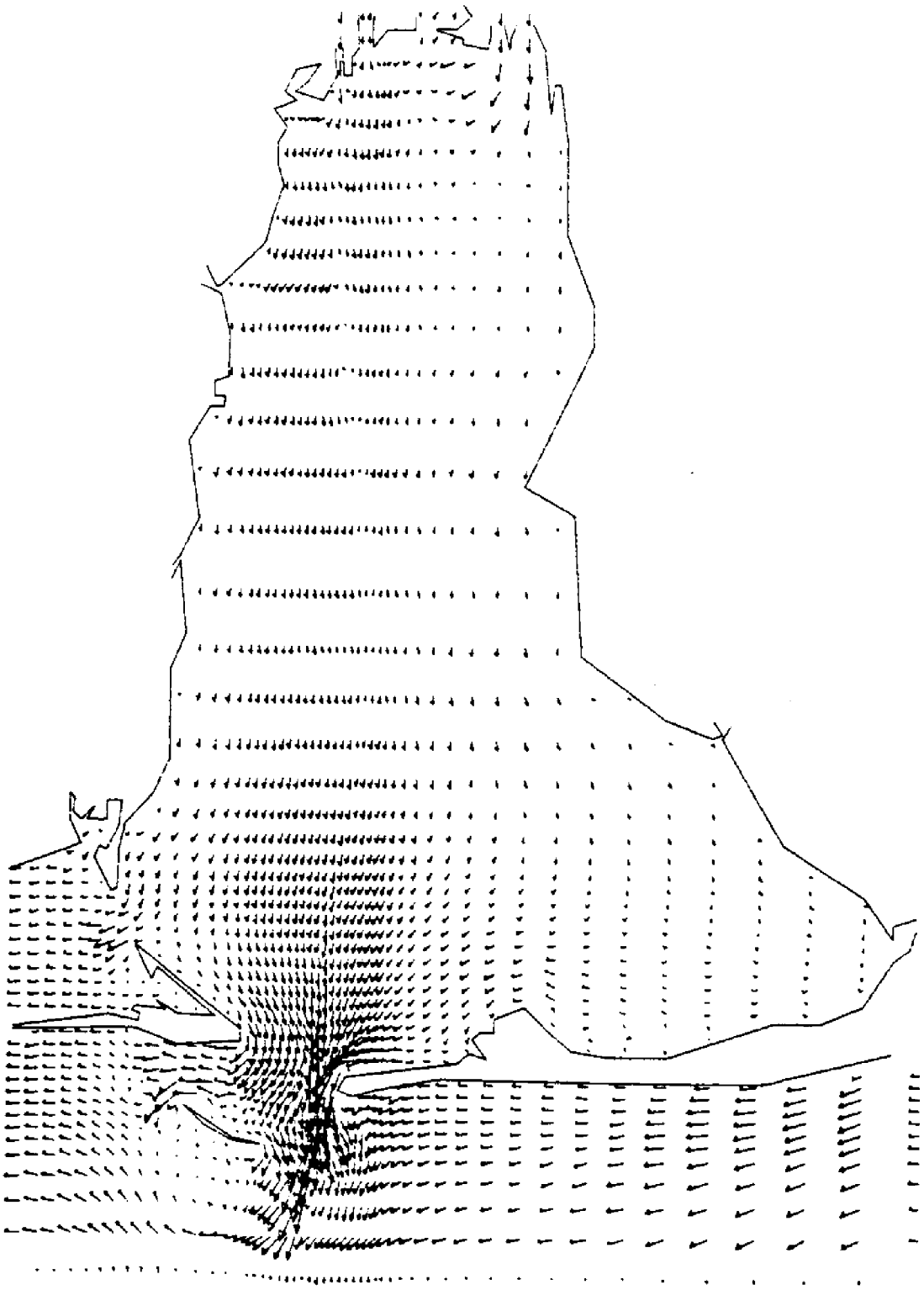

FLOW RATE FIELD AT T(HR) = 40.00
MAXIMUM VELOCITY (FT/SEC) = 2.37

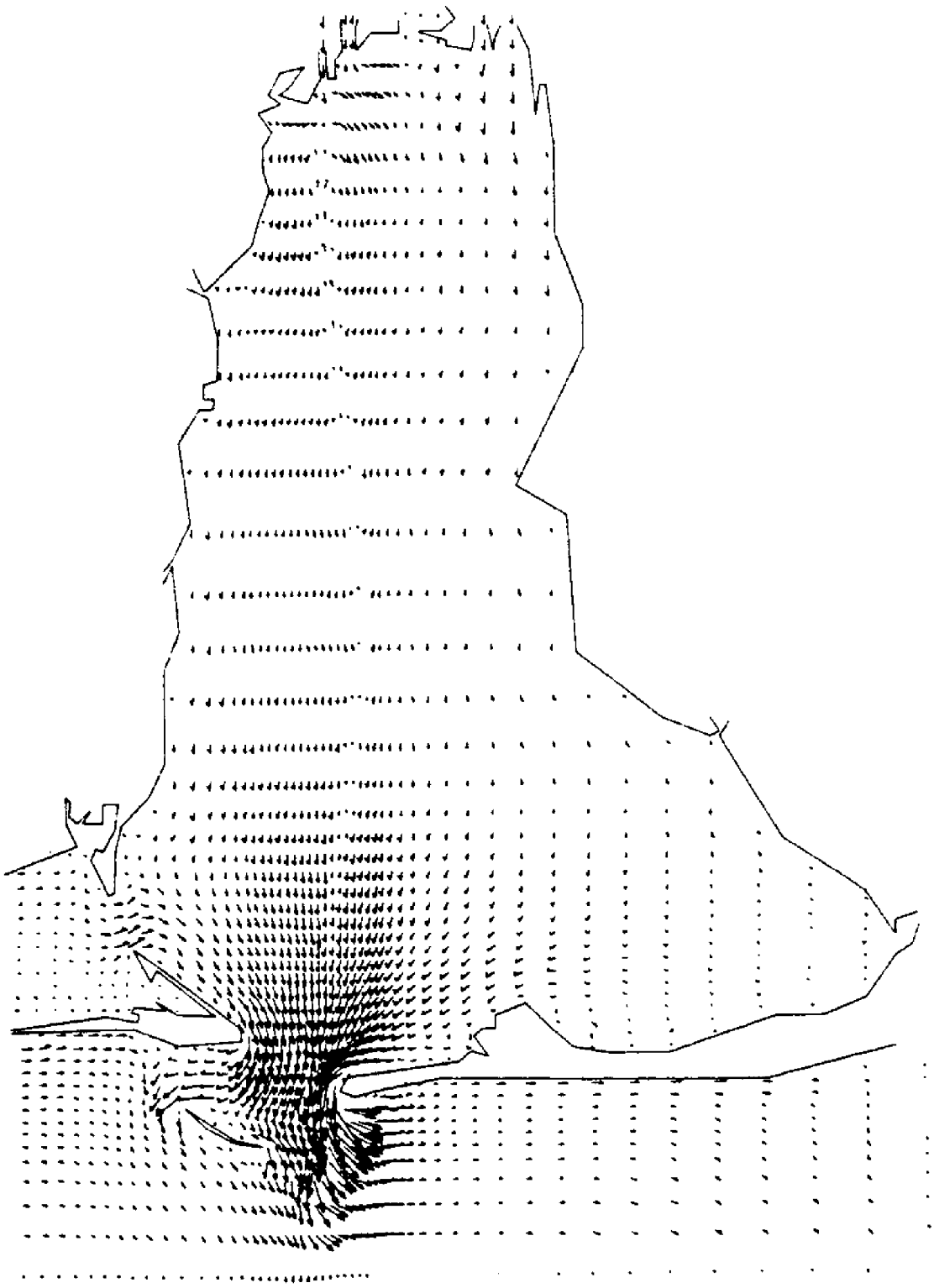

FLOW RATE FIELD AT T(HR) = 4.00
MAXIMUM VELOCITY (FT/SEC) = 2.35

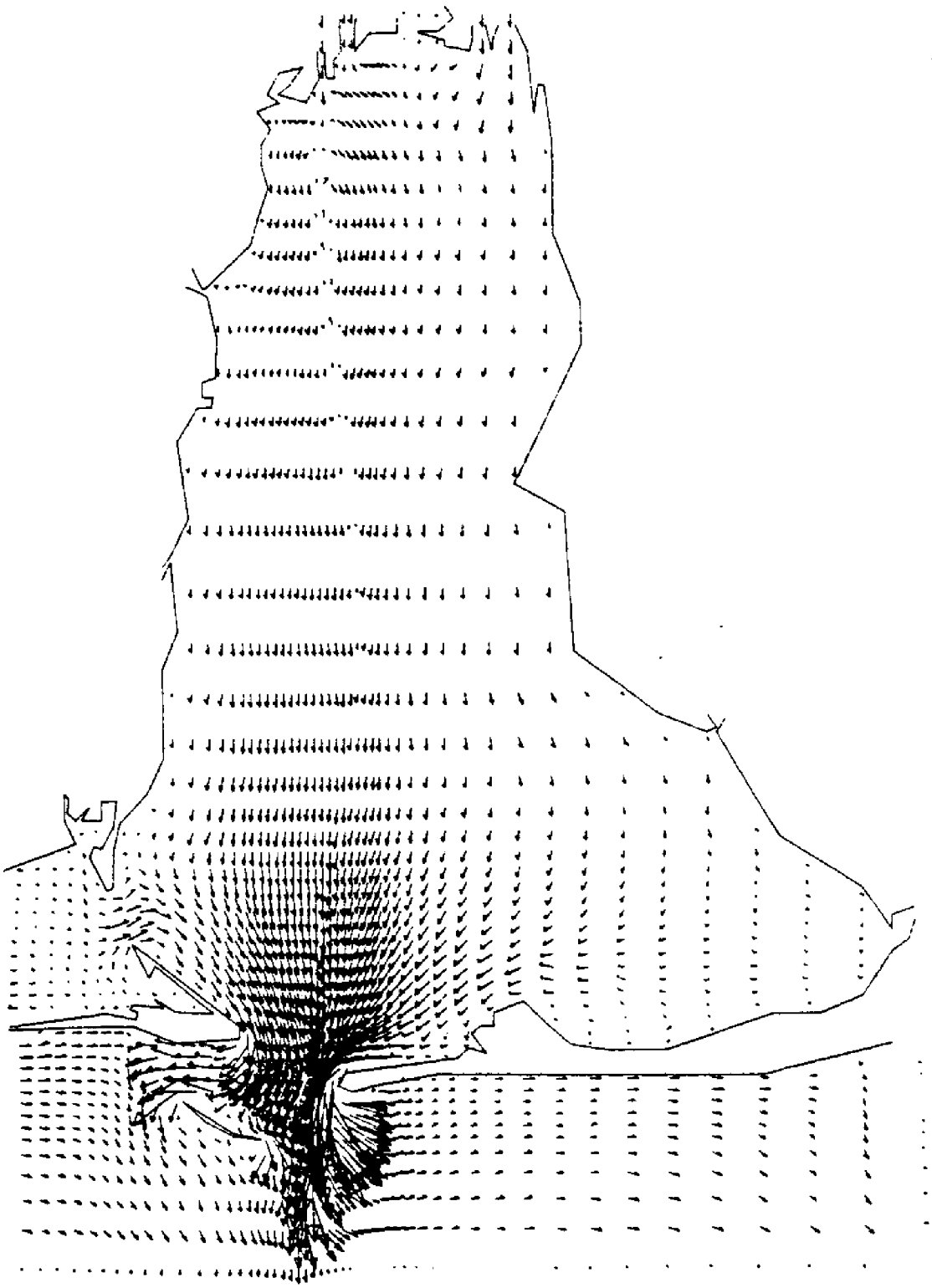

FLOW RATE FIELD AT T(HR) = 8.00
MAXIMUM VELOCITY (FT/SEC) = 4.26

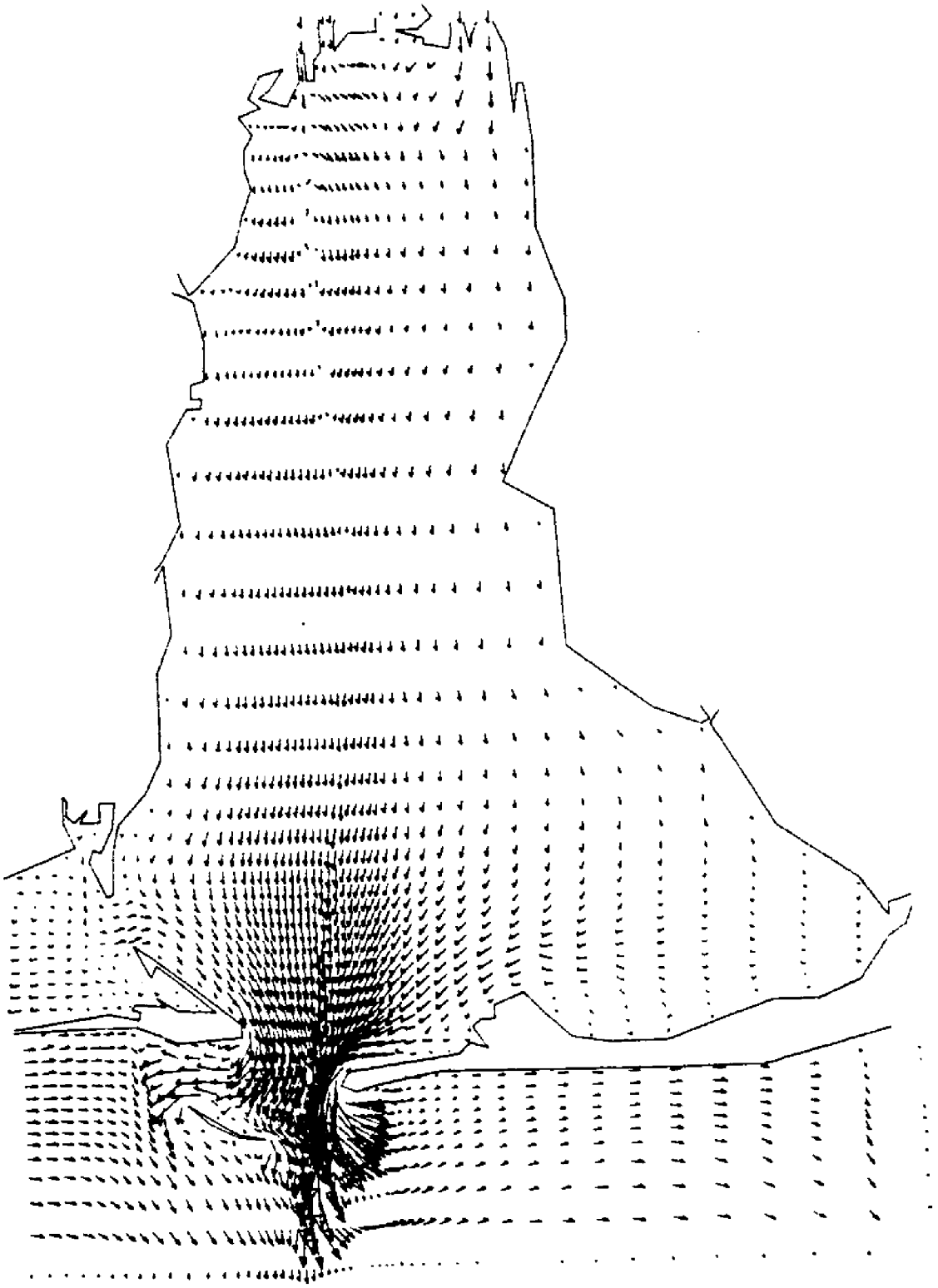

FLOW RATE FIELD AT T(HR) = 12.00
MAXIMUM VELOCITY (FT/SEC) = 3.76

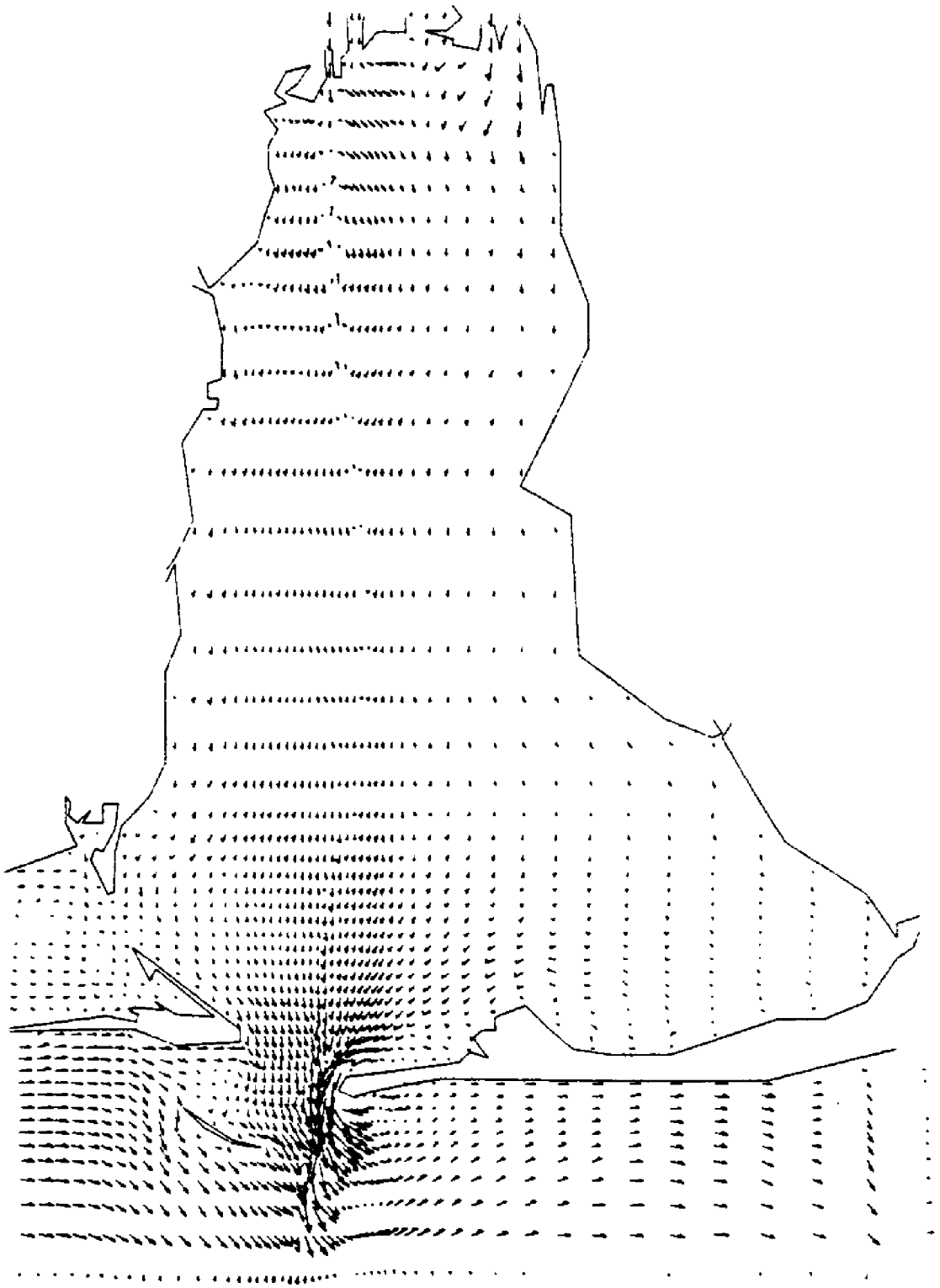

FLOW RATE FIELD AT T(HR) = 16.00
MAXIMUM VELOCITY (FT/SEC) = 1.80

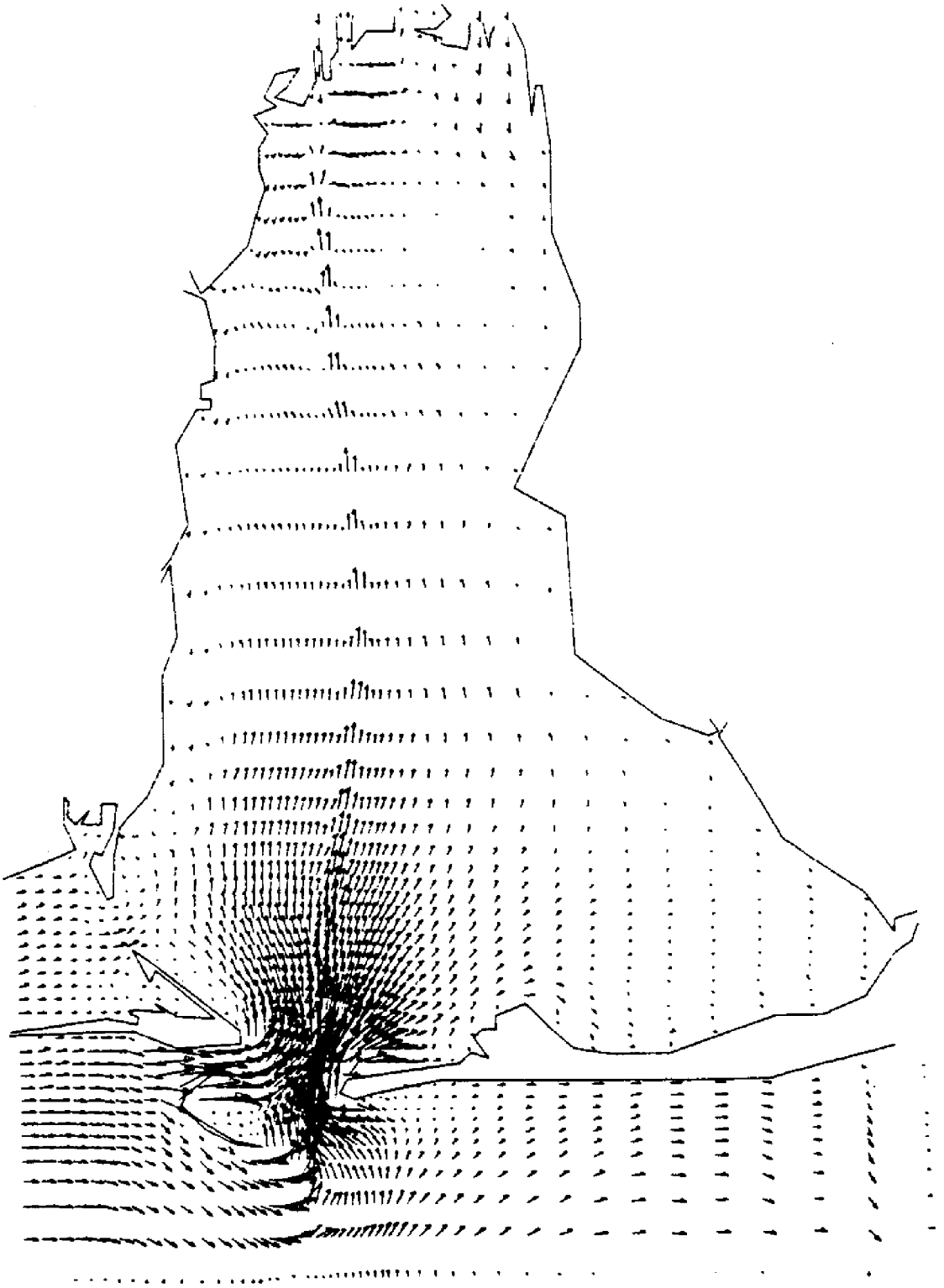

FLOW RATE FIELD AT T(HR) = 20.00
MAXIMUM VELOCITY (FT/SEC) = 3.31

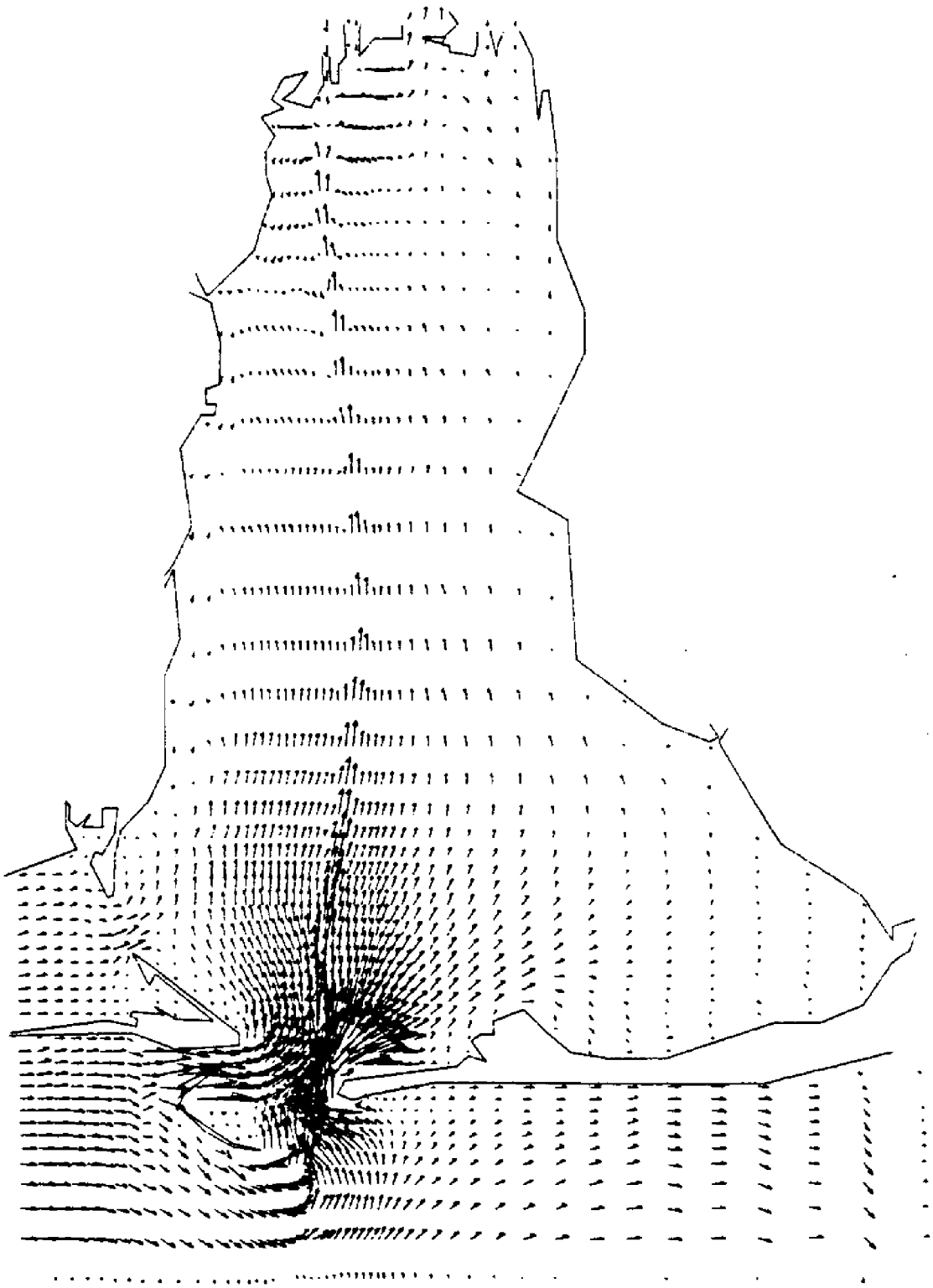

FLOW RATE FIELD AT T(HR) = 24.00
MAXIMUM VELOCITY (FT/SEC) = 3.85

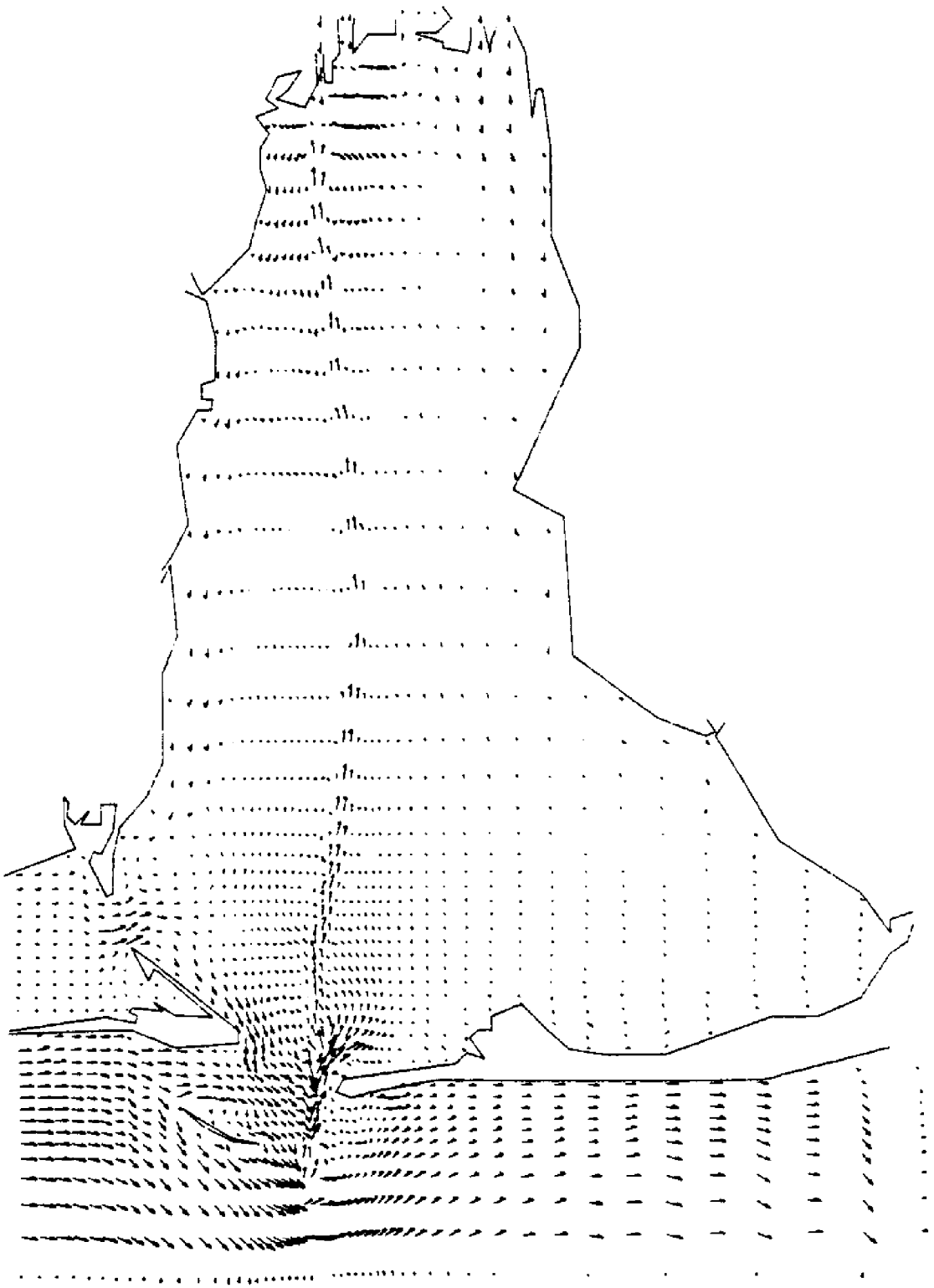

FLOW RATE FIELD AT T(HR) = 28.00
MAXIMUM VELOCITY (FT/SEC) = 1.33

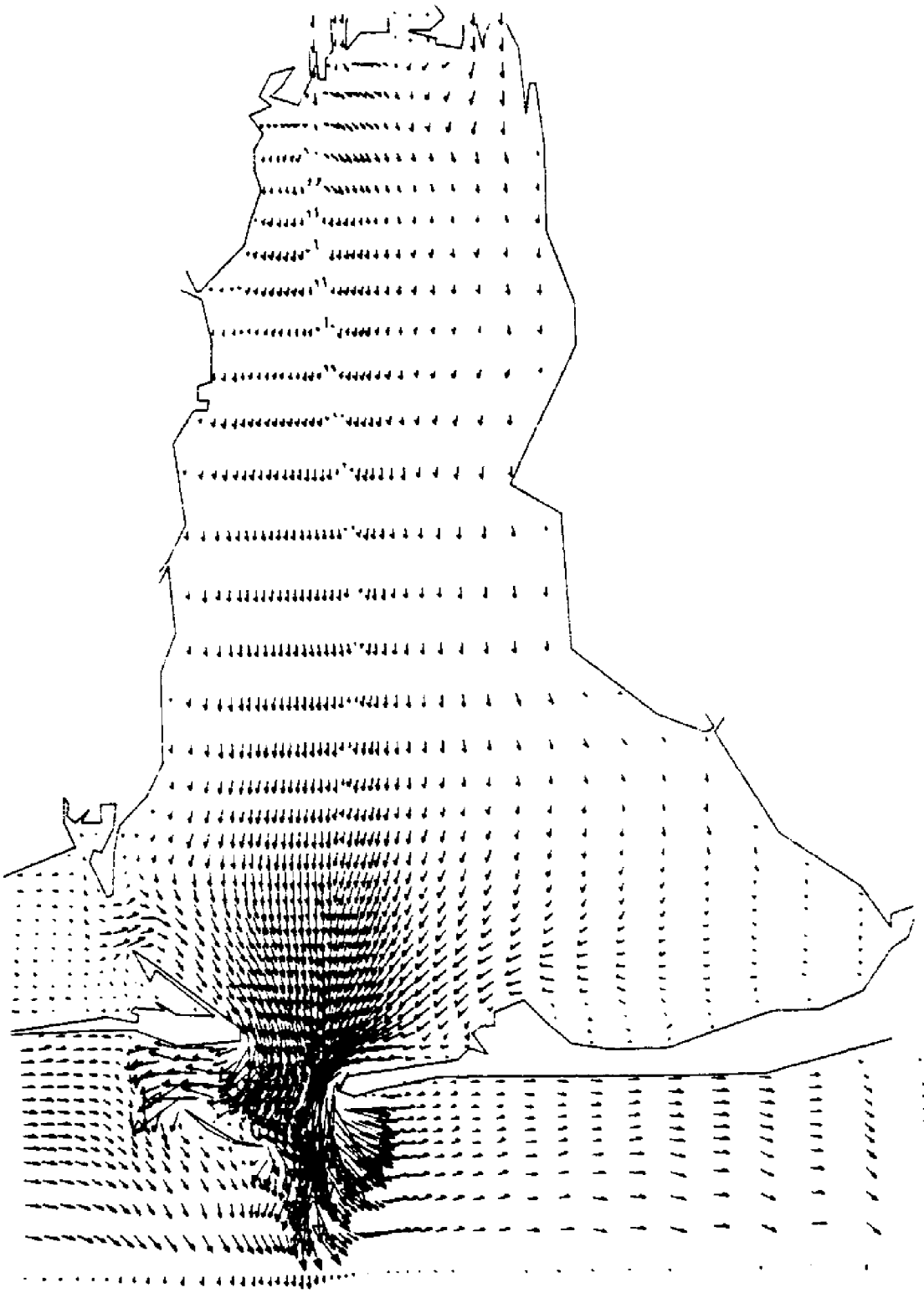

FLOW RATE FIELD AT T(HR) = 32.00
MAXIMUM VELOCITY (FT/SEC) = 4.19

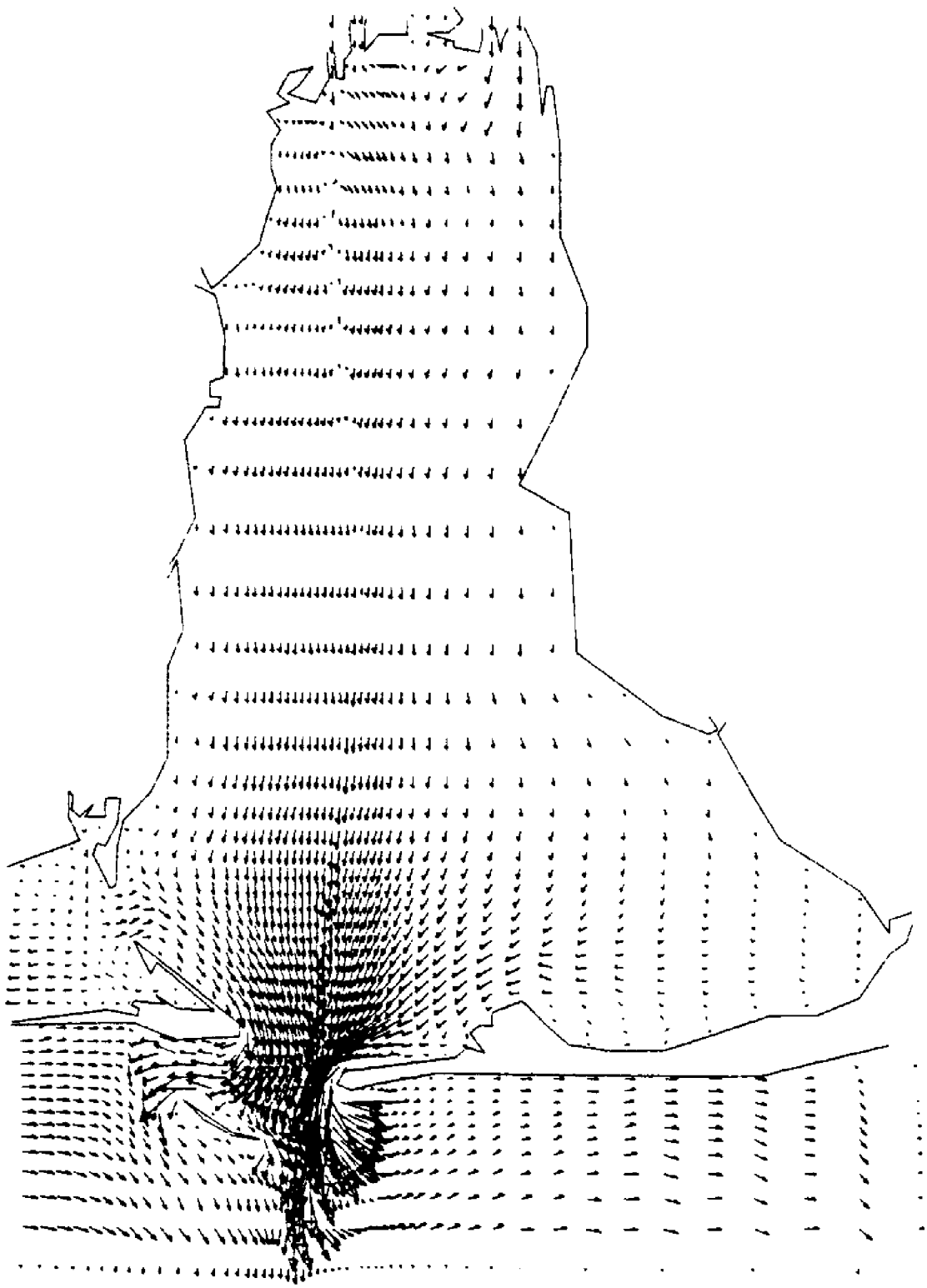

FLOW RATE FIELD AT T(HR) = 36.00
MAXIMUM VELOCITY (FT/SEC) = 4.15

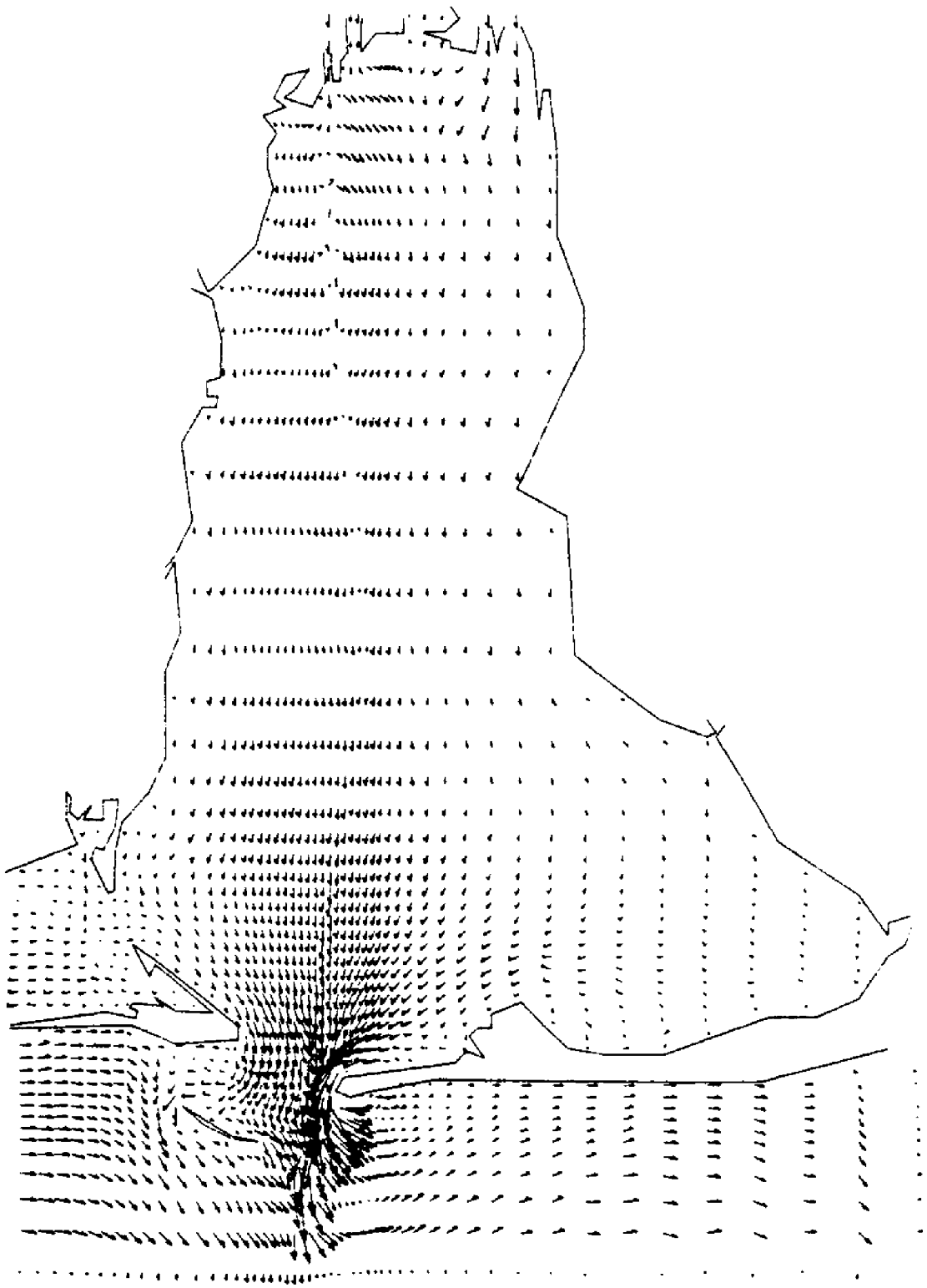

FLOW RATE FIELD AT T(HR) = 40.00
MAXIMUM VELOCITY (FT/SEC) = 2.50

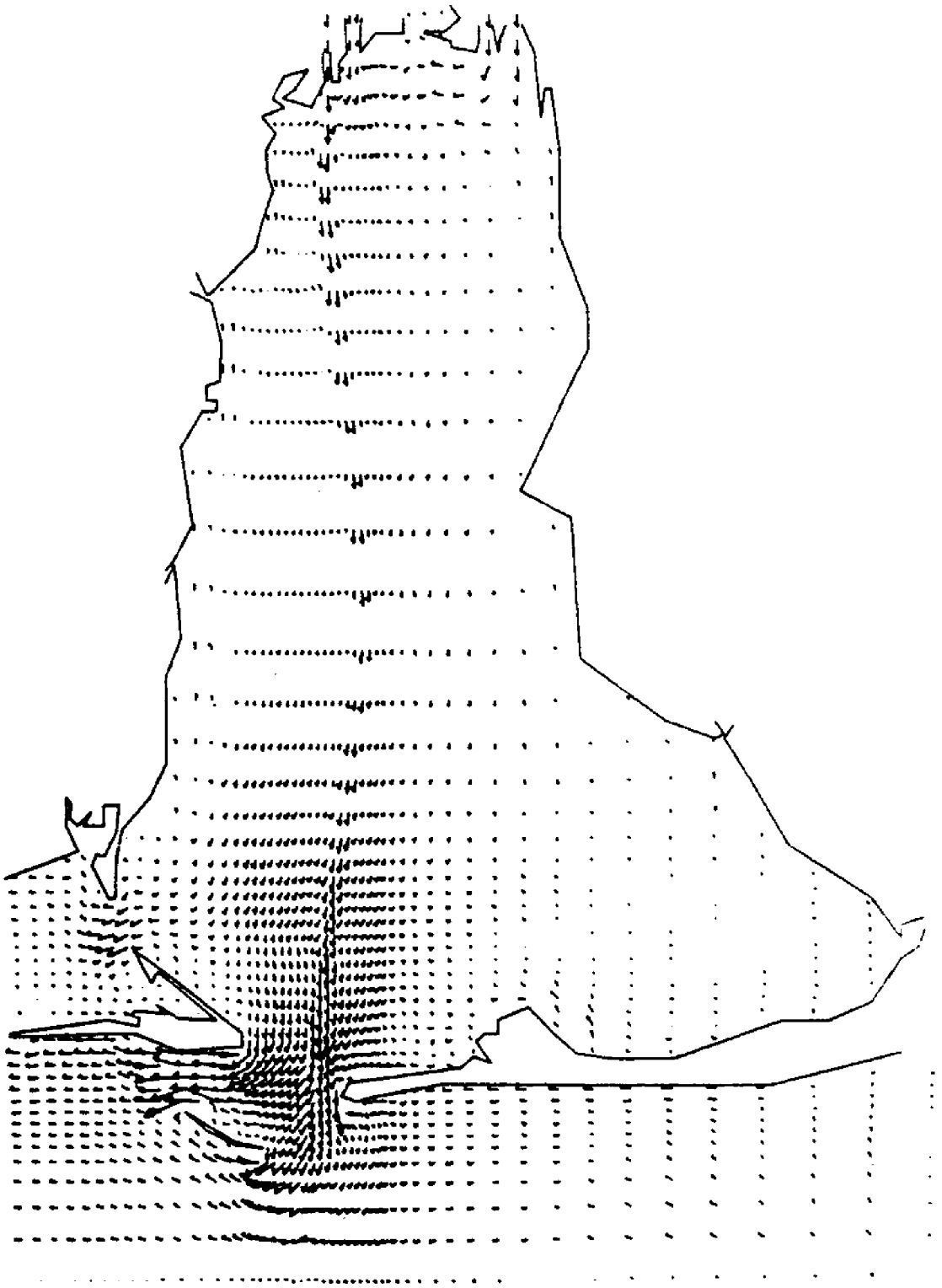

FLOW RATE FIELD AT T(HR) = 4.00
MAXIMUM VELOCITY (FT/SEC) = 1.86

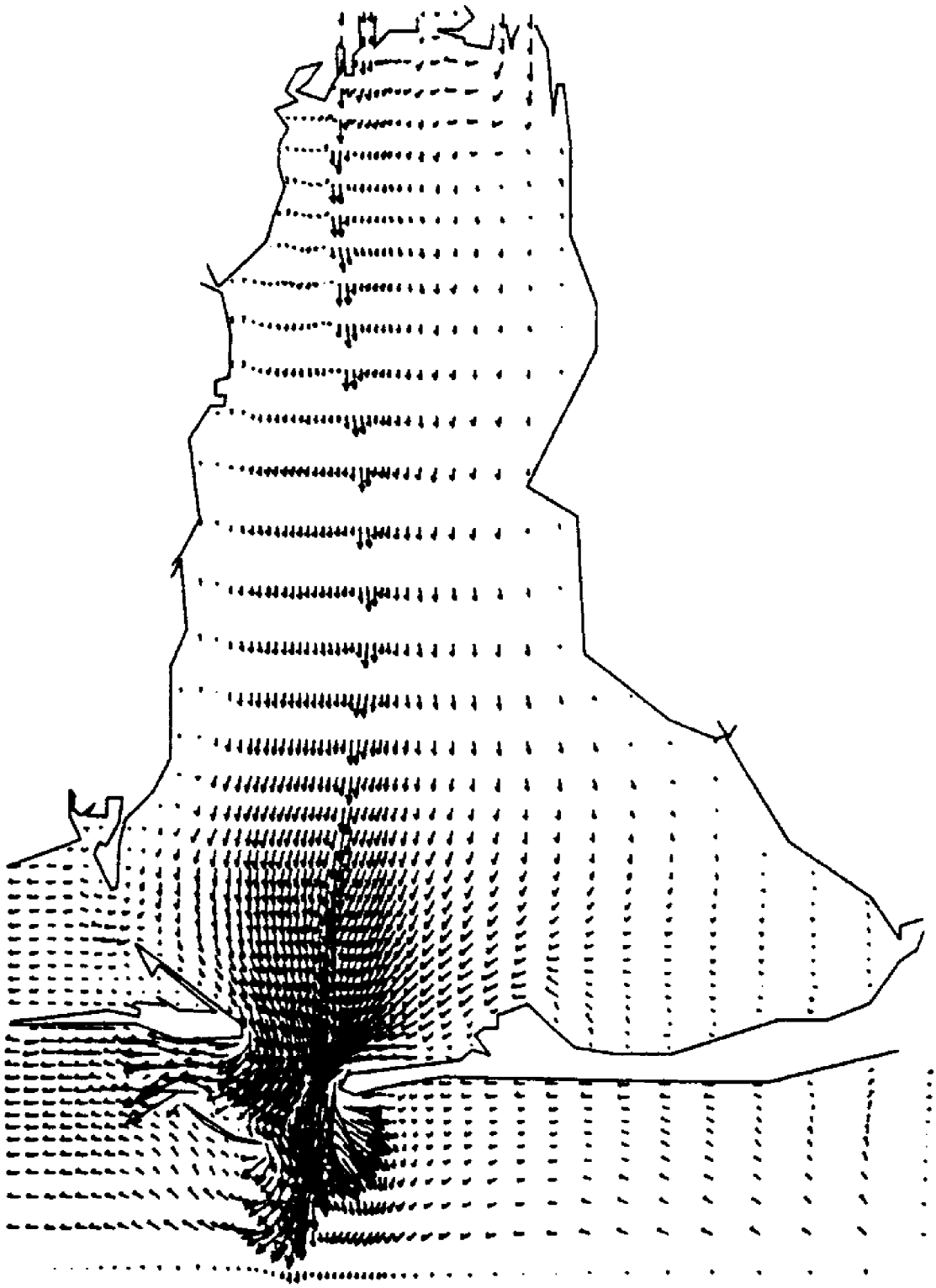

FLOW RATE FIELD AT T(HR) = 8.00
MAXIMUM VELOCITY (FT/SEC) = 4.27

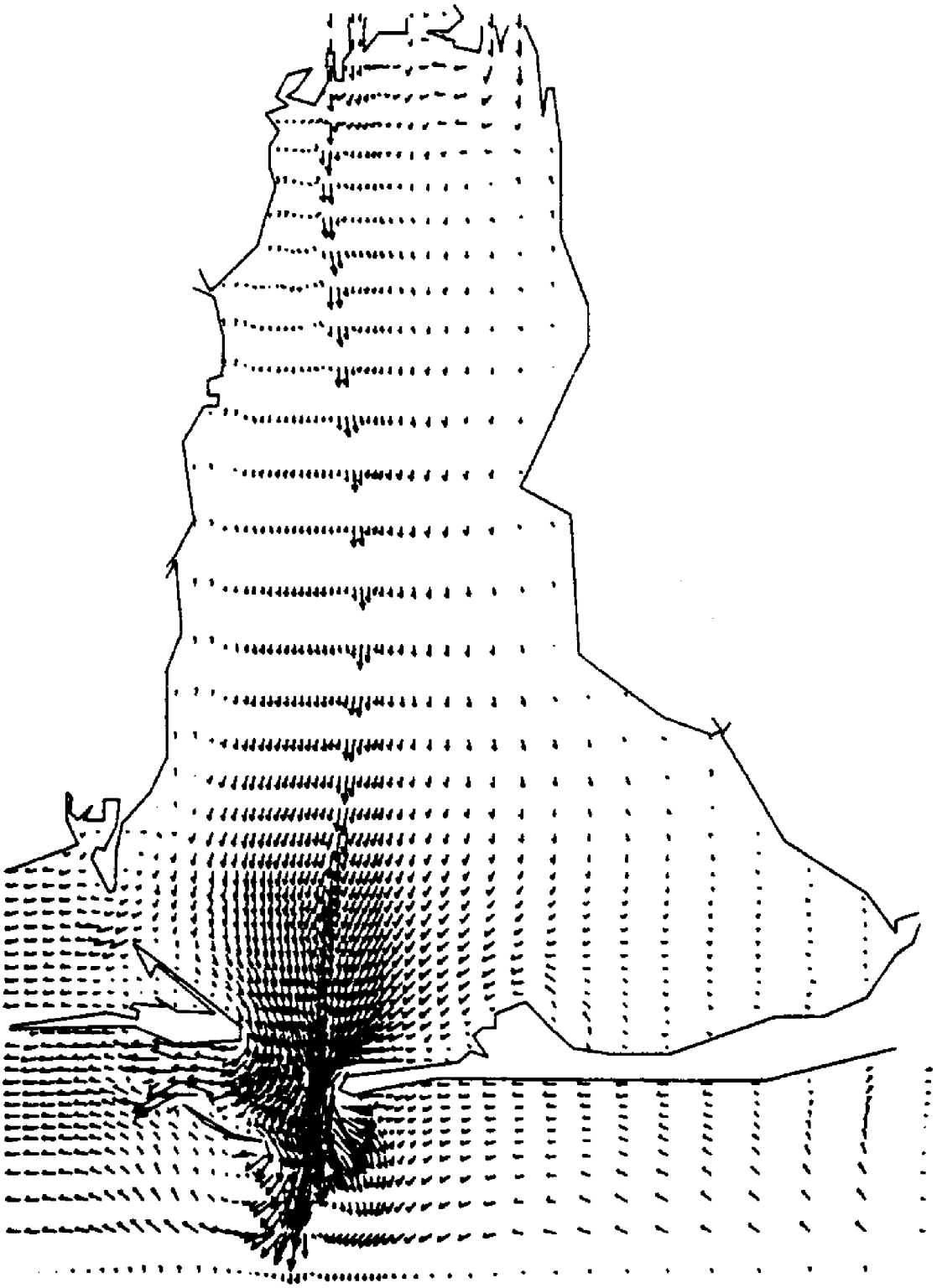

FLOW RATE FIELD AT T(HR) = 12.00
MAXIMUM VELOCITY (FT/SEC) = 3.73

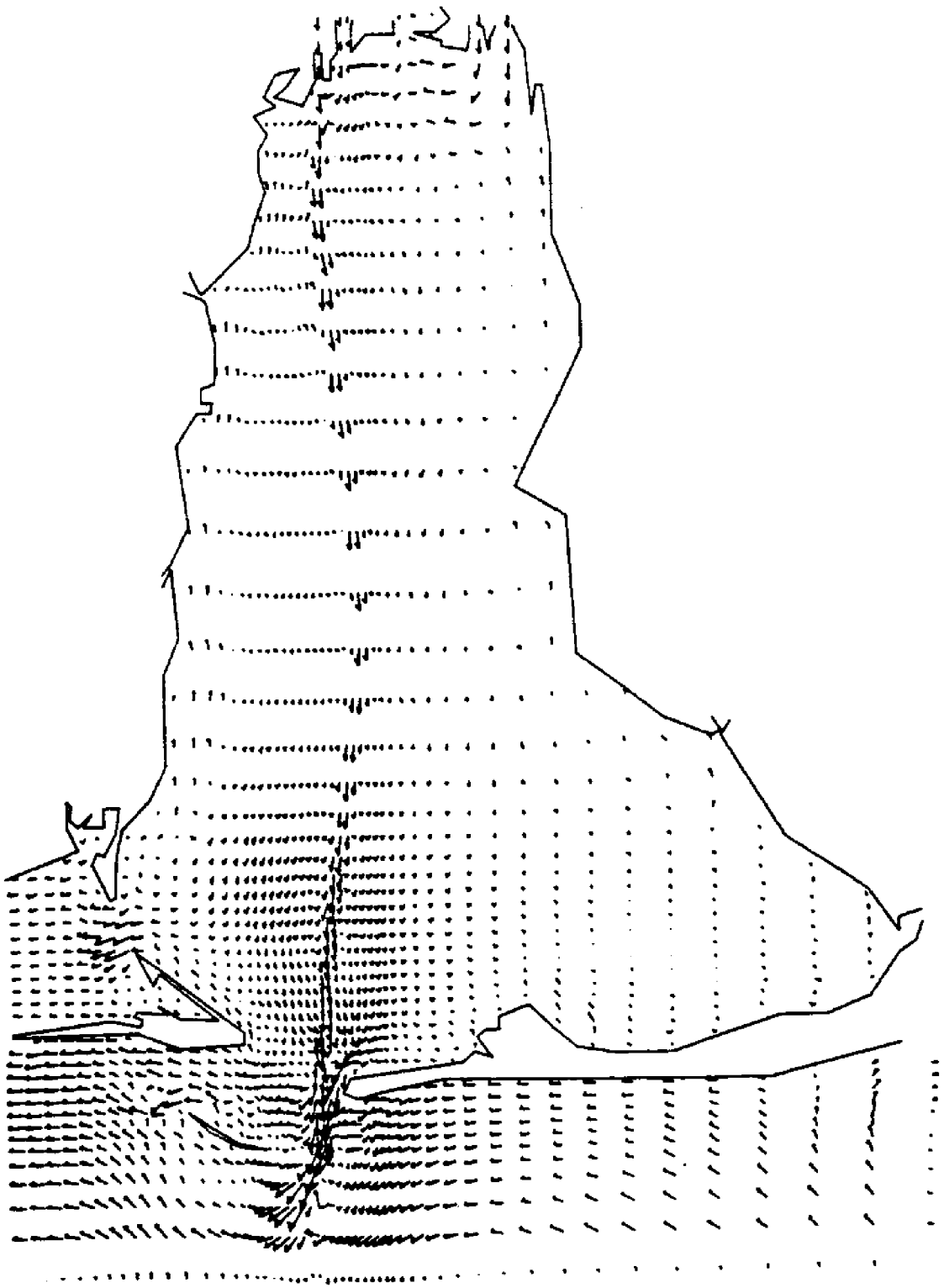

FLOW RATE FIELD AT T(HR) = 16.00
MAXIMUM VELOCITY (FT/SEC) = 1.72

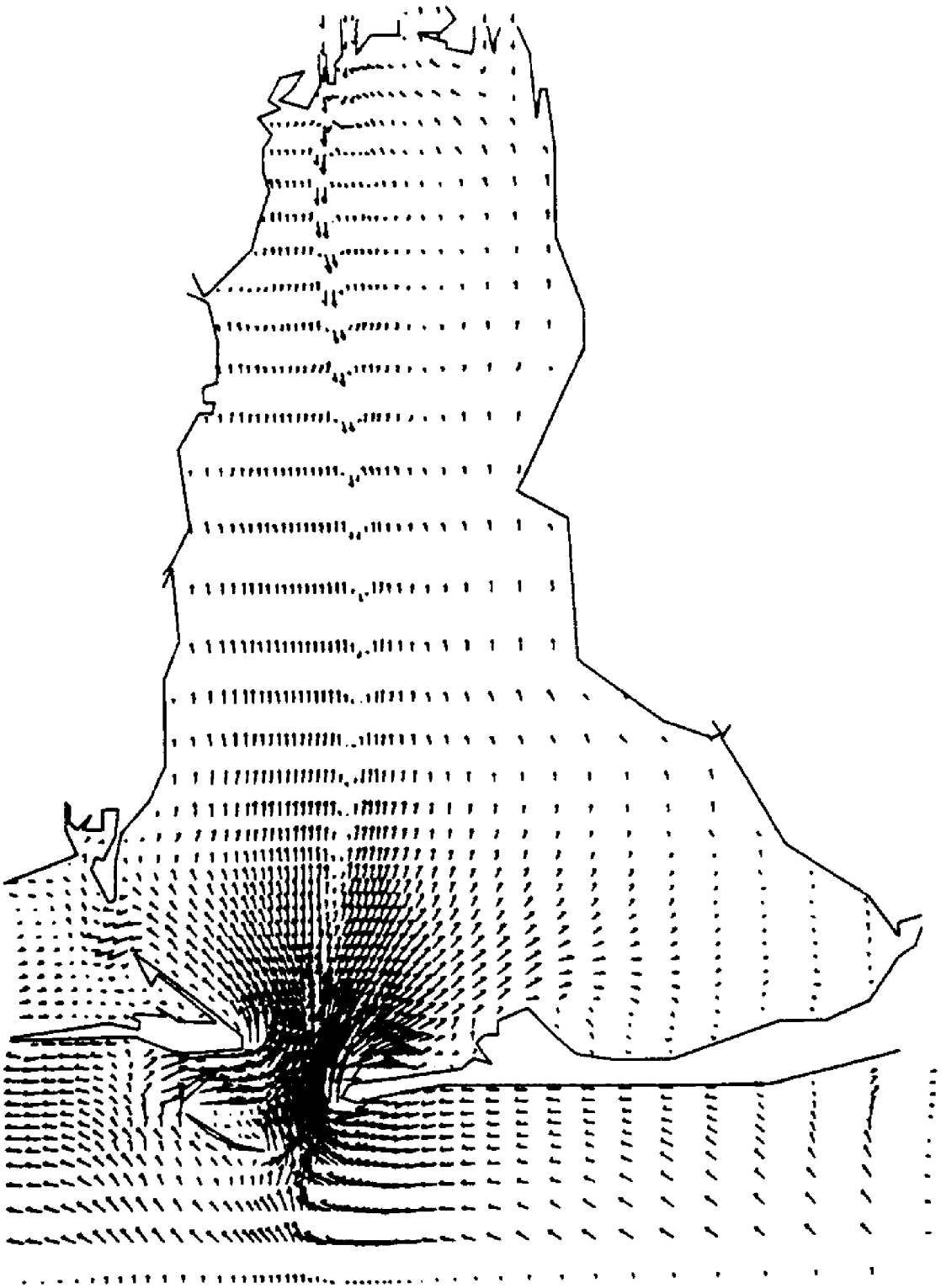

FLOW RATE FIELD AT T(HR) = 20.00
MAXIMUM VELOCITY (FT/SEC) = 3.63

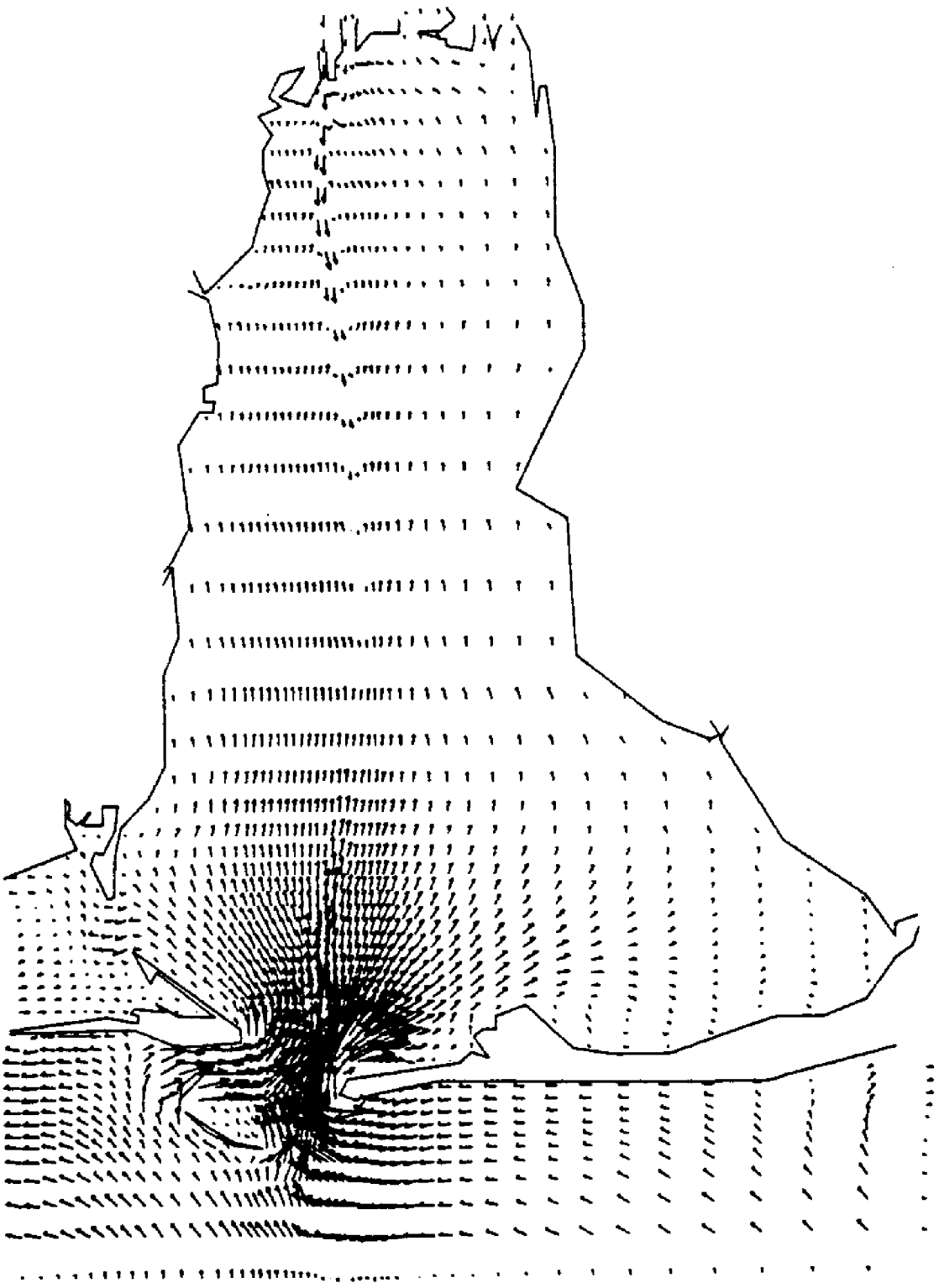

FLOW RATE FIELD AT T(HR) = 24.00
MAXIMUM VELOCITY (FT/SEC) = 3.92

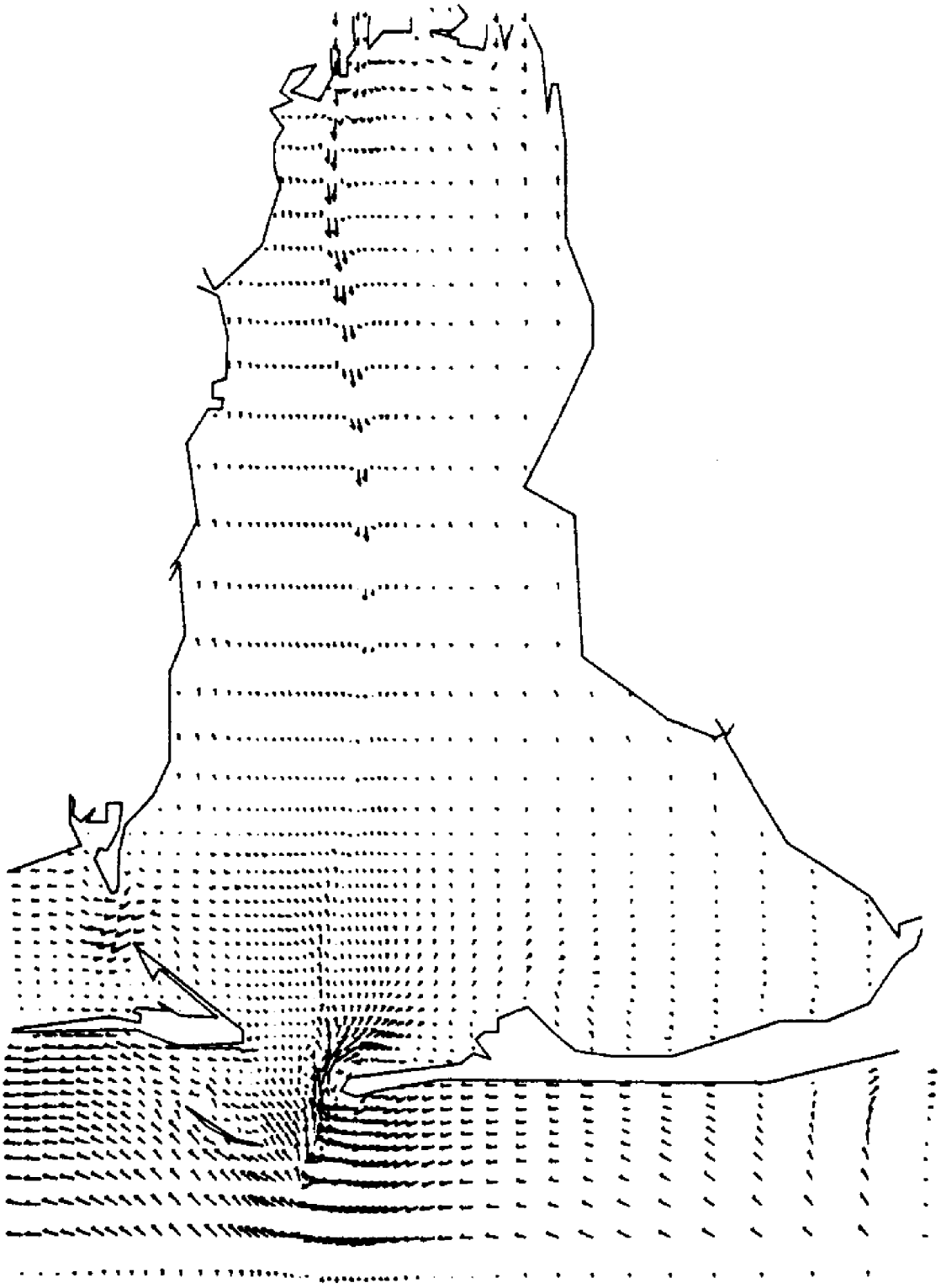

FLOW RATE FIELD AT T(HR) = 28.00
MAXIMUM VELOCITY (FT/SEC) = 1.29

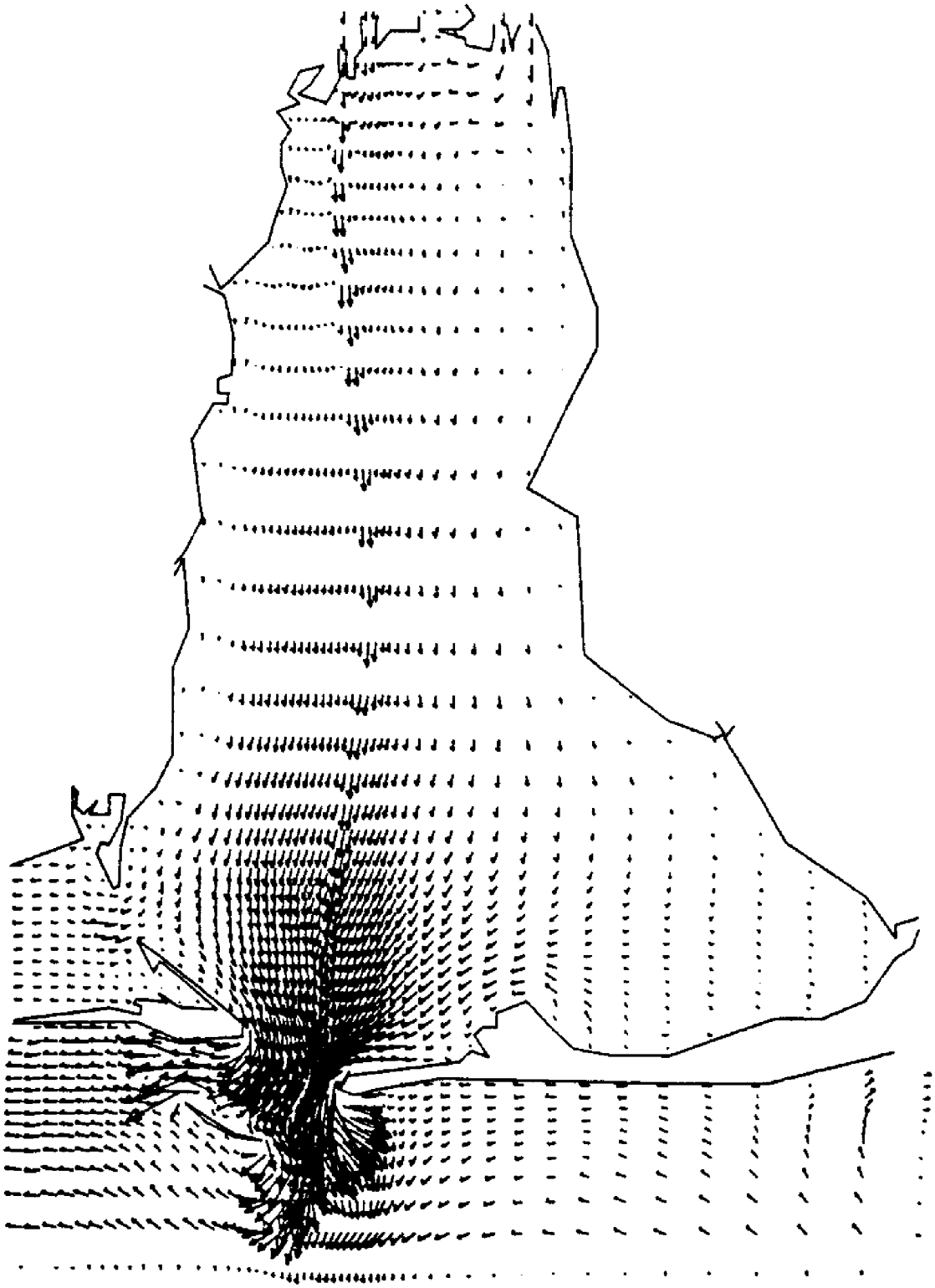

FLOW RATE FIELD AT T(HR) = 32.00
MAXIMUM VELOCITY (FT/SEC) = 4.09

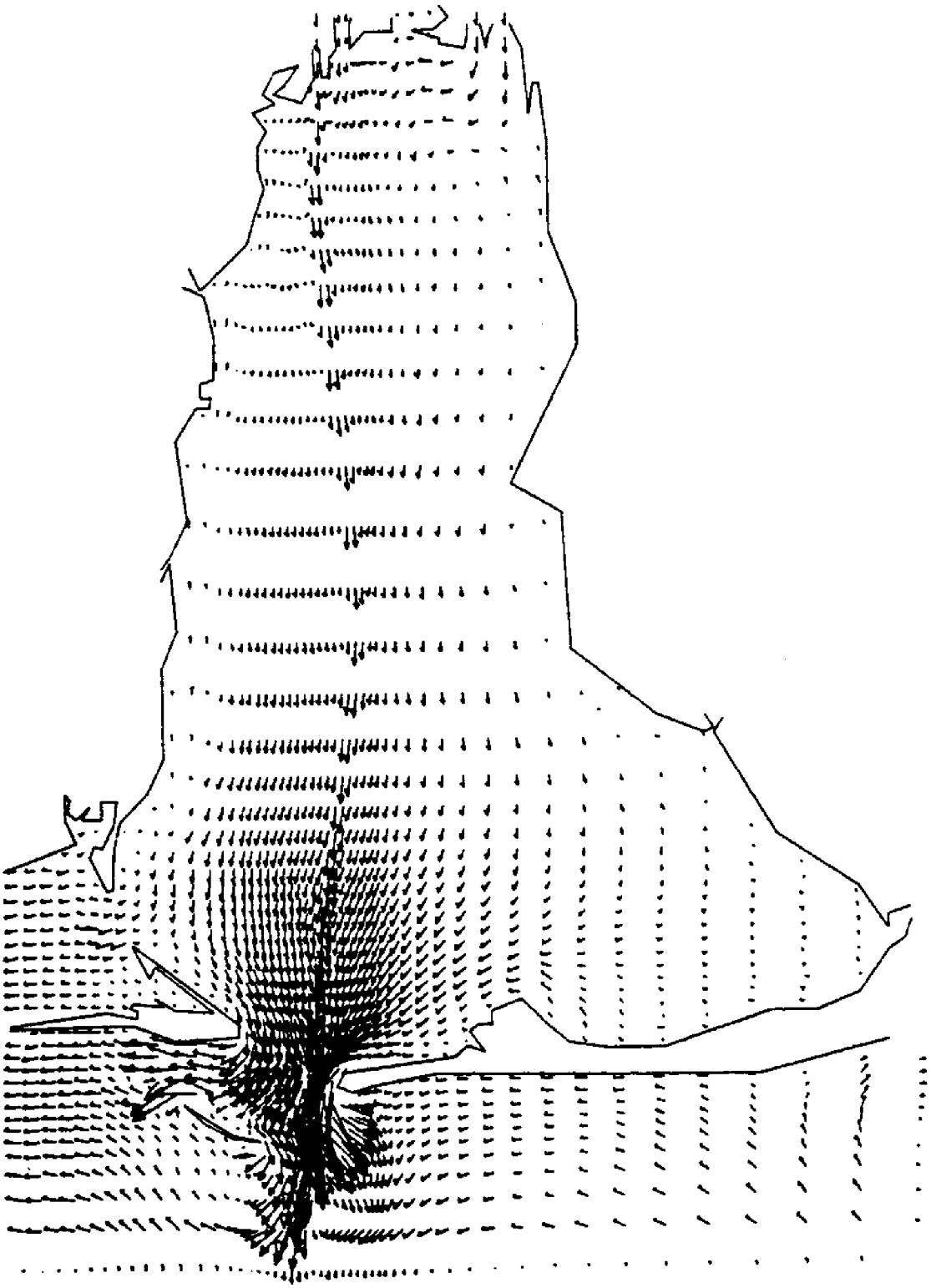

FLOW RATE FIELD AT T(HR) = 36.00
MAXIMUM VELOCITY (FT/SEC) = 4.09

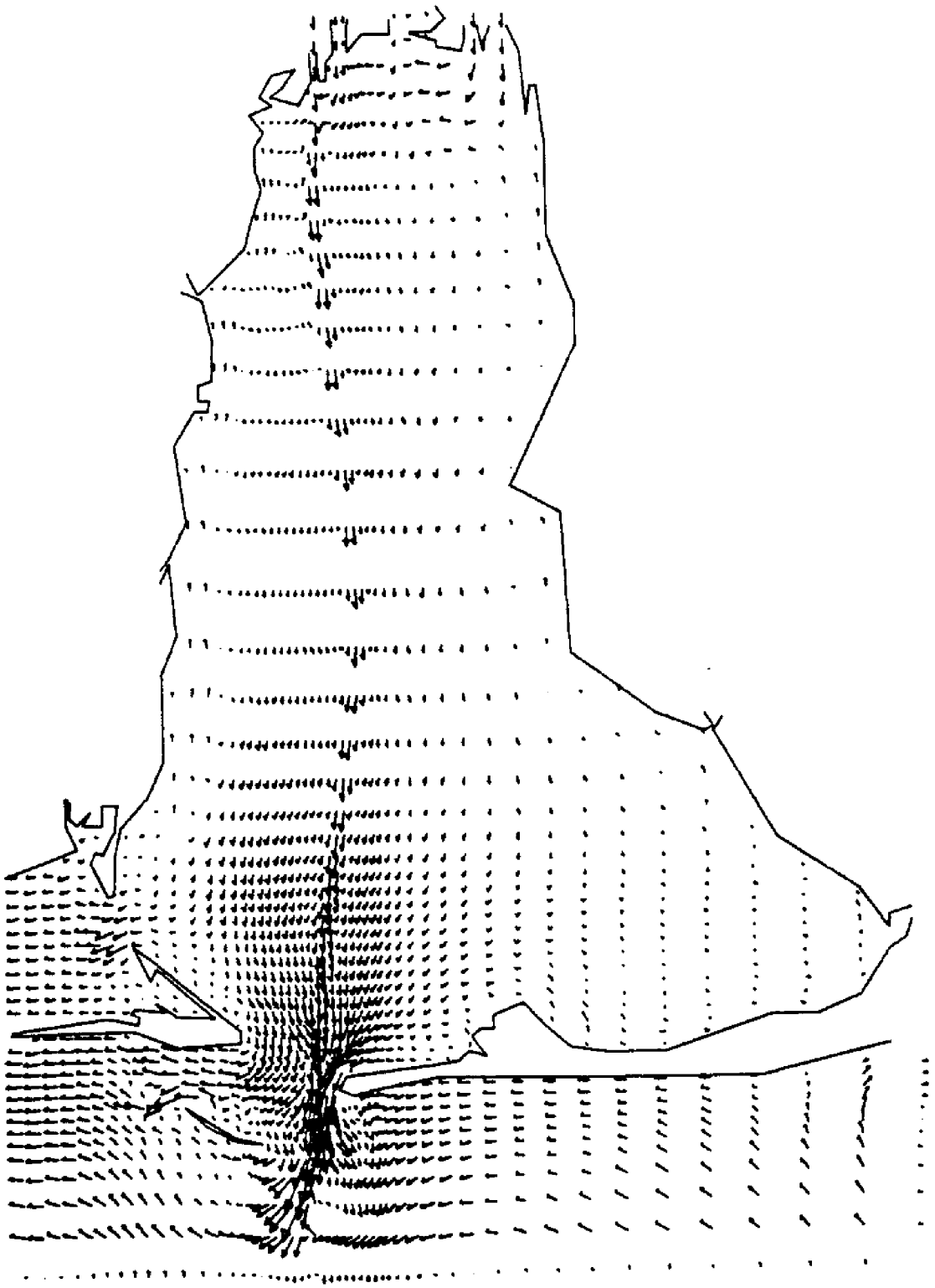

FLOW RATE FIELD AT T(HR) = 40.00
MAXIMUM VELOCITY (FT/SEC) = 2.36

APPENDIX B

CHANGES IN MOBILE BAY CIRCULATION PATTERNS AS A RESULT OF A 20 MPH CONSTANT WIND FROM VARIOUS DIRECTIONS

1. Difference between 20 mph wind from NE and the no wind condition.
2. Difference between 20 mph wind from SE and the no wind condition.
3. Difference between 20 mph wind from NW and the no wind condition.
4. Difference between 20 mph wind from SW and the no wind condition.

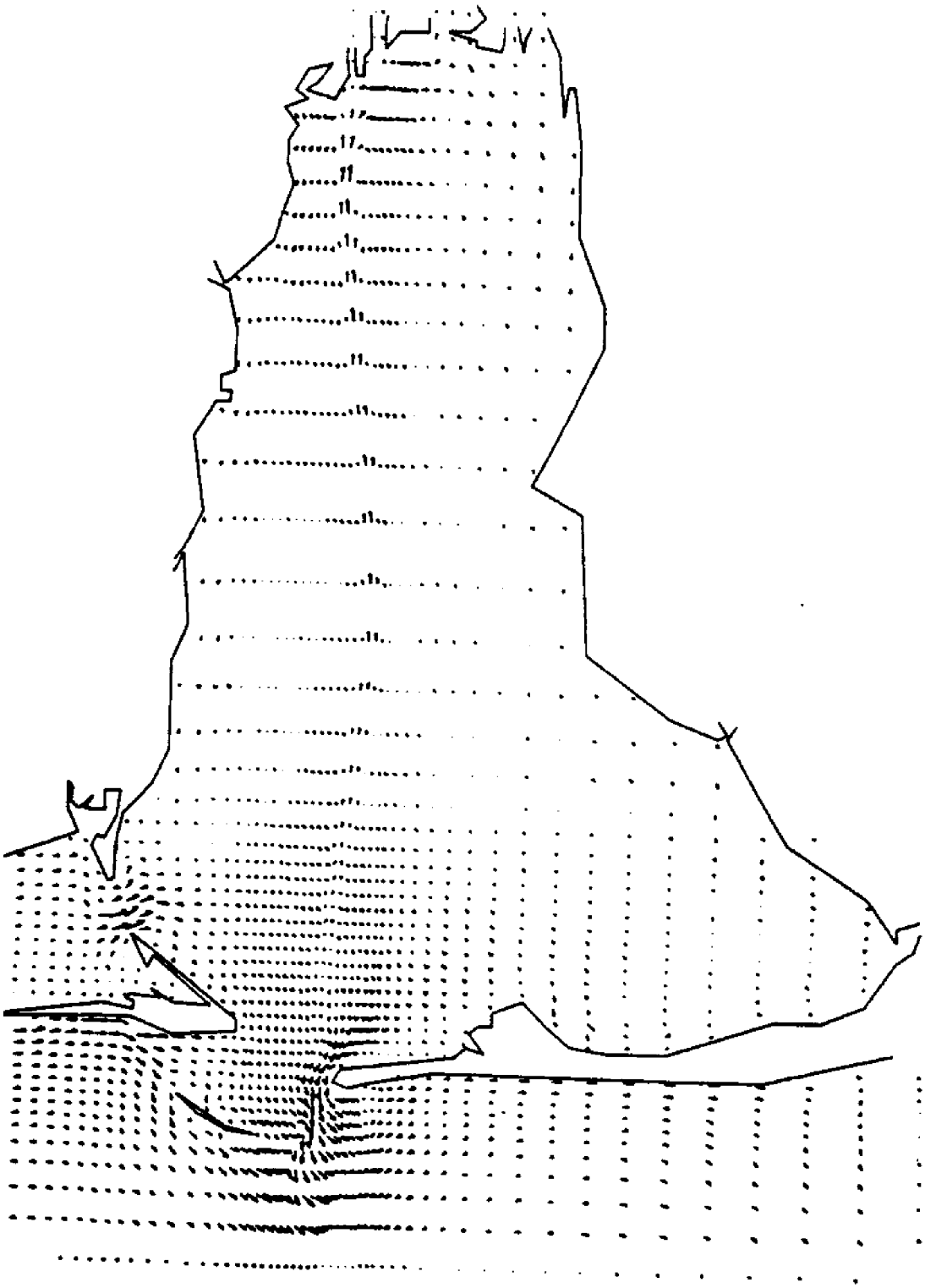

FLOW RATE FIELD AT T(HR) = 4.00
MAXIMUM VELOCITY (FT/SEC) = 1.02

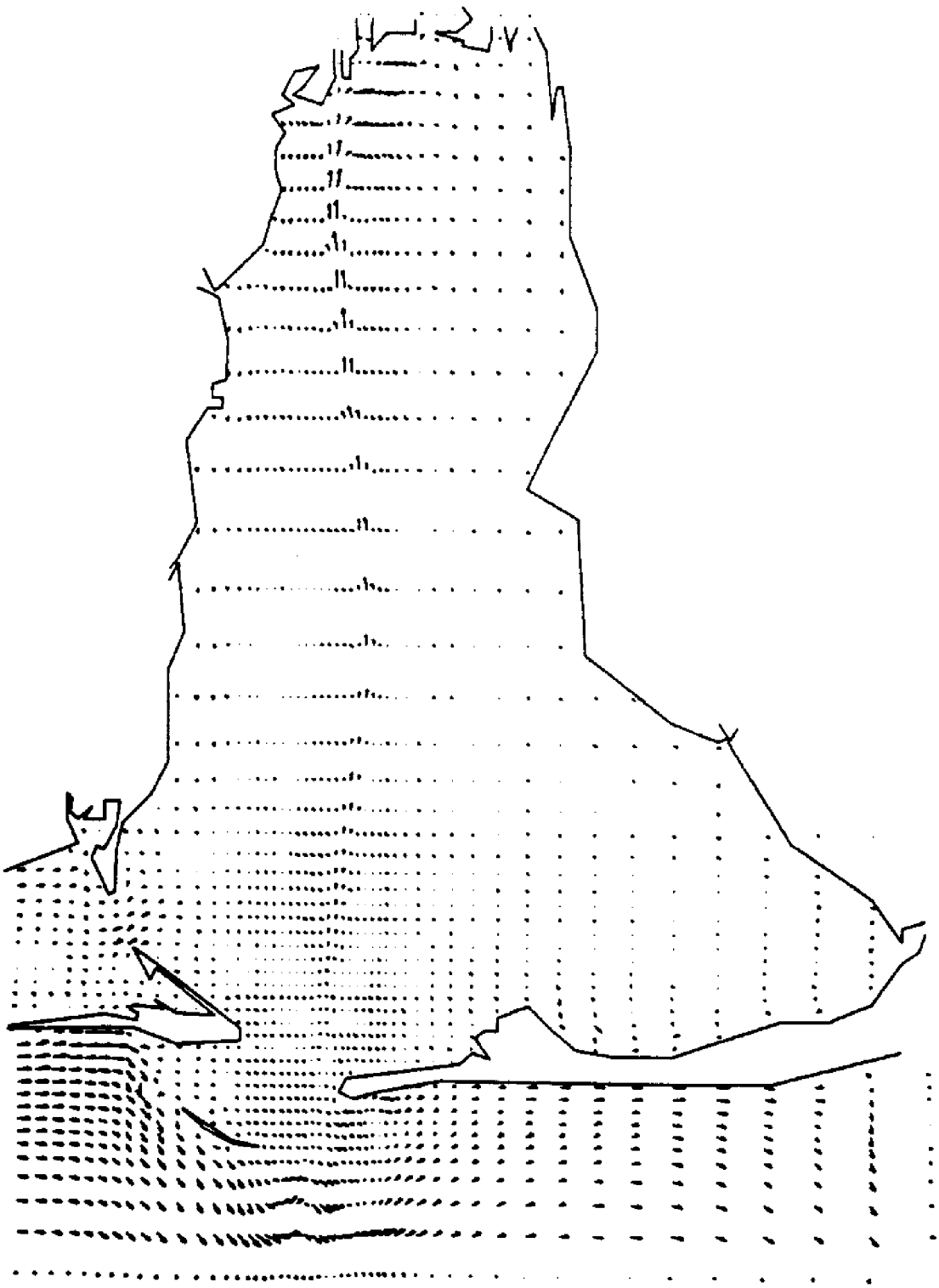

FLOW RATE FIELD AT T(HR) = 8.00
MAXIMUM VELOCITY (FT/SEC) = .99

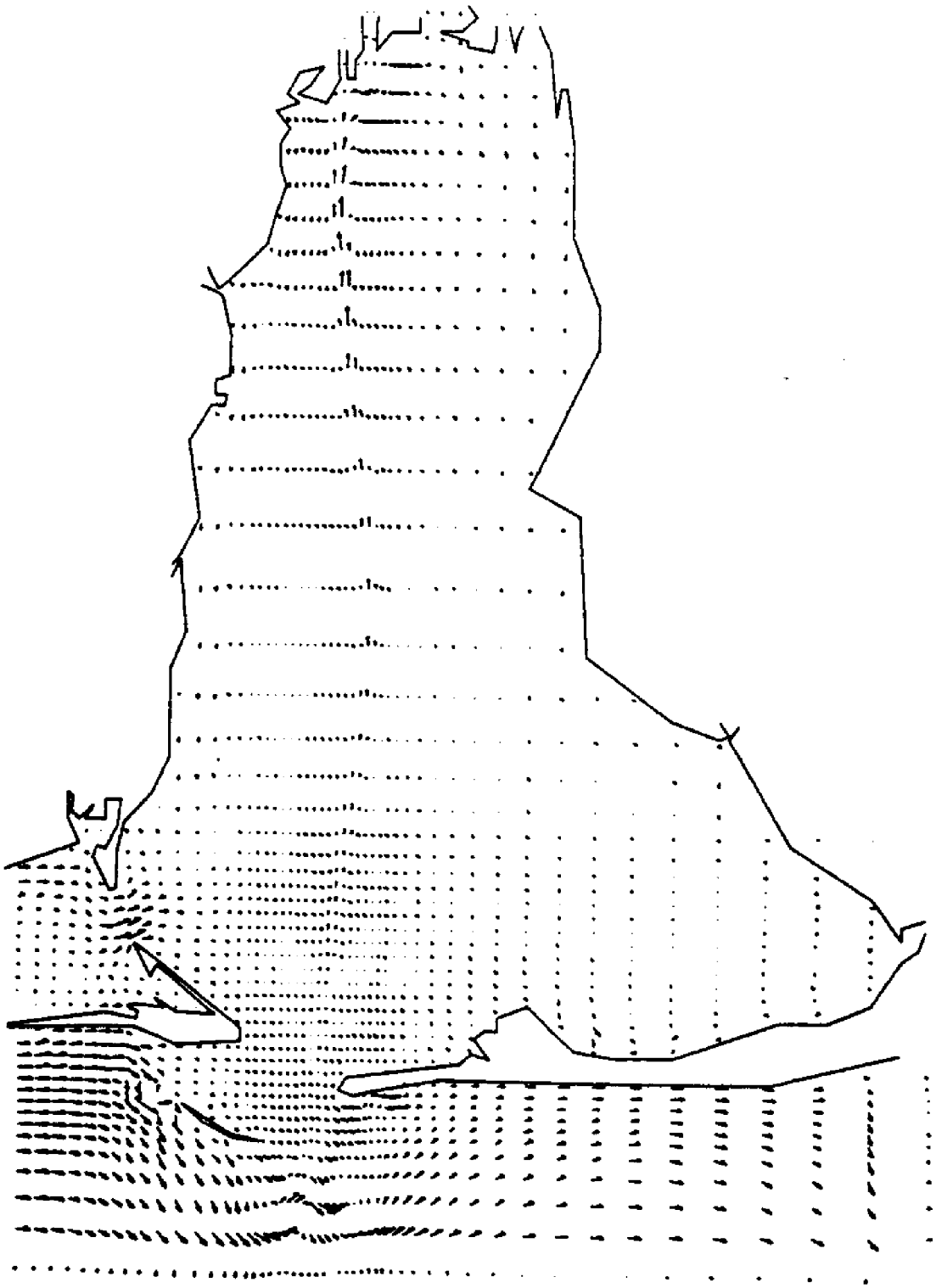

FLOW RATE FIELD AT T(HR) = 12.00
MAXIMUM VELOCITY (FT/SEC) = 1.03

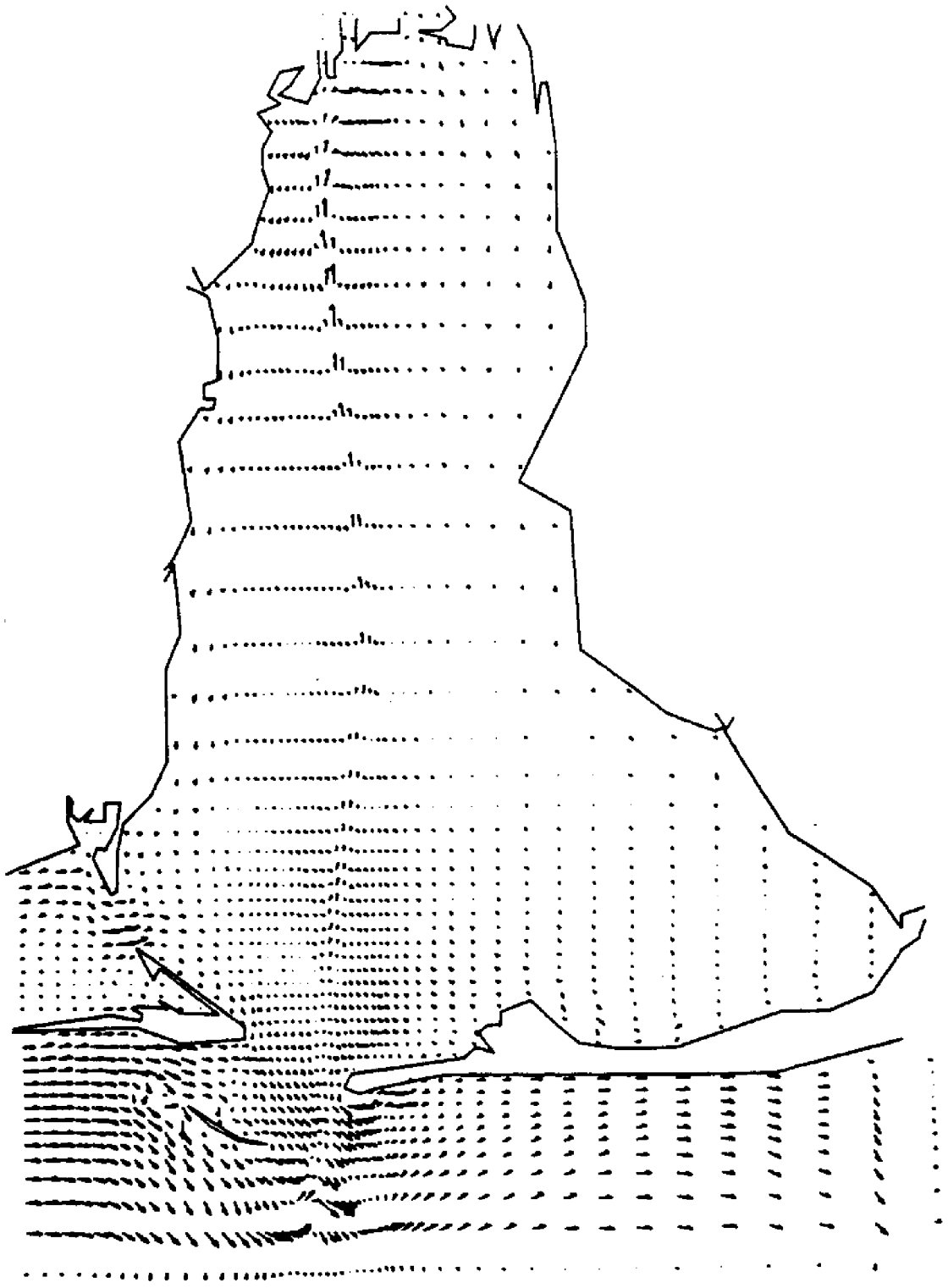

FLOW RATE FIELD AT T(HR) = 16.00
MAXIMUM VELOCITY (FT/SEC) = 1.48

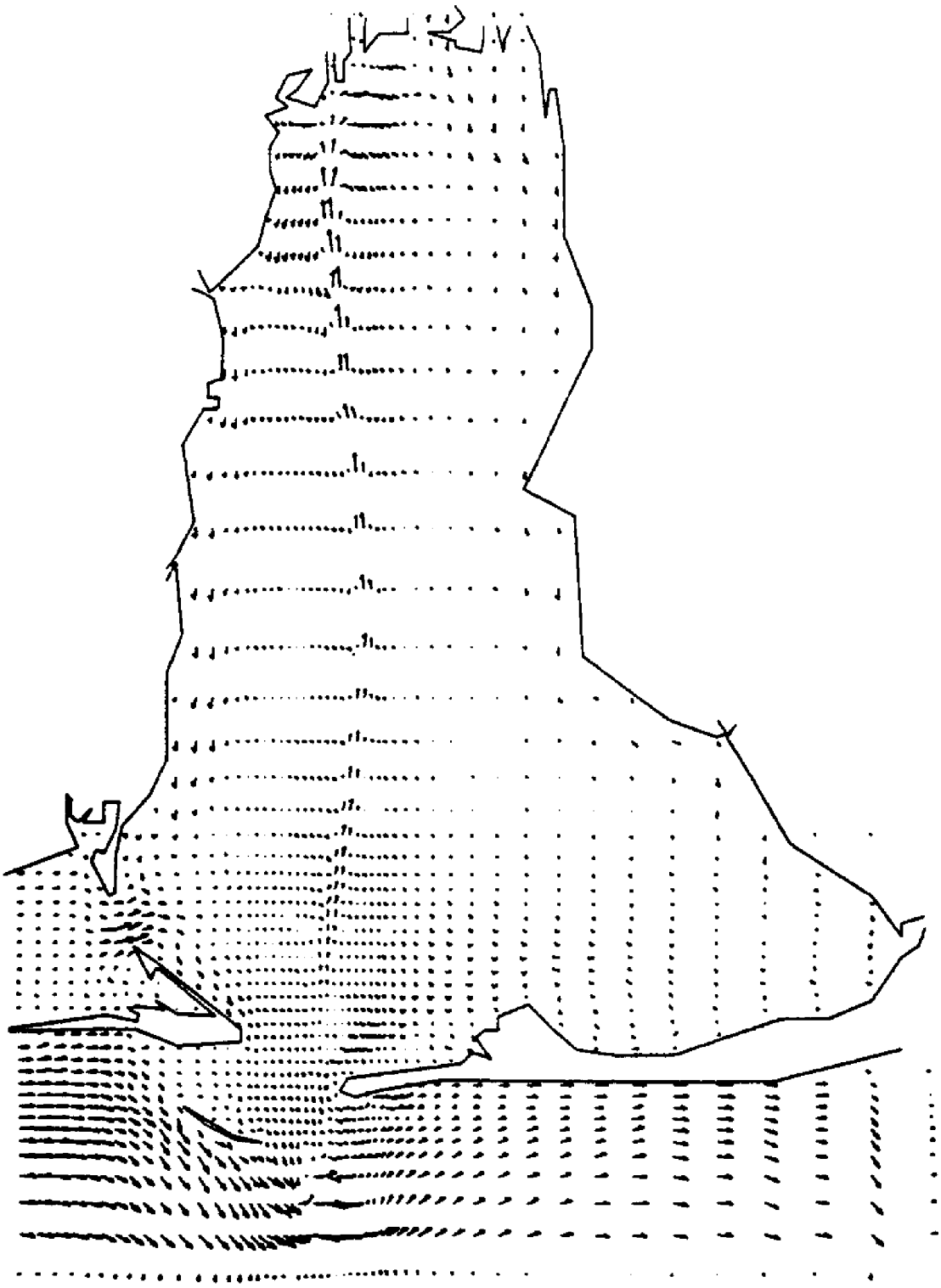

FLOW RATE FIELD AT T(HR) = 20.00
MAXIMUM VELOCITY (FT/SEC) = 1.17

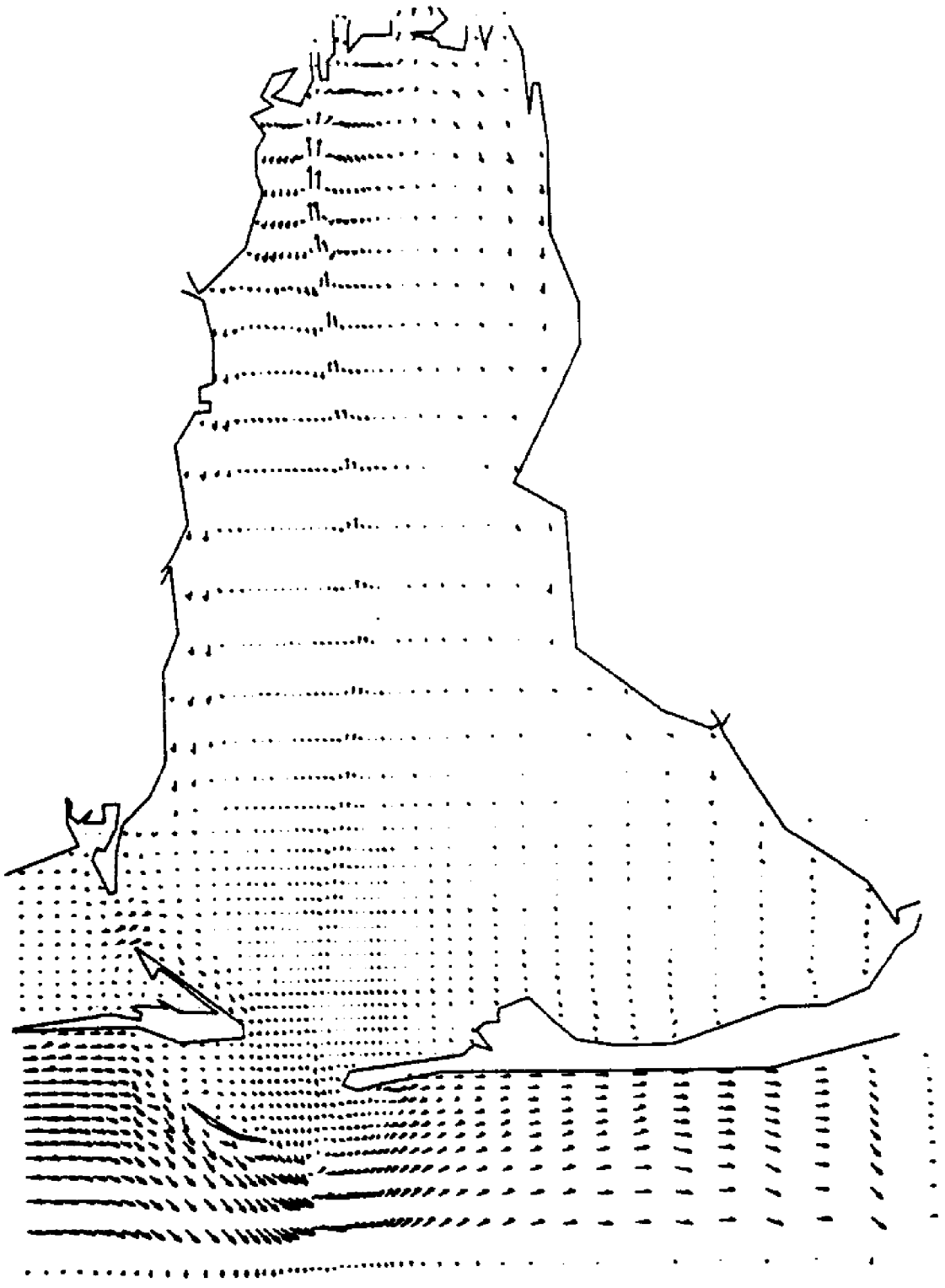

FLOW RATE FIELD AT T(HR) = 24.00
MAXIMUM VELOCITY (FT/SEC) = 1.10

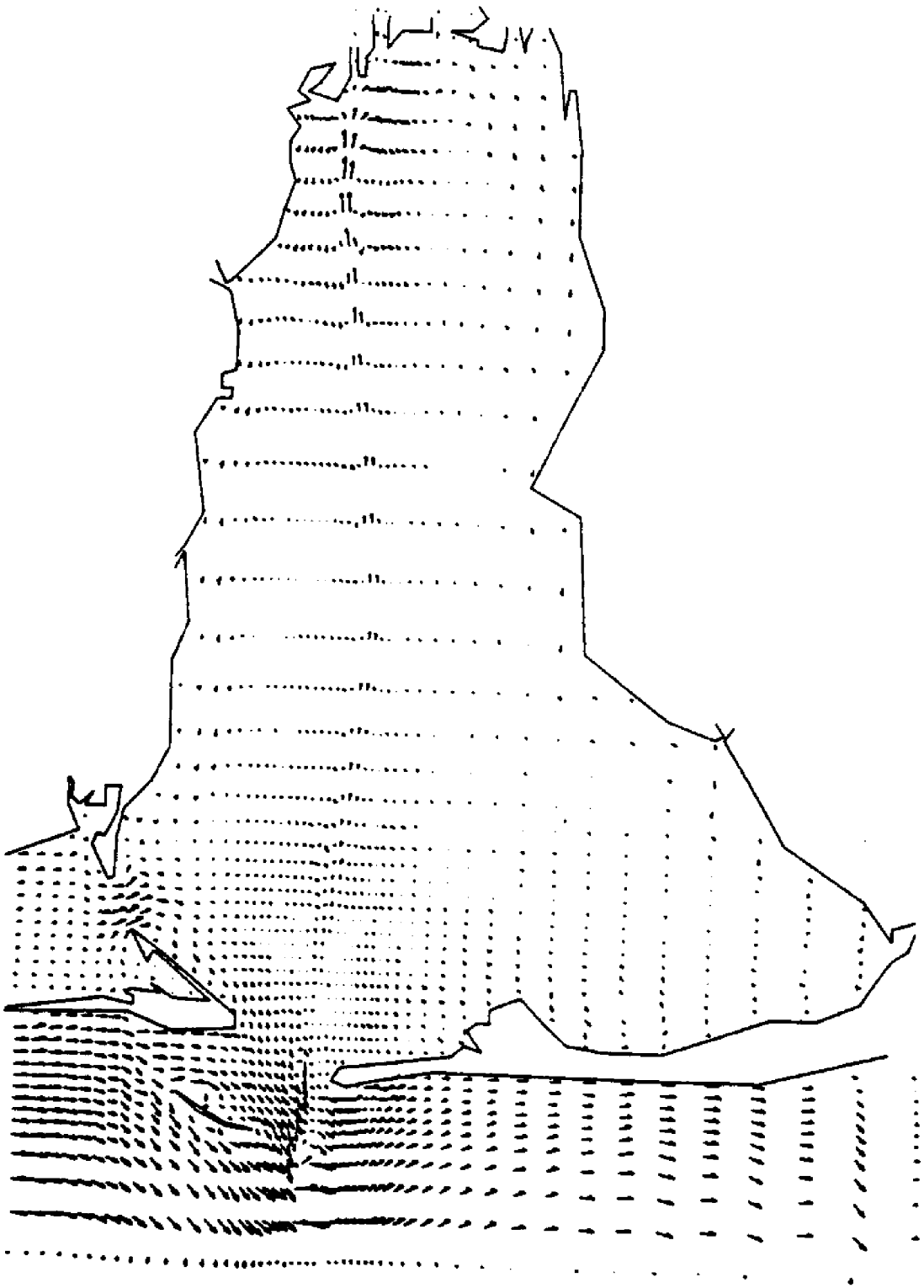

FLOW RATE FIELD AT T(HR) = 28.00
MAXIMUM VELOCITY (FT/SEC) = 1.08

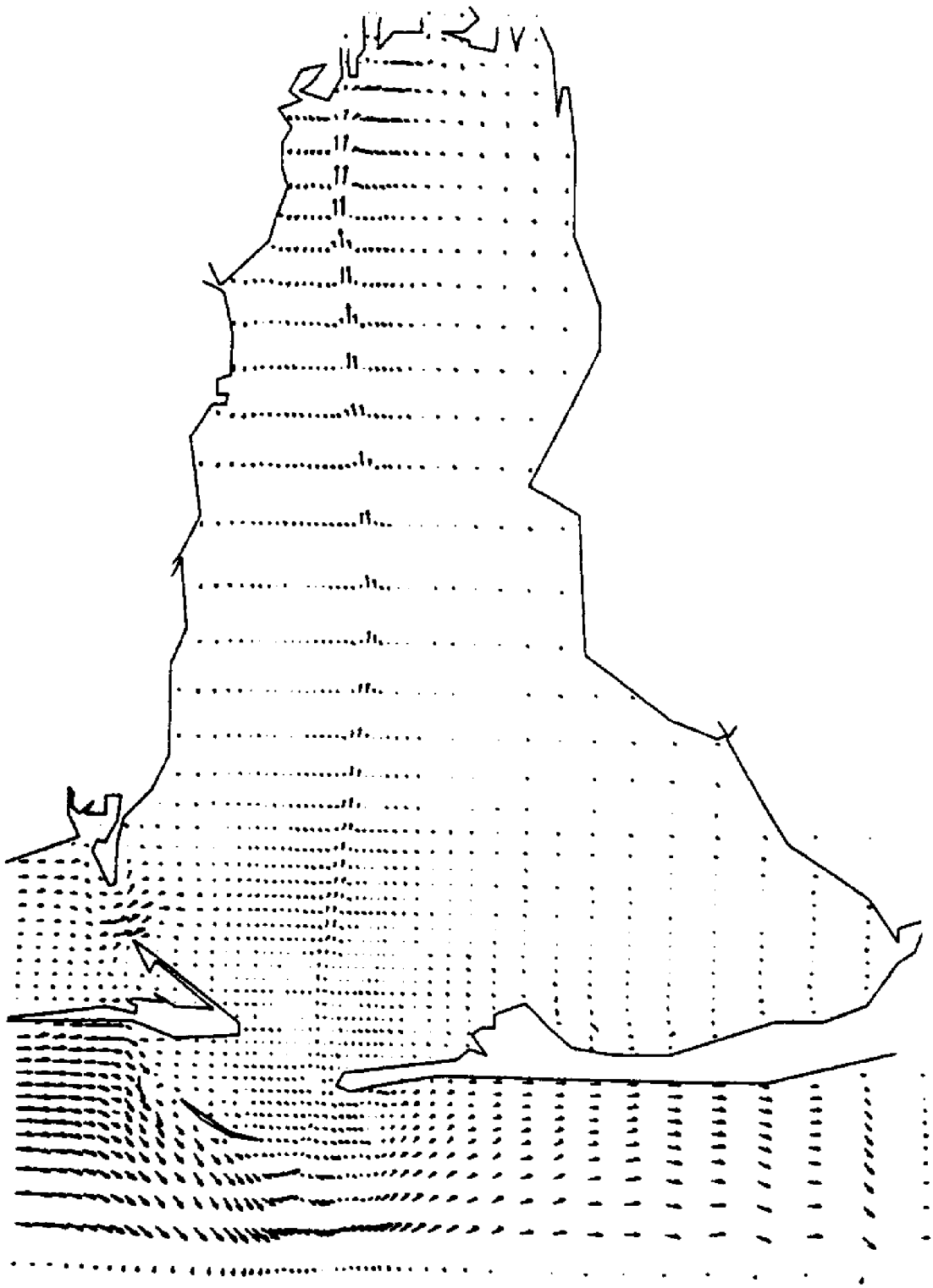

FLOW RATE FIELD AT T(HR) = 32.00
MAXIMUM VELOCITY (FT/SEC) = 1.03

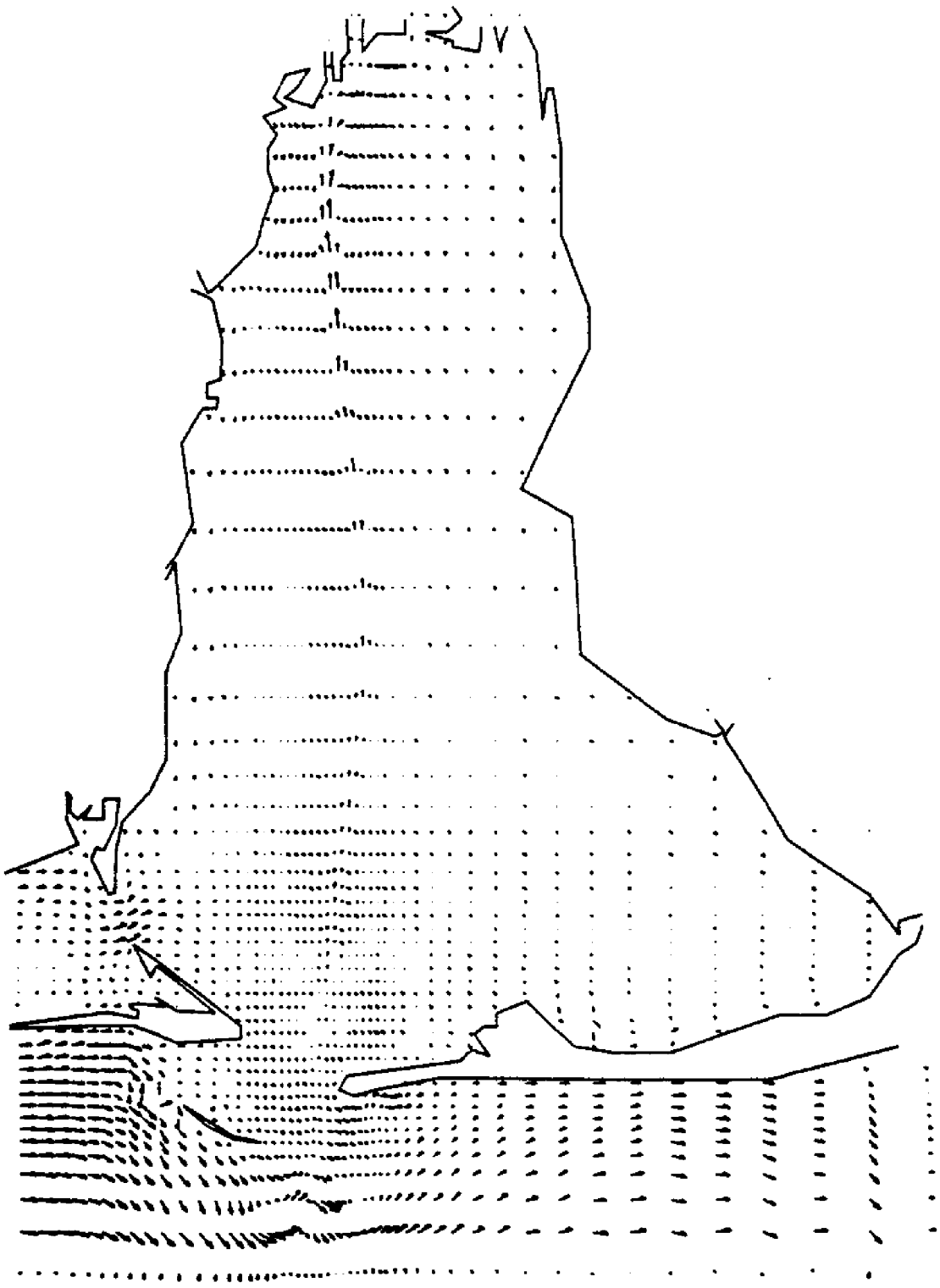

FLOW RATE FIELD AT T(HR) = 36.00
MAXIMUM VELOCITY (FT/SEC) = 1.03

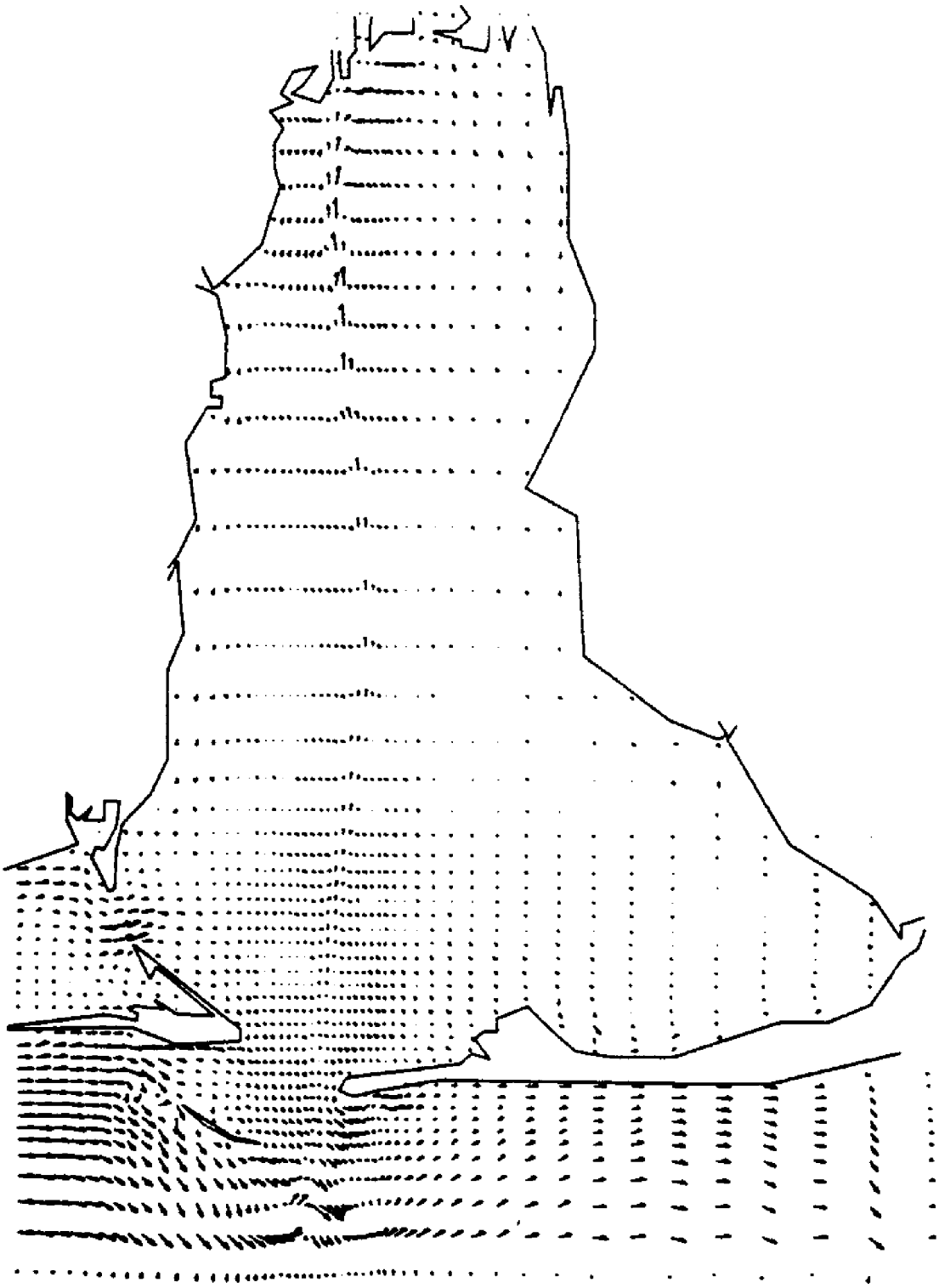

FLOW RATE FIELD AT T(HR) = 40.00
MAXIMUM VELOCITY (FT/SEC) = 1.34

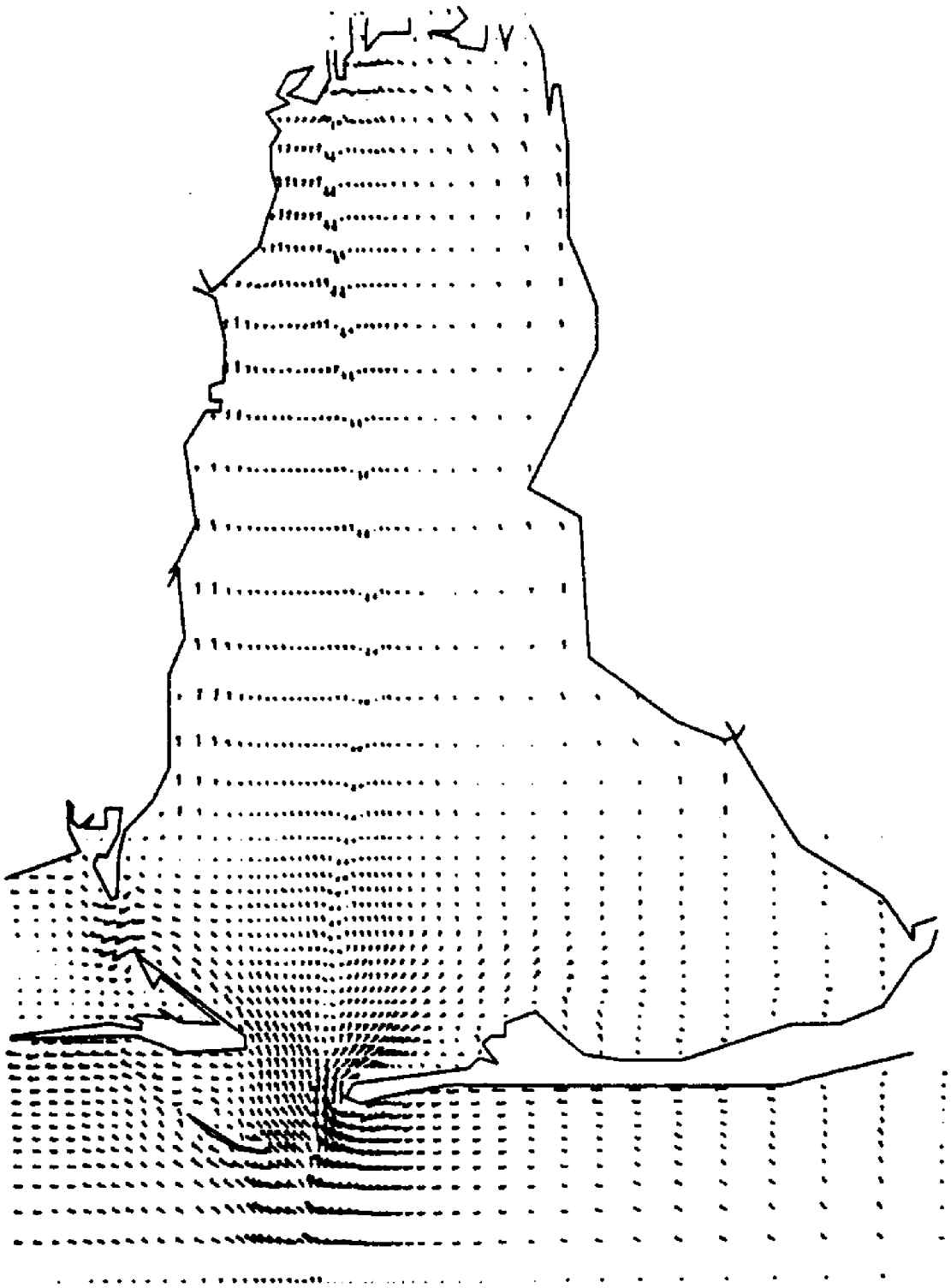

FLOW RATE FIELD AT T(HR) = 4.00
MAXIMUM VELOCITY (FT/SEC) = 1.17

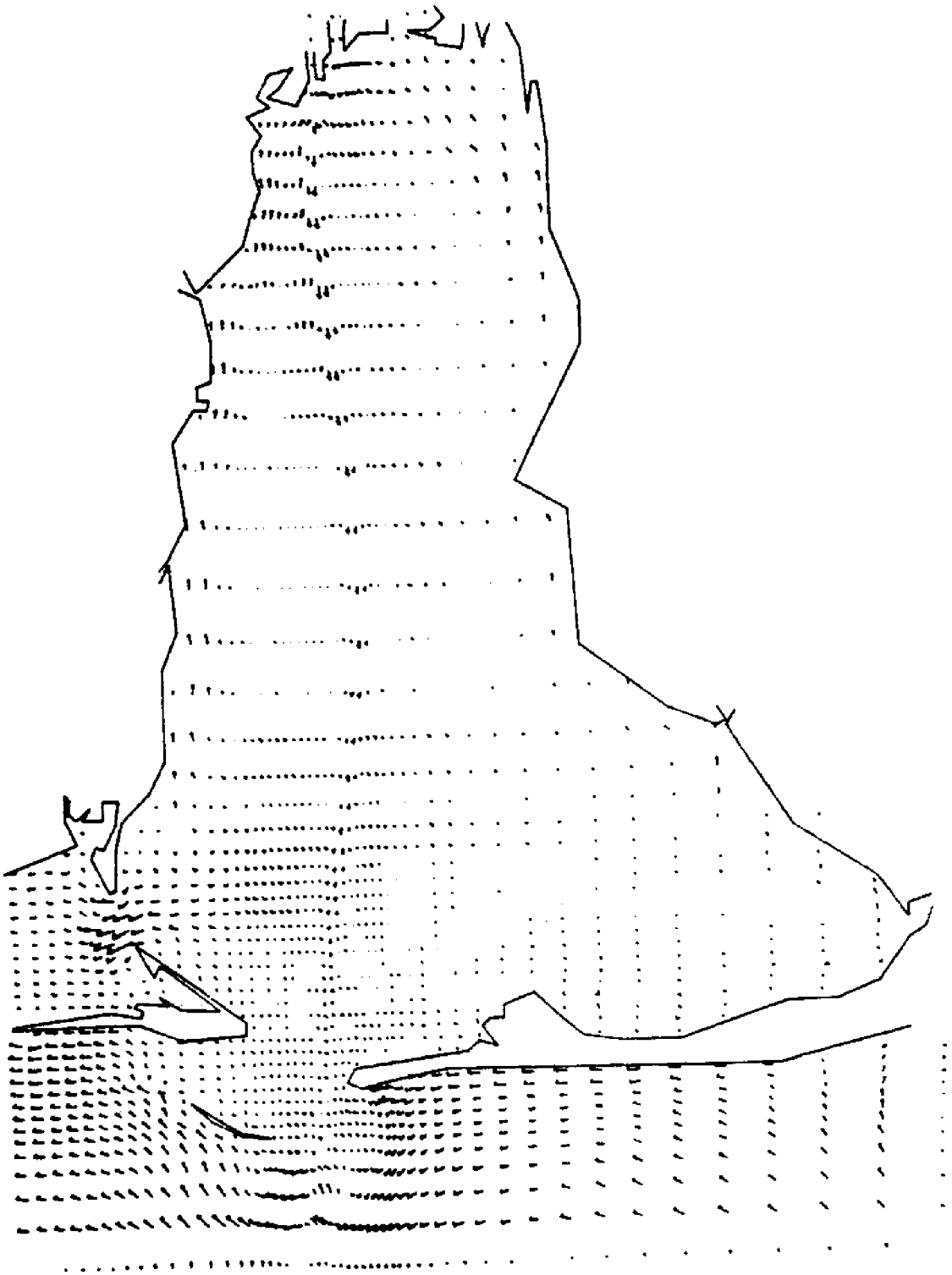

FLOW RATE FIELD AT T(HR) = 8.00
MAXIMUM VELOCITY (FT/SEC) = 1.19

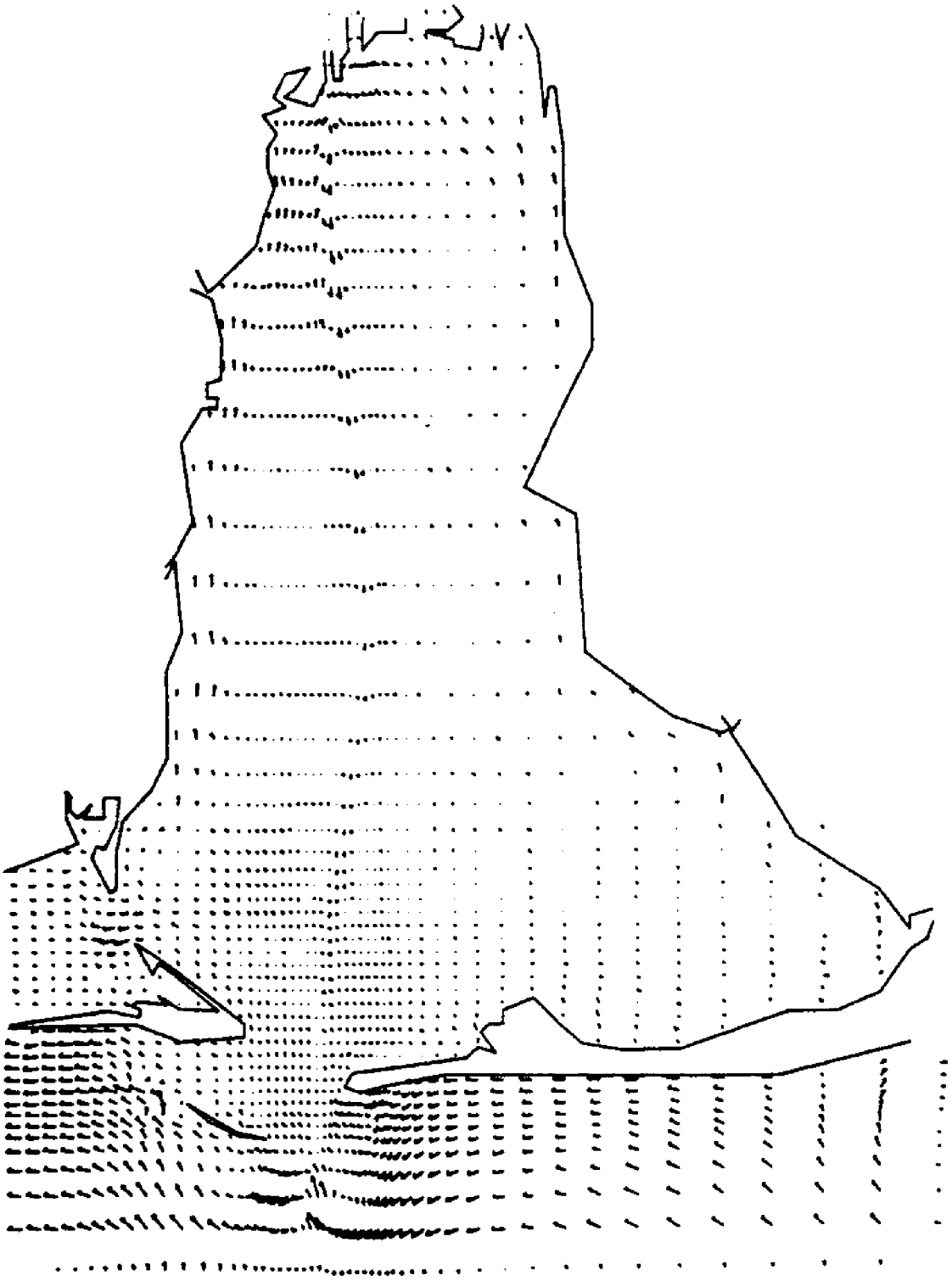

FLOW RATE FIELD AT T(HR) = 12.00
MAXIMUM VELOCITY (FT/SEC) = 1.05

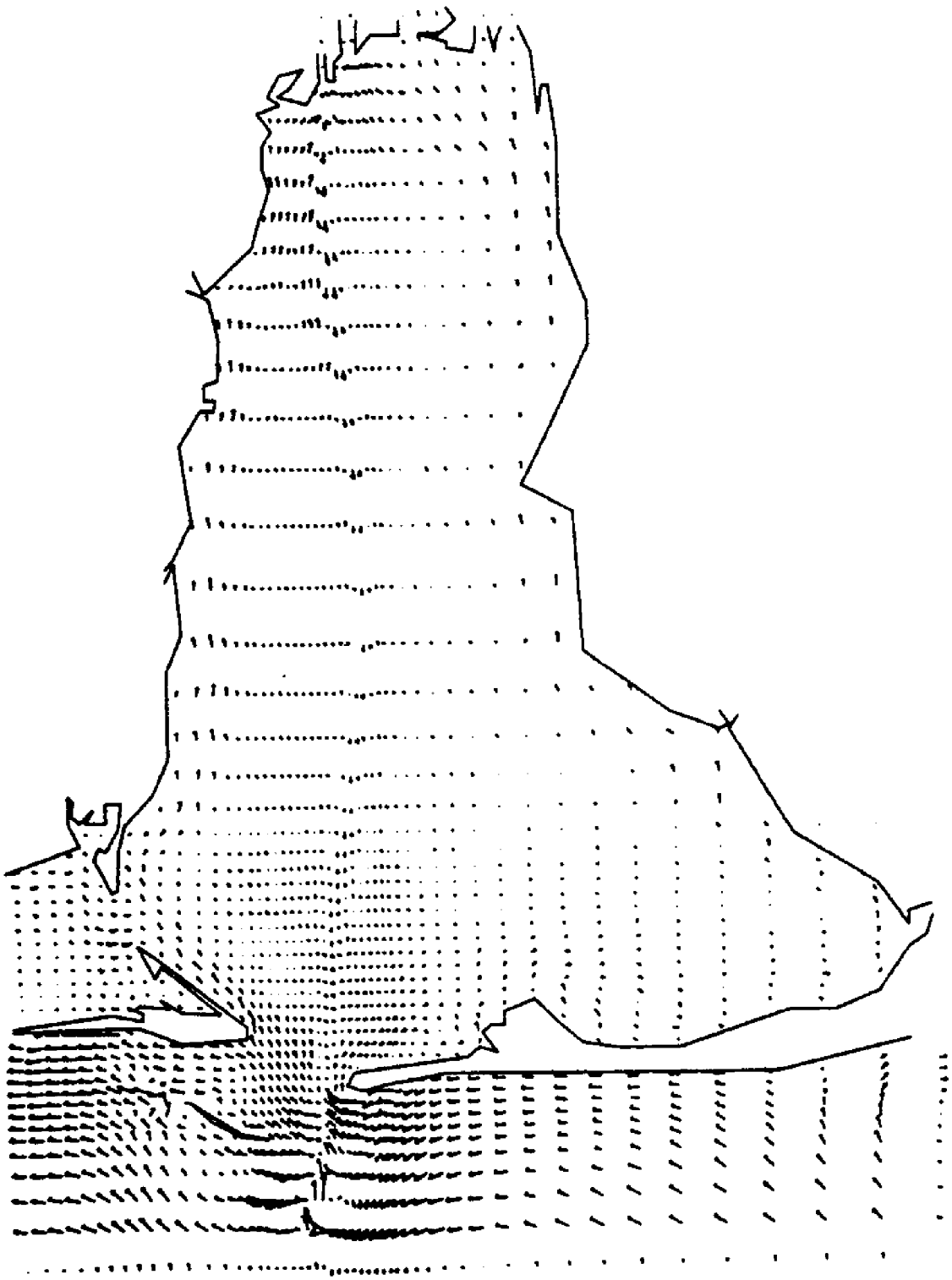

FLOW RATE FIELD AT T(HR) = 16.00
MAXIMUM VELOCITY (FT/SEC) = 1.55

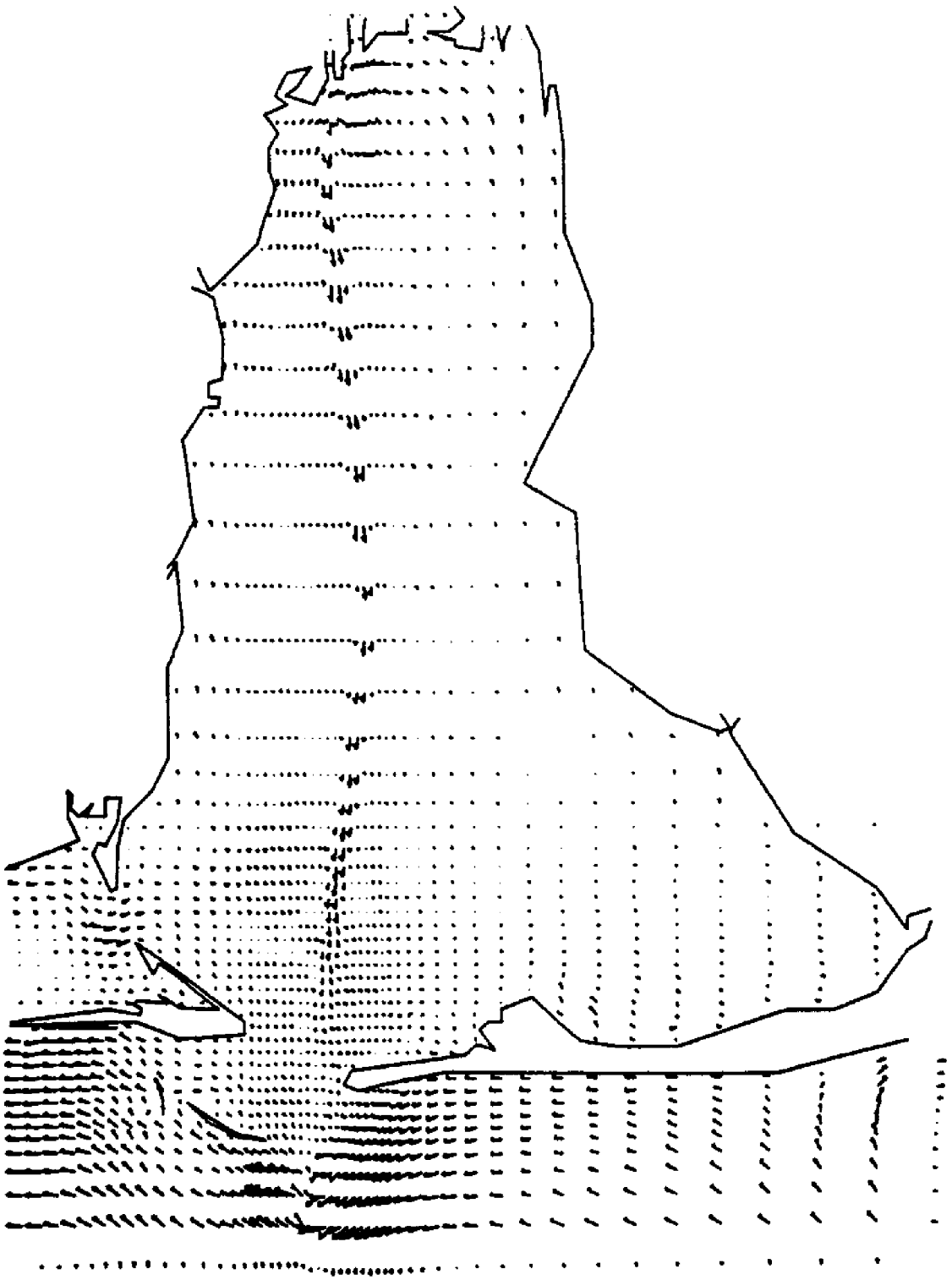

FLOW RATE FIELD AT T(HR) = 20.00
MAXIMUM VELOCITY (FT/SEC) = 1.35

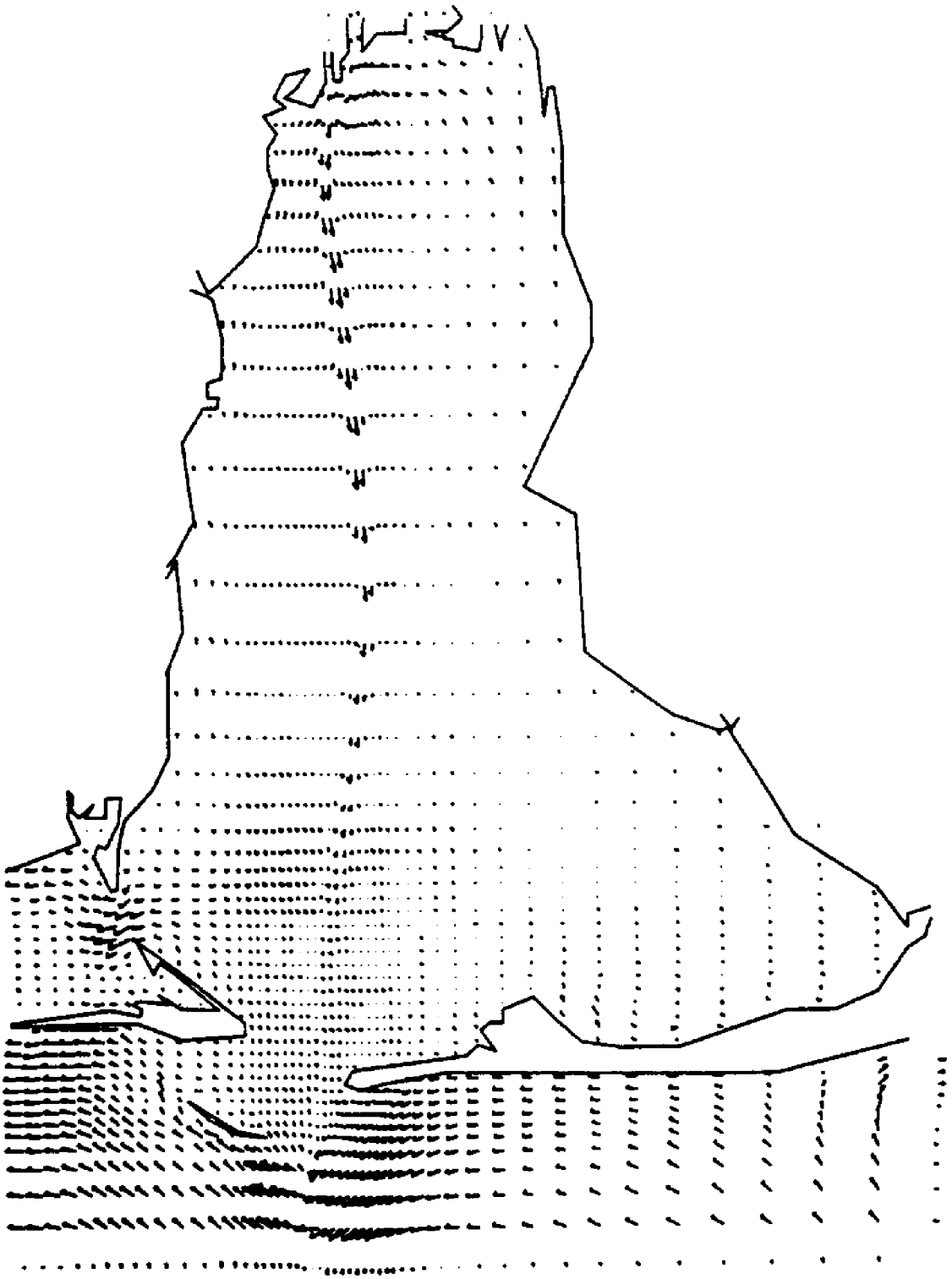

FLOW RATE FIELD AT T(HR) = 24.00
MAXIMUM VELOCITY (FT/SEC) = 1.18

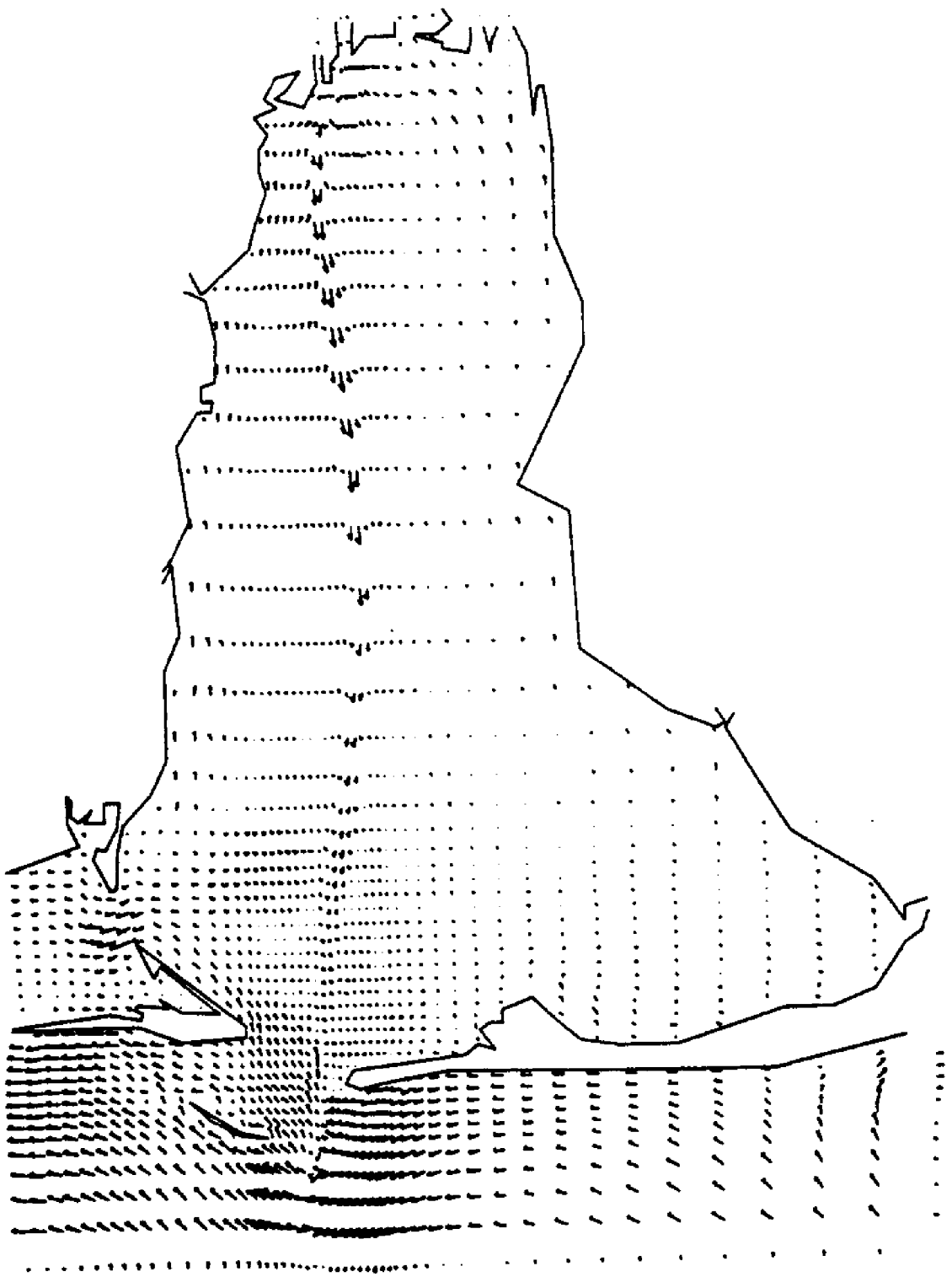

FLOW RATE FIELD AT T(HR) = 28.00
MAXIMUM VELOCITY (FT/SEC) = 1.06

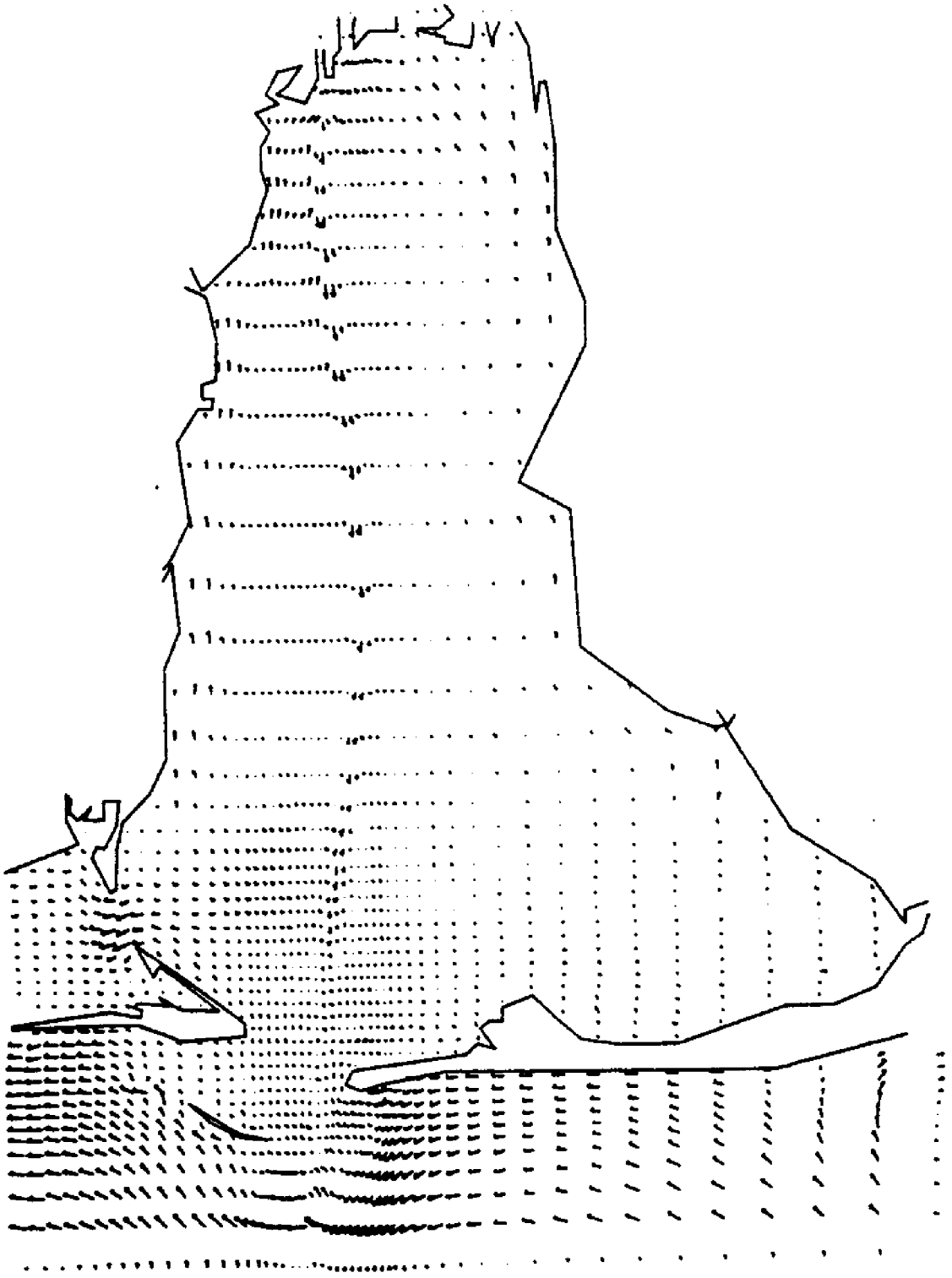

FLOW RATE FIELD AT T(HR) = 32.00
MAXIMUM VELOCITY (FT/SEC) = .922

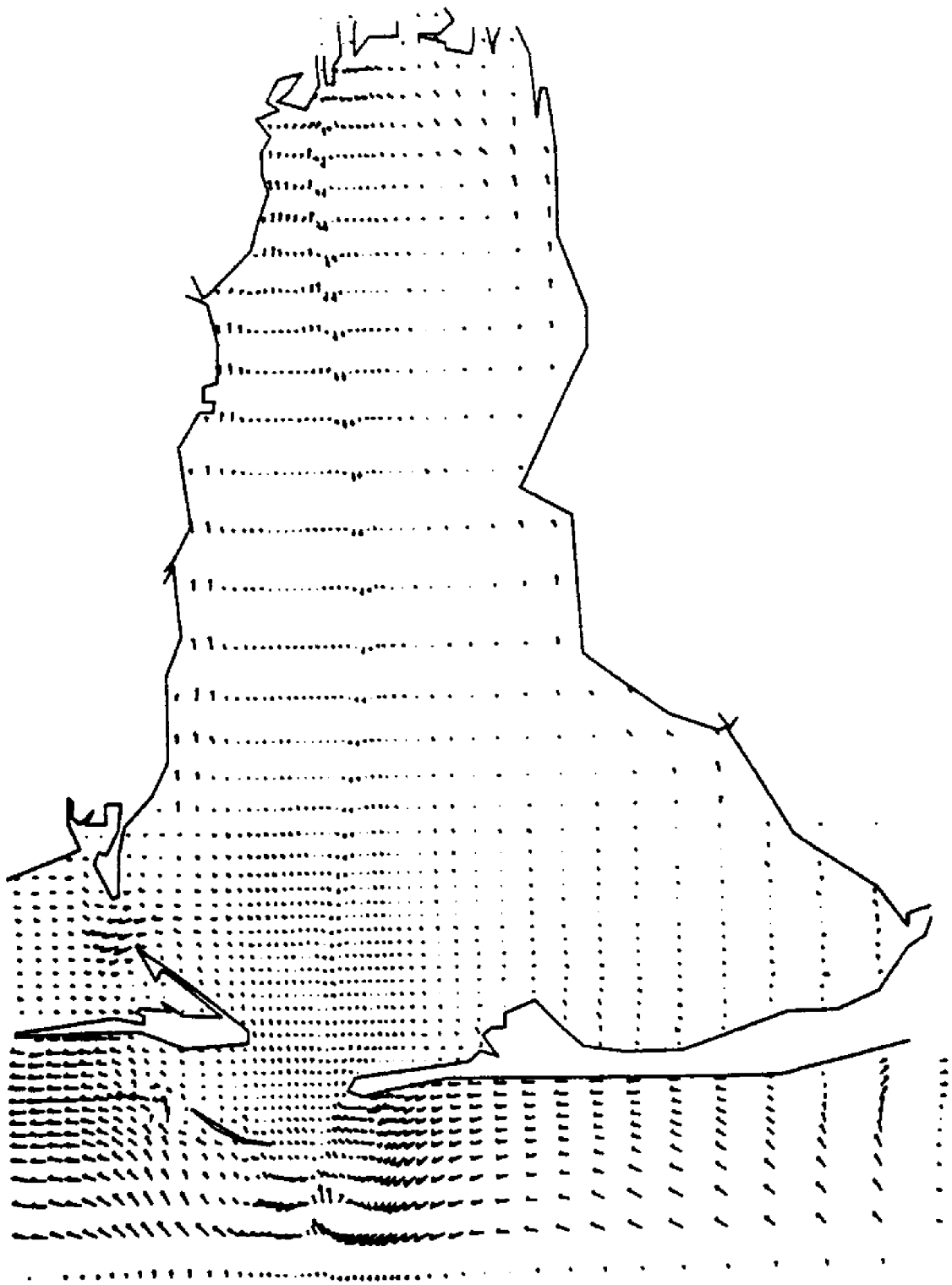

FLOW RATE FIELD AT T(HR) = 36.00
MAXIMUM VELOCITY (FT/SEC) = .97

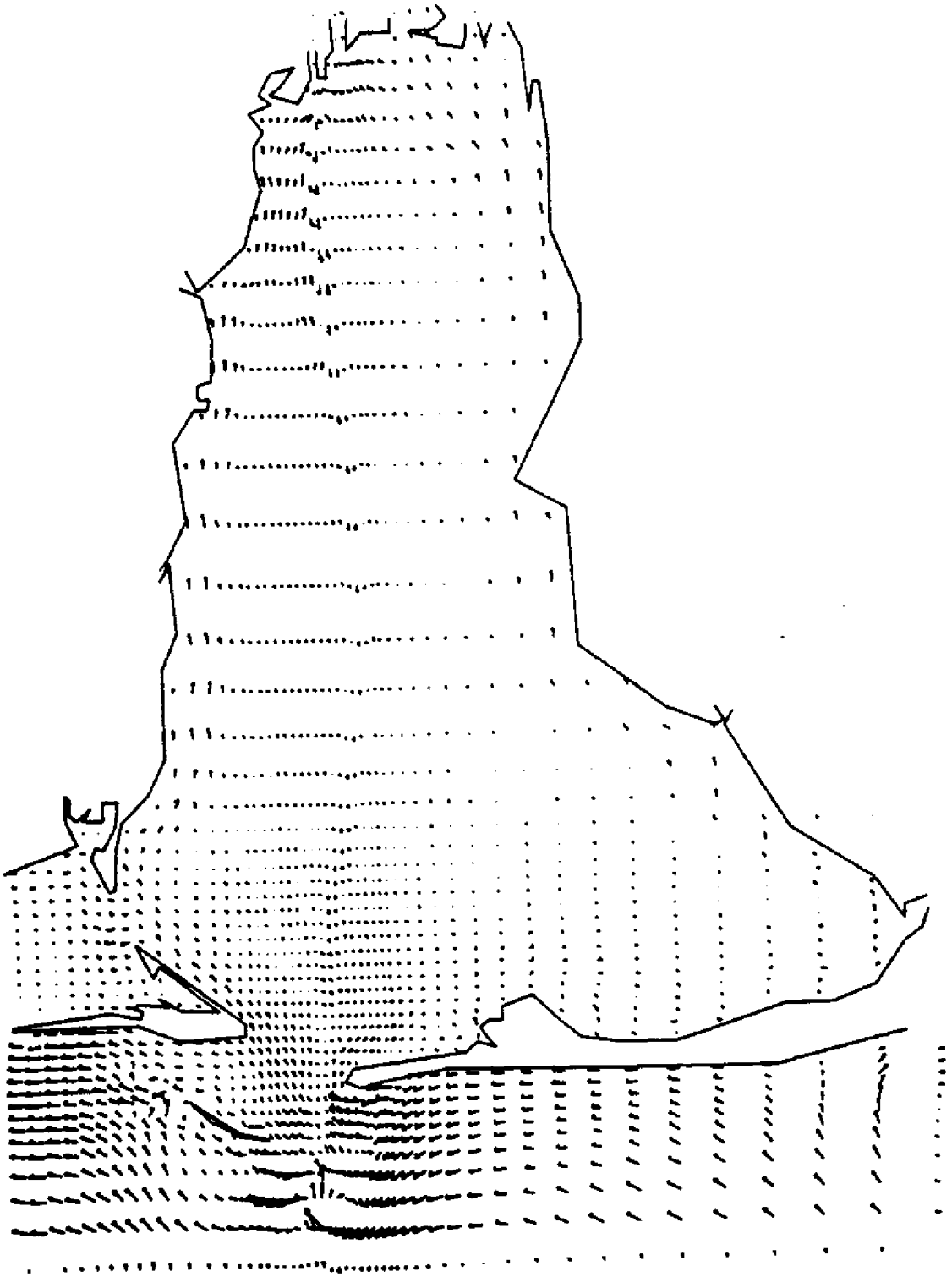

FLOW RATE FIELD AT T(HR) = 40.00
MAXIMUM VELOCITY (FT/SEC) = 1.46

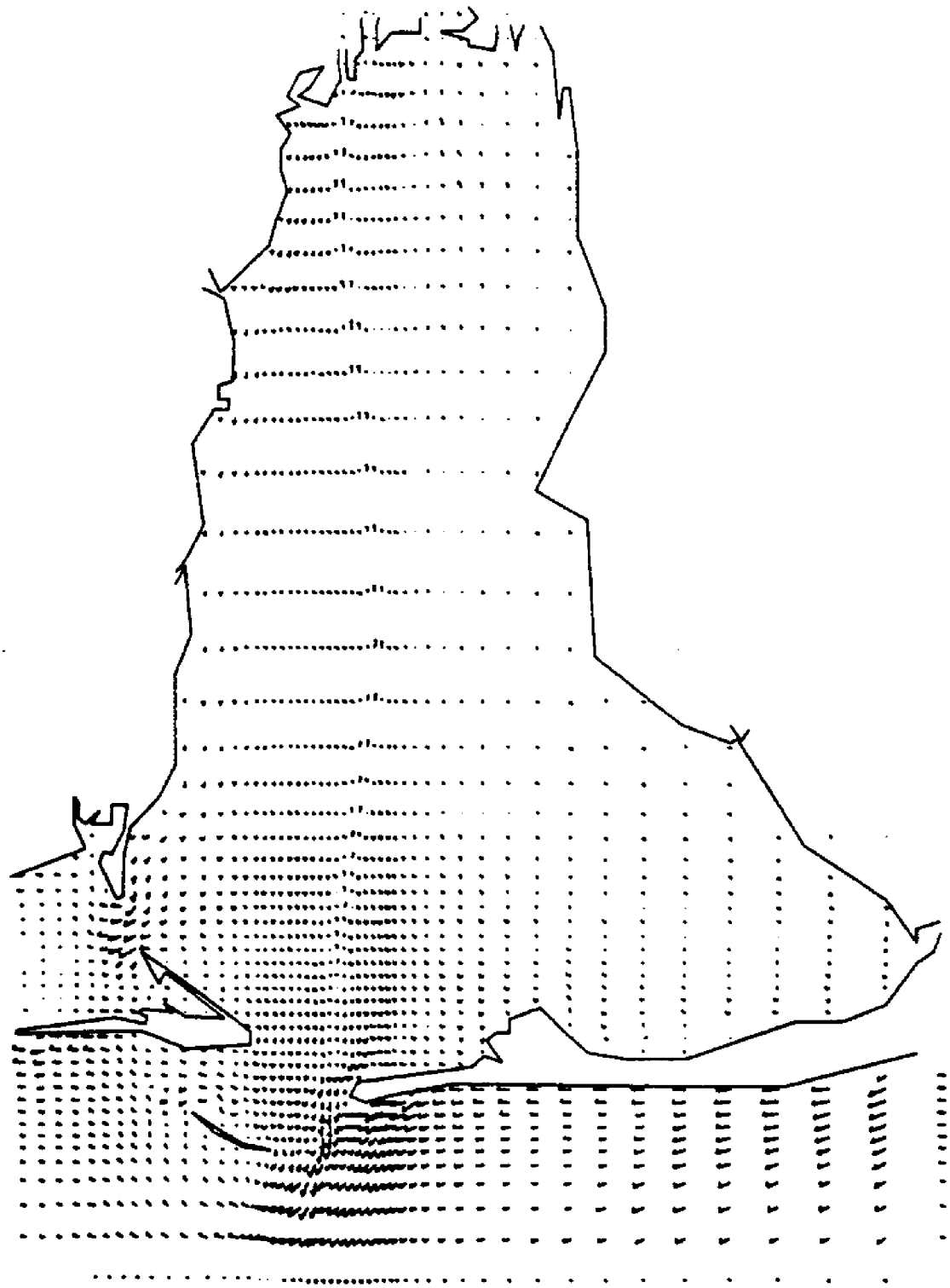

FLOW RATE FIELD AT T(HR) = 4.00
MAXIMUM VELOCITY (FT/SEC) = .90

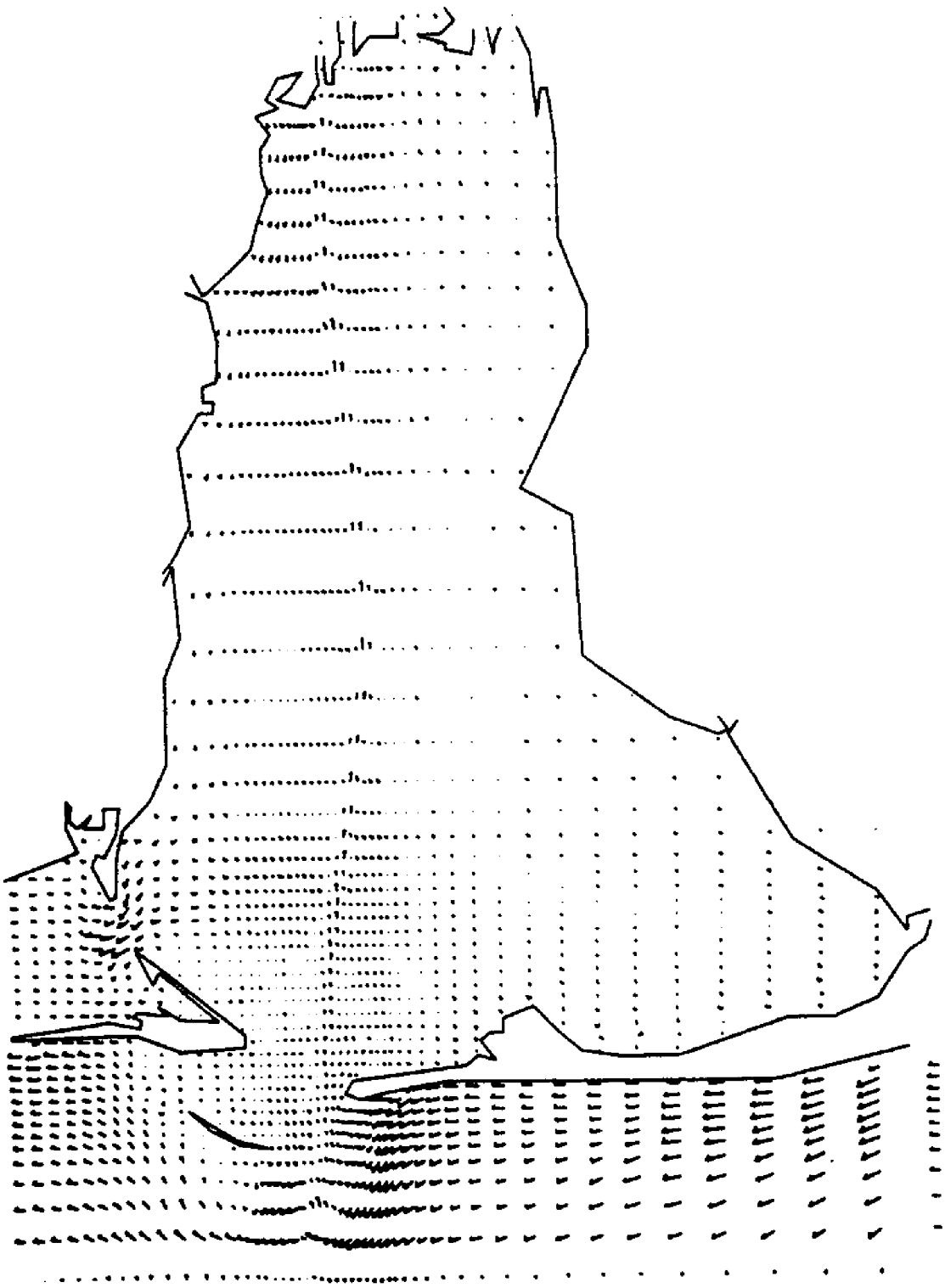

FLOW RATE FIELD AT T(HR) = 8.00
MAXIMUM VELOCITY (FT/SEC) = 1.12

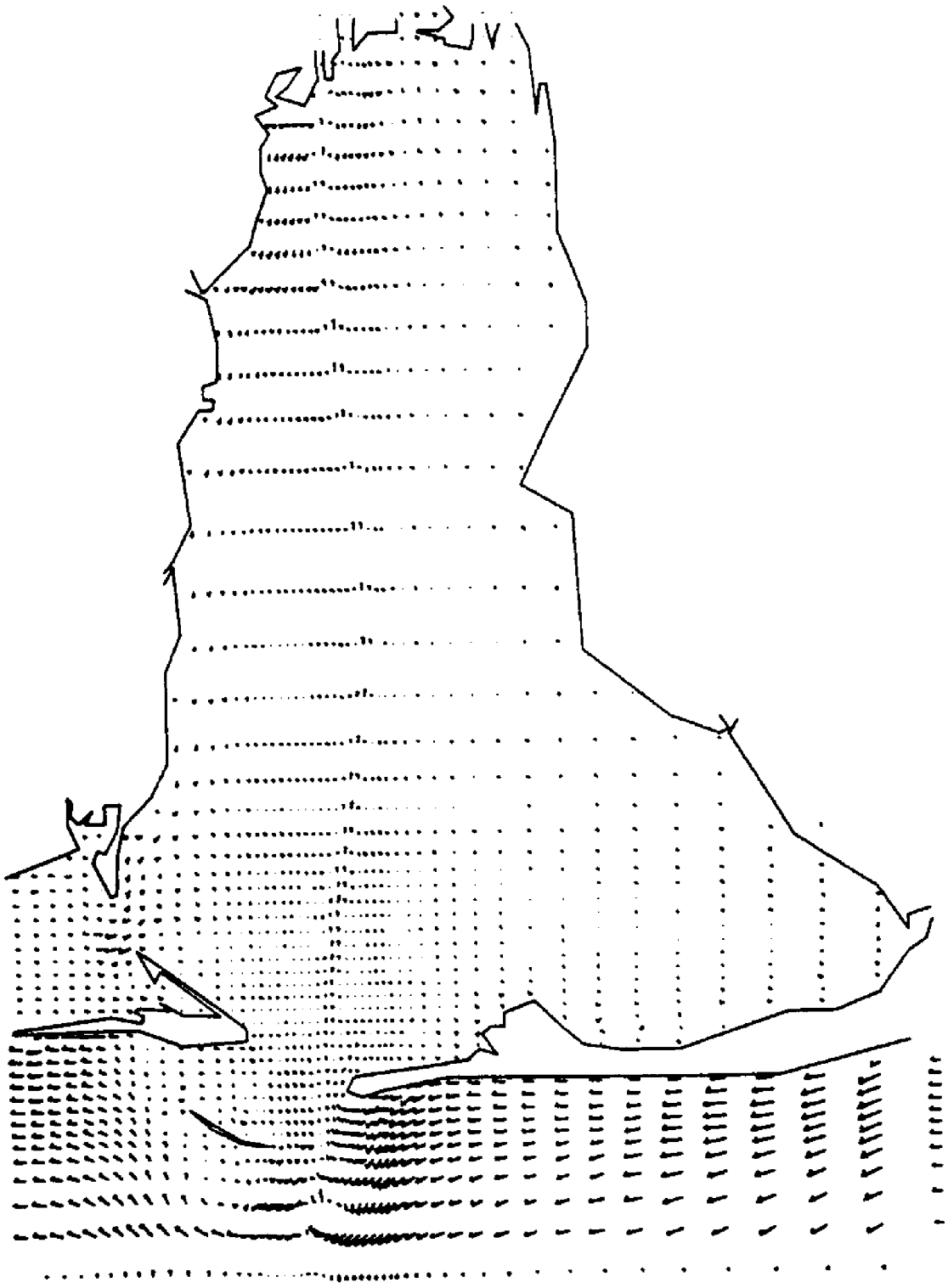

FLOW RATE FIELD AT T(HR) = 12.00
MAXIMUM VELOCITY (FT/SEC) = 1.17

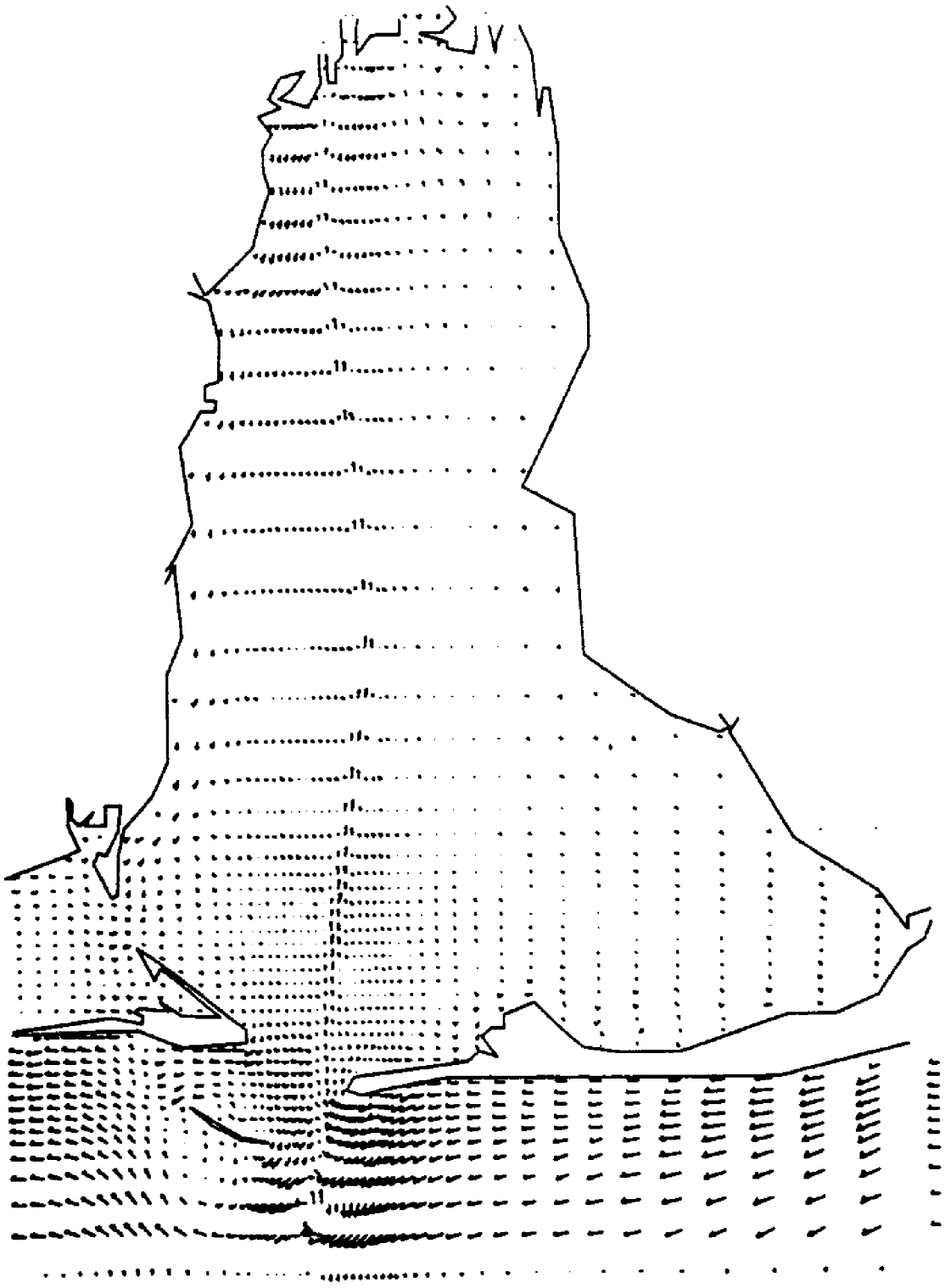

FLOW RATE FIELD AT T(HR) = 16.00
MAXIMUM VELOCITY (FT/SEC) = 1.27

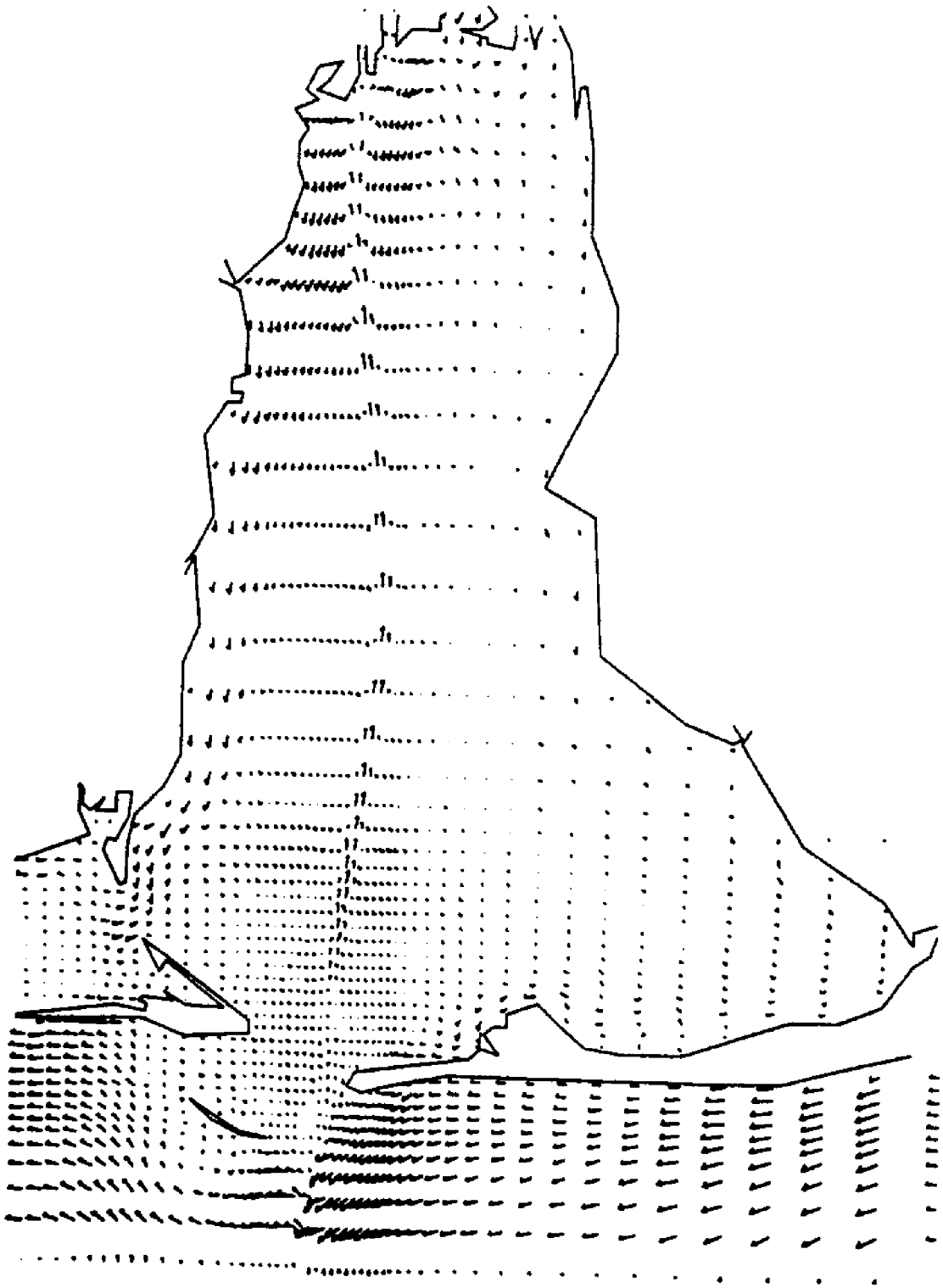

FLOW RATE FIELD AT T(HR) = 20.00
MAXIMUM VELOCITY (FT/SEC) = 1.18

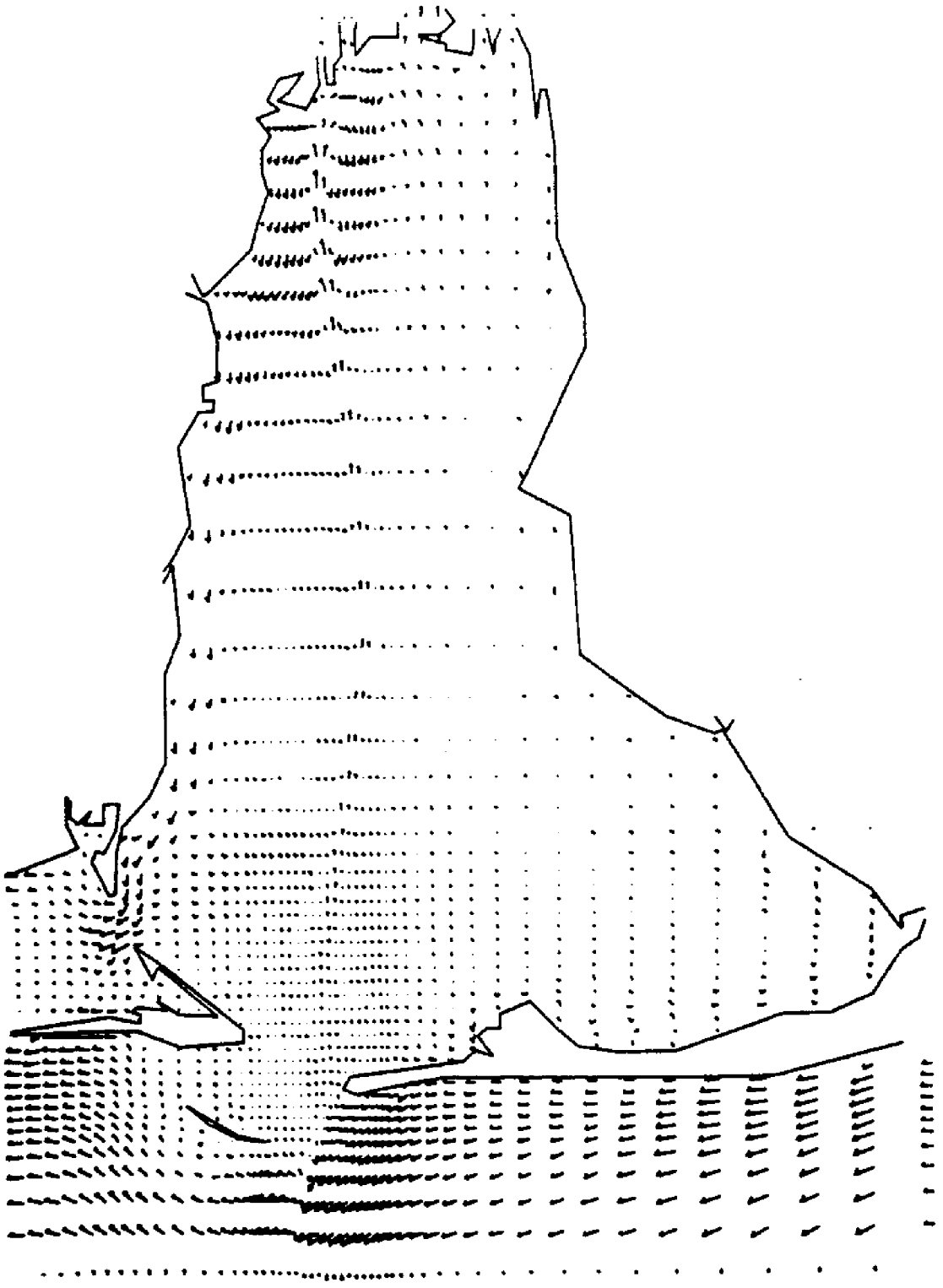

FLOW RATE FIELD AT T(HR) = 24.00
MAXIMUM VELOCITY (FT/SEC) = 1.13

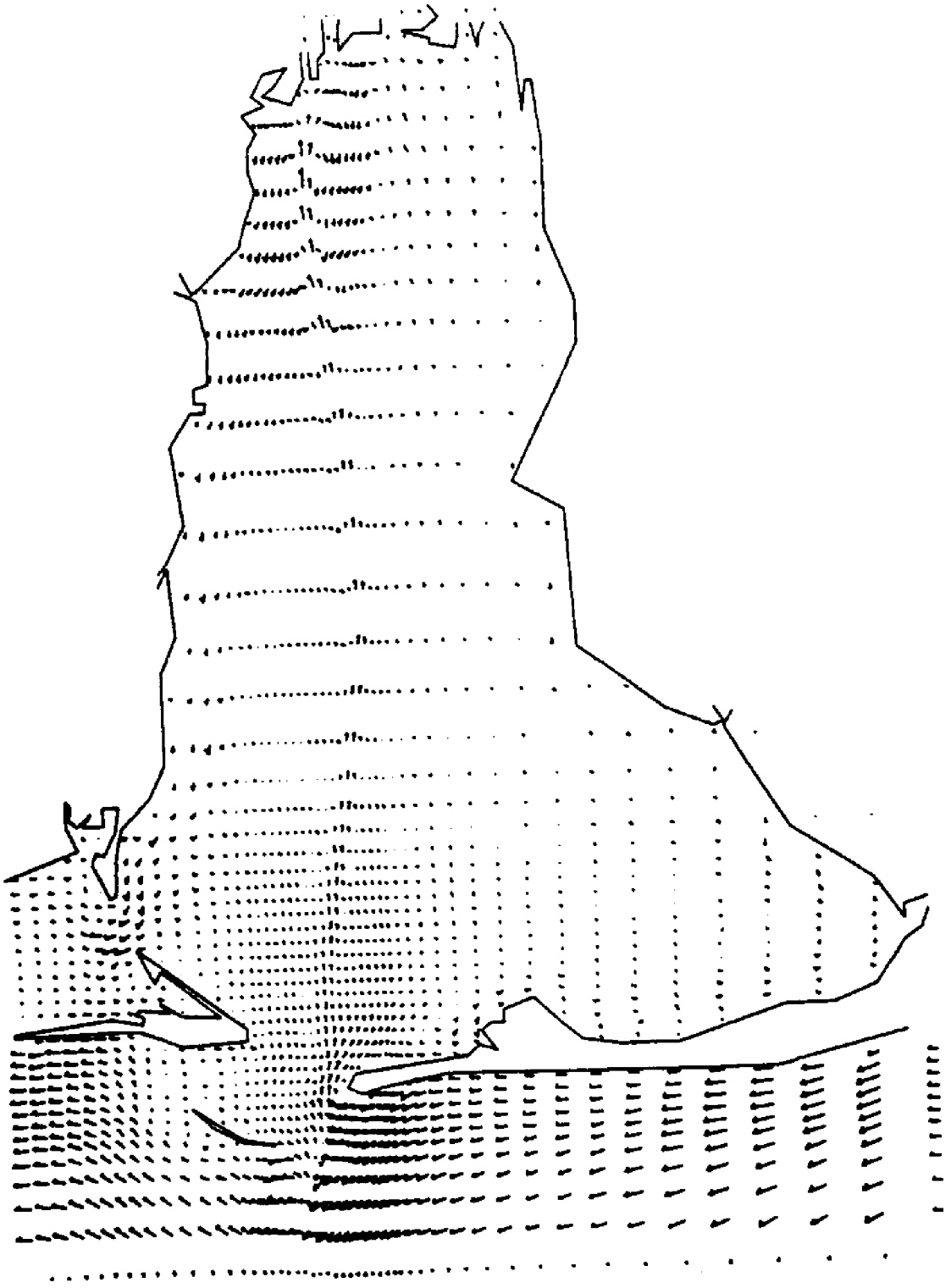

FLOW RATE FIELD AT T(HR) = 28.00
MAXIMUM VELOCITY (FT/SEC) = 1.15

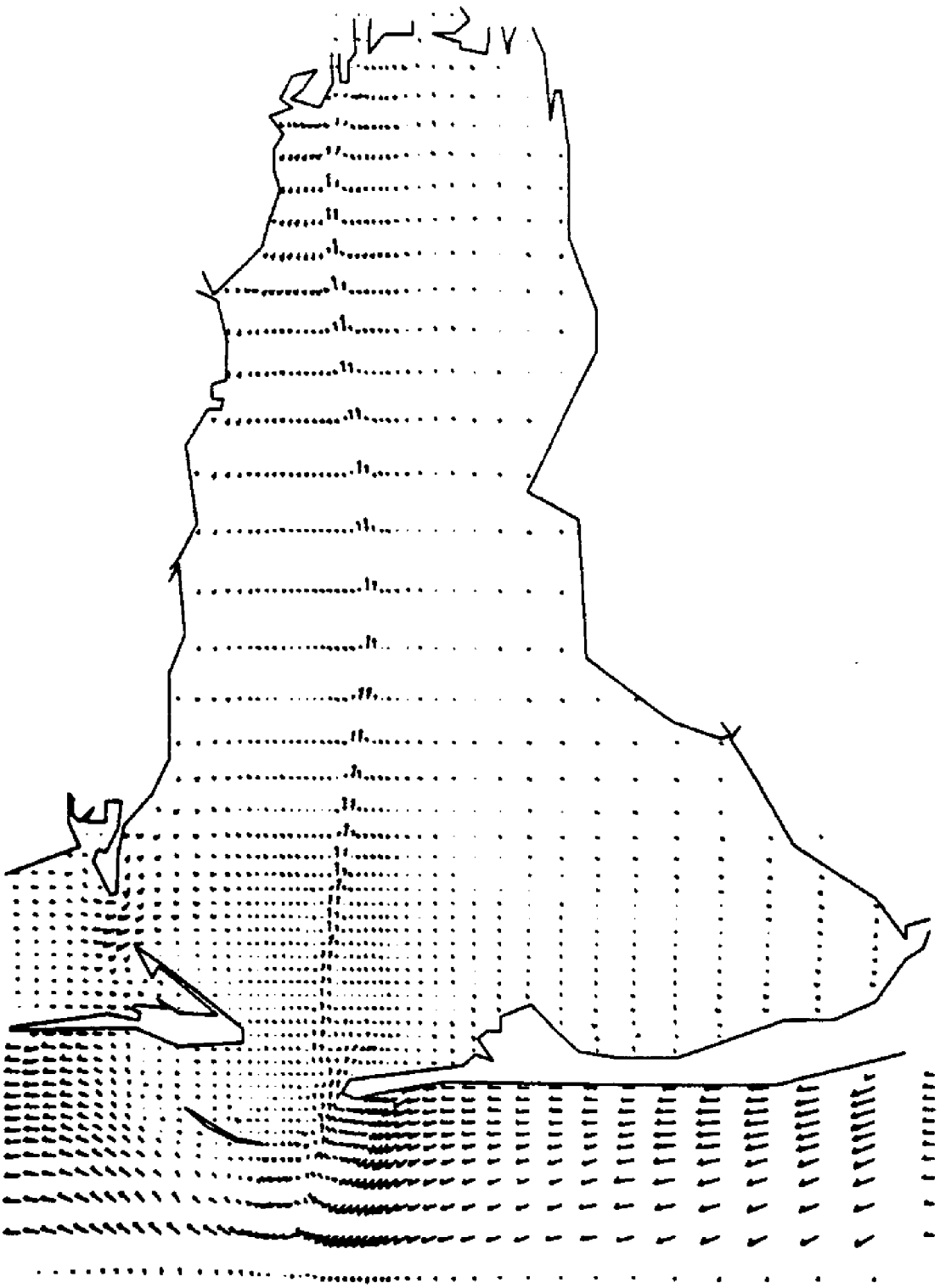

FLOW RATE FIELD AT T(HR) = 32.00
MAXIMUM VELOCITY (FT/SEC) = 1.18

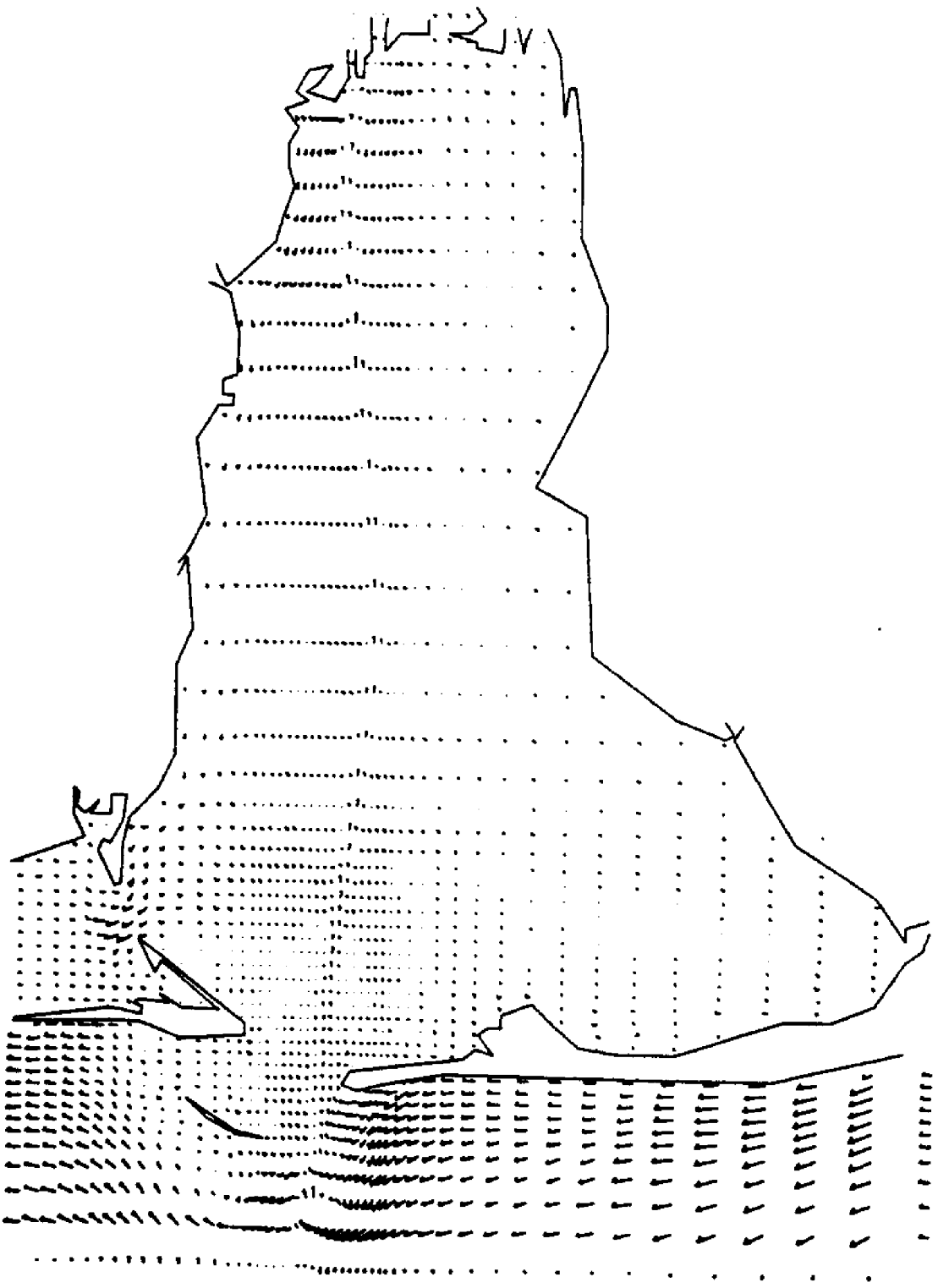

FLOW RATE FIELD AT T(HR) = 36.00
MAXIMUM VELOCITY (FT/SEC) = 1.18

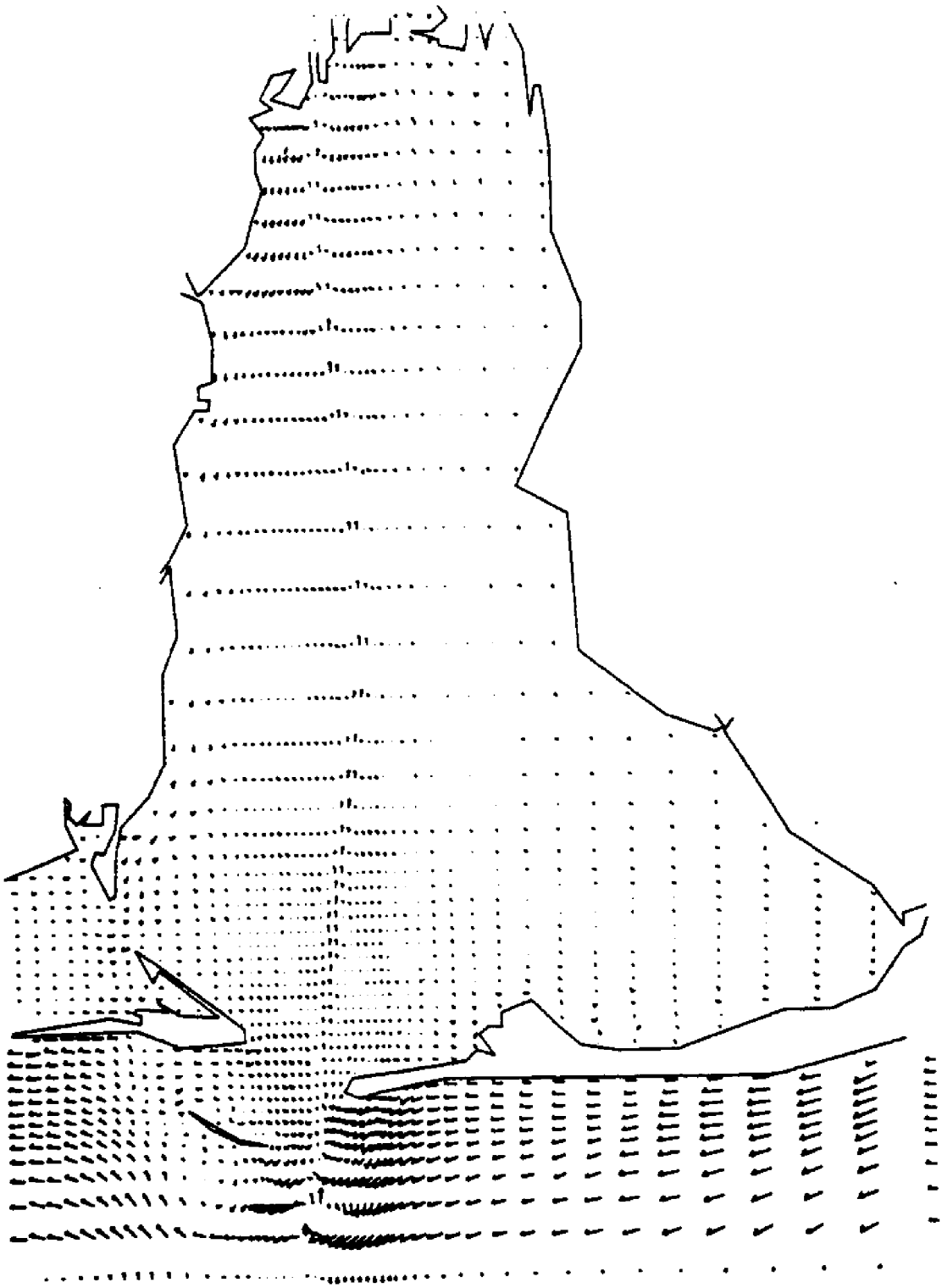

FLOW RATE FIELD AT T(HR) = 40.00
MAXIMUM VELOCITY (FT/SEC) = 1.16

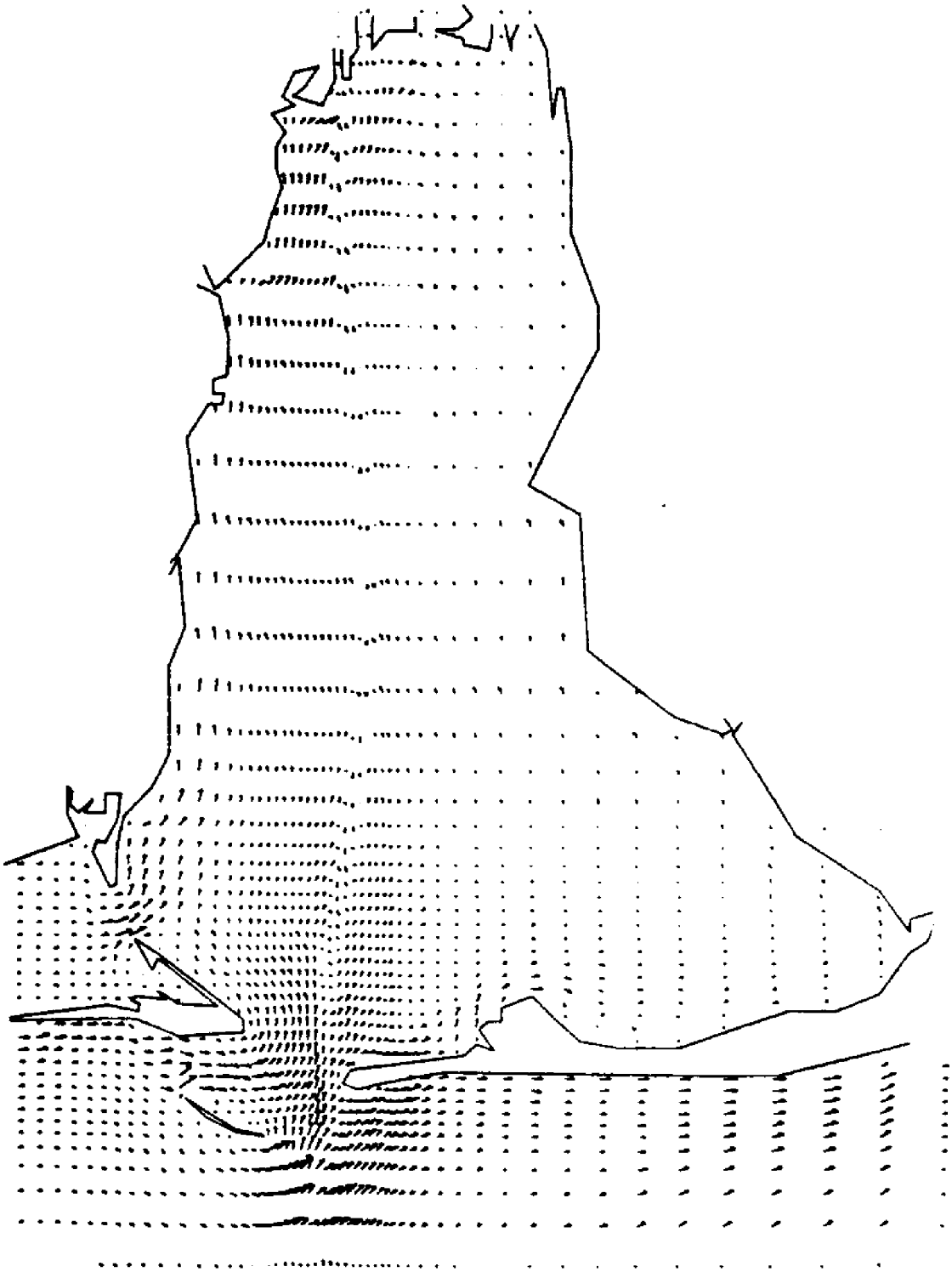

FLOW RATE FIELD AT T(HR) = 4.00
MAXIMUM VELOCITY (FT/SEC) = 1.03

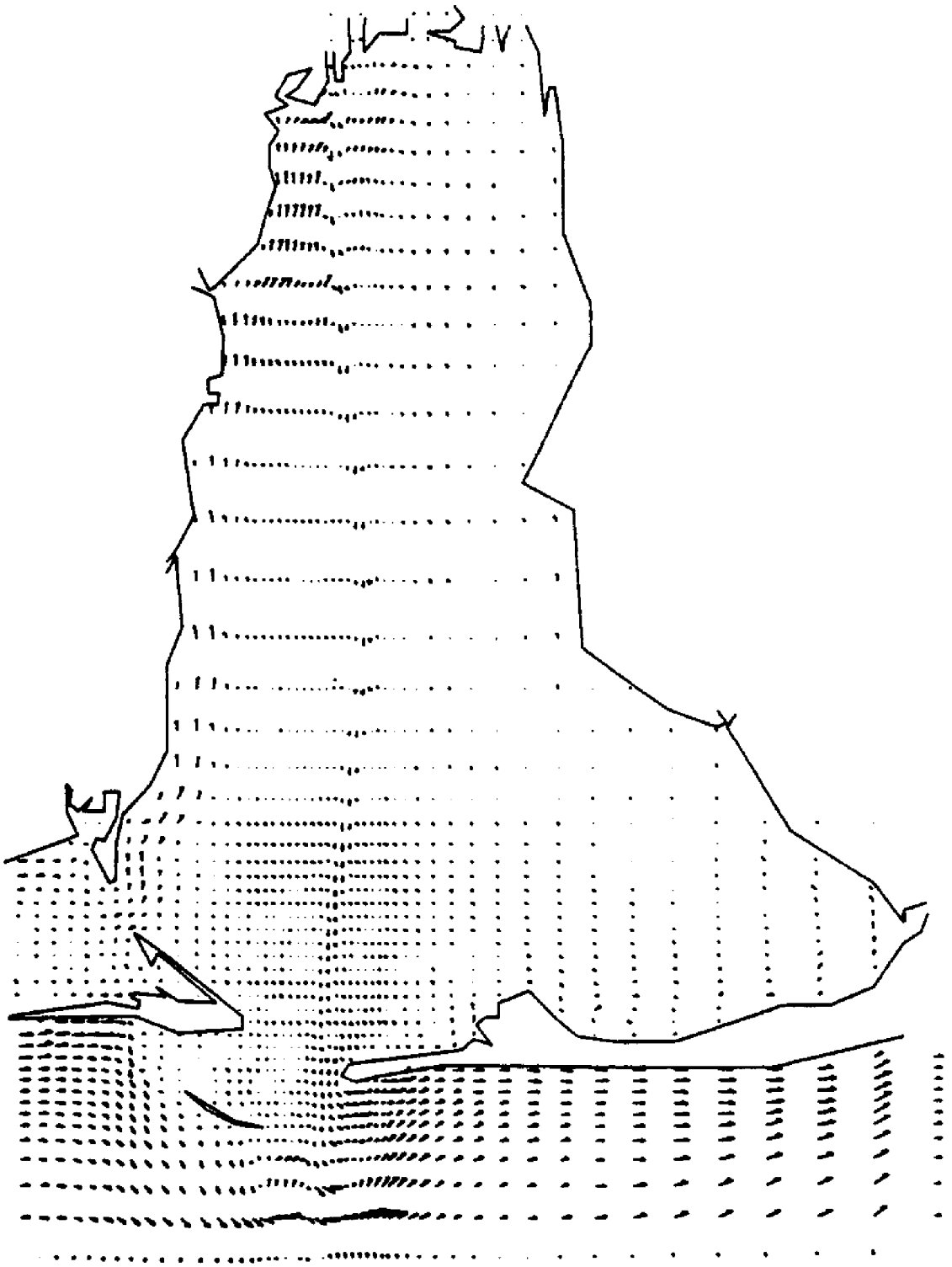

FLOW RATE FIELD AT T(HR) = 8.00
MAXIMUM VELOCITY (FT/SEC) = .89

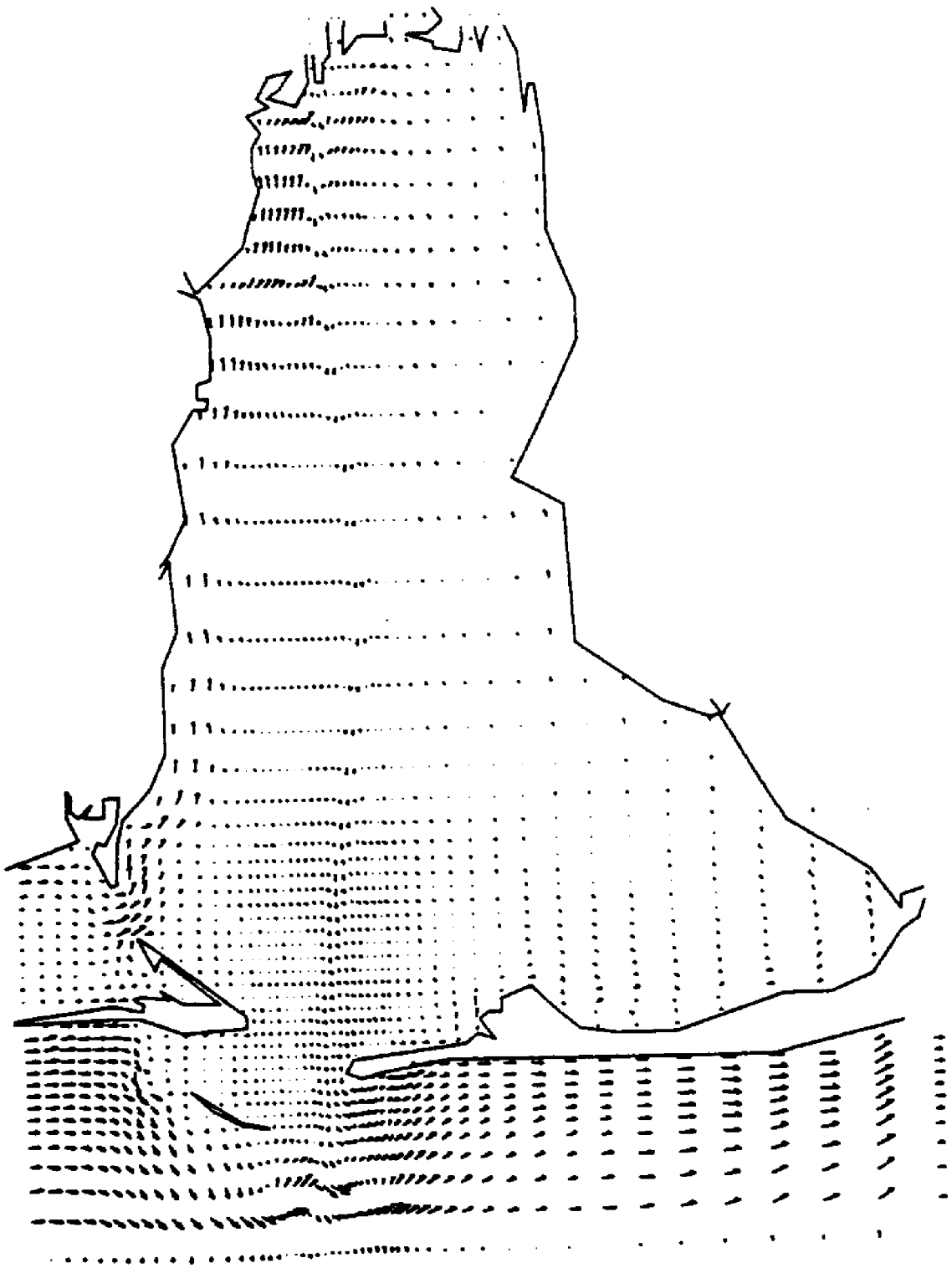

FLOW RATE FIELD AT T(HR) = 12.00
MAXIMUM VELOCITY (FT/SEC) = .96

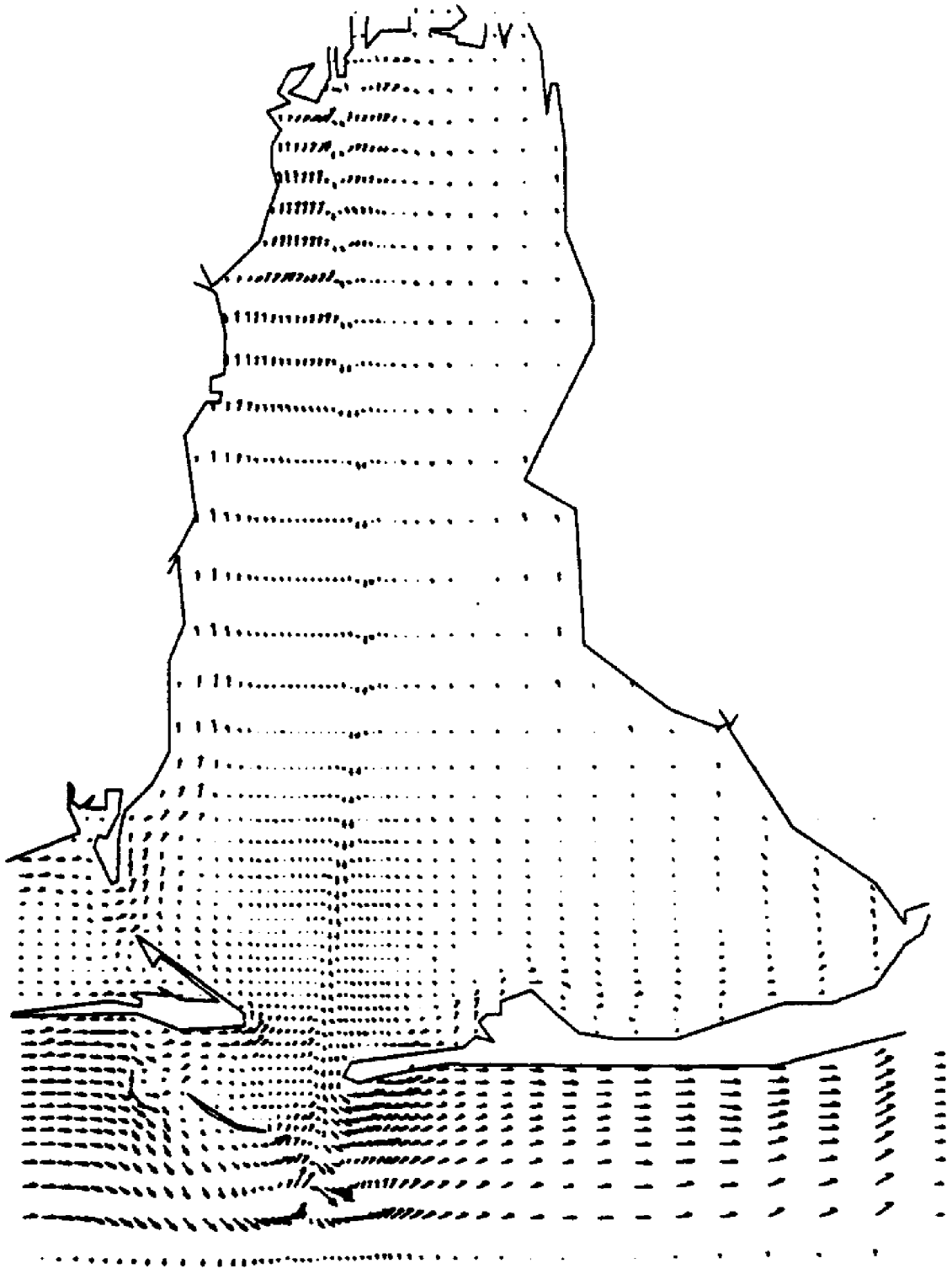

FLOW RATE FIELD AT T(HR) = 16.00
MAXIMUM VELOCITY (FT/SEC) = 1.48

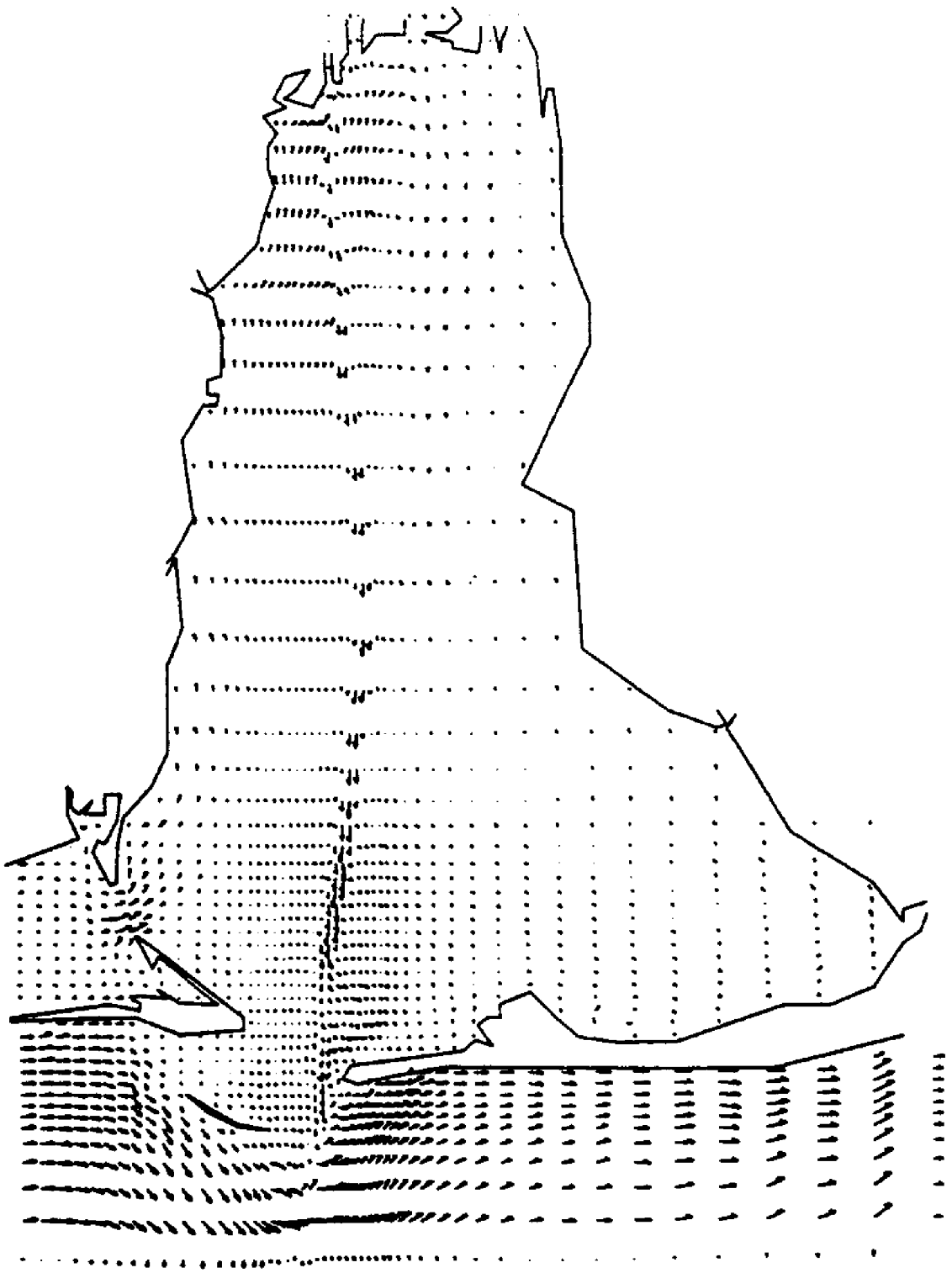

FLOW RATE FIELD AT T(HR) = 20.00
MAXIMUM VELOCITY (FT/SEC) = 1.06

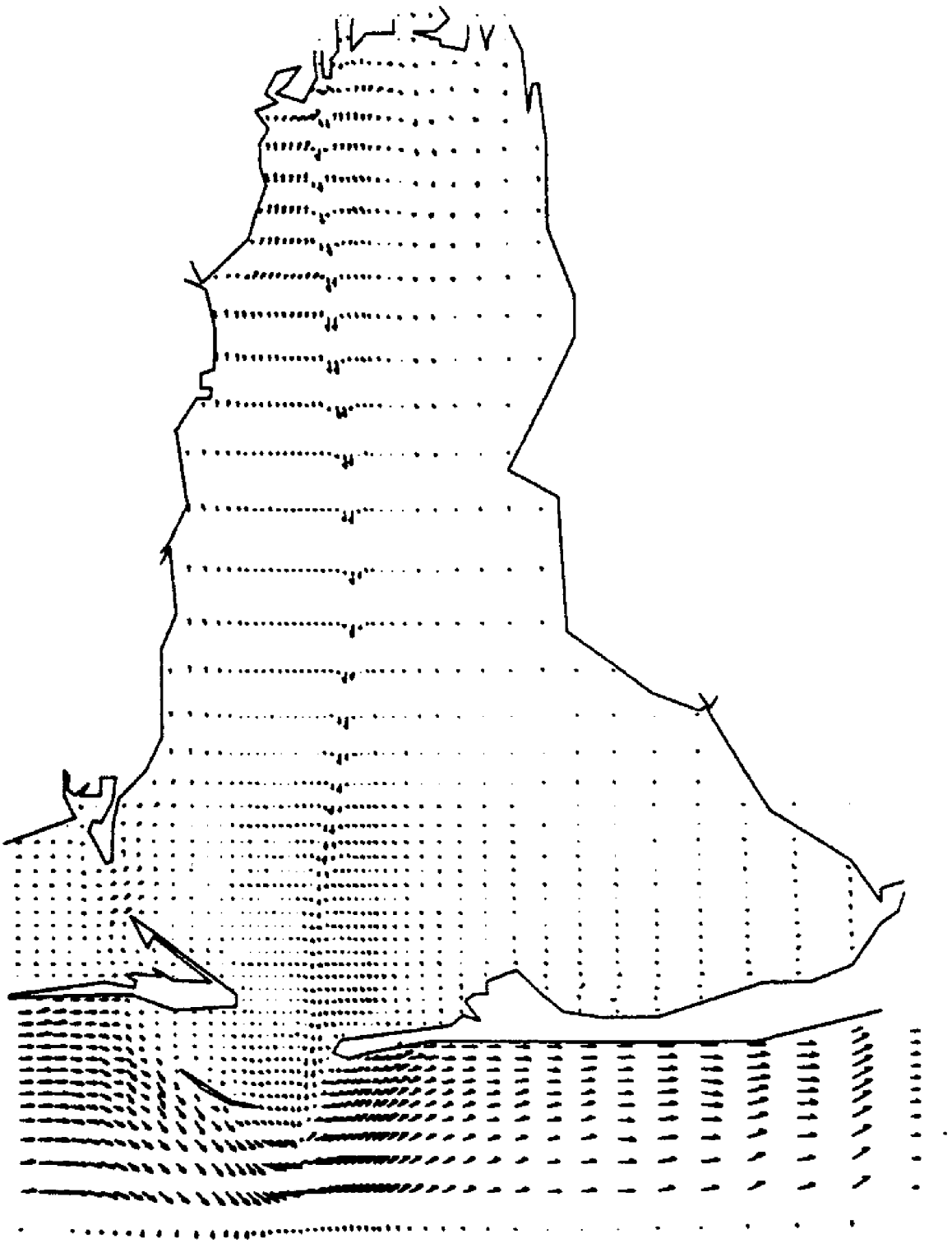

FLOW RATE FIELD AT T(HR) = 24.00
MAXIMUM VELOCITY (FT/SEC) = 1.06

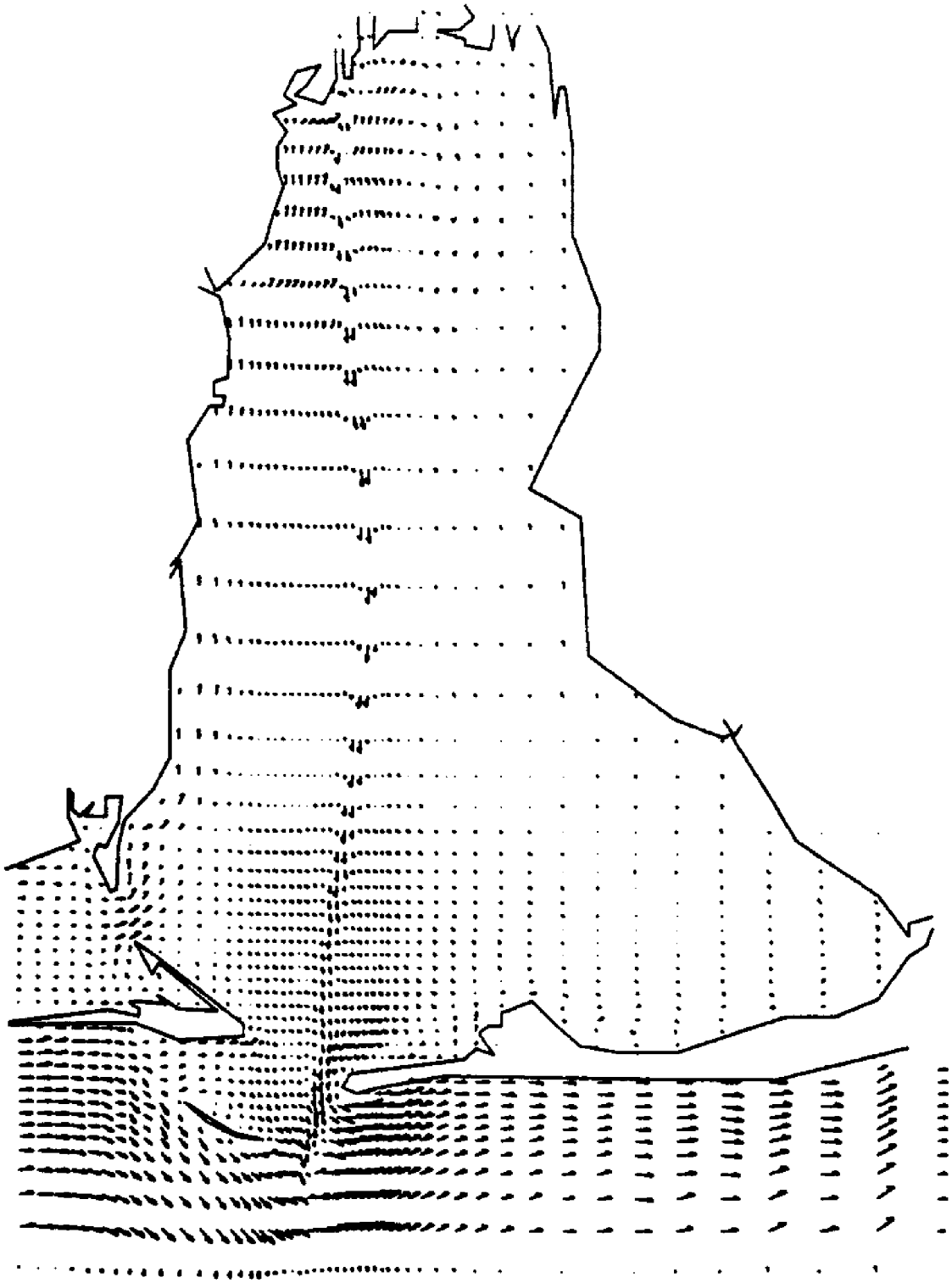

FLOW RATE FIELD AT T(HR) = 28.00
MAXIMUM VELOCITY (FT/SEC) = 1.03

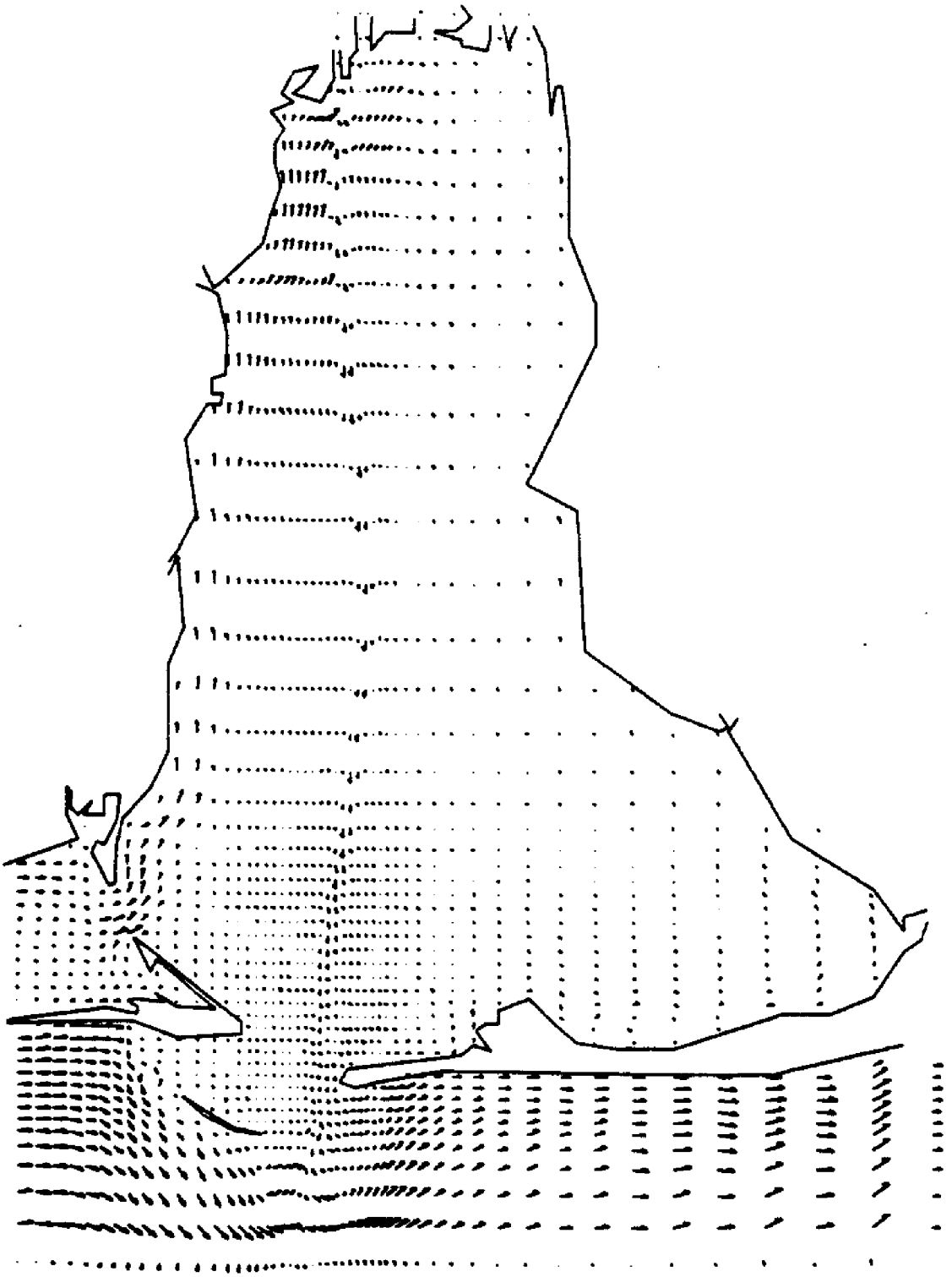

FLOW RATE FIELD AT T(HR) = 32.00
MAXIMUM VELOCITY (FT/SEC) = 1.00

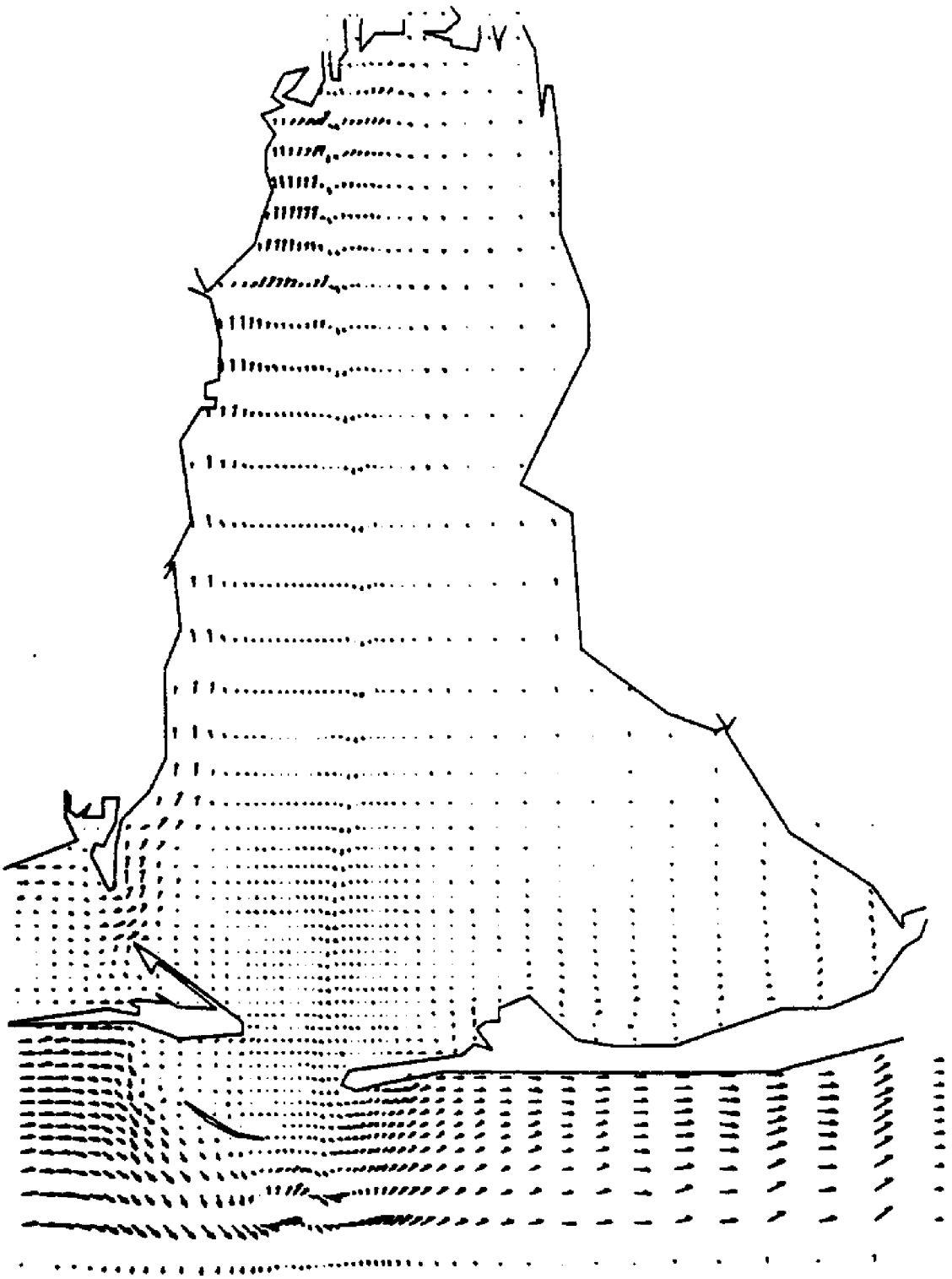

FLOW RATE FIELD AT T(HR) = 36.00
MAXIMUM VELOCITY (FT/SEC) = 1.01

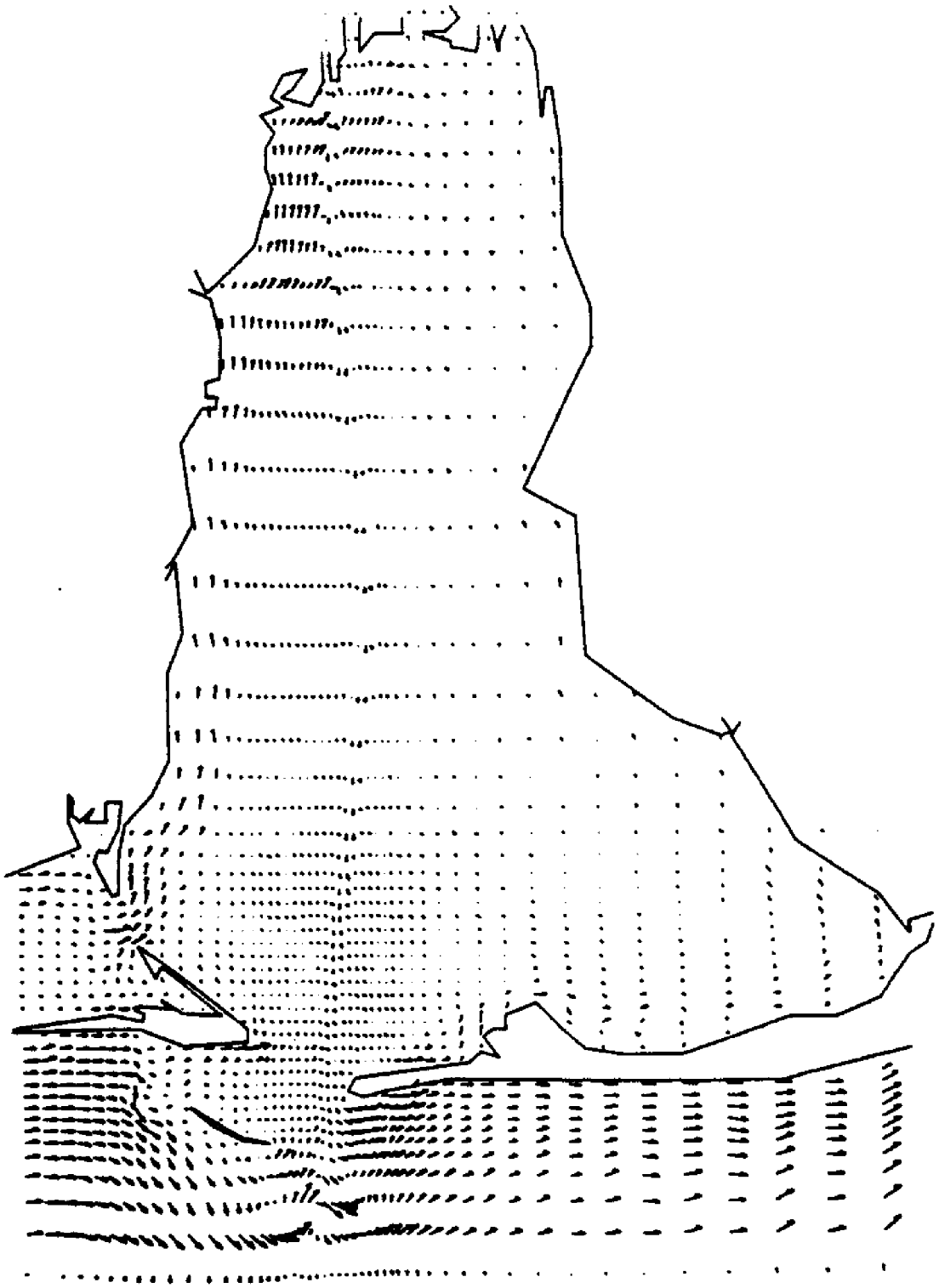

FLOW RATE FIELD AT T(HR) = 40.00
MAXIMUM VELOCITY (FT/SEC) = 1.38

THE UNIVERSITY OF ALABAMA
COLLEGE OF ENGINEERING

The College of Engineering at The University of Alabama has an undergraduate enrollment of more than 2,100 students and a graduate enrollment exceeding 125. There are approximately 100 faculty members, a significant number of whom conduct research in addition to teaching.

Research is an integral part of the educational program, and research interests of the faculty parallel academic specialities. A wide variety of projects are included in the overall research effort of the college, and these projects form a solid base for the graduate program which offers twelve different master's and five different doctor of philosophy degrees.

Other organizations on the University campus that contribute to particular research needs of the College of Engineering are the Charles L. Seebeck Computer Center, Geological Survey of Alabama, Marine Environmental Sciences Consortium, Mineral Resources Institute—State Mine Experiment Station, Mineral Resources Research Institute, Natural Resources Center, School of Mines and Energy Development, Tuscaloosa Metallurgy Research Center of the U.S. Bureau of Mines, and the Research Grants Committee.

This University community provides opportunities for interdisciplinary work in pursuit of the basic goals of teaching, research, and public service.